INVESTIGATION OF TECHNICAL BARRIERS AND SOLUTIONS FOR HIGH PENETRATION OF PHOTOVOLTAIC SYSTEMS IN THE UK

SIVAPRIYA MOTHILAL BHAGAVATHY

PhD

2017

INVESTIGATION OF TECHNICAL BARRIERS AND SOLUTIONS FOR HIGH PENETRATION OF PHOTOVOLTAIC SYSTEMS IN THE UK

SIVAPRIYA MOTHILAL BHAGAVATHY

A thesis submitted in partial fulfilment of the requirements of the University of Northumbria at Newcastle for the degree of Doctor of Philosophy

Research undertaken in the Faculty of Engineering & Environment

October 2017

ABSTRACT

Rising concerns on climate change due to greenhouse gases have led to the UK Climate Change Act 2008 which sets a target to cut CO_2 emissions by 80% of 1990 levels by 2050. Photovoltaic (PV) systems form one of the main technologies capable of delivering the target. Though the ability to deliver reductions in the installed costs of PV will determine the level of sector growth, this growth could be limited by several technical factors. As about 90% of the number of PV systems installed in the UK belong to the category of residential systems with individual ratings less than 4 kW, this study focuses on this sector. This sector represents 20% of the total installed capacity in the UK.

This research aims to identify the key technical barriers and associated solutions to increase PV penetration in a distribution network in the UK. The research defines the realistic worst-case scenario to evaluate the performance of the distribution network with PV and then quantifies the percentage of PV penetration at which the presence of PV may adversely affect the performance of the distribution network. The steady-state analysis conducted shows that the voltage at parts of the feeder violates the statutory limits at 20% penetration for the realistic worst-case scenario, followed by reversal of net active power and low power factor at the secondary of the substation when penetration level is over 30%. The results indicate that the minimum load of the feeder under consideration during hours of daylight and the more common irradiance level at that geographic location should be used rather than a hypothetical worst-case scenario to evaluate the maximum allowable contribution of PV systems in the feeder. Analysis of the performance of distribution networks under fault indicates that the tripping time of the relay may be delayed under the presence of PV. However, the probability of false tripping of the relay is very low.

This research also identifies solutions to increase the contribution of PV systems in the energy mix and evaluates the effectiveness of the solutions. The solutions in the order of decreasing effectiveness are changes to tap changer settings, reactive power control and PV generation curtailment. A strategy to increase the contribution is proposed. This includes changes to the settings of the tap changer (increases the PV contribution from 20 to 40%) followed by active power curtailment (which would increase PV contribution from 40 to 60%). A phased approach like this would enable the regulators to plan for the transitionary period to increase the contribution of PV.

TABLE OF CONTENTS

LIST OF FIGURES

LIST OF TABLES

LIST OF ABBREVIATIONS

ADMD	After Diversity Maximum Demand
ANM	Active network management
CCC	Committee on climate change
CCS	Carbon capture and storage
CHP	Combined Heat and Power
CLNR	Customer Led Network Revolution
CNE	Combined neutral earth
DECC	Department of Energy and Climate Change
DER	Distributed Energy Resource
DG	Distributed generation
DNO	Distribution network operator
EU	European Union
FIFO	First in first out
FiT	Feed-in Tariff
FRT	Fault ride through
GMT	Greenwich Mean Time
IC	Incremental Conductance
IEC	International Electrotechnical Commission
LIFO	Last in first out
LV	Low voltage

LVRT	Low voltage ride through
MPP	Maximum power point
MPPT	Maximum power point tracking
NEC	National Electrical Code
NFFO	Non-Fossil Fuel Obligation
NREL	National Renewable Energy Laboratory
OLTC	On-load tap changers
P&O	Perturb and Observe
PCC	Point of common coupling
PLL	Phase locked loop
PWM	Pulse Width Modulation
REC	Renewable Energy Certificates
RO	Renewables Obligation
ROC	Renewable Obligation Certificates
STC	Standard Test Conditions
SVC	Static voltage compensator
THD	Total harmonic distortion
TNO	Transmission Network Operator
UKGDS	UK generic distribution system
UL	Underwriters Laboratory
VC	Venture capitalists
VSI	Voltage source inverters

LIST OF SYMBOLS

$\alpha_{I_{SC}}$	Temperature co-efficient of I_{SC}
$\beta_{V_{OC}}$	Temperature co-efficient of V_{OC}
η	Efficiency
ΔI_{dc}	Maximum fluctuation in DC-current in the DC/DC converter
ΔP_{max}	Tolerance in the power output of PV system
C_{base}	Base value of capacitance for per-unit calculations
C_{dc}	DC-link capacitance
C_{pv}	Capacitance connected across the PV array
C_{max}	Maximum capacitance value of the LCL filter
E_{curt}	Energy curtailed
F_{nom}	Nominal frequency of operation (50 Hz)
f_{res}	Resonance frequency of the LCL filter
h_{curt}	Hours of energy generation from PV system curtailed
i_{α} , i_{β}	Components of single-phase current along α and β axes of the stationary reference frame
$i_{\omega t+\varphi}$	Single-phase output current of the inverter
$i_{\omega t+\varphi+\frac{\pi}{2}}$	Phase-shifted single-phase output current of the inverter
I_D, I_O	Reverse saturation current of the diode
i_d, i_q	d and q axis components of the current signal
I_{dc}	DC current output of the DC/DC converter
I_{mpp}	Current output of PV array/module at maximum power point
I_{ph}, IL	Component of cell current due to photons
I_{pv}	Output current of PV
I_{SC}	Short-circuit current of the PV module
k	Boltzmann constant

k_i	Integral gain of a PI controller
k_p	Proportional gain of a PI controller
L_{dc}	Inductance of the DC/DC converter
$L_{dc,min}$	Minimum inductance of the LCL filter
n	Number of houses
N	Diode emission co-efficient
P_{base}	Base value of power for per-unit calculations
P_{nom}	Nominal power output of PV system
PV_{gen}	Energy generated by PV systems
R_D	Damping resistance of the LCL filter
R_s	Series resistance of a PV system
R_{sh}	Shunt resistance of a PV system
q	Magnitude of charge of an electron
T	Temperature in K
V_{base}	Base value of voltage for per-unit calculations
V_{dc}	DC-link voltage
Z_{base}	Base value of impedance for per-unit calculations

ACKNOWLEDGEMENTS

I wish to express my sincere gratitude to my principal supervisor, Prof. Nicola Pearsall, for the valuable guidance, support and inspiration at every stage of this research. I would also like to express my gratitude to Prof. Ghanim Putrus, my second supervisor, for the healthy debates on the research and the technical guidance. I would like to express my gratitude to Dr. Sara Walker, under whom I started this research, for her mentorship and continued support by joining the supervisory team as an external supervisor after leaving the university. I would also like to thank them all for their continuous support and feedback throughout the three years. I would also like to thank Northumbria University for the studentship and the financial support.

I would also like to thank Dr. David Johnston and Dr. Edward Bentley for their support at the Lab. I would like to thank my husband, Nagarajan Gopalakrishnan for being the source of happiness and inspiration during the enduring years. I would like to thank my daughter, Srishti Nagarajan, for looking after herself and warming us with her smile. I thank my friends for their support and wish them the best for their future. I would like to thank my dad for supporting me and for being there every time I fell. Last but not least I would like to thank my mum without whom I would not have reached this stage.

(SIVAPRIYA MOTHILAL BHAGAVATHY)

DECLARATION

I declare that the work contained in this thesis has not been submitted for any other award and that it is all my own work. I also confirm that this thesis fully acknowledges opinions, ideas and contributions from the work of others. Any ethical clearance for the research presented in this thesis has been approved. Approval has been sought and granted by the Faculty Ethics Committee on 16/09/2015.

I declare that the word count of this thesis is 45,464 words.

CHAPTER 1

INTRODUCTION

The majority of current energy requirements of the world are fulfilled by oil and natural gas. Figure 1-1 gives the global primary energy consumption, from 1989 to 2016, categorized by source of energy viz. coal, oil, natural gas, nuclear energy, renewable energy and hydro-electricity [1]. Non-renewable sources of energy release significant amounts of greenhouse gases (GHGs) making them unsustainable in all aspects, viz. economically, environmentally and socially. Figure 1-2 gives the global carbon dioxide (CO2) emissions categorized by domain of use of energy [2]. Without any active participation/decision to reduce these GHG emissions, it is predicted that there would be considerable climate change with an average 6 ºC global warming by end of 21st century, the results of which could be fatal to mankind [3]. The need to avoid this irreversible climate change has led the European Union (EU) countries to commit to reducing GHG emissions to 80 – 95%

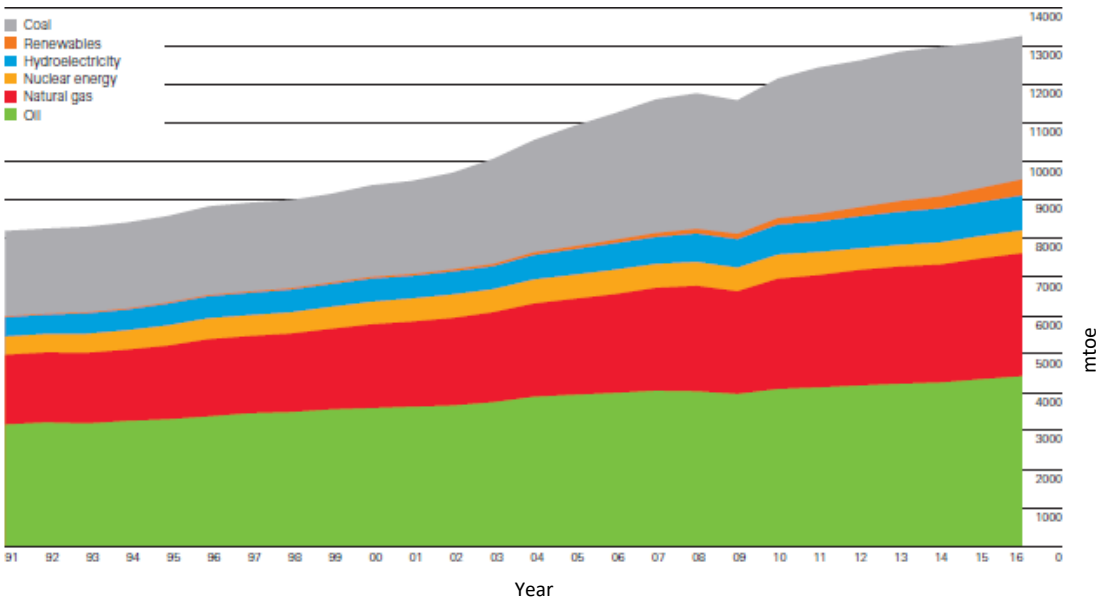

Figure 1-1: Global primary energy consumption (mtoe) [1]

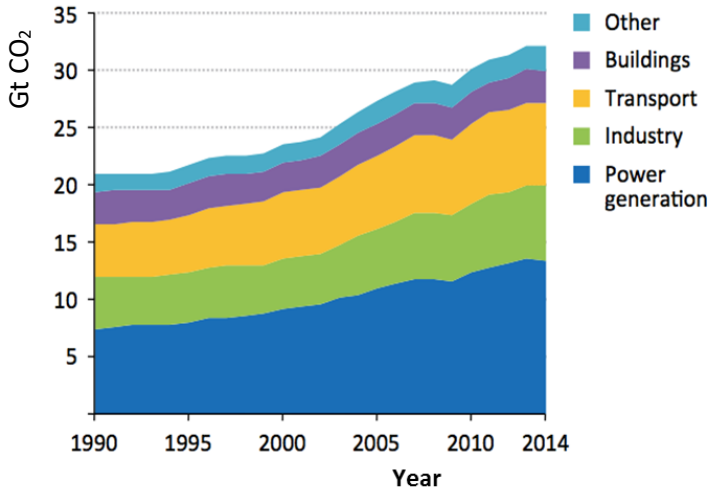

Figure 1-2: Global energy related CO_2 emissions by sector [2]

below the 1990 levels by 2050 [4]. With active participation, the emissions in the years 2015 and 2016 have been maintained at 2014 levels [5].

1.1 Background and Motivation

Since the publication of the Energy White paper in 2003 [6], the UK has stated three fundamental energy policy objectives, commonly referred to as the 'energy trilemma': to reduce emissions of CO_2 that contribute to the manmade climate change, to maintain and increase energy security and to keep the price of energy competitive for business and affordable for households [7]. The UK Climate Change Act 2008 sets a target for cutting GHG emissions by 80% by 2050 from their 1990 baseline levels with an interim target of 26% reduction by 2020 [8]. The act also established the Committee on Climate Change (CCC) to advise the government on progress to a low-carbon economy and set carbon budgets. Figure 1-3 shows the GHG emissions per sector in the UK for the year 2013 [9] and it can be observed that the energy supply sector was the largest contributor to GHG emissions. The UK National Atmospheric Emissions inventory also identifies combustion of fossil fuels in the energy sector as the largest contributor of GHG emissions [10].

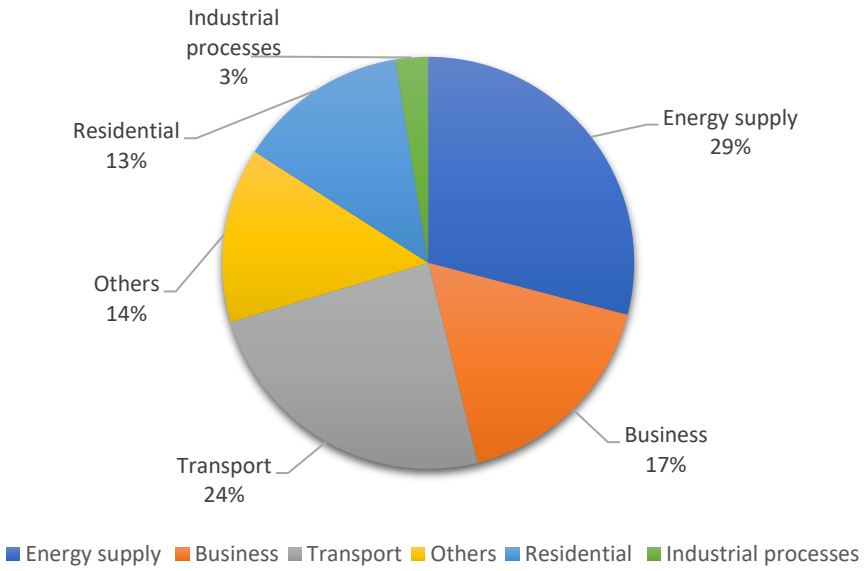

Figure 1-3: GHG Emissions per sector in the UK in the year 2015 (Source: 2015 UK Greenhouse Gas Emissions)

The electricity sector has been identified as one of the areas where the progress on emission reductions can be made most rapidly at relatively low cost and low uncertainty in the timescale to 2030 by Gardner [11]. To decarbonize the electricity sector, UK has four main options, viz. nuclear power, large-scale renewables, fossil fuel power stations with carbon capture and storage (CCS) technologies (though not yet commercially proven) and small-scale renewables [7]. The first three options are operational in transmission networks and the fourth option is operational at low voltage distribution networks. Though nuclear power has the potential to reduce emissions, the current status of the Hinkley Point nuclear power station project makes it a non-feasible option to meet the targets for 2030 [12]. The UK Renewable Energy (RE) Roadmap (2011) states that the target set by the EU for the UK to deliver 15% of total UK energy demand from renewables by 2020 is achievable [13], and photovoltaics (PV) forms one of the 8 technologies capable of contributing to the target with other technologies being onshore wind, offshore wind, marine energy, biomass electricity, ground source and air source heat pumps and renewable transport [14]. The installed capacity of PV in the UK has increased

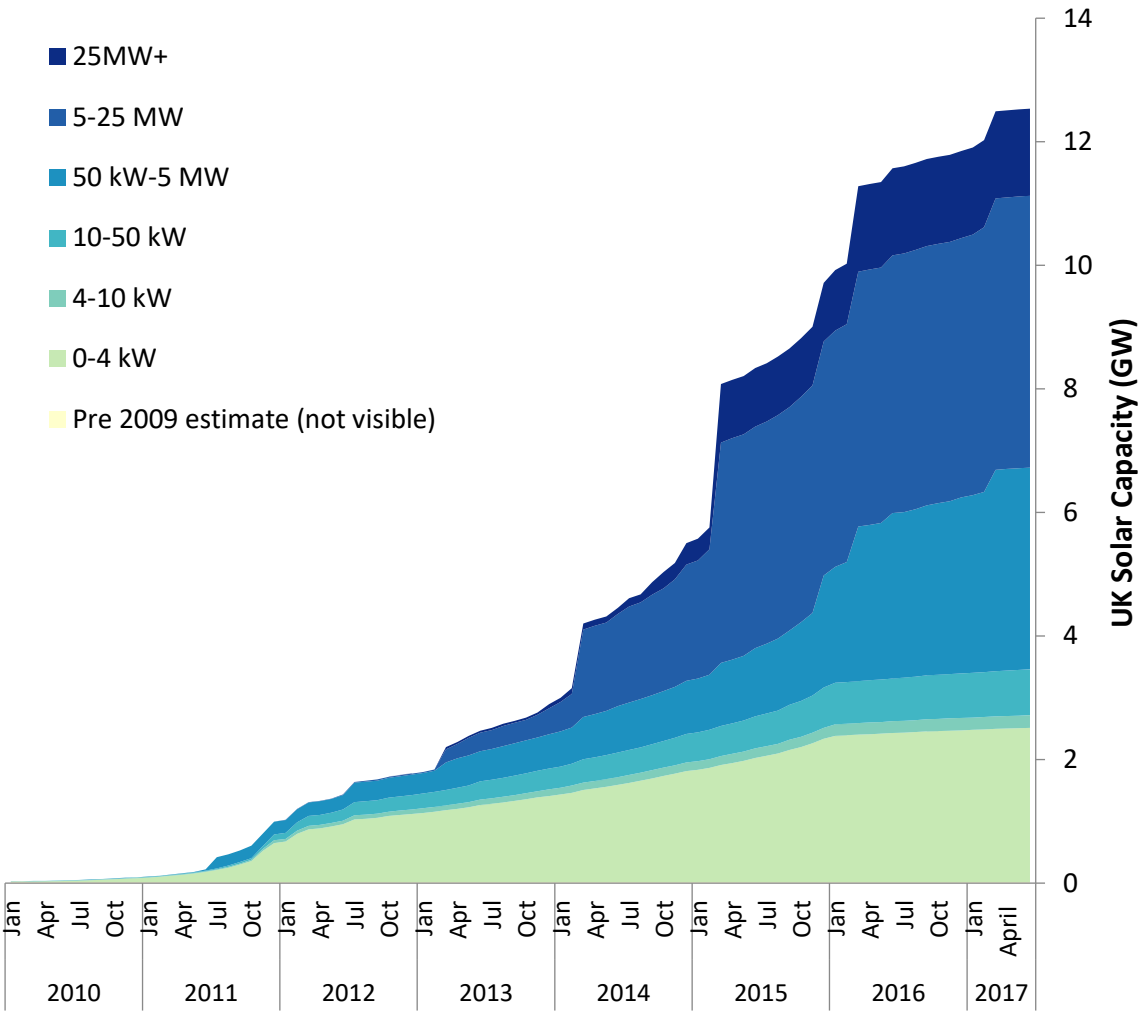

Figure 1-4: Cumulative installed capacity of solar PV in UK (Source: DECC)

significantly over the last decade, as shown in Figure 1-4, ending June 2017 [15]. Though the PV systems with individual capacities less than or equal to 4 kW only contribute 20% to the total capacity, they contribute to more than 90% of installed PV systems by number as shown in Figure 1-5. Their share in installed capacity in the UK has increased over the years reaching 56% of the capacity of newly installed PV systems in the month of May 2017. Experts project that small-scale solar PV generation will contribute around 7.5% of total electricity generation by 2020 and will have a total of 18 GW of PV connected to the grid producing 15 TWh/year by 2030 [11], [16]. These PV systems are connected to the distribution networks that are traditionally passive in control of power flow, with lower amounts of automation and monitoring as compared to transmission networks [17]. Also, the direction of power

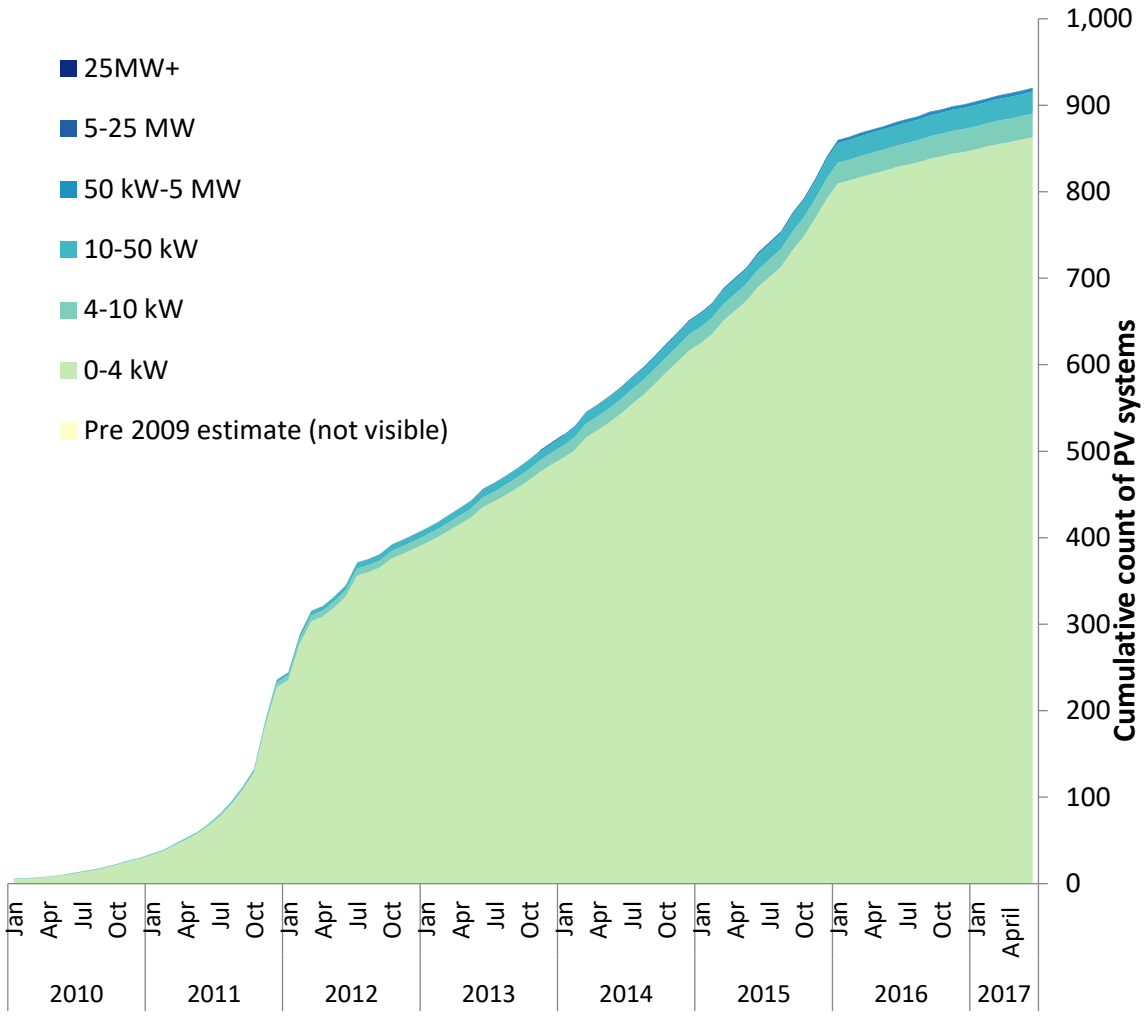

Figure 1-5: Cumulative count of PV systems installed in the UK (Source: DECC)

flow has traditionally been from central generators to the loads located at the end of the distribution network. With increasing penetration of small-scale generators, there arise scenarios of bi-directional power flow, increase in network fault levels and voltage fluctuations in the distribution network [18], which necessitates analysis of the performance of distribution networks. The level of solar PV sector growth and the cost competitiveness will be determined by the ability to deliver further reductions in the installed costs of solar PV systems [19]. Though the ability to deliver reductions in the installed costs of PV will determine the level of sector growth, the contribution from PV could be limited by several technical factors/barriers [20]. With the UK solar PV strategy roadmaps [19], [21] and the UK emission reduction strategies [8] under progress, there arises the need to assess

the barriers and obtain suitable solutions for high penetration of solar PV in the low voltage distribution network.

1.2 Aims and Objectives

The aim of this research is to investigate the key technical barriers and develop associated solutions for high penetration of photovoltaic (PV) systems in the UK.

The specific objectives of this research are:

I. Development of dynamic models of a single-phase PV system and a three phase distribution network representative of the UK distribution network.
II. Definition of probable boundary scenarios for the UK distribution network with PV
III. Evaluation of the steady-state performance of the distribution network under different penetration levels of PV systems. Key performance measures are:
    a. Voltage profile
    b. Real and reactive power variation
    c. Total harmonic distortion (THD)
    d. Reverse power flow
    e. Power factor
IV. Evaluation of the dynamic-state performance of the distribution network under different penetration levels of PV systems. Key performance measures are:
    a. Net fault current
    b. Net current at substation during fault
    c. Current contribution of PV systems during fault
    d. Protection mechanism

V. Evaluation of hosting capacity of PV systems based on results of objectives III and IV

VI. Identification of solutions for the technical barriers identified in objective V, evaluation of the feasibility of the solutions and ranking of the solutions.

1.3 Operational Definition for Penetration of PV

'Penetration' of PV systems is typically used in literature to quantify the contribution of PV to the electricity network and also in identifying the possible impact of PV systems on the distribution network at a particular level of contribution of PV. As there are multiple ways to define the word 'penetration', it is important to define the term as used in this research.

In this research, the definition from [22] has been extended by using the after diversity maximum demand (ADMD). The ADMD for a distribution network is expressed as kVA/house. The definition of percentage penetration in terms of the after diversity maximum demand per house, number of houses in the distribution network and the total installed PV capacity in the network is

$$\%\, penetration = \frac{PVrating}{ADMD \times n} \tag{1.1}$$

where, $PVrating$ is the total installed capacity of PV systems in the distribution network

$ADMD$ is the after diversity maximum demand per house and

n is the number of houses in the distribution network

The use of such a definition based on parameters readily available for a distribution network enables the results to be extended to another distribution network with a different set of technical parameters. Though the definition based on a number of

houses may also be extended, such a definition raises concerns when individual PV systems have different ratings.

1.4 Methodology

The methodology adopted to achieve the objectives are as follows:

I. Develop and validate dynamic models of a single-phase PV system and a residential distribution network representative of the UK distribution network.

II. From literature, evaluate existing installed capacity of solar PV system in the UK to identify the typical size of a single-phase residential solar PV system. Analyse the irradiance and load profile data of the UK to identify realistic worst-case scenarios for evaluation of performance.

III. Perform steady-state simulations on the distribution network to evaluate its performance with balanced and unbalanced distribution of PV across the three phases at different PV penetrations.

IV. Perform dynamic simulations on the three-phase distribution network with different penetration levels of PV systems and different fault locations

V. Identify the parameters adversely affected by the increasing penetration of solar PV at both steady-state and dynamic-state.

VI. Define technical solutions to help improve the parameters adversely affected by the increasing penetration of solar PV and evaluate its effectiveness. The solutions investigated are:

    a. Changing the off-load tap changer setting to improve the voltage profile at peak generation.

    b. Providing reactive power support using PV inverter to improve the voltage profile and power factor at the transformer.

c. Generation curtailment during peak generation and low load scenarios. Evaluate the frequency of occurrence of such an event in the UK from historical data of irradiance and residential load profile.
d. Perform sensitivity analysis to observe the variation of the impact of the solutions with different parameters. Rank the identified technical solutions based on detailed assessment criteria.

1.5 Original Contribution

The original contributions of this research are:

1. Development of a generic dynamic model of a single-phase PV system suitable for ratings from 1 kW to 4 kW.

2. Evaluation of steady-state performance of a distribution network representative of the UK with different penetration levels of PV under realistic worst-case scenarios.

3. Evaluation of dynamic performance of a distribution network with different penetration levels of PV.

4. Evaluation of technical barriers limiting the contribution of PV systems in a distribution network considering the realistic worst-case scenarios.

5. Evaluation of solutions relevant to the distribution network in the UK and its effectiveness to increase the contribution of PV systems under realistic worst-case scenarios.

1.6 List of Publications

Journal papers

1. Sivapriya Bhagavathy, Nicola Pearsall, Ghanim Putrus and Sara Walker. “Performance assessment of a three-phase distribution network with multiple residential single-phase PV systems”, CIRED Open Access Proceedings Journal, pp. 1-4, September 2017.
2. Sivapriya Bhagavathy, Nicola Pearsall, Ghanim Putrus and Sara Walker. “Dynamic performance of a distribution network in the UK with multiple single-phase PV systems”, prepared for submission to Renewable Energy
3. Sivapriya Bhagavathy, Nicola Pearsall, Ghanim Putrus and Sara Walker. “Hosting capacity of a distribution network in the UK considering realistic scenarios”, prepared for submission to Energy

Conference papers

1. Sivapriya Bhagavathy, Nicola Pearsall, Ghanim Putrus and Sara Walker. “Performance assessment of a three-phase distribution network with multiple residential single-phase PV systems”, 24th International Conference & Exhibition on Electricity Distribution (CIRED), Glasgow, UK, 12 – 15 June 2017.
2. Sivapriya Bhagavathy, Nicola Pearsall, Ghanim Putrus and Sara Walker. “Analysis of distribution network performance under different penetration levels of solar PV”, 12th Photovoltaic science, application and technology conference (PVSAT), Liverpool, UK, 6 – 8 April, 2016.
3. Sivapriya Bhagavathy, Nicola Pearsall, Ghanim Putrus and Sara Walker. “Barriers and solutions for high penetration of solar PV in the UK”, Northumbria Research conference, Northumbria University, Newcastle Upon Tyne, UK, 20 May, 2015.

1.7 Overview of the Thesis

This thesis is divided into 8 chapters. The outline of each chapter is as follows.

Chapter 2 – Literature review on barriers for high penetration of PV: This chapter provides a review of the barriers limiting the contribution of PV systems discussed in the literature. The barriers are broadly categorised as technical, socio-economic and policy related barriers.

Chapter 3 – Regulations for distribution networks and grid connection of PV systems: This chapter provides an overview of the technical regulations to ensure safe and reliable connection of PV systems to the distribution network in the UK maintaining the power quality of distribution networks. The regulations for grid connection of PV in Australia, the USA and Germany (countries with significant PV contribution) are also summarised in this chapter. The comparison of regulations is used in the dynamic performance evaluation of the distribution network to discuss the impact of variations in regulations to the performance of the distribution network in chapter 6.

Chapter 4 – Dynamic model of the PV system and the distribution network: A generic model of a small-scale PV system with power rating ranging from 1 kW to 4 kW is developed and presented in this chapter. The generic model of the inverter is capable of replicating the performance of a commercial inverter for faults at different locations of the network. The inverter model is not pertaining to any single manufacturer make and is therefore validated against the standards for PV inverters. The results of performance under fault conditions are validated against experimental results of the performance of a 1 kW PV inverter for faults at its terminals with different fault conditions. The chapter also presents the dynamic model of the distribution network representative of the UK distribution network.

Chapter 5 – Steady-state performance of a distribution network with multiple single-phase PV systems: This chapter evaluates the steady-state performance of the distribution network modelled in chapter 4 for different penetration levels of PV systems. The chapter starts with the methodology used to evaluate the performance, followed by an analysis of the performances of the single-phase distribution network and the three-phase distribution network. Realistic worst-case scenarios based on irradiance monitored at Newcastle upon Tyne and the load profile of households in the UK are developed and presented in this chapter. The impact of changes in the substation voltage, power factor of operation of PV systems and unbalanced distribution of PV systems on the distribution network performance are also analysed. The performance is evaluated in terms of the four power quality indicators namely, voltage profile, THD, net power flow and power factor.

Chapter 6 – Dynamic performance of a distribution network with multiple single-phase PV systems: PV systems act as additional current sources that contribute to the net fault current and may affect the distribution network performance as the existing protection mechanism was not designed for this contribution. This chapter analyses the performance of a distribution network with multiple single-phase PV systems during and after a fault. The chapter then discusses the impact of multiple PV systems on the protective equipment in a 400 V distribution network in the UK, which are typically fuses at all feeders and relays at the substation transformers. The chapter also provides a discussion on the implications of different trip times stipulated by different standards used in other countries on the conclusions drawn using the G-83 standard.

Chapter 7 – Technical barriers and solutions to increase the contribution of PV in distribution network: This chapter draws on the results of the steady-state and dynamic-state performance analysis of the distribution network under different

penetration levels of PV systems in order to quantify the percentage contribution levels of PV at which the presence of PV may adversely affect the performance of the distribution network. The chapter then presents the solutions to increase the contribution of PV systems and evaluates the solutions applicable to low voltage distribution networks. The chapter then evaluates the effectiveness of the chosen technical solutions for a case study of Newcastle upon Tyne, UK, using solar irradiance data for the city and load profile data for the UK. The solutions are ranked based on their effectiveness for increasing PV penetration in residential distribution networks in the UK.

Chapter 8 – Conclusion and future work: Key conclusions of the research are presented in this chapter along with future work.

CHAPTER 2

LITERATURE REVIEW ON BARRIERS FOR HIGH PENETRATION OF PV

This chapter presents a review of the different barriers to increase the contribution of PV. The barriers can be broadly classified as technical, economic and policy-related barriers. As the focus of this research was on small-scale single-phase PV systems in distribution networks, the literature was critically analysed from the perspective of ratings of PV systems, voltage level, type of network and performance parameter(s) considered for the analysis. The gaps in literature were also identified.

2.1 Barriers to High Penetration of PV

The key barriers to high penetration of solar PV considered in literature can be broadly classified as:

- Technical
- Socio-Economic
- Policy-related

The technical barriers discussed in literature are voltage fluctuations, voltage flicker, voltage control, harmonic distortion in current and voltage, load and generation mismatch, fault current, unbalance, protection coordination, need for equipment upgrades, losses in the network, power system oscillations due to lack of inertia of the system and grid vulnerability. The location of PV systems is defined based on their relative distances from the substation transformer. Though barriers in terms of discriminatory interconnection requirements for distributed generation (DG) at remote locations and use of similar standards for a large-scale and small-scale

generation have also been discussed in [23] and [24], it has already been addressed by the community and are no longer considered as barriers. Lack of clear and reliable legal policy framework, the uncertainty of policy subsidies for competing fuels and unfavorable power pricing rules are the policy related barriers [23], [25]. High initial costs, the difficulty of fuel price risk assessment, liability insurance requirement and lack of access to credit are among the economic barriers discussed in the literature [20, 24]. A few social barriers like lack of public interest from repeated surveys/studies, lack of knowledge and limited permissions for construction at some sites were also discussed. The following sections discuss the barriers to high penetration of PV as identified in the literature and the gaps thereof. The literature pertaining to modeling of PV systems, steady-state performance assessment, dynamic-state performance assessment and solutions are discussed further at the beginning of the respective chapters.

2.1.1 Technical barriers

The voltage quality under steady-state conditions has been investigated in [26-33]. Different algorithms like forward-backward sweep method, modified Gauss-Seidel method and modified Newton-Raphson method and its variations for load flow analysis to evaluate the network parameters are typical approaches to evaluate the impact of PV on the steady-state performance of the distribution network, which in turn identifies the barriers.

Fitzer and Dillon analyzed a part of an actual network in the US representative of semi-urban and rural feeders with PV operating at 0.707, 0.866 and 1 p. f. lagging and concluded that presence of PV did not introduce overvoltage up to 30% PV penetration based on number of houses with PV of rating 5.5 kW [26]. The percentage was limited to 30% based on the market saturation values at that period. However, as the after diversity maximum demand of the network is not given, it is

not possible to convert this penetration level to the definition used in this thesis. Favuzza et al. monitored multiple PV systems with rated capacity ranging from 2.9 kW to 20 kW which were considered to operate at 10 to 100% of their rated capacity and concluded that these systems did not result in overvoltage at peak generation [27]. However, for the distribution network considered, authors mention that the maximum generation coincides with the maximum load which is different from the load profile pattern in the UK. Katiraei et al. analysed a network in Canada with PV connected near or far from the substation and observed that, at similar loading conditions, voltage rise was higher when the PV system was far from the substation [28]. The authors also demonstrated that this impact was higher when the base load of the feeder and/or household consumption in the PV neighbourhood is lower but do not evaluate at what penetration levels the presence of PV may adversely affect the performance of the distribution network. Load flow analysis of a part of the actual network in the UK was performed at 1-min intervals by Thomson and Infield, under different penetration levels of PV (0-50%) and they concluded that 50% penetration does not affect the steady-state-voltage for the network under consideration [29]. The authors used the definition of penetration based on the number of houses with individual PV system rating of 2.16 kW which translates to 76% penetration as per the definition in this thesis. However, the authors use mean voltage of the network calculated as the average of the voltage at all points at all time intervals of the day to evaluate overvoltage which may result in cancellation of overvoltage during noon hours against the under voltage at evening peak hours resulting in a overly optimistic result.

McDermott analysed a hypothetical medium voltage distribution network with large-scale DG at far end of the feeder and observed that the presence of PV/wind generators introduced temporary overvoltage [30]. However, the rating of wind/PV

DG was almost 5 times the connected load in the network considered which converts to more than 500% penetration as per the definition used in this thesis. Ali, Pearsall and Putrus analysed the steady-state-voltage under varying load and generation at 25%, 50% and 100% PV penetration using dynamic models in [31]. The authors use a penetration definition based on the number of houses with an individual PV rating of 3 kW and concluded that the voltage upper limit was violated at 100% penetration (230% penetration as per definition of this thesis) during the noon hours. Demirok analysed part of a Danish network with 100 houses with PV systems and concluded that, for a rural network, the voltage upper limit was not violated when 100% of transformer capacity was met by PV generation, whereas for suburban areas the voltage upper limit was violated at 60% [32]. Yan et al. analysed the impact of PV on the number of tap-changer movements and concluded that the number of movements increased with increasing penetration of PV [33]. The authors, however, also highlight that this could be solved using different options including static compensators.

Active power ramp rates for large PV power plants are discussed as a barrier in [34] and the authors concluded that with penetration levels as low as 4%, there arises a need for curtailment, i.e. reduction in the scheduled generation, if the distribution grid does not have the ability to export, thus reducing the plant capacity factor. Reverse power flow and increase in losses are discussed as barriers in [35]. The authors conclude that the network losses increase above the value of losses at no PV level when the penetration level is higher than 70%. Two distribution networks at 11 kV and 33 kV, representative of Malaysian distribution network, are analysed in [36] and the authors conclude that the network losses increase above the network losses at 0% PV penetration at 140% PV penetration for 11 kV distribution network and 108% at 33 kV. Though the authors of [35, 36] do not mention clearly their

definition of percentage penetration, it can be observed from their results that high losses occur after reverse power flow occurs. Therefore, losses are not discussed as a separate performance parameter in this research. Also, it is possible to minimize the network losses by optimally sizing or placing PV systems. However, at the distribution voltage level in the UK, the network operator has no control over the size and location as it is up to individual customers to install PV systems.

The impact of large-scale clustered PV systems on total harmonic distortion (THD) has been analysed in [27, 37-42]. Kotsopoulos et al. monitored three commercial PV inverters and observed zero crossing distortion in all of them [37]. The authors highlight that the distortion arises from the practical limits of pulse width modulation (PWM) technology and that, though complex topologies may result in better waveforms, it comes with an additional expense. The authors also conclude that the presence of multiple PV systems in parallel may result in harmonic limits being violated if there are background harmonics and low grid impedance. Nine commercial inverters were monitored and analysed by Favuzza et al. [27]. The authors observed that the THD of voltage in a network with PV was within a similar range as the network without PV. However, the current harmonics introduced by PV were different for different makes of inverters, with one of the inverters producing a current THD close to 8% at all output conditions. The authors conclude that the current THD may exceed the limit at the point of common coupling (PCC) if the grid impedance is low. Patsalides et al. measured the current THD of a15 kW PV plant in Cyprus and used the values to modify the PV model to incorporate harmonic currents based on actual measurements [38]. The authors then used the modified model to evaluate the impact of multiple PV systems on a 25 bus network and concluded that the voltage THD limit of 8% is not violated even after PV capacity reaches 24% of the transformer capacity. Fekete et al. analysed a part of an actual

network in Croatia with multiple 10 kW PV systems and concluded that the voltage THD limits were not violated in any of the scenarios, even when all the houses had PV [39]. However, current THD was in the range of 60-90% when the PV system was generating less than 20% of the rated power.

The impact of current THD on the voltage THD is dependent on the impedance of the network. Dartawan et al. evaluated the harmonic issues due to the presence of PV in a 12 kV distribution network with capacitor banks [40]. The authors concluded that the voltage THD acts a factor limiting the contribution of PV with the penetration limits being heavily dependent on the individual harmonics contributed by the PV system itself and the presence of other switching capacitors within the network. Pandi et al. used a decoupled harmonic load flow based approach to evaluate the voltage THD and concluded that voltage harmonics limited the PV contributed in only very few scenarios up to 100% PV penetration, though the authors do not clearly define the percentage penetration [41]. Oliveira et al. measured the voltage and current THD of three PV inverters at the inverter terminals and the PCC and also observed that the current THD was higher when PV was operating at less than 20% of its rated power [42].

Harmonic resonance has been discussed as a probable issue in [43-45]. Heskes et al. evaluated the performance of a 2 kW PV system and modelled the harmonics introduced, which were in turn used to evaluate the harmonics in a network with multiple PV systems [43]. Though the authors concluded that harmonic interaction or resonance may become a potential issue in the future at high penetration levels, they do not quantify the penetration level at which it may become an issue. Rangarajan et al. evaluated the impact of multiple PV on an IEEE 319/2007 based system and concluded that the resonance frequency due to the presence of PV moves closer to the fundamental frequency as the number of PV systems and shunt

capacitors in the network increases [44].The same authors also concluded that the current THD was greater than 8% due to the resonance [45]. Though THD is discussed as a factor limiting the contribution of PV, the results are heavily dependent on the network characteristics and the model of the PV system. Most literature uses measured harmonic contribution from a single PV system to evaluate the THD in multiple PV scenarios, which results in a worst-case scenario as, in a realistic scenario, there will be some distance between the inverters which may result in cancellation or phase changes to the harmonic currents. Another gap in the literature is that the networks considered are typically IEEE standard systems or hypothetical networks and not representative of a distribution network in the UK.

The issue of protection co-ordination being adversely affected by the presence of PV has been discussed in [22, 46-50].The impact of high solar PV penetration on the requirement for protection equipment at the 12 kV side in a typical distribution network in the US under different types of fault has been analysed in [22] with the conclusion that upgrades to the protection equipment may be required when PV generation meets 15% of energy usage on a transformer. A part of the 12 kV actual network in the US was analysed by Baran et al. in [46] and the authors concluded that the protection co-ordination and re-closer operating times were affected by the presence of PV systems, though not as heavily as for synchronous generators since inverters tripped almost immediately and the currents from PV were limited during fault. The authors also highlighted that the protection co-ordination becomes more complex as PV is not operational throughout the 24 hours. Azmi et al. analysed a part of an actual network in Norway using digSILENT and concluded that, at 100% penetration of PV (100% as per the definition of this thesis as the authors consider PV rating equal to the maximum demand of the network), the operating times of protection devices were adversely affected and that there is a need to ensure that

both PV and the protection devices operated as per standards [47]. Mourad and Mohamed analysed the IEEE 33 bus test system for the impact of PV on net fault current and concluded that the presence of PV did not significantly affect the net fault current when the PV capacity was almost equal to the total connected load (100% penetration as per the definition in this thesis) [48]. However, the authors assumed that the fault current contribution from PV inverters is around 110-120% of the rated current which is not correct as discussed in sections 4.2 and 4.4 A 10 kV hypothetical network during a fault is analysed in [49] and [50]. The authors concluded that the operation of overcurrent protection devices will be adversely affected at high penetration levels though they do not indicate how they define high penetration [49]. The performance of a hypothetical 4 bus distribution network under fault is analysed in [51] and the authors concluded that the presence of PV affects the performance of the over current relays during the connection and disconnection of PV. The authors also recommend introduction of low voltage ride through (LVRT) to improve the performance. However, the authors consider a simultaneous fault at 4 locations in the network which is very unlikely to occur in practical scenarios. The protection co-ordination issues highlighted in the literature above are at 12 kV and above, whereas residential PV systems are connected at 230 V. To generalise the impact at 12 kV to that at 230 V - is not feasible as the type of protection devices and ratings are different at this level. Also, with the discussions on fault ride through in single-phase PV systems, it is important that the impact of PV on protection devices at distribution levels (mainly fuses at 230 V and relays at primary of the 11/0.4 kV substation) is clearly understood.

The intermittent nature of PV generation in a large-scale PV power plant due to cloud transients has been modelled using a simplified dynamic model of a PV system [52]. The authors simulated the scenarios of cloud transients coupled with

generator trip and observed the variations in real power injection and deviations in the frequency of the grid over a time period of 60 seconds. They observed that, even with sufficient spinning reserves in the system, the grid may still require remedial actions, such as under frequency load shedding, due to the speed of the cloud transients. A steady-state study on the vulnerability of a transmission network with higher penetration of PV has been performed in [53] and the authors concluded that the grid became more vulnerable to planned attacks with an increase in PV penetration and that the attacks resulted in the spread of cascade failures to larger areas in the power grid. The authors demonstrated that the unpredictable fluctuations in generation were the reason for this increased spread of failures.

However, the literature mainly considers the steady-state performance and at higher voltage levels (11 kV and above) and disregards the effects of solar PV on residential distribution networks. Single-phase PV generators at lower voltages are aggregated to one single-phase PV generator in the dynamic model developed in [54], which may not hold true under higher penetration. The dynamic analysis made in [31] considers only the voltage variation under different penetration and insolation levels and does not consider the other performance parameters of the distribution network. Most of the literature discusses the impact during the worst-case scenario of minimum load and maximum irradiance or considers one typical worst-case day in summer to arrive at the maximum permissible penetration level. However, the probability of occurrence of such an event in the UK is very low, as will be discussed in chapter 4. Another gap in the literature is that most studies consider only one performance parameter at a time. However, the performance parameters are inter-linked and the penetration levels at which different performance parameters may be adversely affected are different. Also, a solution that may improve one performance parameter may adversely affect another performance parameter. These gaps

necessitate the re-evaluation of technical barriers for a residential distribution network in the UK considering both the steady and dynamic-state performances, distributed nature of single-phase PV systems and realistic worst-case scenarios.

2.1.2 Economic barriers

Beck and Martinot [23] and Kotsopoulos et al. [55] concluded that subsidies for conventional forms of energy distort the market unfairly and prevent customers from being fully invested in their electricity choices thereby impacting the penetration of RE. Fu concluded that curtailment of renewable energy generation connected to a transmission network when there is a possibility of a network overload introduced uncertainty in the amount of revenue that could be generated from that generating unit [56]. Such an uncertainty affects the growth of the renewable energy sector. Though this study is based on Germany and considers the transmission network, the uncertainty introduced by curtailment is equally applicable to the UK and the distribution network. The uncertainty in revenue becomes more relevant as the same amount of generation curtailed would reflect a greater percentage of the total generation due to the smaller total installed capacity in the distribution network.

2.1.3 Policy barriers

The energy policy of a country plays a significant role in enabling or increasing the contribution from renewables including solar PV. Improper design of guidelines and lack of proper planning/allocation of funds for promoting a renewable technology can also result in the companies going bankrupt as in Spain [57, 58]. The typical policy-related barriers discussed in the literature are lack of a stable market, administrative delays, uncertainty in revenue, lack of support mechanisms and lack of support for innovation and R&D [58-61]. The common policy interventions/mechanisms used across the world for promoting renewable energy are [58, 59, 61]:

1. Enhanced Feed-in Tariff (FiT)
2. Direct capital subsidies
3. Green electricity Schemes
4. Net metering
5. Net billing
6. Sustainable building requirements
7. Tradable Green Certificates/Renewable Energy Certificates (REC)
8. Bidding/tendering schemes
9. Low-interest loans
10. Quota systems
11. Clean Development Mechanism Joint Implementation

The planning and analysis of a policy intervention/support mechanism involves different stakeholders, including those who affect the support mechanism and those who are affected by the support mechanism. The stakeholders for renewable energy policy interventions typically considered in the literature are:

1. Investors
2. Government
3. Policy makers (typically elected representatives of the people)
4. Academic experts and researchers
5. Consultants
6. Society/community
7. Project developers/integrators
8. Industries
9. Renewable energy employees
10. Distributors of both renewable energy and conventional energy

11. Utilities – Distribution network operators (DNOs) and Transmission network operators (TNOs) in the UK
12. Local businesses

The effectiveness of existing policy has to be analysed to understand what aspects of the existing policy are acting as promoters/barriers to increasing the contribution of solar PV. The support mechanisms for RE in the UK existed as far back as 1995 but until 2003 the government had not favoured renewable specific policy resulting in less powerful renewable policies that lacked both clarity and agreement [62]. The Renewables Obligation (RO), increase in public support for R&D and capital grants for demonstration projects were initiated in April 2002 [63]. RO is an obligation on all licensed electricity suppliers in England and Wales to supply 3% of their electricity supplies from renewables in 2002-03 to 15.4% in 2015-16 increased in annual steps [64]. The percentage was planned to remain at that level until 2025-26. The electricity suppliers could comply with RO using

1. Renewable Obligation Certificates (ROCs) issued to qualifying renewable generators
2. Tradable ROCs available in the market
3. Buyout price of 3.0 p/kWh

But by the end of 2004, the renewable generation fell short of the target [65]. The incentives in place in the UK to encourage innovation in sustainable technologies including Solar PV are analysed in [66]. Mitchell and Connor point out that, in 2004, there were major demonstration projects in the pipeline which showed the commitment of the government toward renewables. The work was further extended in [67], where the policy changes introduced in 2003 were analysed. The analysis reveals that the buy-out price was too low to initiate innovation in renewable generation technologies like biomass, wave and Solar PV. Foxon and Pearson

concluded that the UK RE policy from 1990 to 2003 was lacking a clarity in goal which resulted in continuous adjustments of policy. The common support mechanisms, globally, for renewables, are financial subsidy (user subsidy, investment subsidy and product subsidy) and FiT [57]. In the FiT based support mechanism, the owner of a solar PV system is paid for each unit (kWh) of electricity generated by the system at a rate depending on the size and type of solar PV system.

A survey among venture capitalists (VCs) in North America and Europe was carried out to perform risk analysis from an investor perspective in [59]. Burer and Wustenhagen identify market pull strategies as being more preferred over technology push strategies. A FiT based support mechanism was found to be the most favourable policy among the VCs with the consistency of policy affecting their decision on investment. Risk analysis from an investor perspective on two support mechanisms, FiT and Quota obligation, was performed in [68]. Dinica emphasises that proper design and state of the market determines the success of a given support mechanism. Without administrative clarity, even well-designed policy can fail to achieve the targets [69]. The effect of three different support mechanisms, government grants, FiT and REC, on the net present value of hydroelectricity, wind and PV generation was analysed in [70]. The authors concluded that FiT was better for wind and solar systems whereas REC was better for hydroelectric plants. An analysis of the FiT based support mechanisms implemented in Denmark and Germany, the countries close to achieving their respective targets on renewable electricity contribution, was presented in [71]. Lipp also compares the UK's RO policy to FiT based policy and observed that RO did not provide the price and market security needed for increasing the investment. Characteristics that determine the effectiveness of an energy policy were set out and effectiveness of policies in EU

until 2004 was compared in [72]. Harmelink et al. observed that with the existing policy measures, the contribution of renewable electricity generation in the UK would reach only 4-4.5% against the target of 10% by 2010 [73]. The renewable electricity generation in the UK reached around 6.5% by end 2010, slightly higher than that predicted by Harmelink et al. but still short of the target [74]. Adding to existing uncertainties changes in RE policy were introduced in 2006 where exemptions to the Carbon Tax and changes to rules and eligibility criteria were made [75].

An analysis of UK's renewable energy policy since 1990, when privatization of energy industry was initiated, till 2009 was presented in [76]. Pollitt attributed the failure of energy policy to lack of societal preferences and acceptability rather than to lack of financial support mechanisms. Pollitt also condemned the over-ambitious targets set by the government and attributed the failure of the Non-Fossil Fuel Obligation (first policy initiative in the UK for RE) to the sudden drop in energy prices in the years 1999-2001. The details of ROC indicates that if the target was met there would be no need for trading of ROCs resulting in a drop in prices. The author suggests that the NFFO style mechanism with understandings from the initial failure as a better support mechanism than ROC. The author, however, failed to explain how the societal preferences like "not in my backyard" attitude of the residents, resistance from countryside towards large windfarms spoiling their natural beauty etc. resulted in the failure of the national policy as a whole. A similar analysis of UK RE policy until 2010 presented in [77] highlighted that the UK RE policy cannot be analysed in isolation from politics and changes in energy supply. Pearson and Watson observed that the priority of the government towards energy has not been persistent and though it seemed to be of high priority in the year 2010, it may not last for long.

The UK introduced a FiT based support mechanism for RE systems below 5 MW rating in 2010 [78]. The FiT for solar PV systems depended on the total rating of the system and smaller systems had higher tariffs paid. From 2010 to 2015 the tariff was reduced around 10 times and from 2015 to 2017 the tariff was renewed on a quarterly basis [78], resulting in loss of confidence among the investors and introducing lack of stability in the market and increasing the risks. Further to this the Department of Energy and Climate Change (DECC) was merged with the Department of Business and Industry, to be jointly known as the Department of Business, Energy and Industry Strategy. The move, along with the renewed interest in nuclear power plants, highlights that renewable energy may not be the first priority for the current government. Though this warrants a detailed analysis, it is not considered in this thesis.

2.2 Summary

This chapter discussed the literature on barriers to increasing the contribution of PV systems in the UK. The gaps in existing literature on identifying the technical barriers to increasing the contribution of PV systems in a distribution network in the UK has also been highlighted in this chapter. Chapters 5 and 6 provide a further literature review of steady and dynamic performance evaluation with PV. A discussion of existing solutions is included in chapter 7 along with a critical assessment of its applicability in the distribution networks in the UK. The next chapter discusses the regulations guiding the electricity distribution networks and PV systems in the UK.

CHAPTER 3

AN OVERVEW OF REGULATIONS FOR DISTRIBUTION NETWORK AND GRID CONNECTION OF PV SYSTEMS

Regulation in its most generic form represents a rule and can be explained to fit many different domains of knowledge. For this thesis, the term regulation is used in the domain of PV systems and control by government/authority. A regulation, in this context, is defined as a rule or a directive maintained by an authority in order to control the way a PV system is connected to and operated in the electricity network. The regulations are also needed to ensure the quality of the power supply to the customers of the electricity network. These guidelines on power quality are to be satisfied irrespective of the different loading or generation conditions. The regulations are used as guidance to reduce any negative impact of PV systems on the electricity network. The regulations for PV systems control the way the PV systems are installed and operated, the requirements for the existing building on which they are installed and the technical requirements of different parts of the PV system. However, no permission is required from the DNO for installation and operation of small-scale PV systems supplying less than or equal to 16 A per phase. There are also guidelines for ground-mounted PV installations [79] which are not discussed in this chapter as typical single-phase PV systems in distribution networks are roof mounted or mounted on existing buildings.

The installation guidelines for residential PV systems in the UK do not require any planning permissions from the local authority if the PV system installation meets the following criteria [80]

1. The PV system is not installed above the highest point of the property excluding the chimneys
2. A PV system installed on the roof does not significantly affect the external appearance of the property and surrounding area
3. The PV system does not project more than 200 mm from the surface of the roof.

This chapter discusses the technical standards and regulations for quality of supply and grid connection of PV systems in the UK and other parts of the world. The regulations pertaining to the UK are used to evaluate the steady and dynamic-state performance of the distribution network with PV (Chapters 5 and 6) and also to validate the generic PV system models (Chapter 4). The regulations pertaining to other countries are utilised in chapter 6 to discuss the impact of the presence of PV on distribution network when different regulations are adopted for the similar conditions described.

3.1 Technical Regulations in the UK

The technical requirements of PV systems installed in the UK are governed by BS EN 61727-1996, G83 (for small-scale embedded generators up to 16 A per phase) and G59 (for generators producing more than 16 A per phase but less than 50 kW). The standards for PV systems are set on the backdrop of the following standards for electrical systems in the UK:

- EN50160 (2010) – Voltage characteristics of electricity supplied by public electricity networks [81]
- P28 (1989) – Planning limits for voltage fluctuations caused by industrial, commercial and domestic equipment in the United Kingdom [82]

- P29 (1990) – Planning limits for voltage unbalance in the United Kingdom [83]
- G5/4 (2005) – Planning levels for harmonic voltage distortion and the connection of non-linear equipment to transmission systems and distribution networks in the United Kingdom [84]

British Standard EN 50160 guides the voltage characteristics of electricity distribution network in the UK under normal operating conditions [81]. Good power quality is necessary for proper functioning of consumer loads which in many scenarios draw current that is not sinusoidal in nature thus in turn affecting the power quality of the supply. The International Electrotechnical Commission (IEC) defines two different terminologies for voltage in the electricity network, viz. supply voltage and utility voltage. The term ‘supply voltage’ refers to the line-to-line or line-to-neutral voltage at the point of common coupling i.e. the main supplying point of installation which in most cases is the same as the metering point. The term ‘utility voltage’ refers to the line-to-line or line-to-neutral voltage at the plug or terminal of the electrical device. The standard EN50160 deals with the requirements for the supply voltage and categorises electricity networks as low voltage and medium voltage networks based on the supply voltage. An electricity network with phase to phase nominal RMS voltage less than or equal to 1000 volts is considered as a low voltage network and a network with phase to phase nominal RMS voltage between 1 kV and 35 kV as a medium voltage network. Table 3-1 provides the characteristics of a power supply at the supply side of the low voltage distribution network in the UK as per EN 50160.

Engineering recommendation P28 [82], issued in September 1989, provides the limits for voltage fluctuation caused by industrial, commercial and domestic equipment in the UK. The maximum change in magnitude of voltage is limited to 3%

Table 3-1: Supply voltage characteristics of low voltage distribution network in the UK as per EN 50160 [81]

No.	Parameter	Supply voltage characteristics
1	Power frequency	mean value of fundamental measured over 10 s: ±1% (49.5 – 50.5 Hz) for 99.5% of week; -6%/+4% (47 – 52 Hz) for 100% of the week
2	Voltage magnitude variations	±10% for 95% of week, mean 10 minutes RMS values
3	Rapid voltage changes	5% normal; 10% infrequently (measured as single rapid variation of the r.m.s. value of a voltage between two consecutive levels which are sustained for definite but unspecified durations)
4	Supply voltage dip	Majority: duration <1s, depth <60%. Locally limited dips caused by load switching on: 10 - 50%,
5	Short interruptions of supply voltage	(up to 3 minutes) few tens - few hundreds/year Duration 70% of them < 1 s
6	Long interruption of supply voltage	(longer than 3 minutes) <10 - 50/year
7	Temporary, power frequency overvoltage	1.5 kV rms
8	Transient overvoltages	generally < 6kV, occasionally higher; rise time: ms – µs
9	Supply voltage Unbalance	up to 2% for 95% of week, mean 10 minutes RMS values, up to 3% in some locations

irrespective of the shape of change as per P28. Engineering recommendation P29 [83], issued in 1990, provides the planning limits for the voltage unbalance in the UK. The standard limits the voltage unbalance in the LV network to 2% when assessed over any one minute period and the voltage unbalance at point of common coupling should not exceed 1.3% for systems with nominal voltage less than 33 kV and 1% for systems between 33 kV and 132 kV. Engineering recommendation G5/4-1 [84] provides planning levels for harmonic voltage distortion and the connection of non-linear equipment to transmission systems and distribution networks in the UK. The summary of THD limits at different levels of voltages are as given in Table 3-2. Planning levels for harmonic voltages in 400 V systems are as given in Table 3-3.

BS EN 61727-1996 [85] governs the quality of power provided by the PV systems for the utility interface and is the same as the IEC standard IEC1727-1995. The quality of power supply is defined in terms of voltage, flicker, frequency, harmonics and power factor. The standard specifies that

- “The PV system voltage shall be compatible with the utility voltage.”
- “The operation of the PV system should not result in voltage flicker more than allowable limits.”
- “The operation of PV system should not result in excessive distortion of the utility voltage waveform or result in excessive current harmonic injections into the electricity network. Design targets limit the total current harmonics to 5% of the rated peak current of the system and to 2% of the rated peak voltage of the system.”
- “The power factor of the system should have average value greater than 0.85 lagging at the rated conditions or other values of power factor as stipulated by local codes or network operators.”

Table 3-2: THD limits at different voltage levels [84]

System voltage at the PCC	THD limit
400 V	5%
6.6, 11 and 20 kV	4%
22 kV to 400 kV	3%

Table 3-3: Planning levels for harmonic voltages in 400 V systems [81]

Odd harmonics		Even harmonics	
Harmonic order	Relative voltage (%)	Harmonic order	Relative voltage (%)
3	5	2	2
5	6	4	1
7	5	6 to 24	0.5
9	1.5		
11	3.5		
13	3		
15	0.5		
17	2		
19	1.5		
21	0.5		
23	1.5		
25	1.5		

The standard also specifies the following with regard to the protection of the equipment and personnel:

- "The PV system should disconnect from a de-energised distribution line irrespective of the connected loads or other generators within the time limits specified by the local codes."
- "The PV system should disconnect for over/under voltage."
- "The PV system should disconnect for over/under frequency."
- "Following the disconnection of the PV system under any of the conditions, the system shall remain disconnected until the utility service has recovered to within the acceptable limits, typically 30 s to 3 minutes."
- "The PV system shall not inject any DC into the AC or any AC into the DC interface under any conditions."
- "The PV system shall have surge protection as per IEC 1173. IEC 1173 suggests usage of different methods including equi-potentialisation (interconnection with low impedance paths), grounding, shielding, stroke interception and protective devices like diodes, varistors, spark gap devices etc. to provide surge protection."
- "The PV system shall have short circuit protection for the utility grid in accordance with the local and national codes."

As this research focusses on PV systems connected to the low voltage distribution network and with power ratings less than 4 kW, EREC G-83/2 (Recommendations for the Connection of Type Tested Small-scale Embedded Generators (Up to 16A per Phase) in Parallel with Low-Voltage Distribution Systems) [86] is discussed in detail. The guidelines for the PV system interface protection are as given in Table *3-4*. The EREC G83 also recommends that the small-scale embedded

Table 3-4: Protection settings for small-scale generators [86]

Protection Function	Trip setting	Trip delay setting (time)
Under voltage stage 1	$V_{ph\text{-}n}$ – 13% = 200.1 V	2.5 s
Under voltage stage 2	$V_{ph\text{-}n}$ – 20% = 184 V	0.5 s
Over-voltage stage 1	$V_{ph\text{-}n}$ + 14% = 262.2 V	1.0 s
Over-voltage stage 2	$V_{ph\text{-}n}$ + 19% = 273.7 V	0.5 s
Under frequency stage 1	47.5 Hz	20 s
Under frequency stage 2	47 Hz	0.5 s
Over frequency stage 1	51.5 Hz	90 s
Over frequency stage 2	52 Hz	0.5 s
Loss of mains (Vector shift)	12 degrees	0.0 s
Loss of mains (Rate of change of frequency method)	0.2 Hz per second	0.0 s
Loss of main (other methods)		< 1 s

generator should stay disconnected for a minimum of 20 s after the voltage and frequency return to within the limits of Table 3-1. The harmonics of the generator are regulated by the standard EN 61000-3-2 and the limits are as given in Table *3-5* [87]. The standard also stipulates that the DC current injected by the small-scale embedded generator should be less than 0.25% of the AC current rating per phase. In the case of a single generator less than 2 kW, the DC current should be less than 20 mA, the standard necessitates that the small-scale embedded generator should operate between 0.95 lagging and 0.95 leading relative to the voltage waveform unless otherwise agreed with the distribution network operator.

3.2 Technical Regulations in Other Countries

This section explains the regulations for quality of electric supply and grid connection of PV systems in Australia, Germany and the USA, where the contribution of renewable energy in the electricity network has increased significantly in the last decade. The regulations discussed here are utilised in Chapter 6 to discuss the impact of the presence of PV on distribution network when different regulations are adopted for the similar conditions described. The summary of regulations is as given in Table 3-6 and Table 3-7 [88, 89]. Table 3-7 also provides the changes to the regulations that are currently under discussion among the network operators and experts in the respective countries. Further details of regulations in different countries are discussed in [88]. The regulations guiding disconnection of the PV inverters for different voltage and frequency variations as per the standards for Europe (IEC 61727), the USA (IEEE 1547) and Germany (VDE 0126-1-1) are given in Table 3-8.

Table 3-5: Harmonic limits as provided by EN 61000-3-2 [87]

Harmonic order	Maximum permissible harmonic current (Amps)	Harmonic order	Maximum permissible harmonic current (Amps)
2	1.08	21	0.107
3	2.3	22	0.084
4	0.43	23	0.098
5	1.14	24	0.077
6	0.3	25	0.09
7	0.77	26	0.071
8	0.23	27	0.083
9	0.4	28	0.066
10	0.184	29	0.078
11	0.33	30	0.061
12	0.153	31	0.073
13	0.21	32	0.058
14	0.131	33	0.068
15	0.15	34	0.054
16	0.115	35	0.064
17	0.132	36	0.051
18	0.102	37	0.061
19	0.118	38	0.048
20	0.092	39	0.058
		40	0.046

Table 3-6: Technical regulations guiding power quality of electricity networks in Australia, Germany and the USA

Country		Australia	Germany	USA
Standard for steady-state limits at LV		AS61000.3.100	EN50160	ANSI C84.1
	Nominal voltage	230 V (line to neutral)	400 V (line to line)	120 V (line to neutral); 240 V (line to line)
	Maximum allowable voltage	253 V	440 V	126; 252
	Minimum allowable voltage	216 V	360 V	114; 228
	Nominal frequency	50 Hz	50 Hz	60 Hz
	Maximum allowable frequency	varies from 50.25 to 52 Hz depending on the operator	50.5 Hz	60.5 Hz
	Minimum allowable frequency	varies from 47 to 49.25 Hz depending on the operator	49.5 Hz	59.3 Hz

Table 3-7: Technical regulations guiding grid connection of PV systems in Australia, Germany and the USA

Standard for grid connection of PV		AS4777 (Australia)	VDE 0126 -1-1 (Germany)	IEEE 1547 (USA)
	Power factor range	0.8 leading to 0.95 lagging	0.95 lagging/leading	NA
	THD	<5%	<8%	< 5%
	DC current injection limit	0.5% of rated output current or 5 mA, whichever is greater	<1 A; trip time 0.2 s	<0.5% of rated RMS current
	Frequency range of operation	45 – 55 Hz	47.5 – 50.2 Hz	60.5 – 59.3 Hz
	Voltage range of operation	200 – 270 V; Single-phase	85 – 110%	88 – 110%
	Anti-Islanding protection	Must	Must	Must
	Reconnection delay	1 minute	Does not mention	none
	Active and reactive power control	Active communication channel to control output power for systems greater than 5 kW	For <30 kW remote control interface or permanent reduction of active power	Remote curtailment communication by some utilities/network operators
Future changes		Addition of PV systems to standard AS4577, that regulates the demand side management	Intelligent demand side management and information network accessible by relevant stakeholders	LVRT; active voltage regulation

Table 3-8: Comparison of disconnection times as per different standards of PV connection to the grid

Standard	Voltage range (%)	Disconnection time (s)	Frequency range	Disconnection time (s)	Anti-islanding trip time (s)
IEC 61727 (Europe)	V < 50	0.1	51 < f < 49	0.2	2
	50 ≤ V < 85	2			
	110 < v<135	2			
	V ≥ 135	0.05			
IEEE 1547 (USA)	V < 50	0.16	60.5 < f < 59.3	0.16	2
	50 ≤ V < 88	2			
	110 < v<120	1			
	V ≥ 120	0.16			
VDE 0126-1-1 (Germany)	110 ≤ V < 85	0.2	50.2 < f <47.5	0.2	5

3.3 Summary

This chapter provides analysis of regulations that guide the power quality of supply in the UK and the regulations that guide the connection of small-scale embedded generators (including residential PV systems) to low voltage distribution networks in the UK. The power quality is defined in terms of permissible voltage range, permissible frequency range, total voltage harmonics, voltage unbalance and voltage flicker. The guidelines for grid connection regulate the power factor range of the output power of the PV system, limits the total current harmonics and the DC current introduced by the PV system into the distribution network. The regulations also provide maximum delay times for the tripping of the interface (PV inverter) under abnormal conditions and the reconnection delay after the normal conditions of the distribution network are restored. The chapter also discusses the regulations controlling the quality of supply and grid interfacing of small-scale generators to the distribution network in Australia, Germany and the USA.

The regulations guiding the power quality and grid connection of PV systems are used to analyse the steady and dynamic-state performance of distribution network with PV in this research. Discussions are also included in respective sections where a different regulation, other than that in the UK, would affect the conclusions of the analysis. The next chapter provides the details of the developed generic model of the PV system and the distribution network.

CHAPTER 4

DYNAMIC MODEL OF THE PV SYSTEM AND THE DISTRIBUTION NETWORK

As discussed in chapters 1 and 2, in order to identify the technical barriers limiting the contribution of PV systems in the distribution network it is important to understand the impact of small-scale PV systems on that network. The presence of PV systems can affect both the steady and dynamic- state performance of the distribution network. Hence it is essential that the model used is capable of replicating the performance of a real PV system and the distribution network under both these states. Research conducted by the CIGRE/CIRED Joint Working Group (JWG) C4/C6.35 on international industry practice on modelling and dynamic performance of inverter based generation in power systems analysis highlighted the lack of a generic model of inverter based generators for use in power system studies, resulting in the use of a negative load model [90]. The report also highlighted that there was currently no aggregation rules for multiple PV systems connected to the same distribution grid. Also, as different control strategies are available to convert the DC generated by PV into controlled AC current/voltage synchronised with the grid waveforms, the models available were currently dependent on the manufacturer to provide the technical details of the control methodology. The report also points out that there may be discrepancies in the model provided by the inverter manufacturer, as they may not want to completely disclose their control strategy, which provides competitive advantage to that company.

Addressing this gap, this research develops a generic model of a single-phase PV system in MATLAB Simulink, with power ratings ranging from 1 kW to 4 kW, suitable

for power system dynamic studies. The range of power has been chosen based on the statistics that more than 80% of PV systems installed in the UK have a power rating less than or equal to 4 kW [15]. The model of the inverter is capable of demonstrating its performance for faults at different locations of the network. Another feature of the model is the over/under voltage protection strategy as per G-83 guidelines, which have not been addressed in previous literature on inverter control strategy of the inverter. The inverter model uses two-stage, time-delayed tripping in accordance with the guidelines. The magnitude of the voltage at which it should trip and the time delay can be controlled separately by varying the inputs to the model. The inverter model also has provision to change the reactive power supplied by the inverter, which is a service expected from the PV inverter in the future. The inverter model does not pertain to any single manufacturer and is therefore validated against PV inverter standards. The results of performance under faults are validated against experimental results of the performance of a 1 kW PV inverter for a fault at its terminals.

A dynamic model of a distribution network representative of the UK distribution network and its load was also developed in MATLAB/Simulink to evaluate the performance of the distribution network with PV. A three-phase PV inverter model from the MATLAB/Simulink library file was modified to be used with the lumped load to analyse the impact of PV on transients. Appendix A provides the validation of the three-phase inverter model for different ratings of PV system used to replicate different penetration levels of PV.

This chapter starts with the introduction to sunlight and its specification, which is the input for the PV system model. This is followed by a discussion of the PV system model, distribution network model and load model. The state of the art of different models is also discussed in the respective sections.

4.1 Solar Irradiance

The solar irradiance is the measure of the power density of sunlight and is usually measured in W/m^2[91]. The solar irradiance at the outer edge of the Earth's atmosphere, also referred as extra-terrestrial irradiance, is 1367 W/m^2 [91]. As sunlight enters the Earth's atmosphere, some of it is absorbed, some of it is scattered and some passes through unaffected and is absorbed or reflected by objects at ground level. The amount of sunlight absorbed or scattered depends on the length of the path through the atmosphere and the atmospheric conditions (pollution, aerosols, water vapour etc.). The vertical path directly to sea level is referred to as Air Mass 1 (AM1) and is used to compare other distances traveled by sunlight in the atmosphere. At AM1, after absorption has been accounted for the irradiance is generally reduced from 1367 W/m^2 to just over 1000 W/m^2 at sea level [91]. The AM1.5 spectrum, based on specific atmospheric conditions as well as the AM1.5 path length, is accepted as the standard calibration spectrum for PV cells. At a given time or for a given day, irradiance depends on location, weather conditions and time of year.

4.2 Solar Photovoltaic Systems

A solar PV system can be broadly classified as a grid-connected system or stand-alone system. The output of a solar PV array is DC and is usually converted to AC as the electrical appliances widely used require AC voltage. To get maximum possible power from the PV array, some form of maximum power point tracking (MPPT) is used in all types of PV systems. A grid-connected solar PV system consists of two main blocks – solar array and DC/AC inverter with MPPT. Figure 4-1 shows a typical grid-connected PV system without battery back-up. A stand-alone system has two additional blocks - battery bank and DC/DC charge controller.

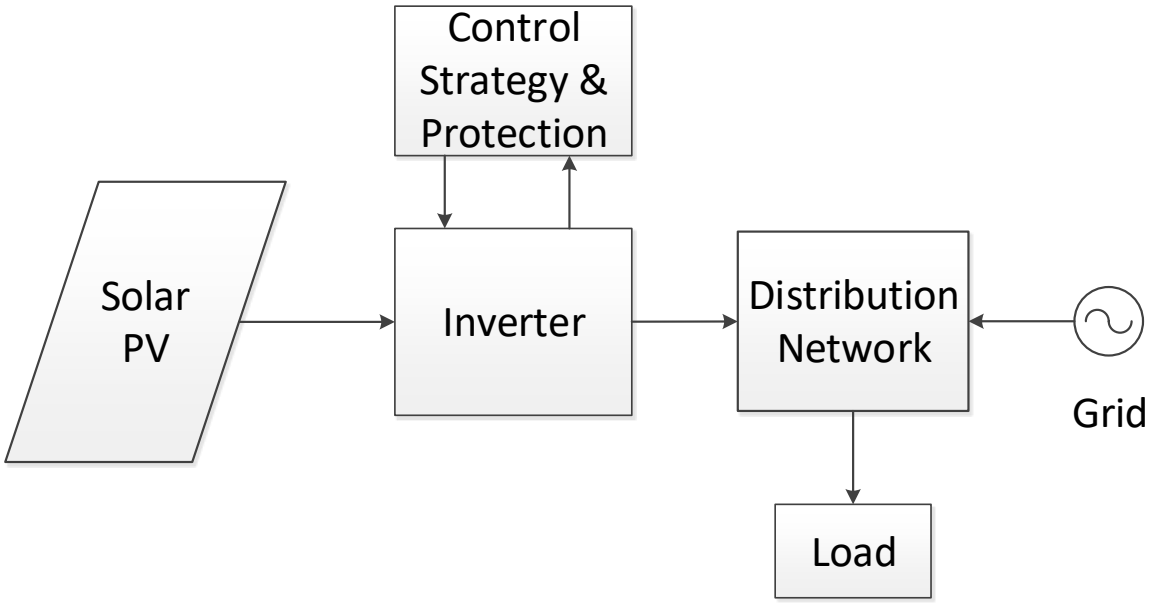

Figure 4-1: Grid-connected PV System without Battery Backup

A hybrid system has the same blocks as a stand-alone system but with an additional source (which may be renewable based or non-renewable based) and a utility switch for supplying power to the grid when there is excess generation and the battery bank is full. Since most of the systems currently prevailing in the UK are grid-connected, the rest of the chapter focuses on a grid-connected system.

4.2.1 Dynamic modelling of PV arrays

Solar cells or photovoltaic (PV) cells are semiconductor p-n junctions that convert sunlight into electricity directly. The energy of visible light excites the electrons in the PV cell to a higher energy state and these electrons then dissipate the energy through an external circuit. The simplified model of PV cell is as shown in Figure 4-2(a). However, the PV cell is not an ideal current source and has both series and shunt resistances to account for the internal losses. The model inclusive of these is as shown in Figure 4-2(b).

As a typical PV cell produces less than 5 W at around 0.5 V, cells are connected in series-parallel combination to produce higher power. The series-parallel

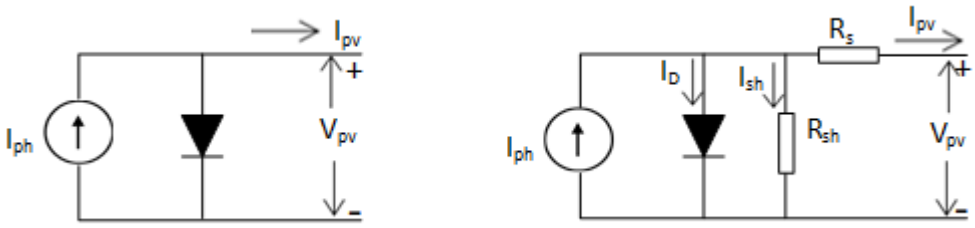

(a) Simplified model (b) Detailed model

Figure 4-2: Model of PV system

combination of cells is encapsulated in an environmentally protective laminate, called a PV module, to prevent damage from exposure to outdoor conditions. A PV array is a set of PV modules connected in series and/or parallel to generate more power than can be achieved from a single module [91]. To model a PV cell, it is important to understand its terminal properties described by the I-V curve. The amount of current and voltage available from the PV cell is dependent on the PV cell illumination level (or irradiance) and PV cell temperature. Figure 4-3 shows the I-V characteristics and P-V characteristics of a typical PV cell. As shown in Figure 4-3(b), the maximum power point (MPP) is the point at which the solar cell produces the maximum power. The corresponding current and voltage are I_{mp} and V_{mp} respectively. In the ideal scenario, the I-V characteristic is defined by the equation

$$I_{pv} = I_{ph} - I_o\left(e^{\frac{qV}{kT}} - 1\right) = I_{ph} - I_D \qquad (4\text{-}1)$$

where I_{ph} is the component of cell current due to photons, I_o is the reverse saturation current of the diode, $q = 1.6 * 10^{-19}C$ is the magnitude of charge of an electron, $k = 1.38 * 10^{-23}J/K$ is the Boltzmann constant, V is the voltage across the cell, T is the

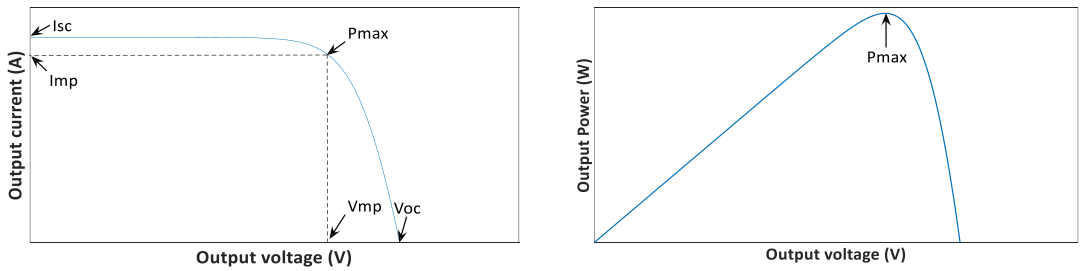

(a) I-V characteristics (b) P-V characteristics

Figure 4-3: Characteristics of a typical solar cell

cell temperature in K and I_D is the diode current. Details of the PV array parameters and the MATLAB/Simulink block are given in Appendix A.

4.2.2 Grid connected inverters

The output of a PV array is DC and changes in magnitude depending on the magnitude of irradiance falling on the array. As described in section 4.1, the grid-connected PV system comprises two major blocks viz. PV modules and DC-AC converter. The DC-AC converter/inverter of the grid-connected system has the following major tasks

1. to ensure that maximum power is generated and transferred from the solar PV array to the grid
2. to generate output voltage and current waveforms that are as sinusoidal as possible whilst ensuring the voltage is synchronised with the grid voltage (grid synchronisation)
3. to disconnect from the grid in the event of a fault in the grid (anti-islanding property of the inverter)
4. to monitor the output and to provide options to transmit/save the information.

Inverter sizing

In order to model the inverter, the nominal rating of the inverter for the corresponding array size has to be determined. The chosen size of the inverter is dependent on the size of the PV system to which it is connected. The optimal sizing of the PV inverter is important to ensure minimum losses. The UK installation guideline [92] gives the ratio of the size of the PV array to the size of the inverter to be in the region between 1.1 to 0.8. Inverters may be undersized for the following reasons:

a. PV modules operate for much of the time below the nominal rated power. Nominal rated power is the output of the module under standard test

conditions (STC) - a condition reached relatively infrequently in the UK as the temperature does not remain at 25 ºC when irradiance is 1000 W/m^2.

b. Following on from the above, inverters will spend much of their time operating at power levels below the nominal array rating.
c. Inverter efficiency reduces drastically when the output power is less than 15% of its rated power (Figure 4-4). By a degree of inverter under-sizing, it is possible to take the normal operating regime higher up the efficiency curve and hence decrease inverter losses at times of normal irradiance levels.
d. Module/array output decreases over the lifetime of the PV system.
e. Inverter cost/watt – cost of the inverter is proportional to the rating of the inverter.

Inverters may be oversized for the following reasons:

a. Limited inverter selection
b. A system with an inverter smaller than the array will on occasions of high irradiance have the output clipped – the inverter will simply not be able to deliver all the available power to the grid
c. May increase inverter life by preventing overloading of components during peak generation

A typical inverter efficiency curve is as shown in Figure 4-4 [93]. From 15% of its rated capacity, the efficiency is above 95%, with maximum efficiency being achieved at a range of 20-40% of rated capacity. The losses are generally constant throughout the operational range of the inverter, however the percentage compared to the output increases as the net output of the inverter decreases, resulting in lower efficiency levels at lower output levels Grid-connected inverters currently operate at unity power factor. Performance of PV inverter with undersized and oversized PV inverters for irradiance and temperature profiles of Denmark and Arizona were

analysed in [94]. The authors concluded that the lifetime of PV inverters with oversized PV array decrease significantly compared to PV array size equal to the rating of PV inverter whereas for Arizona it did not result in significant decrease of lifetime of the inverter. Given the reasons for under sizing and oversizing of inverters, and UK irradiance profile being closer to that of Denmark than Arizona, inverter rating of the same rating as array rating is chosen for this study to ensure

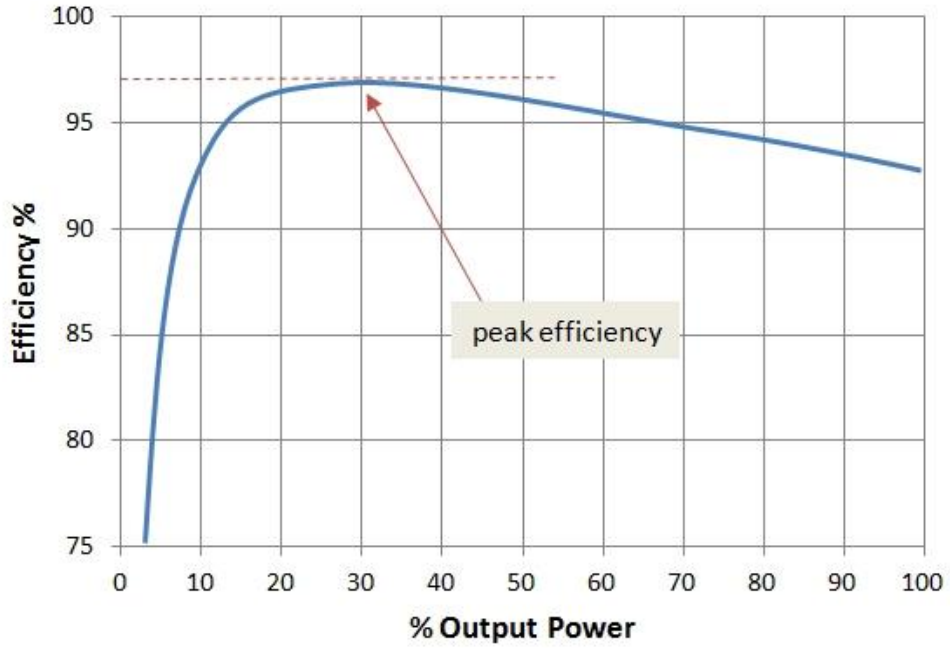

Figure 4-4: Inverter efficiency curve [74]

maximum efficiency for a maximum duration. This also provides opportunities to use the inverter for ancillary services which are evaluated in the later sections of the thesis.

Inverter topology and controls

The PV inverter may use a one or two-stage topology. Single stage topology is currently being favoured in research and is mainly suitable for higher DC input voltages. For the range of ratings considered in this research (PV systems less than or equal to 4 kW), the DC input voltage obtained by connecting modules in series may not be sufficient to maintain a desired DC-link voltage. Therefore, a two-stage topology is used in this research, where the first stage boosts the DC voltage of PV and then a DC/AC inverter is used to produce a 230 V RMS sinusoidal voltage.

According to the type of DC input, these topologies can be considered as voltage source inverters (VSIs), where the DC voltage is constant or as a current source inverter, where the DC current is constant [95]. Single-phase voltage source inverters can be found in half-bridge (Figure 4-5) and full-bridge or H-bridge (Figure 4-6) configurations. Different H-bridge configurations discussed in the literature [89, 91] are:

a. H5, classical bridge with an extra switch in the positive bus of the DC link
b. HERIC (Highly efficient and reliable inverter concept) which has a bypass leg on the AC side
c. REFU inverter which has half bridge configuration with AC side and DC-DC converter side bypass
d. Full bridge with DC bypass
e. Full bridge with zero voltage rectifier

Surveys on commercial inverter topologies [89, 96], highlight that H-bridge is a common topology and that most of the low power commercial inverters do not use an isolation transformer. As the focus of the research is on developing a generic

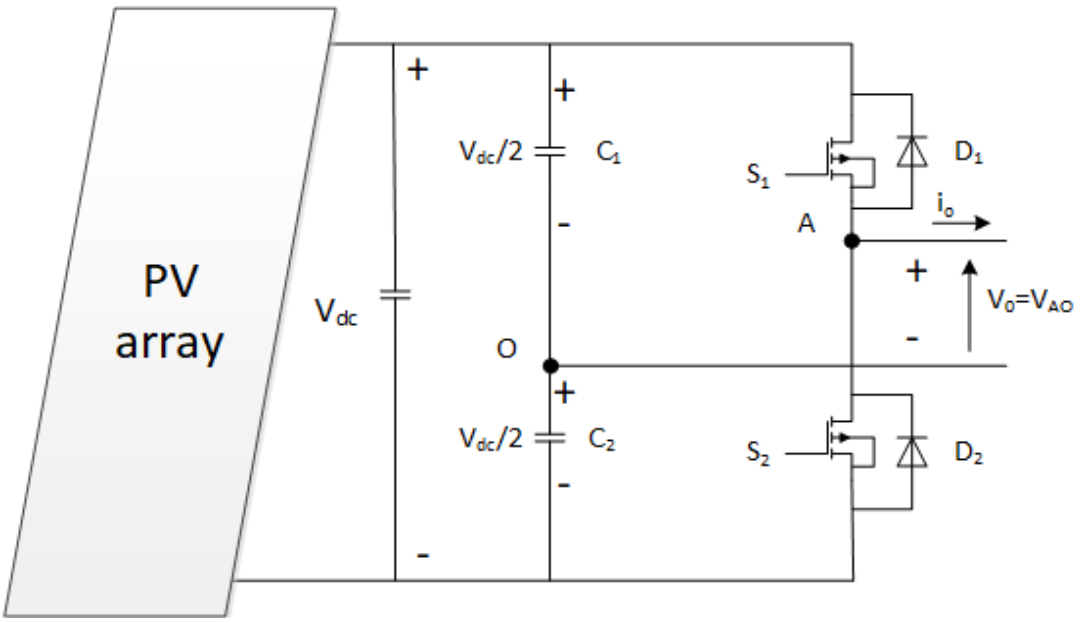

Figure 4-5: Half-bridge topology of a single-phase inverter

model of an inverter, rather than a model specific to a particular make or manufacturer, a common topology and control strategy is chosen.

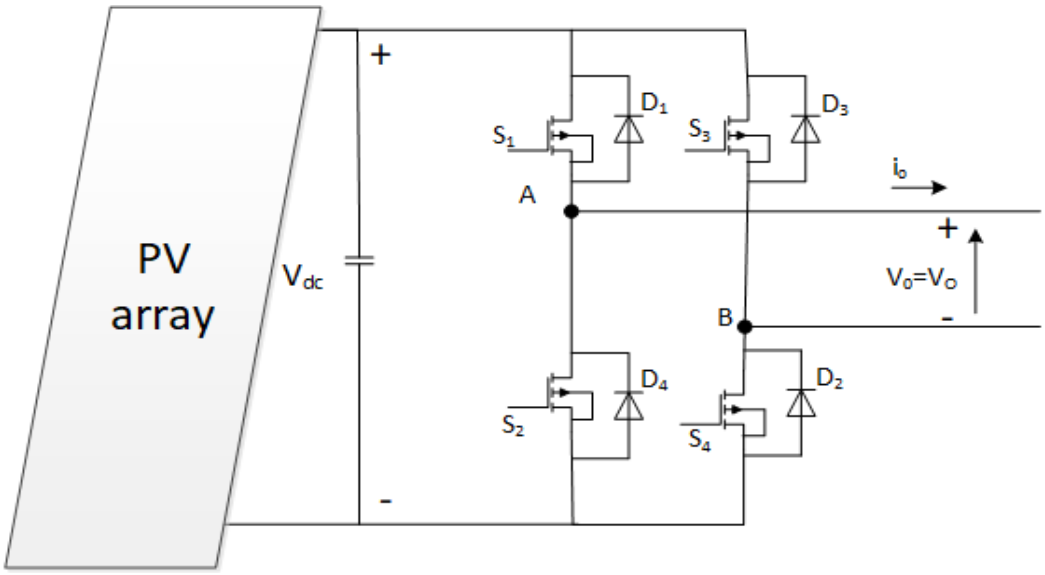

Figure 4-6: Full-bridge inverter topology of single-phase inverter

The most common and popular technique for generating a true sine wave output is Pulse Width Modulation (PWM) [97]. There are 3 basic PWM techniques – single PWM, multiple PWM and sinusoidal PWM (SPWM) for control of the inverter. There are three main modulation strategies, viz. bipolar, unipolar and hybrid modulation. In the case of bipolar modulation, the switches are switched in diagonal whereas, in unipolar modulation, each leg of the H-bridge is switched according to its own reference. In hybrid modulation, one leg is switched at grid frequency and one leg at high frequency. The MATLAB Simulink block for the PWM generator provides the options for unipolar and bipolar switching. The model developed uses bipolar modulation as it produces reduced levels of low order harmonics [98]. The output voltage of a PWM inverter is not purely sinusoidal and a filter is required to smoothen the waveform. The DC-link voltage should be greater than the peak AC voltage (325 V for 230 V RMS sine wave) plus the voltage drop across the inverter and the AC filter. Hence the DC-link voltage is chosen as 425 V and the DC-DC boost stage

provides a constant 425 V from the variable output voltage of the PV array. The detailed block diagram of the PV inverter is shown in Figure 4-7.

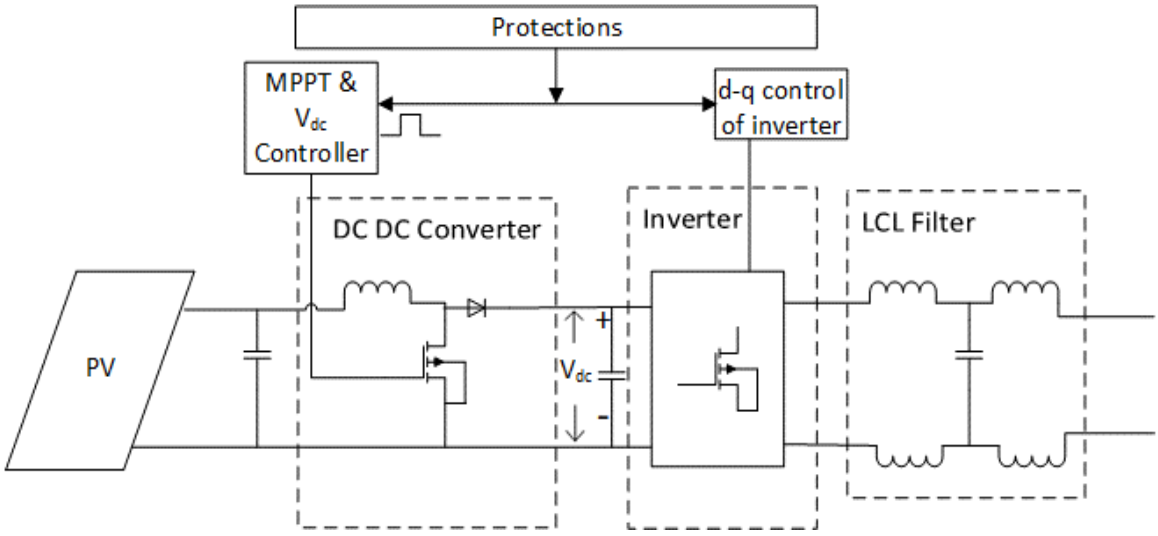

Figure 4-7: Detailed block diagram of PV system

4.2.3 DC/DC boost converter

As the DC voltage from the PV array is less than 425 V and also varying with irradiance, a DC/DC boost converter is used to increase the voltage and to maintain the DC-link voltage close to 425 V. Changes in irradiance affect the PV current significantly more than the PV voltage, i.e. the range of values across which the current varies is much higher than the range of variation of voltage for the same change in irradiance as shown in Figure 4-8. Control for such current variations would require fast dynamics and might lead to controller saturation [99, 100]. Hence, a voltage control based DC/DC converter was modelled in this research. A capacitor was added to the input in order to achieve a voltage source topology. The DC/DC converter not only performs the voltage boost but also the maximum power point tracking (MPPT) i.e. adjusts the operating point of the PV array so that maximum possible power at that instance is transferred to the grid.

MPPT of solar PV system

Many MPPT techniques have been discussed in the literature, and these vary in many aspects including simplicity, convergence speed, hardware implementation,

sensors required, cost, the range of effectiveness and need for parameterization. The most widely used MPPT techniques are [101]:

1. The Perturb and Observe (P&O) and its variants
2. Incremental Conductance (IC) methods and its variants

Comparison of different MPPT techniques under different types of irradiance variations for a period of 0.5 s was performed in [101] and the authors observed that energy extracted from the array is maximum for the IC based method followed by the P&O based method. The authors also compared the techniques in terms of the cost of the system and evaluated IC and P&O based methods to be of low/medium cost. The analysis performed in [102] compared the energy generated from solar for different tracking techniques and observed that, for step variation of irradiance, a modified P&O method provides better tracking than the IC based method but with both being better than constant voltage, open voltage and short circuit current based techniques. In the modified P&O based method used above, increment/decrement of voltage is dependent on the rate of change of power with voltage instead of a

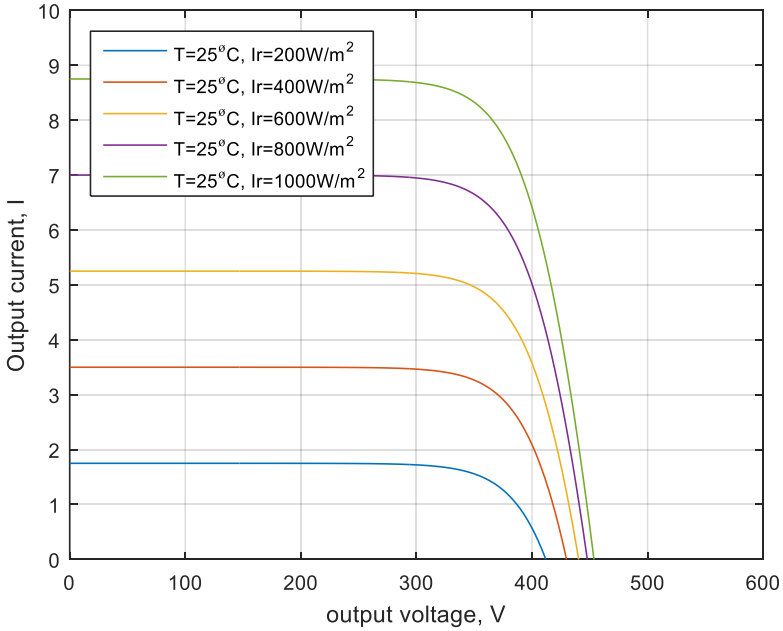

Figure 4-8: I-V characteristics of a 2.5 kWp PV array at different irradiance levels

constant value. Based on these observations and the ease of implementation, the P&O based MPPT technique was chosen for the proposed generic model.

P&O algorithms operate by periodically perturbing (i.e. incrementing or decrementing) the array terminal voltage or current and comparing the PV output power with that of the previous perturbation cycle. If the PV array operating voltage changes and the power increases, the control system moves the PV array operating point in that direction; otherwise the operating point is moved in the opposite direction. In the next perturbation cycle, the algorithm is repeated to identify the direction of change of power and suitably move the operating point. Figure 4-9 gives the flowchart of the P&O based method [102]. A common problem in P&O algorithms is that the array terminal voltage is perturbed every MPPT cycle; therefore when the MPP is reached, the output power oscillates around the maximum, resulting in power loss in the PV system. This is especially true in constant or slowly-varying atmospheric conditions. Another problem with the P&O algorithm is that the operating point may rest in local maxima instead of the global maximum. The model of P&O based MPPT has been implemented using the code and the details of the code for the MPPT model is provided in appendix B.

4.2.4 DC/AC converter (inverter)

The second stage of the PV inverter generates a variable magnitude AC waveform from the constant DC voltage produced by the DC/DC converter. The output voltage waveform should be synchronised with that available at the point of connection to the grid. Grid-connected PV inverters can be either voltage controlled or current controlled and they supply power to the local load and the grid. An appropriate controller is required to ensure that there are no errors in synchronisation with the grid, as the error can result in damage of the inverter. Current controlled inverters provide peak-current protection, overload rejection and higher-accuracy control than the voltage controlled inverters [103]. Therefore, current controlled inverters are

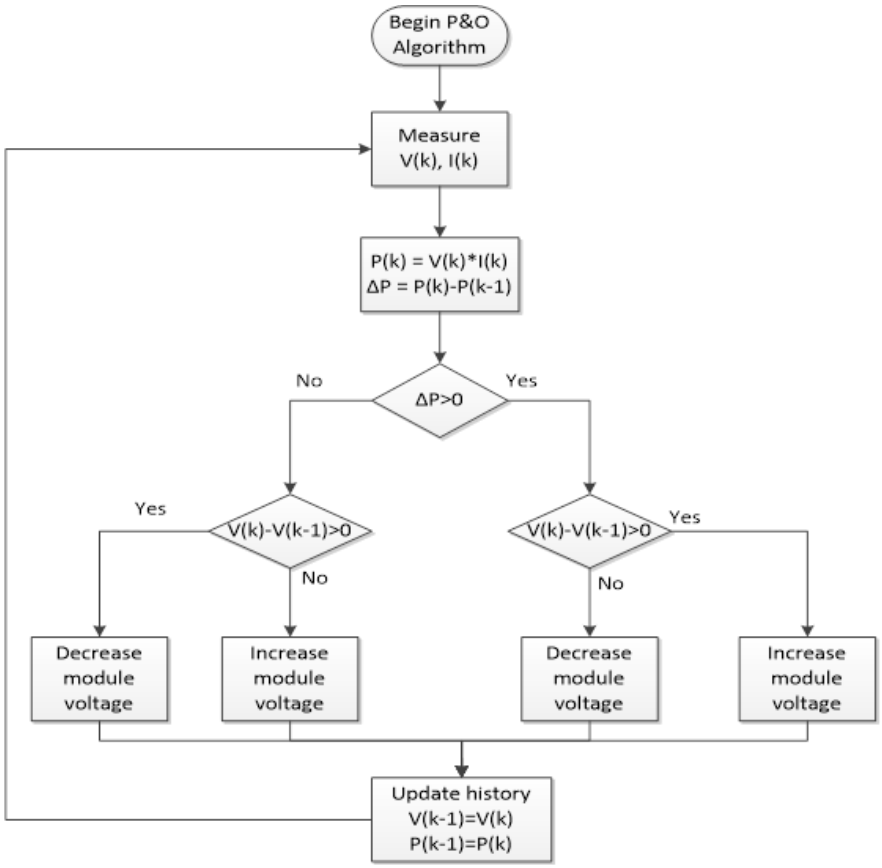

Figure 4-9: P&O Algorithm for MPPT [82]

more suited for grid-connected inverters. Grid synchronisation can be performed using phase locked loop (PLL) or non-PLL (Fourier based) methods.

The PLL based method has been chosen for the generic model, due to the ease of use and availability of a built-in block in MATLAB Simulink (see Appendix B). PLL is a closed-loop system, with a phase detector, a proportional-integral-derivative (PID) controller, an internal oscillator and a low pass filter, that controls the phase of the external sinusoidal signal by using the feedback loop as shown in Figure 4-10. Also, the load conditions usually change and the AC voltage output waveforms would have to be adjusted to the new conditions. Such adjustments can be made using a closed-loop approach which can use a feedforward or feedback approach. The feedback approach can compensate for the DC fluctuations and controls the gating signal depending on the deviation of the output of the inverter. The feedback control can be implemented via hysteresis current control or linear control.

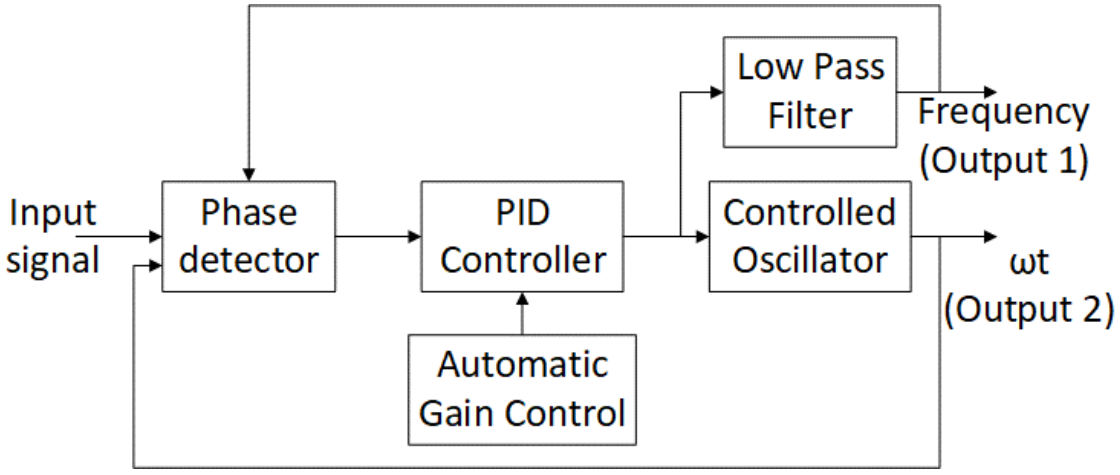

Figure 4-10: Block diagram of phase locked loop method for grid synchronisation

Hysteresis current control forces the AC line current to follow a given reference. The status of the switches is changed whenever the actual output current goes beyond a given reference. The drawbacks of hysteresis control for single-phase inverters are:

a. Switching frequency cannot be predicted in a similar manner to the control using carrier-based modulators and therefore the harmonic content of the AC line voltages and currents become random. This is a disadvantage when designing the filter components.
b. The controllers cannot fully eliminate the DC component in the load current in one waveform cycle.

Therefore linear current control is used in the model developed. Linear controllers can be implemented using different reference frames viz. abc, αβ (stationary) and d-q reference (rotating) frames. An error between the actual output current and the reference current is inherent in linear control while operating on abc or αβ reference frame. The inherent error is due to the fact that the controller needs a sinusoidal error to generate sinusoidal modulating signals required by the modulator. This can be minimised by increasing the gain of the controller, which in turn increases the noise of the circuit resulting in the deterioration of the overall performance of the

control scheme. To eliminate the steady-state error, rotating transformation based control is used, i.e. linear control in d-q reference frame. In a three-phase system Clarke transformation is first used to transform the signal in the abc reference frame to the αβ reference frame and Parks transformation is applied on the resultant signal to convert it into a d-q stationary reference frame. Parks transformation was first developed for three-phase signals and later extended to single-phase signals [104-107]. The αβ components of a single-phase signal can be calculated using equation 4.2.

$$\begin{bmatrix} i_\alpha \\ i_\beta \end{bmatrix} = \begin{bmatrix} i_{\omega t+\varphi} \\ i_{\omega t+\varphi+\frac{\pi}{2}} \end{bmatrix} \tag{4.2}$$

where, i_α and i_β are the components of single-phase current along α and β axes of the stationary reference frame

$i_{\omega t+\varphi}$ is the single-phase output current of the inverter

$i_{\omega t+\varphi+\frac{\pi}{2}}$ is the phase-shifted single-phase output current of the inverter

That is, the original signal is complemented with an imaginary signal which is phase shifted by π/2 radians to create an orthogonal system similar to three-phase systems. These signals are then transformed to the d-q reference frame using

$$\begin{bmatrix} i_d \\ i_q \end{bmatrix} = \begin{bmatrix} \sin(\omega t) & -\cos(\omega t) \\ \cos(\omega t) & \sin(\omega t) \end{bmatrix} \begin{bmatrix} i_\alpha \\ i_\beta \end{bmatrix} \tag{4.3}$$

where, i_d and i_q are the d and q axis components of the current signal.

The output 2, ωt, of the PLL is used to perform the Park's transformation on the grid variable (i.e. grid voltage and current) to generate the respective d-q components. The d-q components of inverter current are passed through a low pass filter to eliminate the higher order harmonics introduced by the PWM controller in the signal. The direct axis current reference value is obtained from the DC-link voltage and DC reference value. The PI controller is reset on the rising edge of the external reset

signal. The section 4.2.6 on controller saturation during fault describes the necessity of the reset after tripping. The output of the inverter is connected to a filter before connecting to the grid to remove the harmonics in the voltage and current waveforms introduced by the PWM switching. The d-q controller of the inverter compensates for the voltage drop across the filter.

Output AC filters

The output voltage of a PWM DC/AC converter consists of pulses of different widths, which are determined by the Uref signal. The output current is a sine wave with harmonics. The filter is necessary at the output of any DC/AC converter to limit the harmonics in the output waveforms. A passive filter not only affects inverter harmonic injection but impacts on the harmonics produced by a coupled non-linear load. Passive filters are often used to reduce voltage harmonics and current distortion in distributed generation systems. The harmonic currents injected by a grid-connected inverter can be classified as

a. Low frequency harmonics
b. Switching frequency harmonics
c. High frequency harmonics

The three main existing harmonic filter topologies are (Figure 4-11):

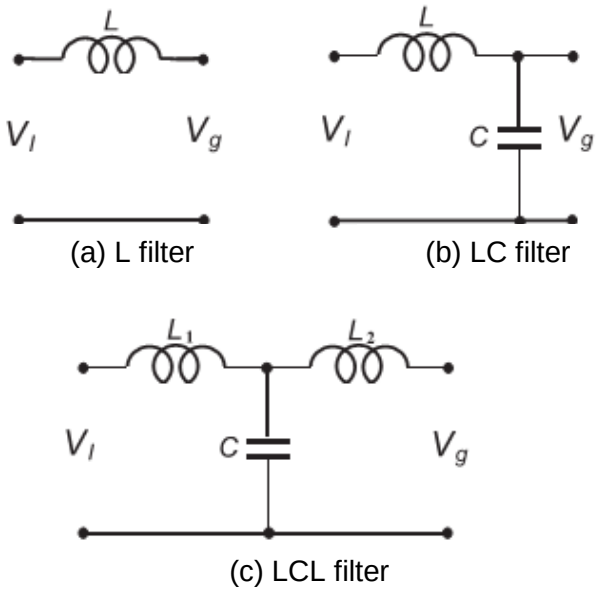

(a) L filter (b) LC filter

(c) LCL filter

Figure 4-11: Different types of filters

a. L – Filter – first order filter

b. LC Filter – Second-order filter

c. LCL Filter – Third order filter

A basic L filter is as shown in Figure 4-11(a). Attenuation of the basic inductor filter is -20 dB/decade over the whole frequency range. Using this filter, the inverter switching frequency has to be high in order to sufficiently attenuate the inverter harmonics. The harmonic currents injected into the grid network must be less than 0.3% of the rated current for harmonic orders (h) greater than 35(IEEE Standards 519-1992 [108]). The L- filter cannot achieve the harmonic limit mentioned in the standards unless the switching frequency is greater than 20 kHz.

The LC Filter is a second order filter as shown in Figure 4-11(b) and gives an attenuation of -40 dB/decade. The resonant frequency is calculated using equation (4.4)

$$f_0 = \frac{1}{2\pi\sqrt{LC}} \tag{4-4}$$

The limitation of the LC Filter is that the shunt element is ineffective when connected to a stiff grid network, where the grid impedance is insignificant at the switching frequency.

An LCL filter is a third order filter with a circuit as shown in Figure 4-11(c). It produces better attenuation of inverter switching harmonics than the L and LC Filters. Key advantages of the LCL filter are:

1. Low grid current distortion and reactive power productions
2. Attenuation of -60 dB/decade for frequencies in excess of the resonance frequency
3. The possibility of using a relatively low switching frequency for a given harmonic attenuation.

The resonant frequency of the LCL filter is given by equation (4.5)

$$f_0 = \frac{1}{2\pi\sqrt{\frac{L_1+L_2}{L_1 L_2 C}}} \tag{4.5}$$

An LCL filter can achieve reduced levels of harmonic distortion with lower switching frequencies and with less overall stored energy. The harmonic requirement of IEEE 1547 can be achieved using an LCL filter at switching frequencies greater than 3500 Hz. For the developed model, LCL filter is used as it helps meeting the requirements mentioned by the guidelines. The following constraints have to be maintained to avoid excessive voltage drop on the AC side across the inductors, maintain good controllability of the output current and suppress the ripple in the AC side current [109]:

a. The capacitor value should be limited such that it can supply a maximum reactive power of not more than 5% of the rated power in order to maintain almost unity power factor.
b. The total value of inductance should be around 0.1 p. u. to limit the AC voltage drop during operation otherwise a higher DC link voltage would be required to ensure current controllability.
c. The resonant frequency should be in the range between 10 times the line frequency and one-half of the switching frequency, to avoid amplification of unwanted harmonics in the lower parts and upper parts of the harmonic spectrum.
d. Passive damping must be sufficient to avoid oscillations under transients.

The damping resistor of resistance equal to 1/3rd of the capacitive reactance at the resonant frequency is connected in series with a capacitor to effectively damp down the oscillations [110].

4.2.5 Over and under voltage protection

As discussed in chapter 3, the PV inverter is designed to trip under different circumstances defined by the regulations/specifications pertaining to the respective country of use. As this research aims to evaluate the impact of PV on the dynamic performance of the distribution network, the under/over-voltage trip has been included in the generic model of the PV system developed. Figure 4-12 shows the flow chart of the over/under voltage trip signal generation and the delayed resetting of the parameters. When the voltage at the terminals/point of grid connection goes beyond the normal range of values, the inverter trips after a delay depending on the magnitude of voltage sag/swell as stipulated by G-83. The threshold values are as discussed in section 3.1. The signals are reset after a delay of 0.5 s which is smaller than the delay in practical scenarios to ensure that the simulations are run faster. Figure 4-13 shows the MATLAB/Simulink implementation of the over/under voltage protection.

4.2.6 Inverter control saturation during fault and modification thereof to the model

The short-circuit fault is typically the most common and is usually implied by the term fault. A fault occurs when one energized electrical component contacts another at a different voltage. The short-circuit fault current can be orders of magnitude larger than the normal operating current. The current from such an event can damage electrical equipment and pose safety concerns to both utility and non-utility personnel. During a fault condition, the inverter disconnects from the grid due to the controllers sensing any of the following factors: overcurrent at the AC side, excessive DC link voltage, loss of grid voltage synchronisation, reactive current injection imbalance [111], [112].

During fault or voltage sag, the operating point of the inverter deviates from the MPP as the power from the PV system is not fully transferred to the grid due to the voltage drop at its terminal resulting in build-up of charge in the DC link capacitor and higher

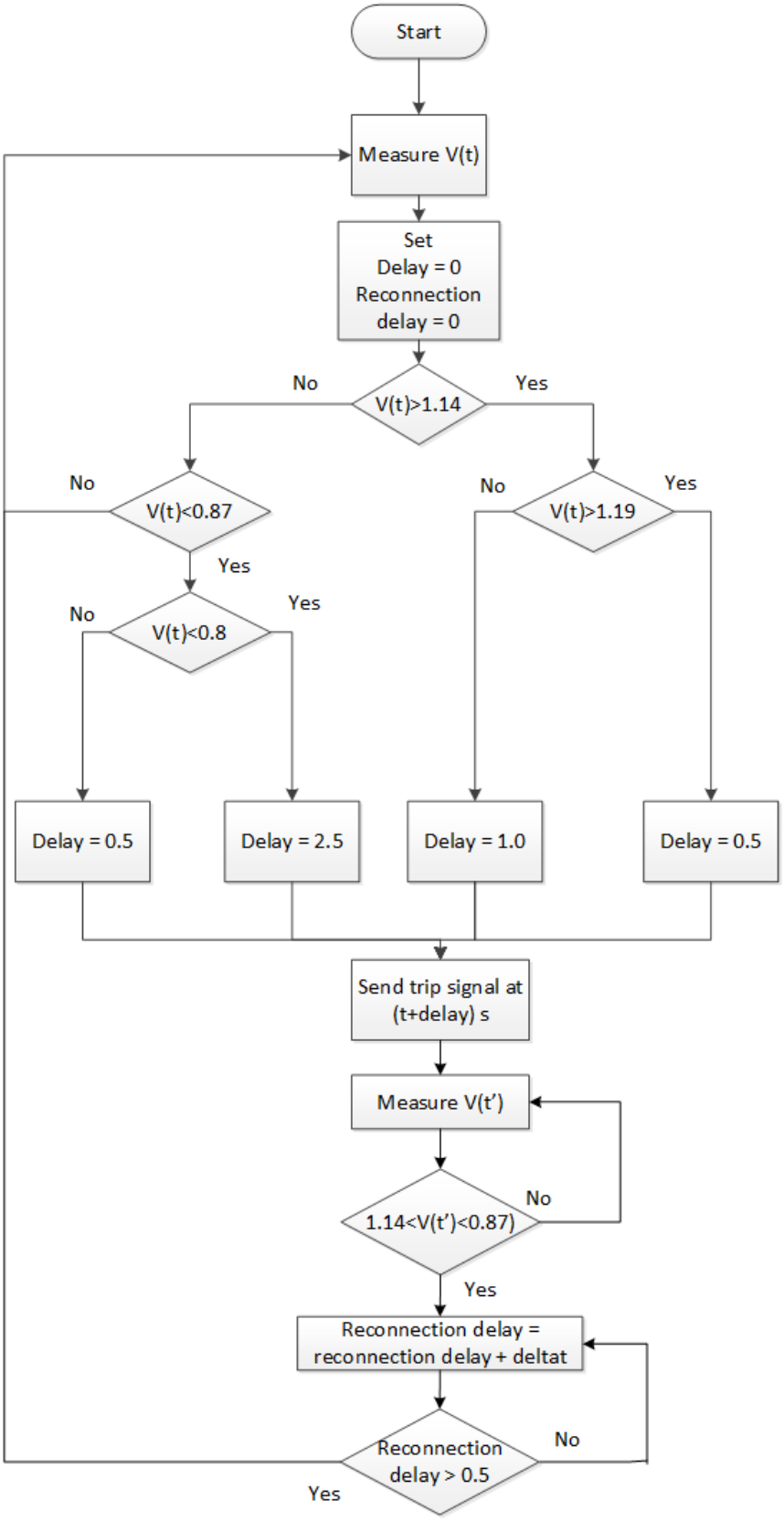

Figure 4-12: Flow chart of Over/under voltage protection

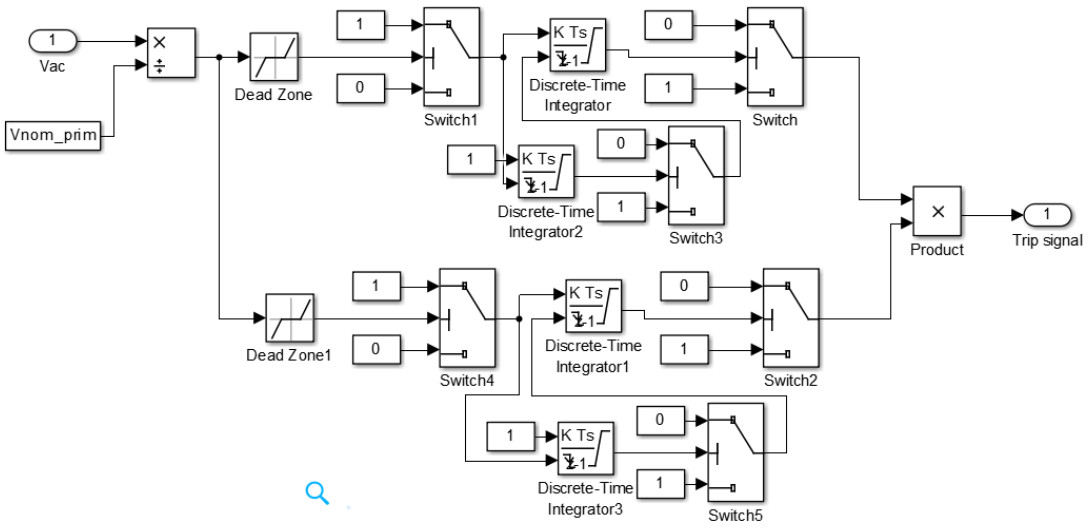

Figure 4-13: Over/Under voltage protection of inverter

than rated current at the AC side. A problem that may appear because of the deviation of the operating point is that, after the fault is cleared, the DC-link voltage and the AC currents may take more than 3 s to reach the pre-fault values [112]. The reason is that the error in the DC-link voltage is accumulated in the 'integral' part of the PI controller. This accumulated value is limited by the current limiter and thus it has no effect on the grid currents. However, when the voltage sag ends, the excessive control action accumulated in the 'integral' part of the controller has to be compensated by an input error in the opposite direction. As a consequence, the DC-link voltage is reduced below the reference value. This may be overcome by using an anti-windup technique to stop the PI controller from accumulating the control action when it exceeds a specified value or using an external reset triggered by the fault clearance or voltage sag clearance. The model described in this chapter faced this issue when the simulations were carried out to understand the performance of the distribution network under fault. The output power of the inverter started to reduce almost 1s after the fault was cleared and went to almost zero before increasing again to reach the MPP power. An external reset was added to the current controller block, which resets the PI controller once the fault is cleared thus resolving the transients introduced by the accumulation of value in the PI controller.

4.3 Generalisation of PV Model for Different Ratings

All the blocks discussed in sections 4.2 are converted into a subsystem with a mask as shown in Figure 4-15. Appendix B also shows the overall model of the PV system. The block takes irradiance and temperature as input and produces AC output synchronised with the point of grid connection. As each module used has a rating of 250 Wp, the size of PV system can vary from 1 kW to 4 kW in steps of 250 W. For 4 kW system, 16 no.'s of 250 Wp modules are required. If all 16 are connected in series, it results in DC voltage of around 495 V at MPP, which is higher than the DC link voltage. Hence, 8 modules are connected in series and two such strings are connected in parallel to achieve an overall capacity of 4 kWp. This is also a common practice among installers to limit the DC input voltage. Also, a 3.75 kWp system would require 15 modules of 250 Wp each which results in a DC voltage of around 465 V at MPP. As the number of modules is odd, it cannot be converted into parallel connection. Combinations using smaller rating of PV modules, like 200 Wp, 125 Wp etc., did not result in a feasible combination of a number of modules in series and parallel. Hence this rating is not considered for the general model developed. The equations described in section 4.3 are used to define the operating parameters of

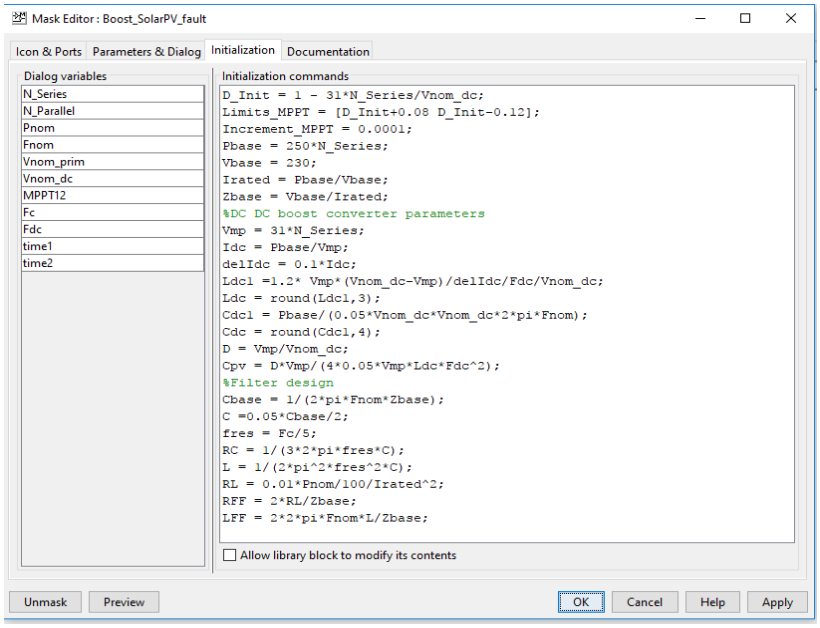

Figure 4-14: Masked block initialisation of generic model of PV system

the model in the ‘initialization’ pane of the mask editor so that the values of different components change automatically for any change in the rating of the PV system as shown in Figure 4-14.

4.4 Validation of the Generic Model of PV System

The two stages viz. the DC/DC controller with MPPT and the DC/AC inverter are validated individually as the published literature focussed on the performance of one of the two blocks at a time.

4.4.1 Validation of MPPT model

Faranda and Leva compared the energy extracted from the Solar PV system under different irradiance conditions for different MPPT methods [101]. The same set of data signals a – n, shown in Figure 4-16, was used to calculate the efficiency of the MPPT model. The results of the efficiency of the MPPT in [101] were for a 4.65 kWp system and were used to arrive at the range of efficiencies. The efficiency of the P&O method in the published paper was slightly lower for signals j and l, around 97%, than most of the other signals, greater than 98%. The signals j and l have low average irradiance levels, where the DC/DC converter losses will be more visible in

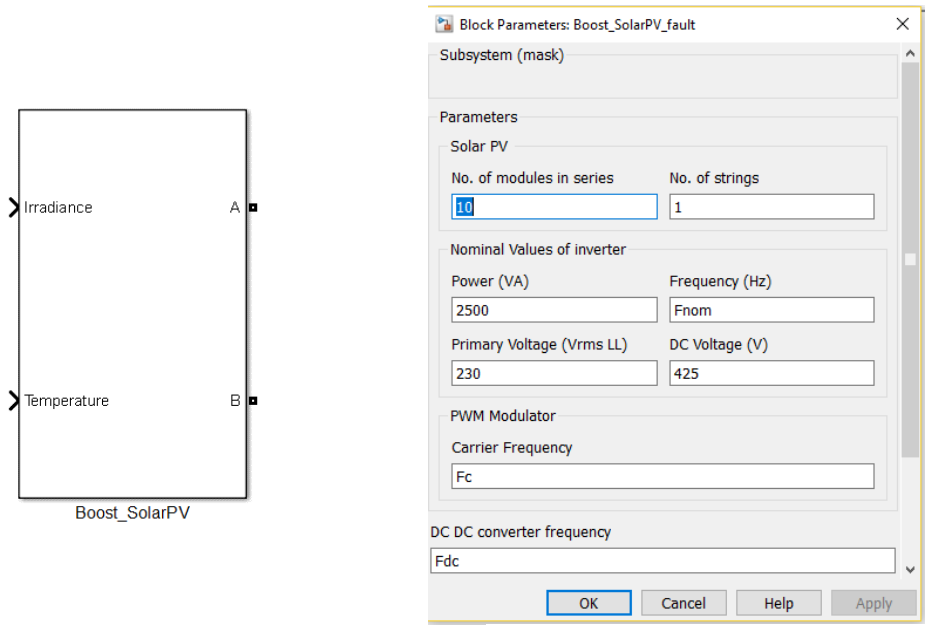

(a) Masked block (b) Parameters

Figure 4-15: Generic model masked block and its parameters

comparison to higher irradiance levels. The efficiency of conversion is calculated as the ratio of energy extracted using the specified tracking method to the theoretical energy that can be extracted calculated based on area under the graph. Figure 4-17 shows the efficiency of MPPT for different ratings of the PV system for different

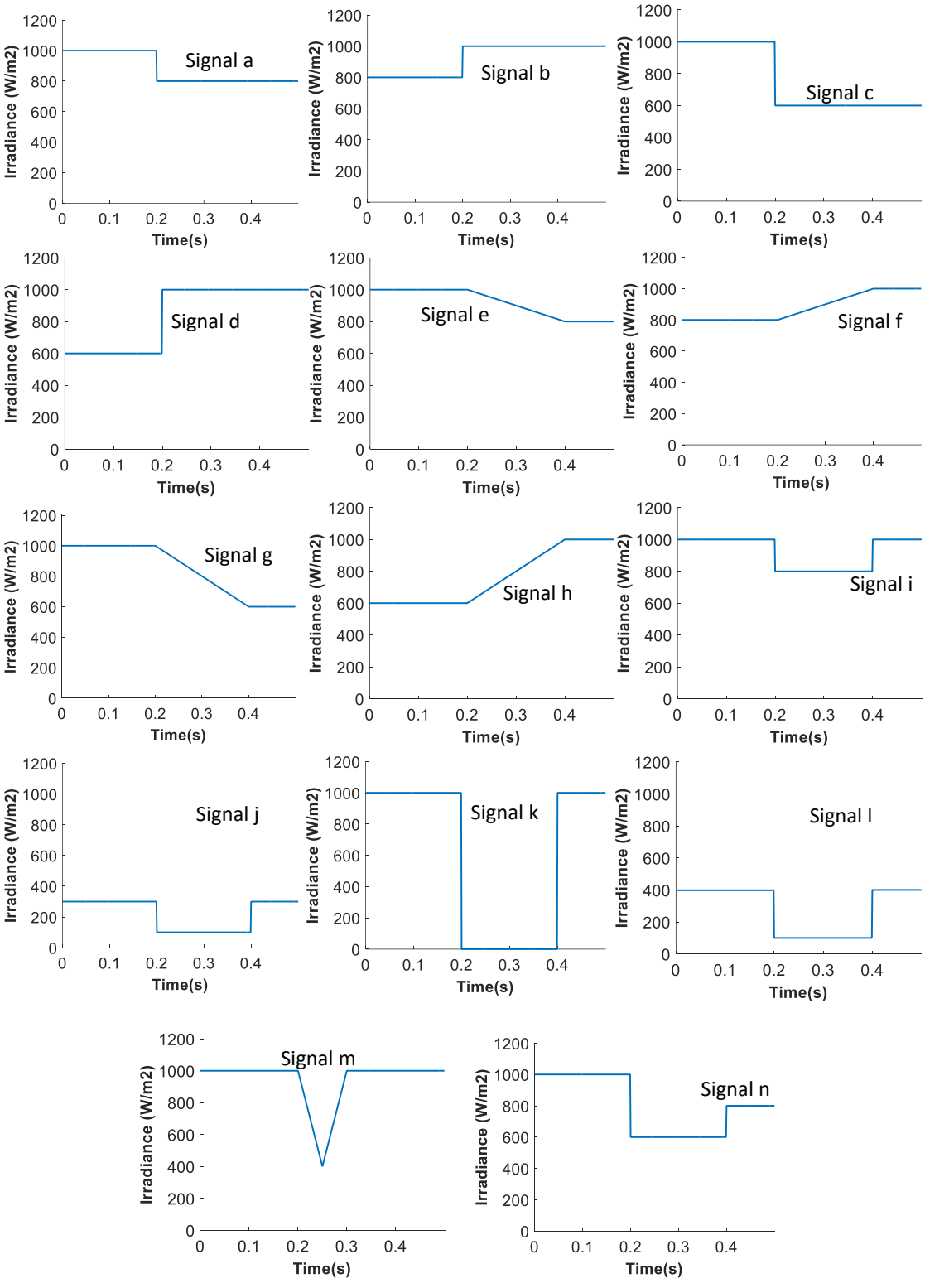

Figure 4-16: Signals a- n used for validation of MPPT model [81]

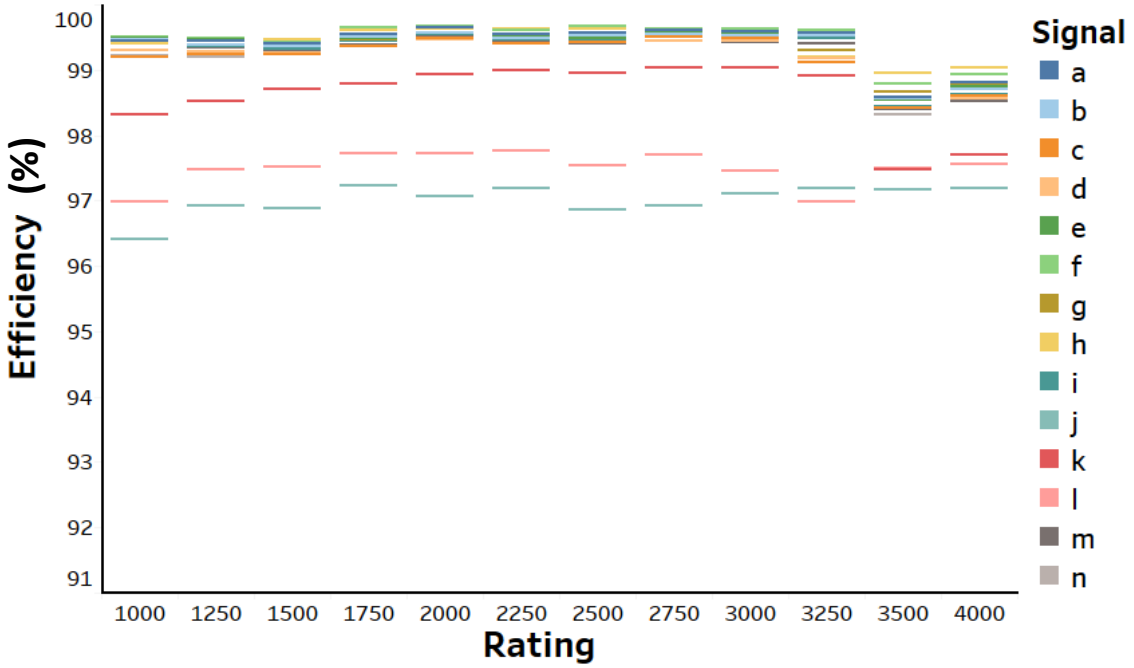

Figure 4-17: Efficiency of the developed MPPT model at different ratings of PV system for the signals a - n

signals. From the graphs, it can be observed that efficiency obtained using the developed model is more than 98% for all ratings for all signals except for signals j and l, similar to the published efficiencies.

4.4.2 Validation of steady-state DC/AC inverter model

The National Electrical Code (NEC) and IEEE 1547-2003 are the common standards that deal with PV systems [91]. IEEE 1547 -2003 specifies the maximum allowable harmonic amplitudes for PV inverter output in terms of percentage of maximum load current as given in Table 4-1. Even harmonics are limited to 25% of odd harmonic limits. Figure 4-19 and Figure 4-18 show the odd and even harmonic current as a percentage of rated peak output current for different ratings of the PV system. From the graphs, it can be observed that the harmonics of the output current are within the limits specified by the standards.

Table 4-1: Maximum harmonic current distortion in percent of rated current capacity

Individual harmonic order (h) (odd harmonics)	h<11	11≤h<17	17≤h<23	23≤h<35	35≤h	THD
% of rated current	4.0	2.0	1.5	0.6	0.3	5

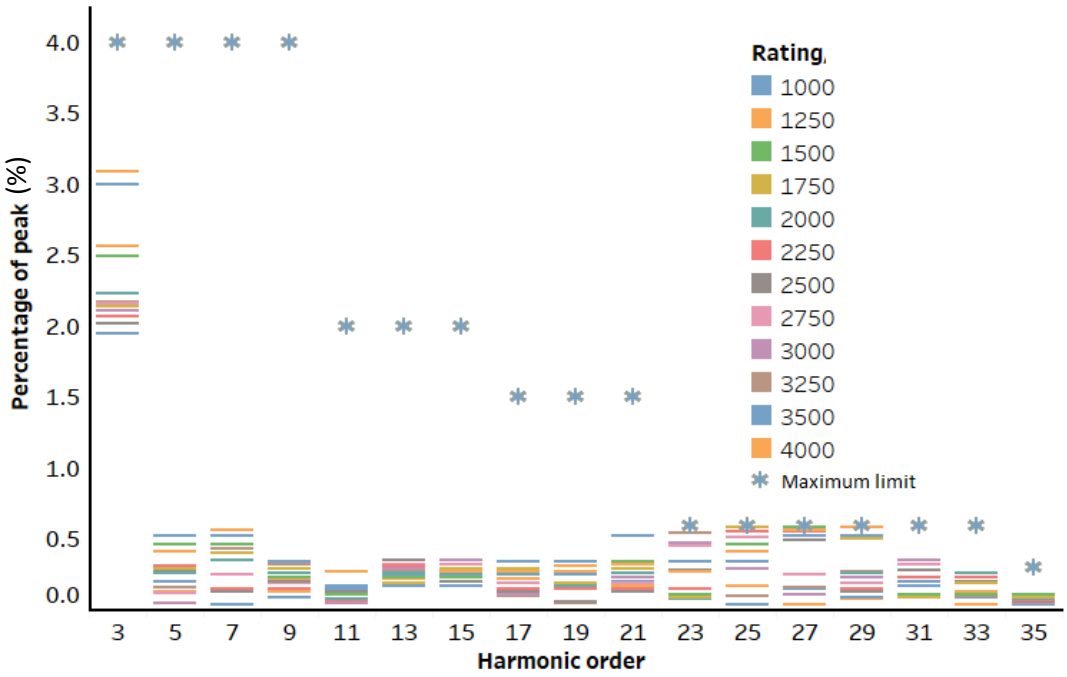

Figure 4-19: Odd harmonic currents as percent of rated current as obtained from simulations and as per standards

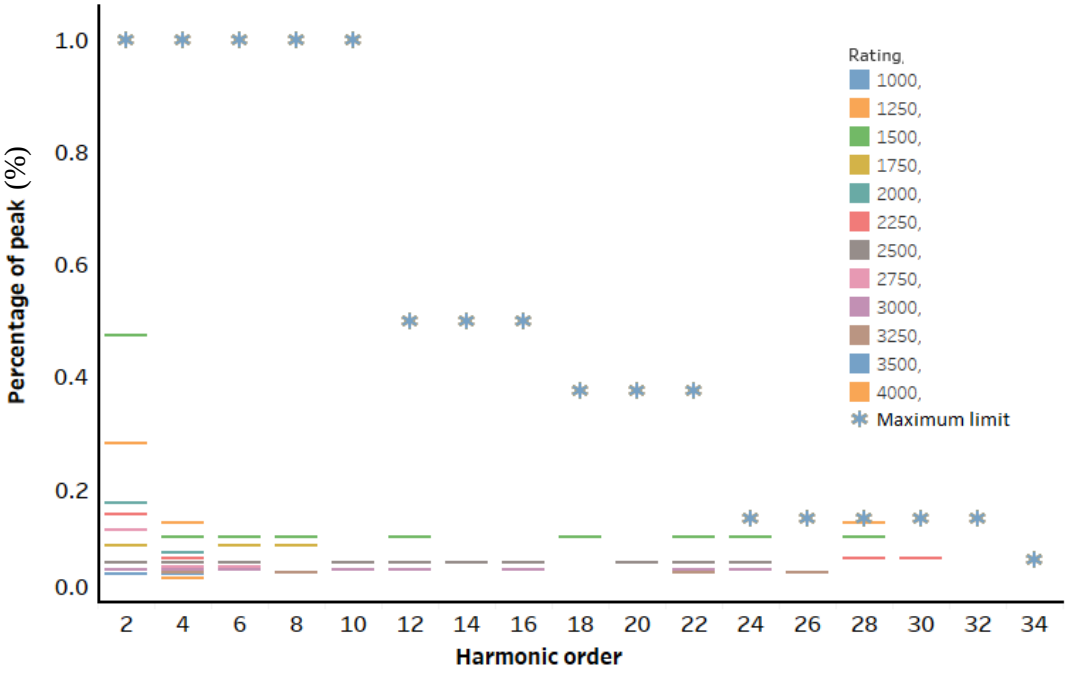

Figure 4-18: Even harmonic currents as percent of rated current as obtained from simulations and as per standards

4.4.3 Validation of dynamic performance of the inverter model

The contribution of the inverter to fault current is often considered minimal and has not been a subject of research until recently. Therefore the number of publications with experimental results of the performance of a grid-connected inverter during a fault is limited. The report from the National Renewable Energy Laboratory (NREL) provides the results of 1 kVA single-phase and 500 kVA three-phase inverters during different types of faults using a test procedure designed by Underwriters Laboratory (UL) [113]. The results of the experiment indicate that for a short circuit at the terminals of the inverter, the 1 kVA inverter produced an output current peak of around 5 times the rated current. This current lasted only for one-tenth of a cycle and can be attributed to the capacitor discharging under sudden reduction in voltage across its terminals. However, the inverter disconnected almost immediately contradictory to the expectation of time delay between detection of fault and tripping of the inverter. Similar tests of a 500 kVA inverter at the manufacturer's premises yielded an output current peak of around 2 to 3 times the rated current during fault and lasted between 1.1 to 4.25 ms. Two three-phase 30 kVA inverters were tested in [114]. The two inverters produced 120% and 180% of their rated current for the first cycle after fault and then reached their rated current levels. Both the inverters stayed connected to the grid for 9 and 7 cycles after fault introduction respectively. Four commercial inverters (three single-phase 5 kVA inverters from ABB, KACO and SMA and one three-phase 10 kVA inverter from SMA) were tested for faults of 0.3 s duration with different resistances to ground in [115]. The single-phase inverters from ABB and SMA tried to maintain the output power as equal to the pre-fault conditions, when the pre-fault condition was less than 100% of the rated power of the inverter, by increasing the output current during a fault. The increase in current during fault was also found to be dependent on the voltage at the terminals during a fault. For very low voltages (less than 32% of rated voltage), the inverter output

current decreased during a fault. The output current of the KACO inverter increased during fault and there was also a gradual increase in reactive power output of the inverter during a fault. This increase in reactive power during fault has been attributed to controller saturation. The inverters did not trip for all the tested scenarios as the guidelines provide a delay of 0.5 s before tripping under fault and the fault in the experiment lasts only for 0.3 s. However, for the test scenarios where the inverters did trip within the 0.3 s, the inverters did not synchronise with the grid as soon as pre-fault conditions were restored. This is in-line with the requirements that, in the case of tripping of the inverter, the inverter should wait for 30 s to 3 minutes after the restoration of the grid. The authors observe that the output current of the inverter was not higher than the rated current of the inverter in any of the tests, which contradicts the results from [114] and [116].

As the results in published literature contradict each other, it was decided to conduct similar experiments on commercial low-cost inverters available in the local market. A 1 kVA grid tie inverter by Solarepic with specifications as given in Appendix C was used for experiments. The test set-up shown in Figure 4-20 has been used to validate the model. The set-up is similar to that explained in [116] but using the actual grid instead of a grid simulator. The use of the actual grid necessitates an additional resistance in series with the fuse to limit the grid current during a fault. A multi-function timer relay was used as S3 to introduce the fault for different durations

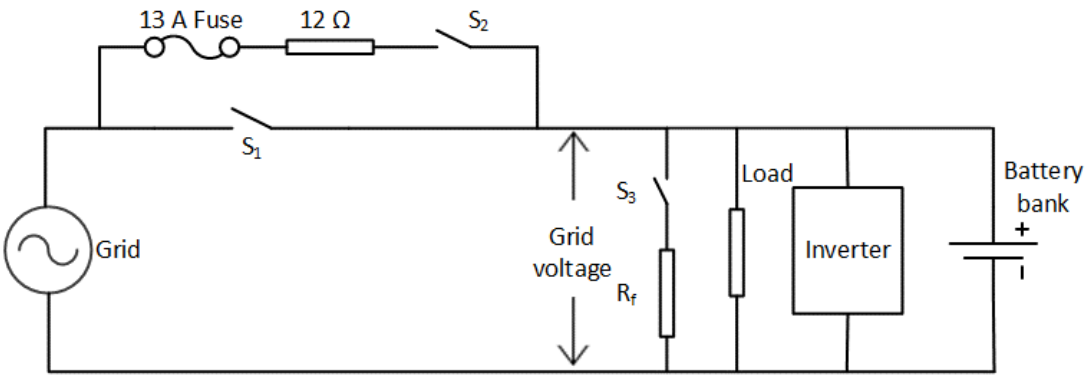

Figure 4-20: Test circuit diagram

(0.5 s to 3 s) and DSPACE set up was used to monitor the inverter voltage, inverter current and grid current. A load bank comprising of six 220 Ω resistors was used as "Load" and the current drawn from the grid was minimum with four such resistors in parallel. Figure 4-21 shows the experimental set-up in the lab.

The test procedure is as follows:

a. Close switches S1 and S2
b. Adjust load to make the current from/to grid as close to zero as possible
c. Open switch S1
d. Initiate record measurements in DSPACE
e. Close switch S3 to simulate fault for different durations depending on the time setting of the multi-function timer relay.

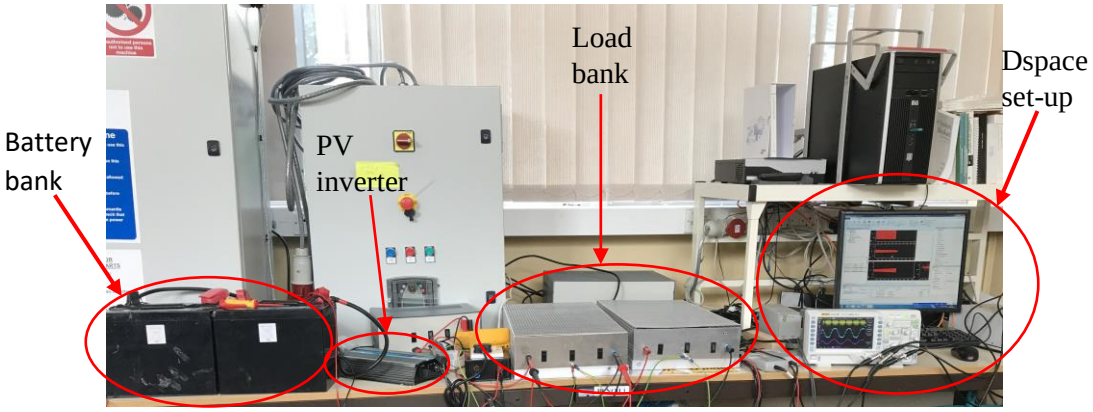

Figure 4-21: Experimental set-up to validate dynamic model

The steady-state output voltage and current of the inverter are nearly sinusoidal with a voltage THD of around 4% and current THD between 12 – 18%. The higher current harmonics could be attributed to the harmonics in the grid voltage which was around 3% with no inverter connected to the grid [117].

When Rf = 6 Ohms, the voltage at the inverter terminals falls to around 90 Vrms (Figure 4-22(a)) and the inverter trips after 7 cycles. The inverter output current increases to 9.3 A peak during a fault, almost twice the pre-fault peak current as shown in Figure 4-22(b). Rf = 12 Ohms results in a voltage sag to 122 V RMS (Figure

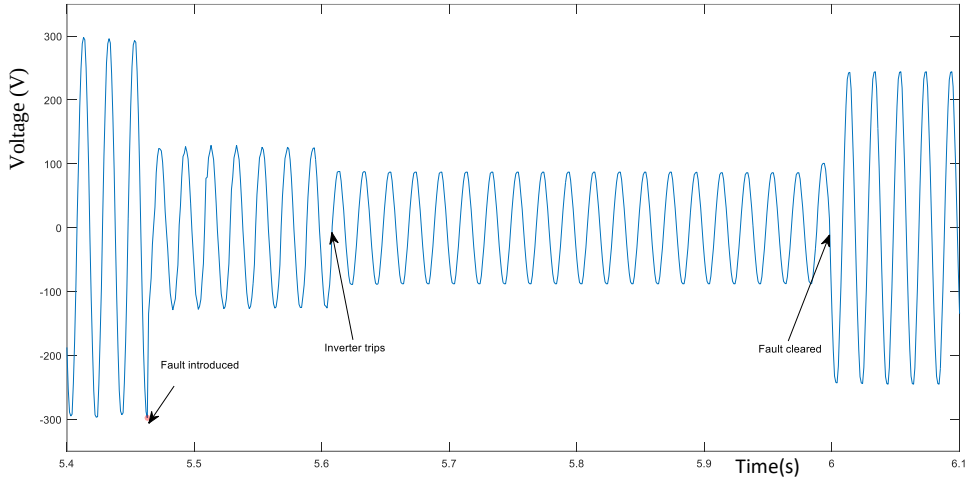

(a) Voltage across the terminal

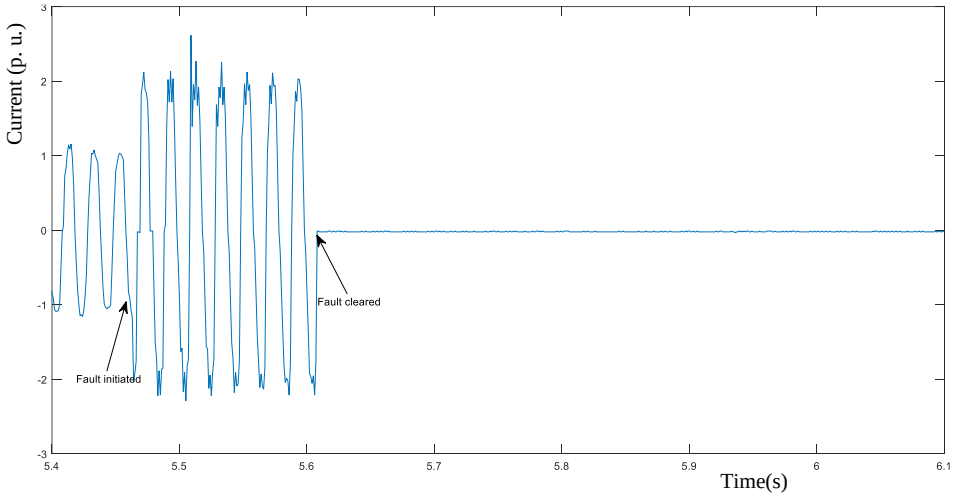

(b) Output Current

Figure 4-22: Inverter output before, during and after fault for Rf = 6 Ohms

4-23(a)), resulting in tripping of the inverter after 14 cycles. The inverter output current peak varies between 1.5 to 2 p. u. during the fault as shown in Figure 4-23(b). When Rf = 24 Ohms, the inverter does not trip even though the voltage at the terminals drops to 154 Vrms and the current increases to 1.5 times the rated current (Figure 4-24).

As the generic model is not replicating any particular manufacturer, the fault current contribution from the PV inverter is modelled to be limited to 2 p. u., which can be changed if necessary by changing the upper limit of the PI controller in the d-q controller of the inverter. Also, the delay in tripping is set as equal to the maximum allowed time delay dependent on the voltage magnitude at the inverter terminals.

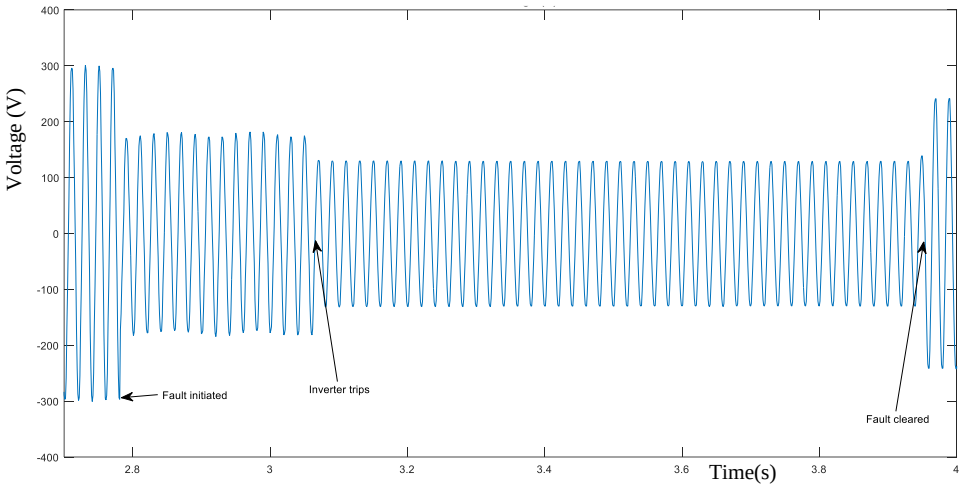

(a) Voltage across the inverter terminals

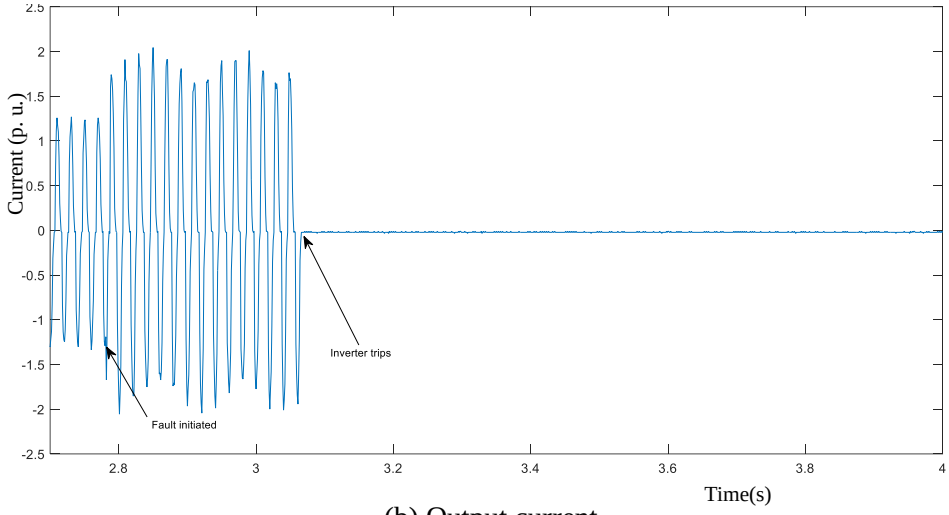

(b) Output current

Figure 4-23: Inverter output before, during and after fault for Rf = 12 Ohms

Figure 4-25(a) shows the output current of the PV inverter of the generic model developed during a fault at the far end of the distribution network that results in a voltage sag at the terminals of the inverter. The output current increases but remains less than 1.5 p. u. similar to the experimental results. Figure 4-25(b) shows the output current of the inverter of the generic model of the PV system for a fault near its terminals resulting in a significant voltage drop across its terminals. The inverter trips after a delay of 0.5 s in-line with the UK guidelines. The output current peak in the first cycle after the fault is slightly higher than twice the rated current which can be attributed to the response time of the controller and is similar to the experimental result of the 1 kVA inverter in [116]. The continued contribution of the inverter to the fault current remains less than 2 p. u. after the first cycle.

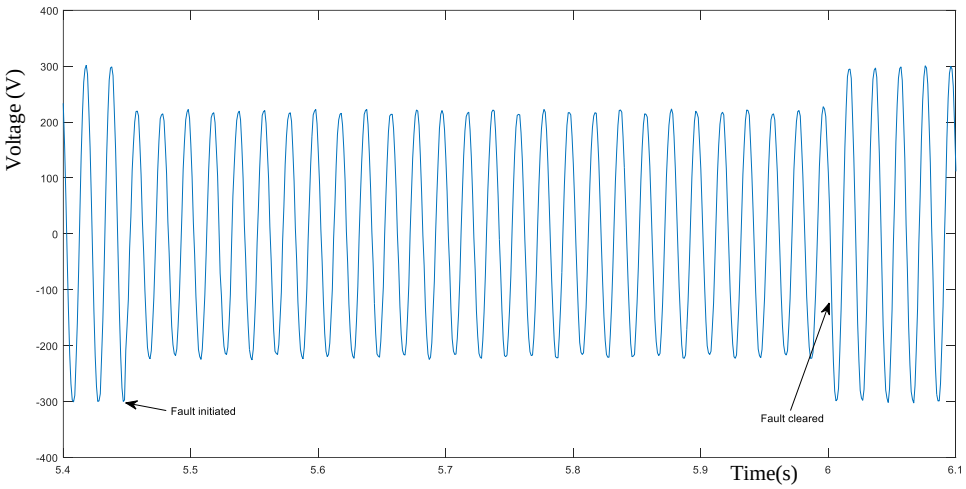

(a) Voltage across inverter terminals

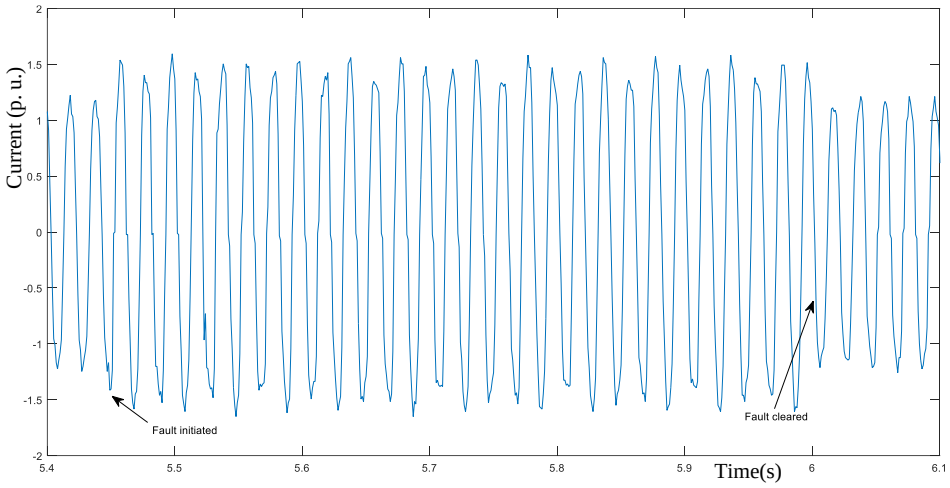

(b) Output current

Figure 4-24: Inverter output before, during and after voltage sag

4.5 Dynamic Model of a Typical Network and Load

A typical network representative of the UK residential network, as shown in Figure 4-26, has been chosen for the analysis [118]. The network consists of a 33/11 kV substation with two 15 MVA transformers with on load tap changers supplying six 11 kV outgoing feeders and each 11 kV feeder, in turn, supplies eight 11/0.4 kV substations equipped with off load tap changers. Each 11/0.4 kV substation supplies 384 houses through 4 feeders. As the research focuses on residential solar PV, only one 11 kV feeder is modelled in detail and the remaining 5 feeders are modelled as lumped loads. Similarly, one of the eight 11 kV/400 V substations and one of the four 400 V feeders are modelled in detail and others as lumped loads. The detailed

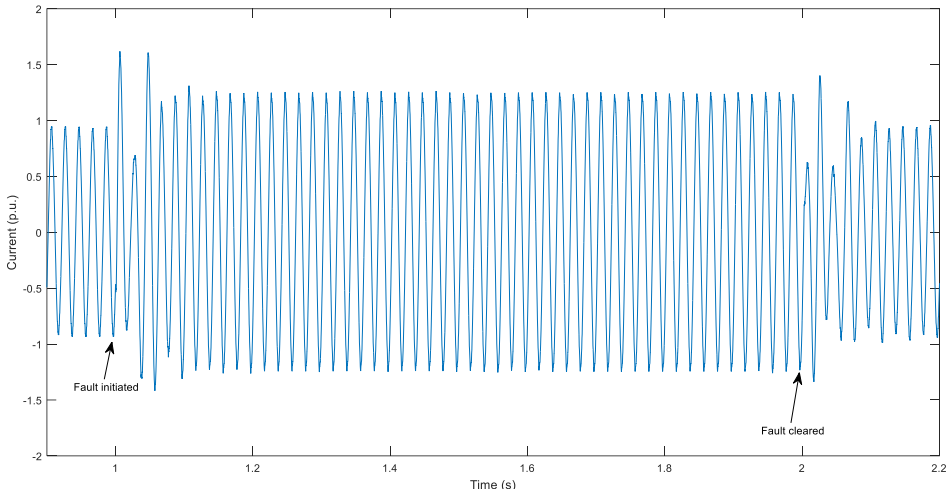

(a) Voltage sag

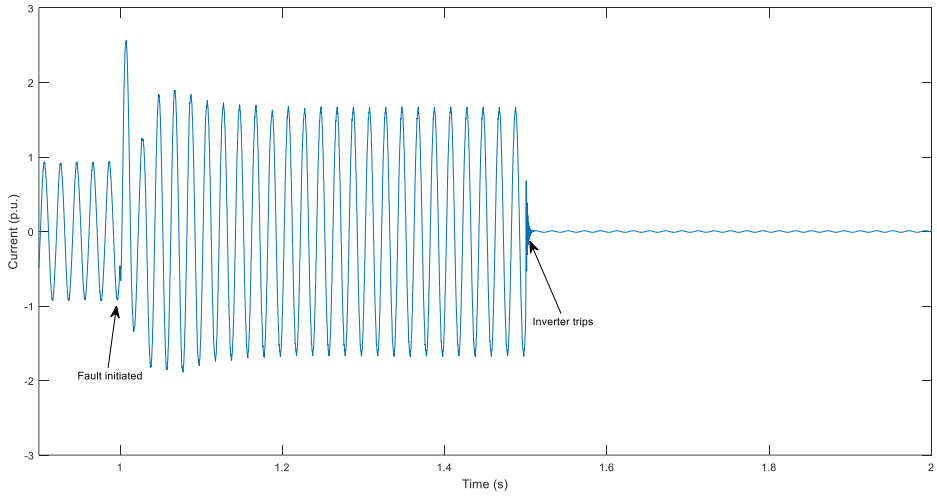

(b) Fault near the inverter terminal

Figure 4-25: Output current of the generic model of the PV system (in p. u.) before during and after a voltage sag and fault

400 V feeder supplies 57 houses and it is assumed that these houses are uniformly distributed in the three phases across 6 node points (buses). The six nodes have 11, 8, 15, 4, 6 and 13 houses respectively and Table 4-2 shows the number of houses in each phase in each node. The details of the sample network are as given in Appendix D. The steady-state simulation of the network at minimum load results in a voltage around 1.01 p. u. at the secondary of the 33/11.5 kV substation transformer and around 1.09 p. u. at the secondary of the 11/0.433 kV substation transformer, similar to the voltages published in [118].

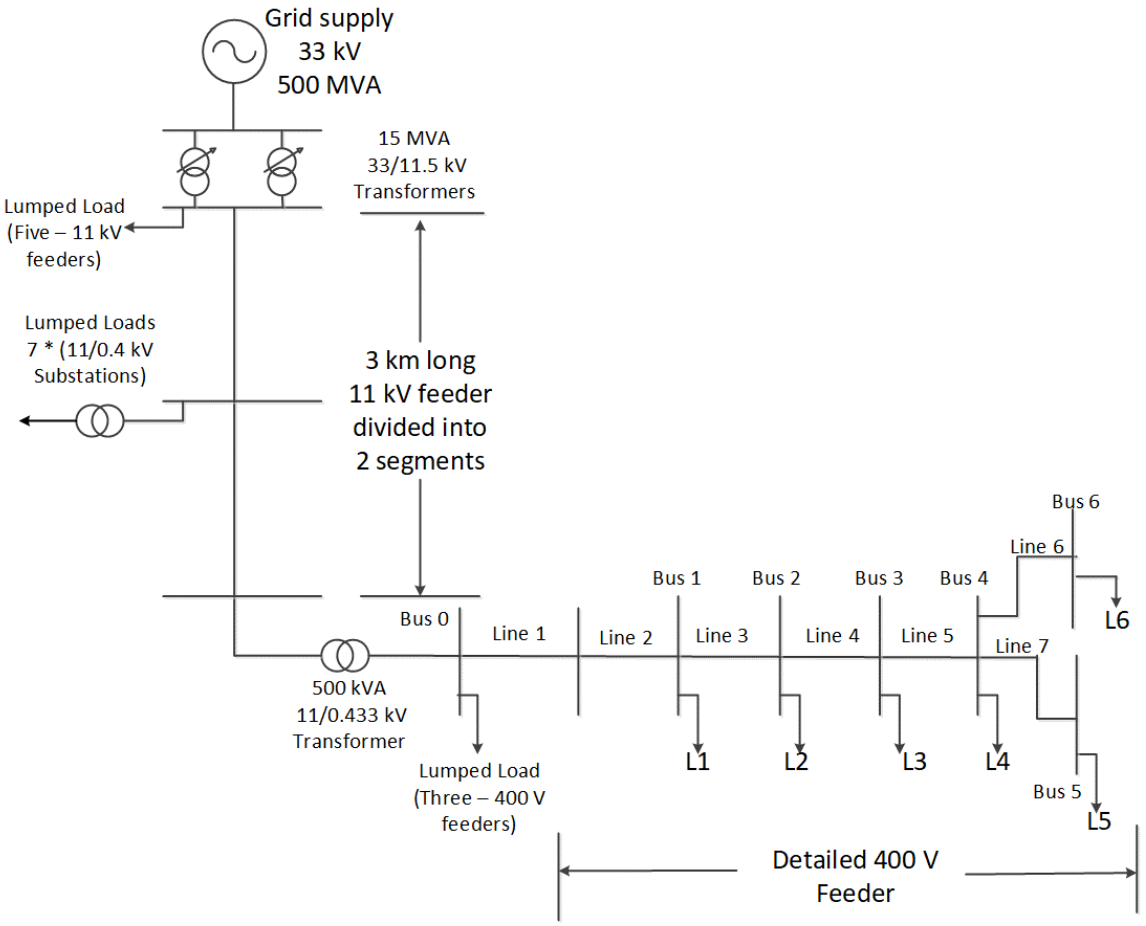

Figure 4-26: Typical distribution network

For the first stage, only one low voltage (LV) feeder (supplied from a 500 kVA transformer), together with its connected loads, was modelled in detail. The tap changer is set to provide a secondary per phase voltage of 250 V in order to ensure that the voltage is within the statutory limits under maximum demand conditions. The single-phase feeder supplies 19 houses and is distributed across 6 node points L1 to L6 (see Figure 4-27).

Table 4-2: Details of number of houses per phase per node

Node no.	L1	L2	L3	L4	L5	L6
Ph A	4	2	5	2	4	2
Ph B	4	3	5	1	4	2
Ph C	3	3	5	1	5	2

Table 4-3 gives the number of houses in each node point and the house numbers. The After Diversity Maximum Demand (ADMD) per house is 1.3 kVA and after diversity minimum demand per house is 0.16 kVA [118]. Power factor of the load is considered as 0.95 lagging.

Table 4-3: Details of number of houses per node for single-phase feeder

Node no.	L1	L2	L3	L4	L5	L6
No. of houses	4	2	5	2	4	2
House no.	1-4	5,6	7-11	12,13	14-17	18,19

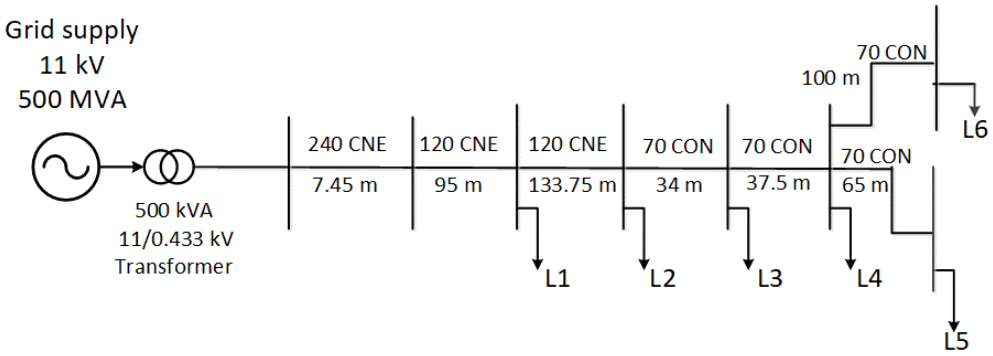

Figure 4-27: Single-phase feeder network

The built-in dynamic load block in MATLAB/Simulink uses an ideal controlled negative current source to model the dynamic load. MATLAB does not allow connection of two current sources in parallel and as PV is another current source, the dynamic model block was modified to include a high resistance in parallel with the end terminals of the dynamic model. The built-in masked block was also modified to accept external control of the real power of the load. The time constants which control the dynamics of the real and reactive power of the load were assigned zero, so as to permit the evaluation of the impact of PV on the dynamic performance of the network ignoring the load dynamics. The power factor of the load was assumed as 0.95 lagging. Also, constant impedance load is assumed by setting the values of np and nq as 2. As a future scenario, it is possible to include the time constants of different household loads and also different types of loads like constant

current load or constant power load. The load model was used to represent individual households in the detailed feeder and the input to the model was dependent on the scenarios considered which are discussed in chapters 5 and 6.

4.6 Summary

In this chapter, a generic model of a single-phase PV system capable of replicating the steady and dynamic-state performance has been developed. The capacity of PV system can range from 1 kWp to 4 kWp. The chapter provides an introduction to solar irradiance and the different blocks of the grid-connected solar PV systems. State of art of different topologies and control strategies of the grid-connected inverters are also discussed. A d-q control based two-stage inverter with sinusoidal PWM has been chosen for the model keeping in the mind the pros and cons of the different options and their suitability for low voltage applications. The model of the MPPT and inverter are individually validated using irradiance data from published literature and standards. This model, when used to evaluate the performance of a distribution network under fault, produced a reduction in output power once the fault is cleared. This reduction of power was attributed to the accumulation of excessive control action of the PI current control block inside the inverter. A simple external reset has been used to reset the controller after the fault is cleared. This ensures that the inverter remains synchronised to the grid after the fault is cleared. The dynamic performance of the model has been further validated against experimental results of 1kVA grid-connected inverter operated under voltage sag and published results of the performance of the inverter under short-circuit at its terminals. A dynamic model of a distribution network representative of the UK distribution network has also been developed. The single-phase load model from the built-in blocks has been modified for connecting them in parallel with PV systems which act as a current source. The developed generic model of the PV system, along with the models of the distribution network and load, is used to evaluate the steady and

dynamic-state performances of the distribution network under different penetration levels of PV systems as discussed in chapters 5 and 6.

CHAPTER 5

STEADY-STATE PERFORMANCE OF A DISTRIBUTION NETWORK WITH MULTIPLE SINGLE-PHASE PV SYSTEMS

The technical issues arising from the increasing contribution of PV, as discussed in the literature, are voltage fluctuations, voltage flicker, voltage control, harmonic distortion, fault current, system unbalance, protection coordination, need for equipment upgrades, losses in the network, power system oscillations due to lack of inertia of the system and spread of outage to a wider area of power supply in case of a fault at certain locations [22, 27, 31, 34, 37, 53]. Barriers in terms of outdated interconnection requirements and lack of standards have also been discussed [23, 24]. The technical issues discussed in the literature can be broadly classified as those occurring in the steady-state and those occurring in the dynamic-state. The majority of the available literature focuses on large-scale solar systems and on the system analysis at the transmission level. Extending the results of these studies may not be suitable for a distribution feeder as their characteristics are significantly different. Traditionally, distribution networks have evolved to be passive with very limited automation and monitoring as compared to transmission networks [17]. Also, the direction of power flow has been from central generators to the loads typically located at the end of the distribution network. With increasing penetration of small-scale generators, including PV systems, there arise scenarios of two-directional power flow and real-time power mismatch in the distribution network. In order to identify the technical issues in the distribution network, the performance of the network with PV has to be analysed. This chapter aims to evaluate the steady-state performance of the distribution network with different contribution levels of PV

systems. The models of the PV system and the distribution network models developed in Chapter 4 are used to analyse the performance of the distribution network. The chapter starts with the methodology used to evaluate the performance, followed by the performances of the single-phase distribution network and the three-phase distribution network. The impact of changes in the substation voltage, the power factor of operation of PV systems and unbalanced distribution of PV systems on the distribution network performance are also analysed. The performance is evaluated in terms of the voltage profile, THD of current at the secondary of the 11/0.433 kV substation transformer, net power flow at the secondary of the substation transformer and power factor at the secondary of the substation transformer.

5.1 Review on the Impact of PV on Steady-state Performance

The following paragraphs describe the impact of PV on the steady-state performance parameters as discussed in the literature and the gaps thereof. The performance parameters used to evaluate the hosting capacity are: voltage profile, total harmonic distortion (THD), reverse power flow, power factor, and voltage unbalance.

The impact of PV systems on the voltage profile is the most studied performance parameter [28, 29, 31, 32, 118-120] and the majority of the research uses load flow-based analysis. The impact of distributed generation on the voltage profile of an LV distribution network at has been analysed in [118]. The analysis was further extended to include reverse power flow and unbalance in [119]. However, the DG considered in these are CHP units which have a different generation profile and performance as compared to the PV systems. Therefore, these results cannot be directly extended to analyse the impact of PV. The impact of location of PV on voltage fluctuations for a network in Canada at 50% penetration (12.5% as per our

definition) has been analysed in [28]. The authors observed that at 50% penetration, the maximum voltage at the furthest point from the substation was 1.03 p. u. at 900 W/m^2 irradiance, i.e. the voltage upper limit was not violated at 50% penetration of PV. The scenarios for evaluation of performance are a range of generation from 0 to 90% of the rated capacity of PV and range of loads from no load, light load (1.1 kW/house) to peak load (7.5 kW/house). An analysis of a feeder containing more than a thousand customers, considering the single-phase nature of house loads and its variability, was performed by authors in [29] using an unbalanced load flow based approach. The authors used synthetic 1-minute load data generated using the algorithm given in [121] and irradiance from one clear sunny day in summer and winter each to calculate the load profile across the feeder for different instances of time. The authors observed that at 50% penetration (82% as per our definition if the after diversity maximum demand is assumed as 1.3 kVA as the network is part of an actual network in the UK), the voltage mean does not violate the upper limit. However, the authors do not provide the range of irradiance levels and the loads on the days considered. Also, the use of an average of the voltage at each point over a day results in more optimistic results as the average tends to cancel the voltage rise at high generation against the voltage drops at peak loads. An unbalanced load flow based approach was further used in [32] on hypothetical networks representative of urban, semi-urban and rural networks to evaluate the impact of PV on the voltage fluctuation. However, the author considers a no-load scenario to evaluate the hosting capacity which results in a pessimistic limit as the load in the network is never zero. A dynamic model based approach is used to evaluate the impact of PV on the voltage profile of a distribution network in [31]. The authors use the distribution network as described in [118] along with typical summer load and irradiance profiles and observed that even at 50% penetration of PV, which translates to 115% as per the definition used in this research, the voltage profile was

within the limits. A load flow based approach utilizing 1-minute synthetic load profiles and satellite-based hourly irradiance data interpolated to obtain a 1-minute resolution data were proposed in [120]. The author uses a correlation of load with irradiance to evaluate the performance of the distribution network with PV. This paper adopts a similar strategy of correlation of irradiance with load profile, utilizing the measured data of load and irradiance in the UK, to identify the realistic worst-case conditions to evaluate the hosting capacity of the network.

The next parameter that is affected by the presence of PV is the total harmonic distortion (THD) of current. The measurement of THD in a network with 19 single-phase PV systems showed that the THD was within the limits [122]. However, the measurements at nine inverters given in [27] showed that the upper limit of current THD was violated by one of the inverters. The authors attribute this violation of THD to the type of inverter used as the THD was always greater than 8% irrespective of the DC power input. The authors of [40] observe that the harmonics introduced by PV are dependent on the existing harmonics in the transmission network introduced by non-linear loads in the network. However, the literature focuses on single PV system connected to the distribution network and has not considered the impact of multiple single-phase PV systems on the distribution network. This research aims to evaluate the impact of PV on the distribution network assuming linear loads i.e. with no existing harmonics in the grid.

Another parameter that is affected by the presence of PV systems is the net power flow at the substation. When power generated by the PV systems is higher than the load in the feeder supplied by the substation, it results in a reversal of the direction of power flow at the substation. Though reverse power flow is mentioned as a factor to be considered in the performance analysis, it has not been discussed in detail in any of the above studies on the steady-state performance of the distribution network

with PV or as a factor affecting the contribution of the PV system. The power factor at the substation is also affected by the presence of PV systems. Currently, all commercial PV inverters operate at unity power factor. This affects the power factor as seen by the network operator. This research also observes the variation of power factor with increasing penetration of PV systems. Unbalance introduced by single-phase PV of capacity 6 kW each on a 6 bus network and a 28 bus network are discussed in [123]. The authors observed that the voltage unbalance does not reach 2% even when all the houses have a PV system. However, the authors consider that the phase at which PV is connected is independent of the phase at which the house is connected. This research evaluates the impact of unbalanced distribution of PV on the voltage unbalance at the substation.

5.2 Methodology of Steady-State Analysis

Steady-state analysis typically assumes that the changes to load and generation are small and happen at time intervals such that each instance can be considered individually as steady-state. The steady-state analysis is performed in two stages here. In the first stage, the single-phase feeder alone (sample network 1) is analysed and in the second stage, the three-phase distribution network (sample network 2) is analysed. In order to evaluate the performance of the distribution network, it is important to identify the different operating conditions of the distribution network, which can be described mainly in terms of the connected load and the irradiance. The irradiance level affects the actual contribution of the PV systems and in turn, affects the performance of the distribution network. The typical performance evaluation for the electricity network considered in the literature uses a worst-case scenario which is the maximum generation and after diversity minimum load. However, the probability of occurrence of such an operating condition is very low as the maximum generation from PV systems occur at noon and the minimum after diversity demand for the UK occurs in the early morning. A case study using the

irradiance data from Northumberland Building in Newcastle upon Tyne, UK and load data from the Customer Led Network Revolution (CLNR) project has been used to identify the more probable operating conditions of the distribution network in the UK (discussed in section 5.3). After identification of the probable operating condition, the contribution of PV systems is increased from 0% (no PV scenario) to 100% in steps of 10% to evaluate the impact of PV on the performance of the distribution network. The location of the PV system in the LV network is assumed to be distributed either near the substation or near the far end of the feeder. The next section defines the operating conditions of the distribution network under which its performance is evaluated.

5.3 Scenarios for Performance Evaluation – A Case Study Based Approach

The operation of the distribution network is controlled by the net load which is dependent on the connected load and the local generation. The generation from PV systems is dependent on the irradiance and the temperature, with a change in irradiance having a higher impact than the change in temperature. Irradiance falling on a horizontal surface and a south facing surface on Northumberland Building on the Northumbria University campus at Newcastle upon Tyne and measured at a 1-minute frequency over a three year period has been used for analysis as described in section 5.3.1. The load profile data from CLNR project are analysed as discussed in section 5.3.2. The irradiance and load profile data are correlated to arrive at the possible operating conditions of the distribution network as described in section 5.3.3.

5.3.1 Analysis of irradiance data of Northumberland Building, Newcastle upon Tyne

Irradiance data was collected as a part of the performance monitoring of the Northumberland Building 40 kW PV façade. The sensors were located on the roof of the building and measured irradiance on a horizontal surface and that on a south facing vertical surface. The irradiance on horizontal and south facing surfaces measured at 1-minute intervals from 1998 to 2000 was used to analyse the characteristics of irradiance. The erroneous data resulted in 24 days in three years to be ignored. The erroneous data was identified based on the meter showing a continuous constant value throughout the day. Bins of horizontal irradiance, with a bin size of 50 W/m^2, were created to plot the histogram of the irradiance. Figure 5-1 shows the histogram of the horizontal irradiance measured at Northumberland Building at 1-minute intervals over the three years. The bin 0 includes all values of horizontal irradiance between 0 and 49, including 0. The bin can be mathematically represented as [lower limit, upper limit). The measurement device recorded a value of +/-0.000049 kW/m^2 for 0 W/m^2. Therefore all irradiance values less than zero in

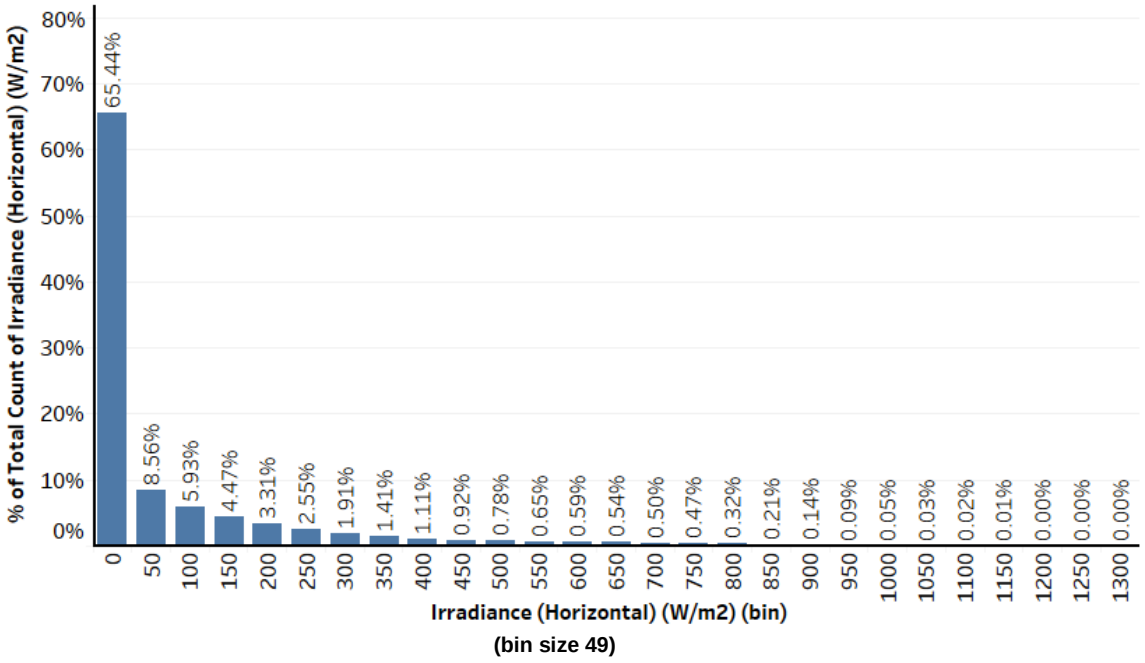

Figure 5-1: Histogram of horizontal irradiance measured in Newcastle upon Tyne from 1998 – 2000

the initial data were assigned as zero. The data of irradiance shows that around 0.06% of the total minutes in the three years, i.e. 5 hours in the three years, had horizontal irradiance greater than or equal to 1000 W/m^2 and around 0.87% of the total minutes in the three years, i.e. 71 hours, had horizontal irradiance greater than or equal to 800 W/m^2 excluding the 24 days of erroneous data. Figure 5-2 shows the histogram of irradiance on a south facing wall in Newcastle upon Tyne measured at 1-minute interval for the three years. It can be observed that the irradiance was greater than or equal to 1000 W/m^2 for 0.11% of the time, i.e. about 9 hours in the three years and greater than or equal to 800 W/m^2 for 1.76% of the time, i.e. about 144 hours in the three years. Considering the daylight hours instead of all the hours in the year, about 2% of the sunshine hours had horizontal irradiance greater than or equal to 800 W/m^2 and about 5% of the sunshine hours had irradiance on south facing wall greater than or equal to 800 W/m^2. In this research, the irradiance level is varied from 200 W/m^2 to 1000 W/m^2 in steps of 200 W/m^2 to analyse the impact of PV on the single-phase feeder. The results of performance evaluation of the single-phase feeder highlighted that the adverse impact of penetration of PV occurred mostly at high irradiance levels (as discussed in Section 5.4). Therefore,

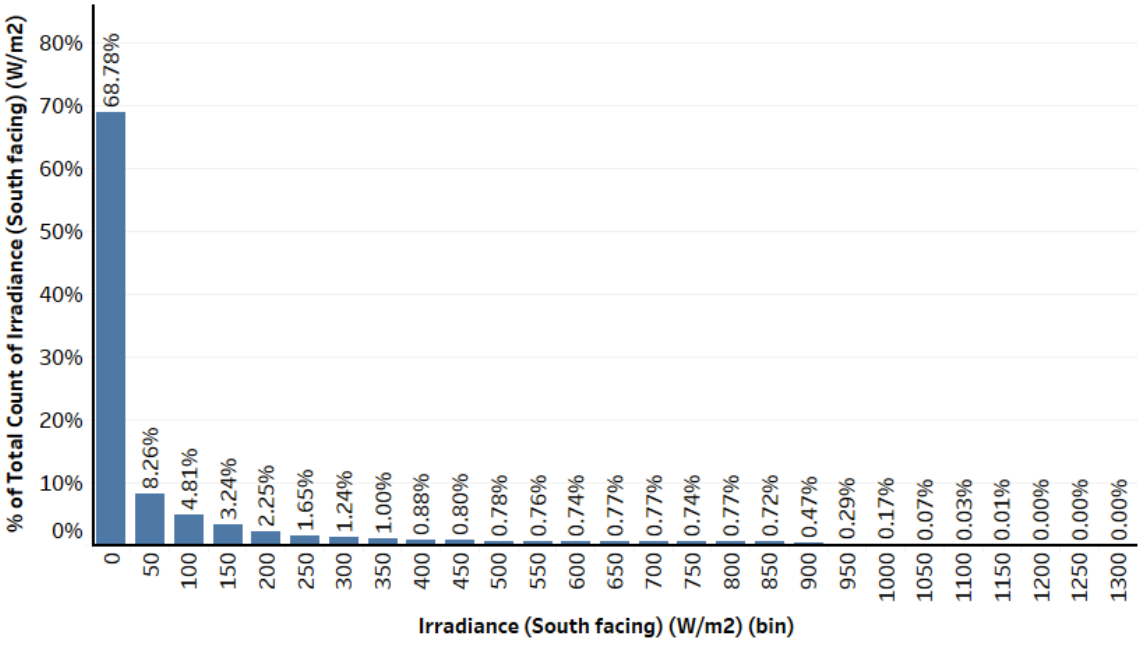

Figure 5-2: Histogram of irradiance on a south facing wall in Newcastle upon Tyne measured from 1998-2000

for the analysis of the three-phase network, a more probable high irradiance value of 800 W/m^2 is chosen based on the above analysis. However, the network is also analysed at 1000 W/m^2 irradiance level to compare the realistic worst-case results at 800 W/m^2 against the typical worst-case scenario considered in the literature.

5.3.2 Analysis of load profile data from Customer Led Network Revolution project

The load profile represents the pattern of electricity usage over a typical day, month or year. It is also sometimes aggregated as variations over a day for a particular season. With increasing penetration of distributed generation, electric vehicles, storage options and increasing interest in smart grids, it is all the more important to understand the load profile at the individual household level. Understanding of the load profile at house level provides better options for demand-side management as well as for prediction of the voltage fluctuations, peak loads and imbalances that can occur in the distribution network. There is a need to be able to generate load profiles at household levels replicating the characteristics of households with aggregate level data of that region. Newborough et al. have observed households in the UK with measurements being monitored at 30 households at time steps ranging from 1s to 10 minutes and conclude that the optimal time step for readings to reflect accurate load power and energy consumption to understand the factors influencing load profile is 1 minute [124].

There are two approaches to generate a load profile – top-down and bottom-up approach. The bottom-up approach has been more common in load profile generation and is typically based on statistics of ownership of different appliances at the national level. The prominence of the bottom-up approach is also due to the necessity of a large amount of data for the top-down approach, which is rarely available in the public domain. The literature on load profile generation based on

measured data uses data from around 5 to 100 households and typically at a 30-minute interval.

Details of the Data

Customer Led Network Revolution (CLNR) was a flagship project under Ofgem's low carbon network funds. The project monitored around 8,800 houses belonging to different categories/mosaic classes distributed across the UK at half-hour intervals for more than a year [125]. This dataset was the largest available measured value of loads at individual households monitored over more than a year. Though 1-minute interval was mentioned as more suitable than 30-minute interval to identify the factors influencing the load profile, i.e. to identify the type of load used in a given time-period, 30 minute time interval was chosen for this research as the focus was on the overall load profile not the characterisation of individual loads. Another factor that affected the choice is the number of houses monitored and the diversity of the types of houses which enables evaluation of the load profiles for different categories of households in the UK.

Around 11,000 houses were initially identified for the CLNR trials. All houses belong to one of the 15 classes of houses (Mosaic classes) identified by Experian. The different classes and their percentage populations in the UK are as given in [125] and is provided in Appendix E. 8811 houses were monitored at half hourly intervals over a period starting from 01/10/2009 to 31/03/2014. The percentage of houses monitored belonging to each category is as given in Appendix E. As this percentage is different from the percentage of houses for each class in the UK, the measured data cannot be directly averaged to generate an average demand profile as a representative of the demand profile of a typical distribution network in the UK. Another inconsistency in the data is that not all houses were monitored for the entire duration and not all measurements started at the beginning of the month. However,

all days monitored had 48 data points i.e. measurements were complete for each day of the measurement period. The data was available in two ".csv" files, the first one containing the information of location id, measurement date and time, measurement type and measurement. The second file contained the information of location id, mosaic class, measurement start and end dates and tariff type.

After diversity load profile as seen from the secondary substation

The proposed method uses data available from CLNR trials to generate typical after diversity load profile for households in the UK using the UK national average percentage composition of households. The steps to calculate the after diversity load profile, using Tableau software, are:

1. Two CSV files containing the data, as mentioned in the previous section, were joined by matching the "location id" of both the files
2. Any zero values indicate an error in measurement. The data was checked to identify any such errors and any missing measurements. The data did not have any zero values or missing data points.
3. The data was checked for British Summertime corrections but required no adjustments. Any such change in time would have resulted in one day in a year with 50 data points per household and one day with 46 data points per household. However, there were no such days in the data. This implied that the data was measured on Greenwich Mean Time (GMT). No particular corrections were done to this time as the data on irradiance also used GMT to record the data.
4. The average demand profile for each category of the household for each day of the year was created. The after diversity load profile was calculated for each day of the year using a weighted average of the average demand profile for each category of the household. The weight of the average for each

category was the percentage of that category of household in the UK national average.

Figure 5-3 shows the after diversity load profile of a household in the UK for a year. From the figure, it can be observed that the minimum load of 150 W occurs during the time interval 1 a.m. to 4 a.m. and that the load during hours of daylight is almost always higher than the minimum load of the individual households. The minimum load during hours of daylight is greater than 300 W and occurs during the time interval 12 noon to 3 p.m. The minimum load of 150 W occurred in the month on September and the minimum load of 300 W occurred in the month of July.

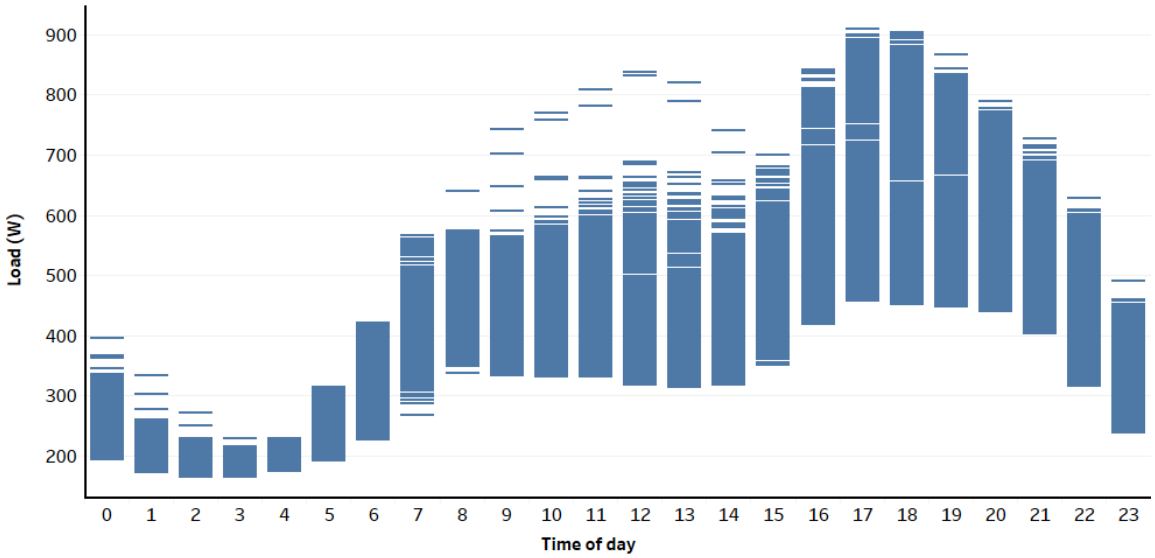

Figure 5-3: After diversity demand profile of a household in the UK over a year

5.3.3 Correlation of irradiance with load profile

The 1-minute irradiance values on the horizontal and south facing wall were averaged over half hour intervals. The half-hour irradiance values at Newcastle were correlated to the half-hourly after diversity load profile as shown in Figure 5-4(a) and (b). From the figures, it can be observed that for high irradiance levels (>600 W/m^2) on both horizontal and south facing wall, the load is always greater than 300 W. The after diversity minimum demand for the network under consideration is 160 VA @ 0.95 p. f. lagging.

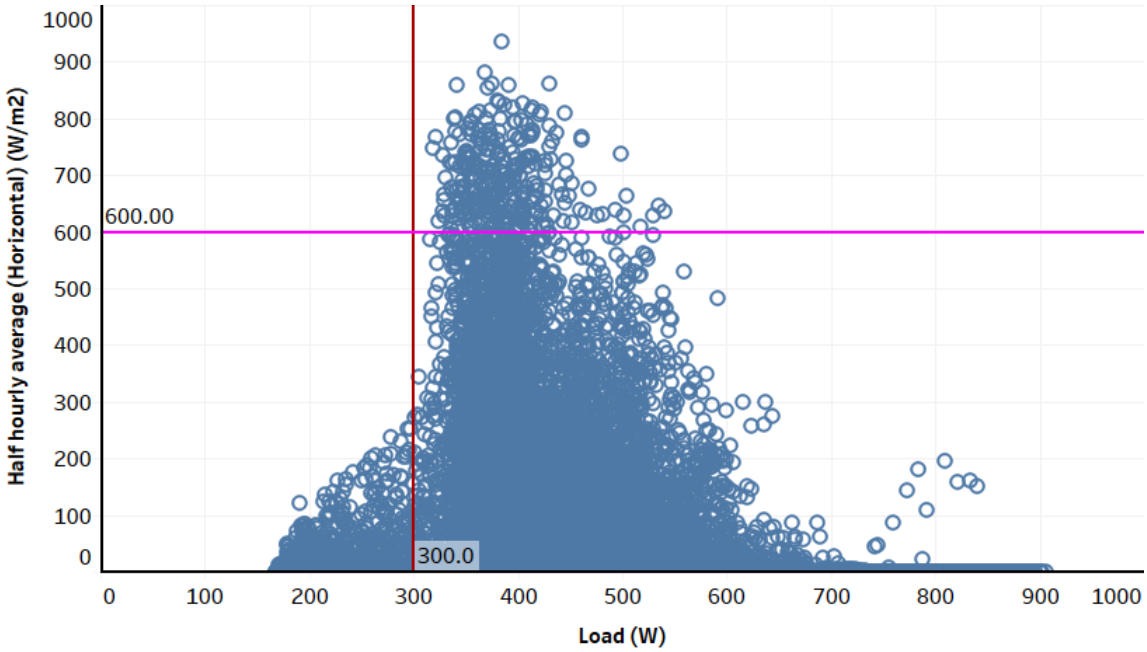

(a) Horizontal surface

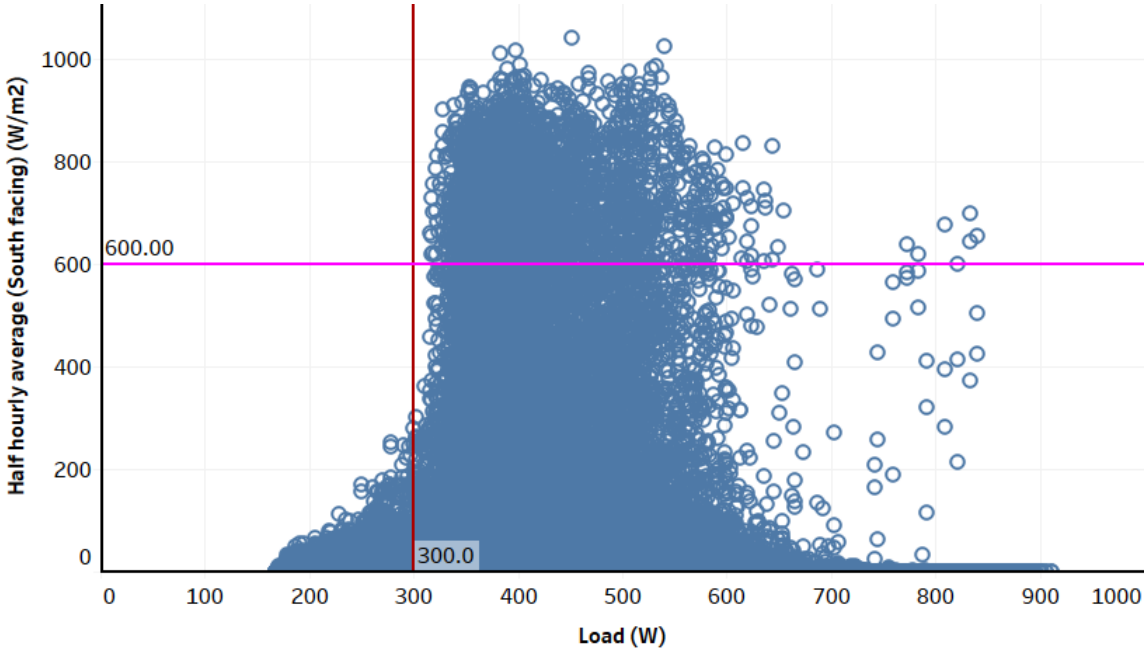

(b) South facing vertical surface

Figure 5-4: Plot of irradiance on horizontal and south facing vertical surface vs. load

5.3.4 List of scenarios for evaluation of performance

The performance of the single-phase feeder was analysed by evaluating its performance for the following different values for the parameters

a) Load: Minimum load (152 W per household), Minimum daytime load (300 W per household),

b) Irradiance: 200 – 1000 W/m^2 in steps of 200 W/m^2

c) PV location – near the substation, far from substation

d) Substation no-load voltage – 250 V, 240 V and 230 V

e) Percentage of PV – 0 to 100% in steps of 10

The percentage penetration of PV has been defined as the ratio of total PV capacity to the after diversity maximum demand of the feeder (number of houses times the after diversity maximum demand of individual house). The results of the single-phase analysis indicated that as the penetration level increases, the impact of PV on the distribution network performance was higher at high irradiance levels than at low irradiance levels as would be expected. To evaluate the performance of the three-phase distribution network the following scenarios were chosen based:

1. Typical worst-case scenario: Minimum load (152 W per household) and irradiance of 1000 W/m^2
2. Realistic worst-case scenario: Minimum load during hours of daylight (300 W per household) and irradiance of 800 W/m^2
3. Futuristic scenario: Load of 500 W and irradiance of 800 W/m^2

The values for the different parameters for three-phase analysis are:

a) PV location clustered at the far end of the feeder

b) PV distribution – balanced across three phases; unbalanced with all PV in one phase

c) Percentage of PV – 0 to 100% in steps of 10 for balanced distribution; 0 – 60% in steps of 10 for unbalanced distribution (limited to 60% as when percentage PV penetration is greater than 60%, all houses in one phase of the detailed feeder would have PV and additional PV would be distributed in the second phase)

d) PV power factor – unity power factor, 0.98 p. f. leading (generator convention), 0.95 p. f. lagging (generator convention)

5.4 Results of Steady-State Analysis of the Single-Phase Feeder

The performance of the single-phase feeder was evaluated in terms of the voltage profile, total harmonic distortion at the secondary of the substation, net real power at the distribution substation and power factor at the distribution substation. The distribution substation is marked as bus '0' in Figure 4-27. At irradiance levels less than 800 W/m^2 the penetration level at which the performance is adversely affected is higher than those at irradiance levels greater than or equal to 800 W/m^2 as discussed in Appendix F. Therefore, the following sections focus on the impact of PV on the performance of the single-phase feeder at irradiance levels of 1000 and 800 W/m^2.

5.4.1. Voltage profile

Figure 5-5(a) shows the voltage profiles (in p. u. at 230 V base) of the single-phase feeder for minimum loading of 152 W per household at different penetration levels of PV under irradiance of 1000 W/m^2 and with PV distributed near the distribution substation i.e. PV is connected to houses in bus 1 and as the penetration increases to bus 2. Figure 5-5(b) shows the voltage profiles for PV located at the far end of the feeder i.e. bus 6. The voltage at each bus is within the statutory limits of +10% and -6% [126] for penetration of PV up to 50% for PV located near the substation and up to 20% for PV located at the far end of the feeder. This is in line with the existing literature which indicates upper voltage limitation being violated when PV is located at the far end of the feeder [28, 29]. The voltage profiles for minimum load during hours of daylight (300 W) and irradiance of 800 W/m^2 indicates that the upper voltage limit is not violated for up to 80% and 40% penetration of PV, for PV located

near the substation and at the far end of the feeder respectively, as shown in Figure 5-6(a) and (b).

5.4.2. Total harmonic distortion

Figure 5-7 shows the variation of THD of the current at the secondary of the substation transformer at different penetration levels of PV systems for irradiance

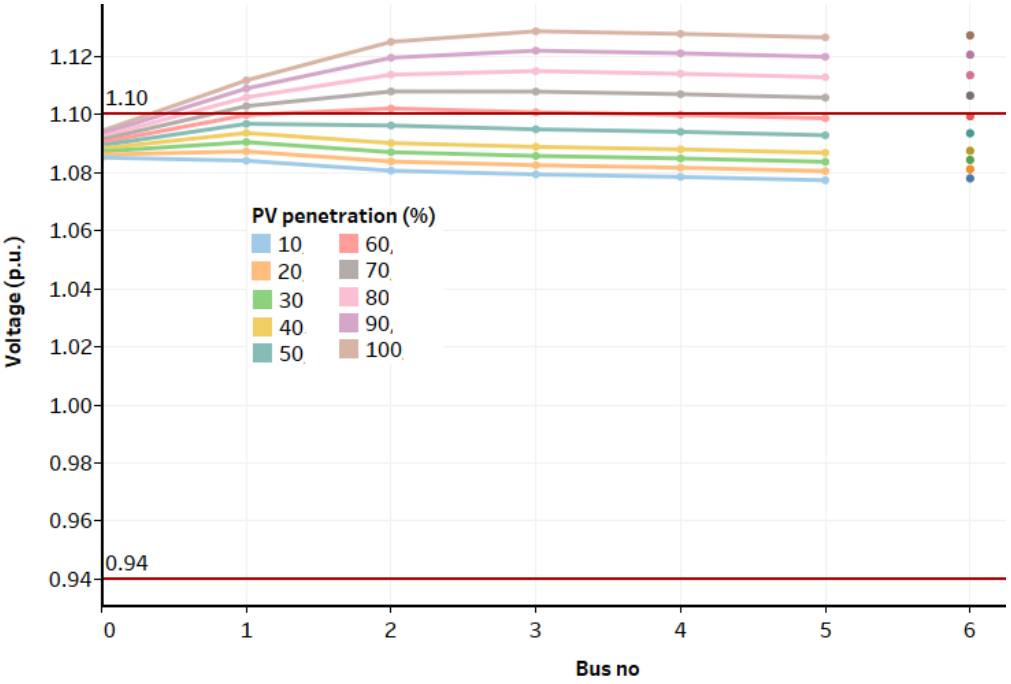

(a) PV distributed near the distribution substation

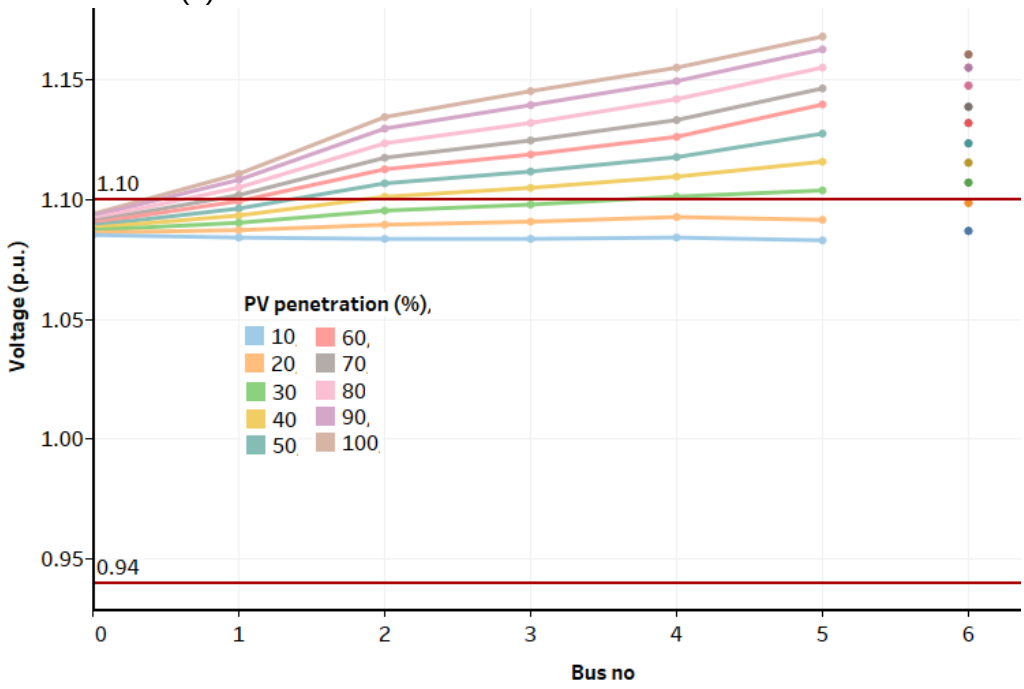

(b) PV distributed at the far end of the feeder

Figure 5-5: Voltage profile for minimum load of 152 W and irradiance of 1000 W/m² at different penetration levels for different PV locations

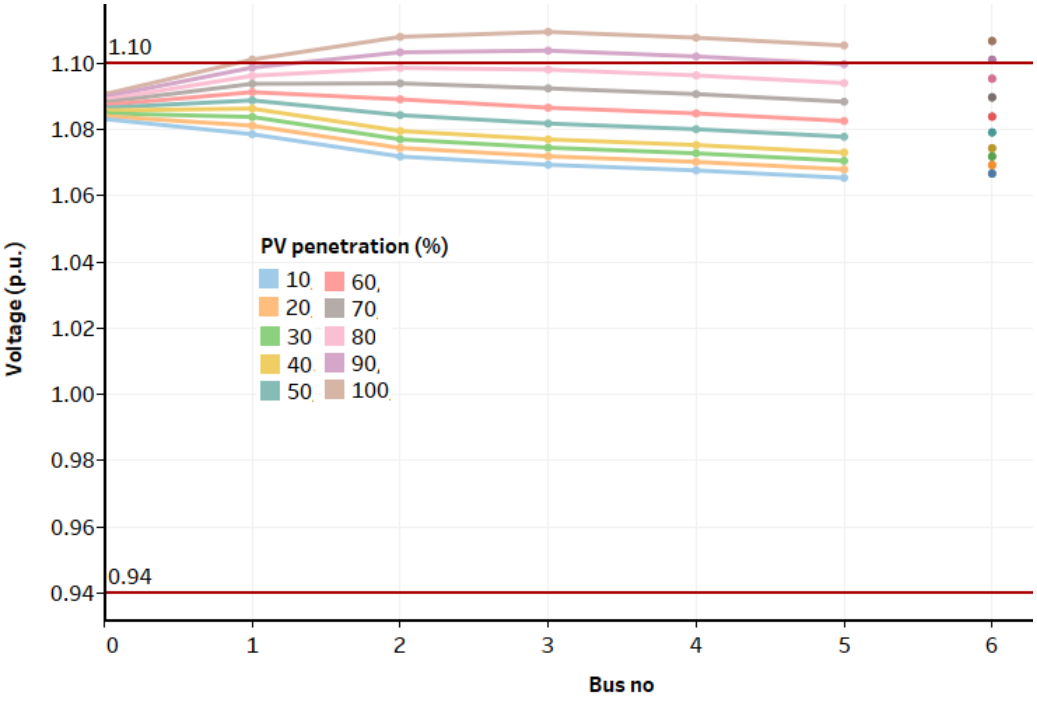

(a) PV distributed near the distribution transformer

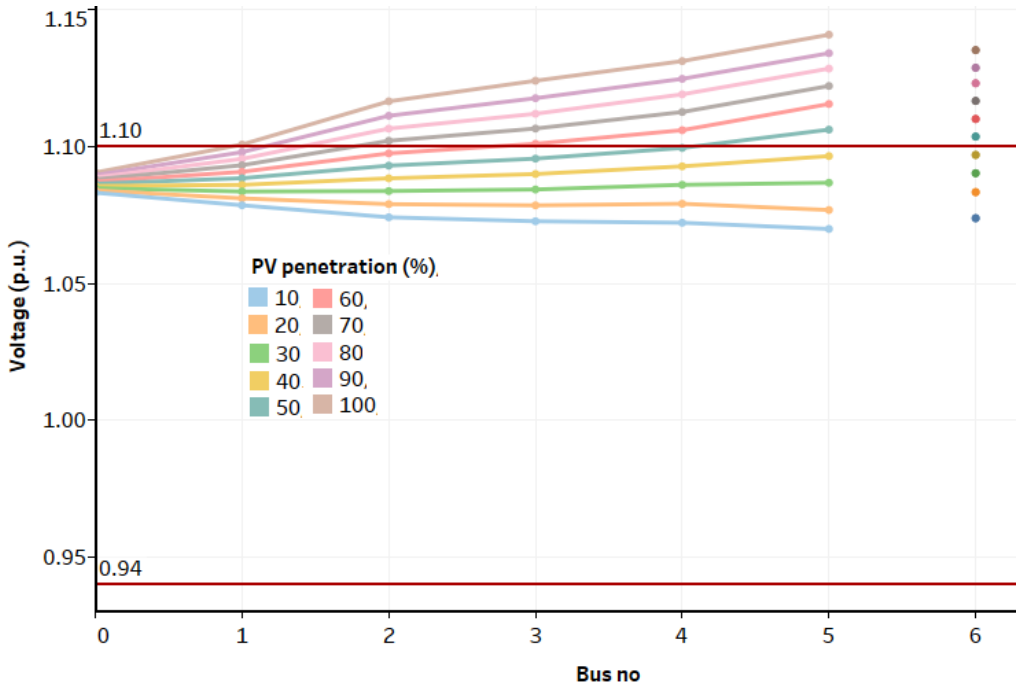

(b) PV distributed at the far end of the feeder

Figure 5-6: Voltage profile for load of 300 W, irradiance of 800 W/m^2 and different PV locations

levels of 1000 W/m^2 and 800 W/m^2 and a load of 152 W and 300 W for PV distributed near the substation at different penetration levels. For the typical worst-case scenario considered in the literature, the THD of current is greater than 5% at 10% penetration of PV systems. However, when the realistic worst-case scenario is considered the THD of current is greater than 5% at 20% penetration. The

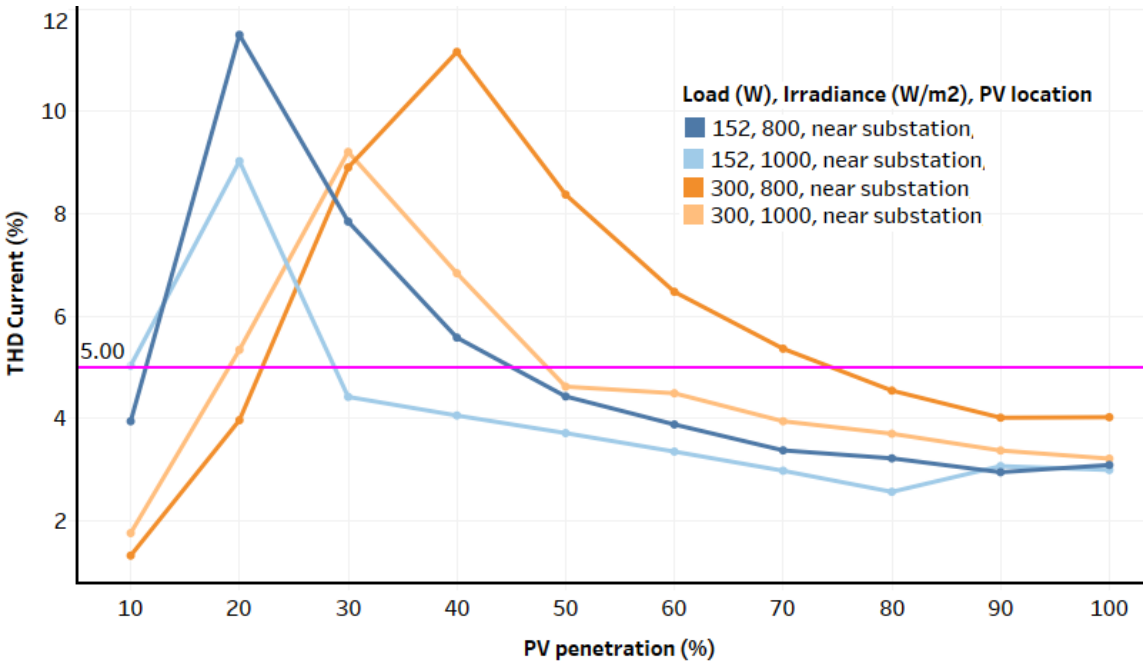

Figure 5-7: THD of current at the secondary of the distribution transformer for different penetration levels for loads of 152 W and 300 W with PV distributed near the substation for irradiance levels of 1000 and 800 W/m²

guidelines limit the voltage harmonics and therefore, it is desirable to limit the current harmonics as increase in current harmonics in turn results in an increase in voltage harmonics. The presence of non-linear load or background voltage harmonics (harmonics in the grid voltage before PV is connected) may aggravate the THD of current. The location of PV does not have a significant impact on the THD of current at the substation. The peak of THD occurs at the penetration level when the active power demand of the load is almost completely met by the PV generation as at that point only harmonic currents will be circulating through the distribution network.

5.4.3. Net power at the distribution substation

Figure 5-8 shows the variation of net active power at the secondary of the substation transformer for different penetration levels and for irradiance levels of 800 and 1000 W/m². Net power has been considered negative when power is fed by the grid and positive when the power is fed to the grid. Positive net power indicates that the generation is higher than the load in the feeder. Typical distribution network has been designed for power flow from the substation to the loads and when the

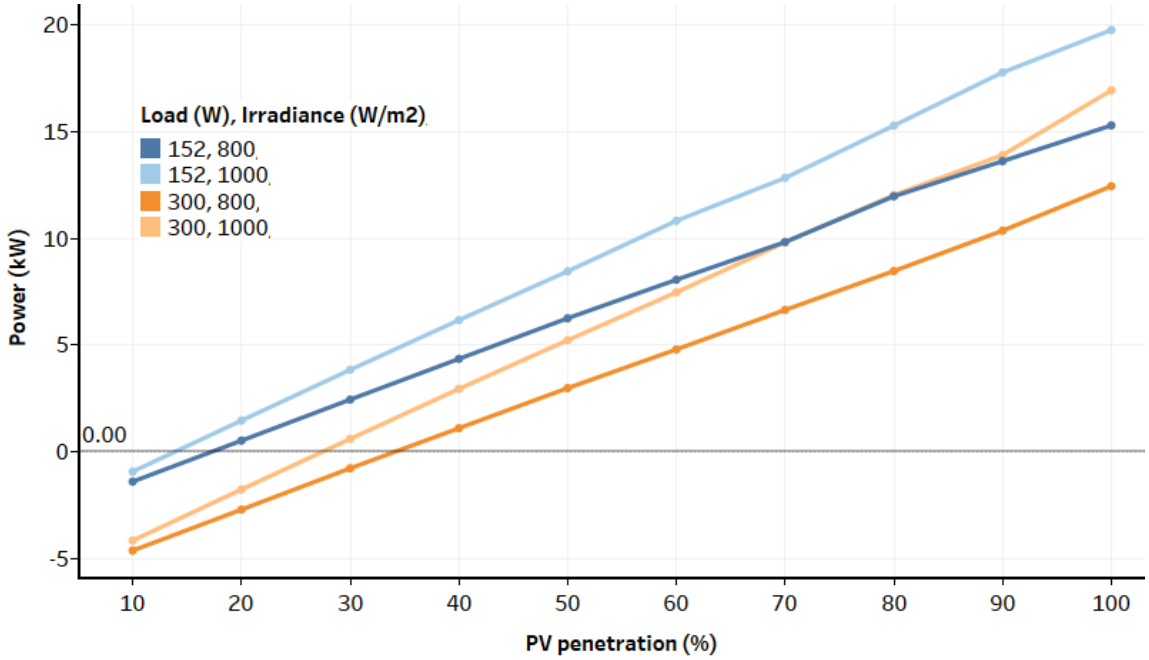

Figure 5-8: Net active power flow at the substation transformer for different penetration levels of PV for different scenarios

direction of this power flow changes, it is termed as reverse power flow. For the typical worst-case scenario, the reverse power flow occurs when the penetration of PV increases above 10%. For the realistic worst-case scenario, the reverse power flow occurs at greater than 30% penetration of PV. The penetration level at which reverse power flow occurs is independent of the location of PV on the feeder. However, it is dependent on the load profile and maximum local irradiance at the feeder. Even a very small reverse power flow for a duration less than 3 cycles may result in tripping of network protectors and create an island at 480 V in distribution networks in the US [127]. However, the substation transformers at 11/0.433 kV in the UK typically does not have directional protection. When the overall penetration increases the reversal would be reflected at the 33/11 kV transformer which typically has directional protection.

5.4.4. Power factor at the distribution substation

Figure 5-9 shows the variation of power factor at the substation transformer for different penetration levels and irradiance of 800 and 1000 W/m^2. When the PV inverter is operating at unity power factor, the power factor at the secondary of the

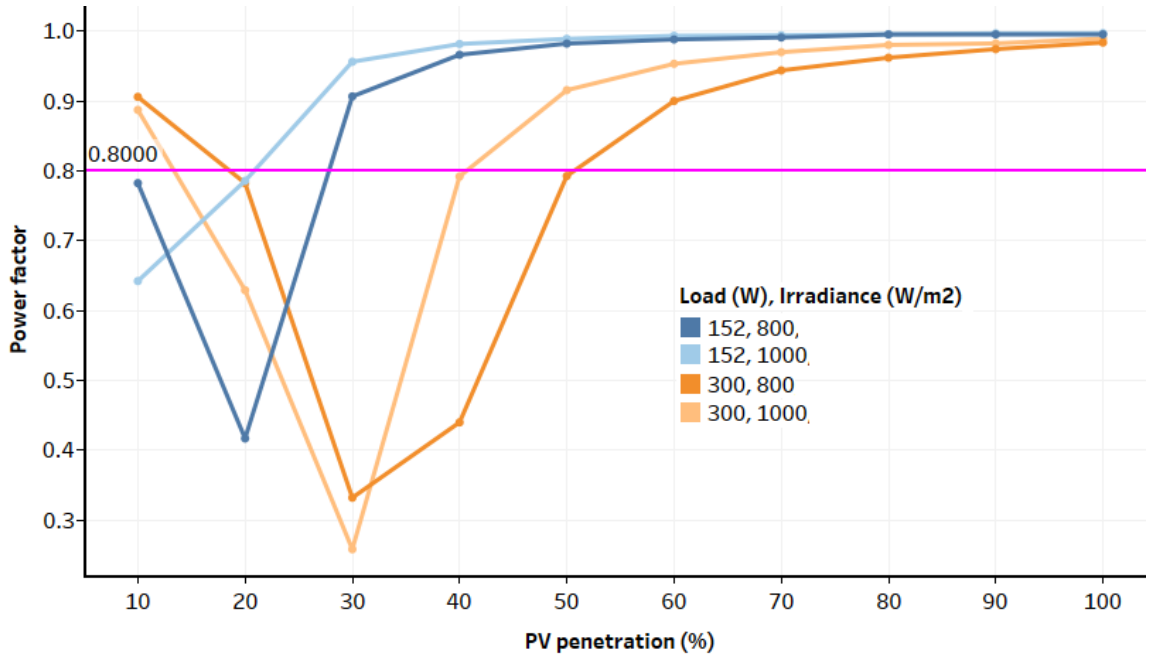

Figure 5-9: Power factor at the substation for different penetration levels of PV

substation transformer goes below 0.8 lagging at 10% penetration of PV system for the typical worst-case scenario of 1000 W/m^2 irradiance and 152 W load. When the PV penetration level increases, the real power requirement of the loads is increasingly met by PV generation reducing the net real power demand at the secondary of the substation. Since the inverter is usually operated at unity power factor and the reactive power demand of the load remains constant, the increase in penetration of PV and/or irradiance would result in a reduction of power factor at the secondary of the substation.

The increase in power factor in the right-hand part of the graph is due to the increase in reverse power flow when the PV penetration level increases further, i.e. the real power being supplied to the transformer is increasing while reactive power is still being drawn from the transformer to meet the load demand. If the realistic worst-case scenario of 300 W load and 800 W/m^2 irradiance is considered, the power factor goes below 0.8 lagging at a penetration level of 20%. This is well before the violation of voltage limits of the feeder and forms a barrier to increase the contribution of PV.

5.4.5. Impact of change in substation tap-changer on the performance parameters

The 11/0.433 kV substation has an offload tap changer which is typically set to maintain a fixed value slightly higher than 433 V (line to line) under no load conditions. The substation voltage is maintained at higher than the nominal value to ensure that the voltage across the feeder remains within limits at different loading conditions. When the tap changer of the substation transformer is set to reduce the secondary voltage to 415 V (line to line) or 240 V (phase to neutral), the upper limits of the voltage at individual households is not violated for up to 100% penetration even when PV is clustered at the far end of the feeder as shown in Figure 5-10. However the power factor falls below 0.8 at lower penetration level than when the substation voltage was maintained at 250 V. Maintaining unity power factor at the inverter may be beneficial for the customer, but, from the substation point of view, it would be more beneficial if the PV inverter could supply some reactive power i.e. the PV inverter operated at lagging power factor. The power factor at which each inverter should operate in order to maintain near unity power factor at the secondary

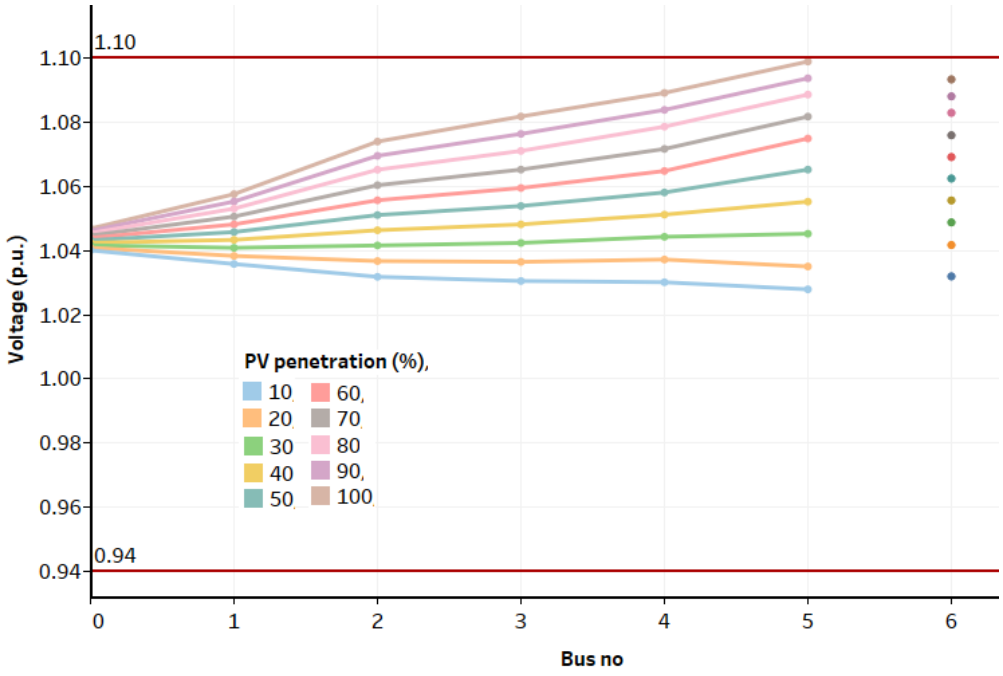

Figure 5-10: Voltage profile (in p. u. on 230 V base), of the single-phase feeder for different penetration levels for reduced substation voltage of 240 V

of a substation transformer is dependent on the load power factor and penetration level of PV. Also, the maximum reactive power that each inverter can supply is dependent on the irradiance at that instant and the rating of the inverter with respect to the rating of the PV system.

5.5 Results of steady-state analysis of the three-phase distribution network

The performance of the three-phase distribution network is also analysed in terms of the voltage profile, total harmonic distortion at the substation, net real power flow at the substation and power factor at the substation. The substation is marked as bus '0' in Figure 4-26. The impact of the change of operating power factor of PV systems from unity power factor to 0.98 p. f. lagging and 0.95 p. f. lagging is also discussed. The impact of unbalanced distribution of single-phase PV on the performance parameters is also analysed.

5.5.1. Voltage profile

Figure 5-11 shows the voltage profile of the three-phase distribution network for a minimum load of 152 W and maximum solar irradiance of 1000 W/m^2 and Figure 5-12 shows the voltage profile for the more probable scenario of 300 W load and 800 W/m^2 irradiance. The increase in substation voltage for an increase in load from 152 W to 300 W is due to the action of the tap changer. The tap setting at the 33/11 kV transformer changes from 0 to -1 when the loading changes from 152 W load to 300 W. For the typical worst-case scenario, the voltage at buses at the far end of the feeder exceed the upper voltage limit when the percentage of PV reaches 30%. However, for the realistic worst-case scenario of 300 W and 800 W/m^2, the voltage at most of the three-phase feeder exceeds the upper voltage limit as penetration of PV increases beyond 20%. This implies that the hosting capacity of the network would be around 20% of the after diversity maximum demand of the network or in

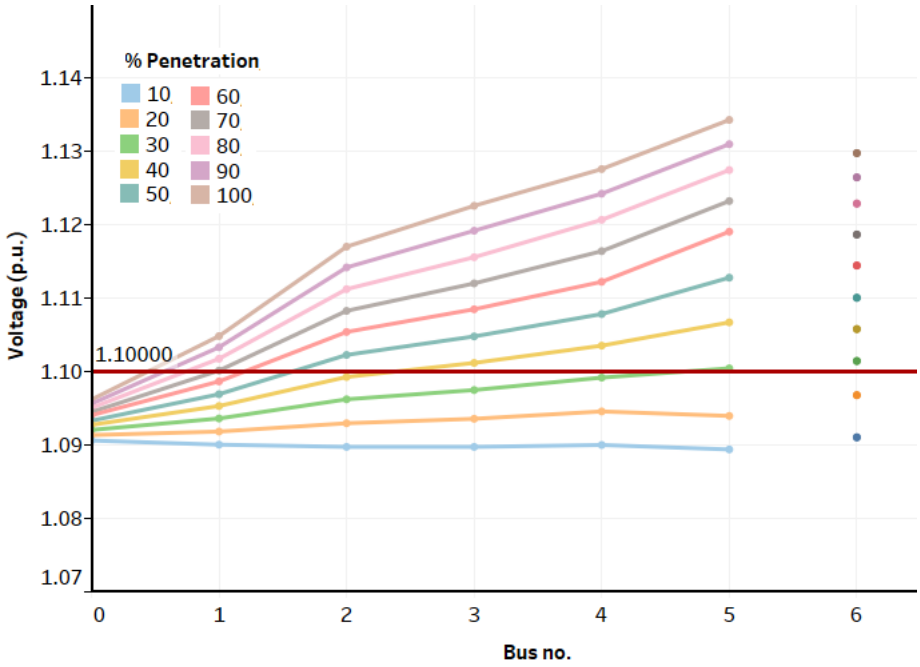

Figure 5-11: Voltage profile of the three-phase distribution network for different penetration levels of PV systems at load of 152 W and irradiance of 1000 W/m²

terms of the number of houses, around 10% of houses with PV of average system size 2.5 kWp would result in voltage limits being violated for the realistic worst-case scenario. The hosting capacity is also dependent on the voltage step per tap and the number of taps in the transformer. For a slightly higher average load per household of 500 W, the voltage at the buses does not violate the upper limit for

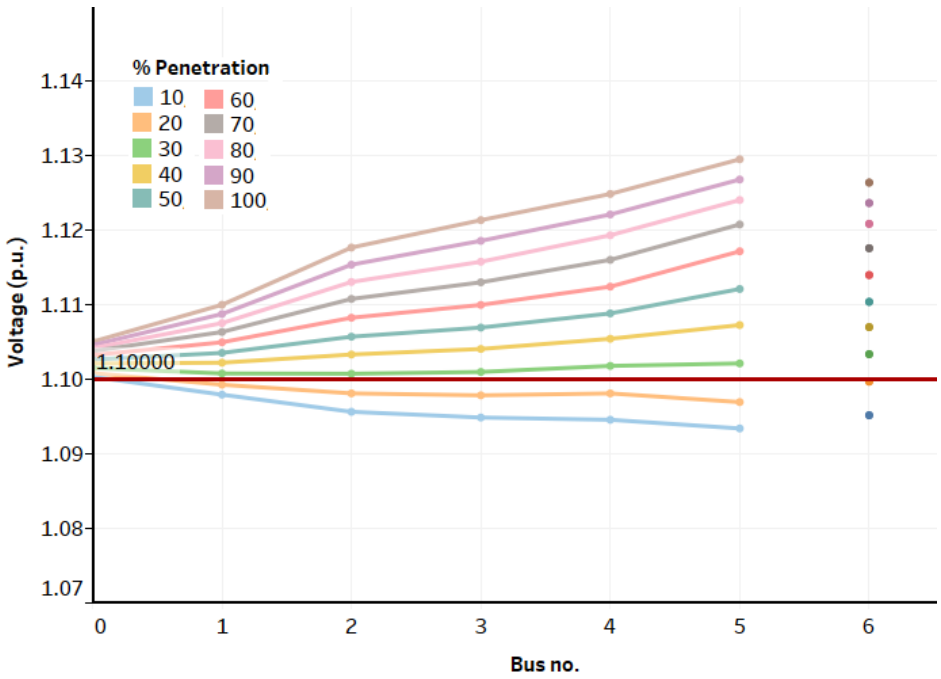

Figure 5-12: Voltage profile of the three-phase distribution network for different penetration levels of PV systems at load of 300 W and irradiance of 800 W/m²

percentage penetrations up to 90% as shown in Figure 5-13.

5.5.2 Total harmonic distortion at the distribution substation

The THD of the voltage is not significantly affected by the presence of multiple single-phase PV systems. The THD of current at the secondary of the substation for the typical worst-case scenario of 152 W load and 1000 W/m^2 irradiance is below 5% for different penetration levels of PV as shown in Figure 5-14(a). For the more probable scenario of 300 W load and 800 W/m^2 irradiance, the THD of current is less than 3% at all penetration levels as shown in Figure 5-14(b). For the scenario with 500 W load and 800 W/m^2 irradiance, the THD of current at the secondary of the substation is less than 5% for different penetration levels of PV (Figure 5-14(c)). From the results, it can be observed that THD of the system is not significantly affected by the presence of PV when there are no pre-existing harmonics in the grid.

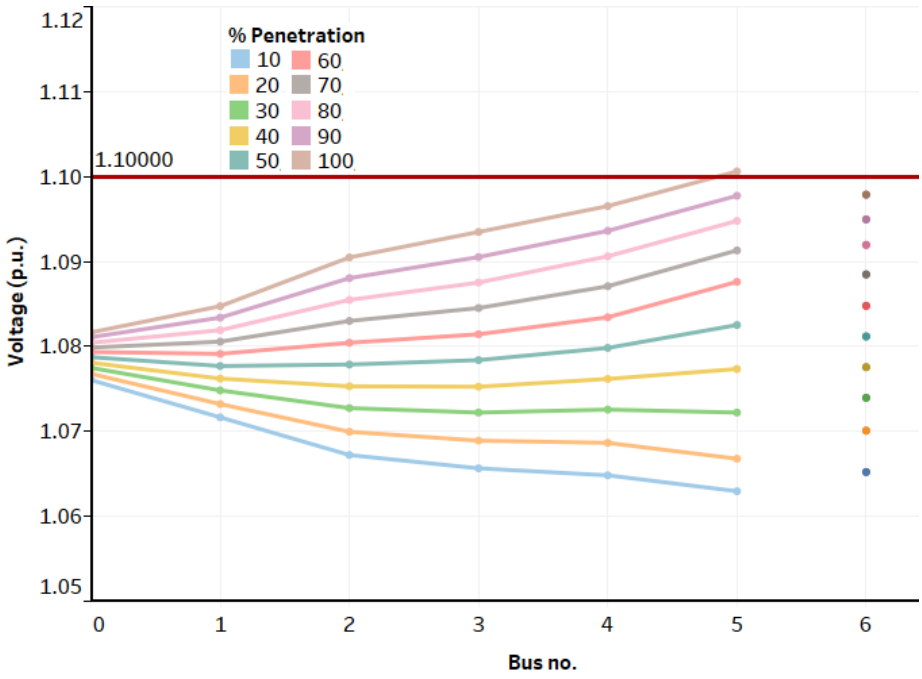

Figure 5-13: Voltage profile of the three-phase distribution network for different penetration levels of PV system at 500 W load and 800 W/m^2 irradiance

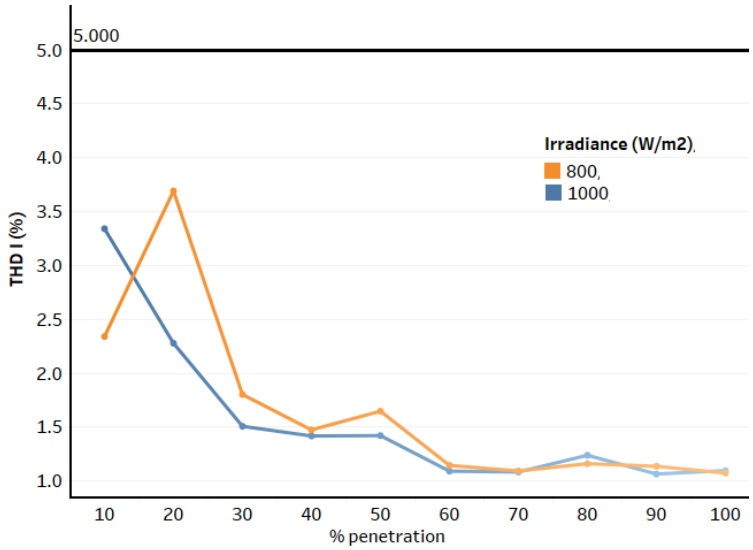

(a) Typical worst-case scenario

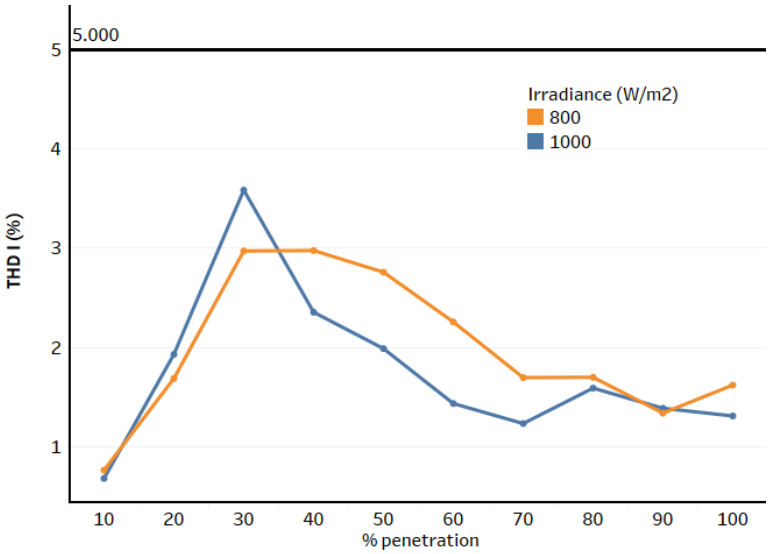

(b) Realistic worst-case scenario

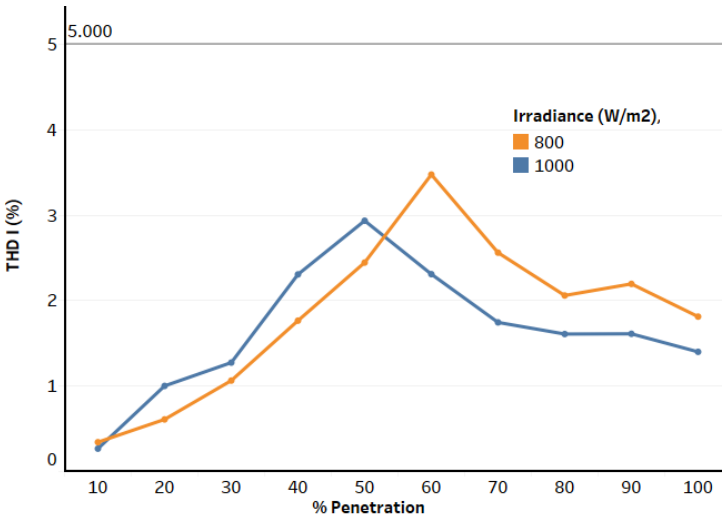

(c) Futuristic scenario

Figure 5-14: Total harmonic distortion of current at secondary of substation for typical worst-case scenario and realistic worst-case scenario

5.5.3 Net power at the distribution substation

The net power at the substation becomes positive at less than 20% penetration of PV systems under minimum load and maximum solar irradiance of 1000 W/m^2 (Figure 5-15). This implies that with just 42 of 384 houses having a single-phase PV system of 2.5 kWp each this would result in a reverse power flow at the supply transformer of the feeder when worst-case scenario is considered. For the more probable scenario of 300 W and 800 W/m^2 irradiance, the net power reverses at around 30% penetration of PV systems. For this scenario, more PV can be installed without adversely affecting the performance of the distribution network, with the increase in PV being approximately 40% if we consider the number of houses or 50% if we consider the rating of the PV systems. The net power at the substation becomes positive only after 50% penetration if the 500 W load and 800 W/m^2 irradiance is considered. That is, when 105 of 384 houses (around 30% of houses) have PV installed, reverse power flow at the substation occurs in this scenario.

5.5.4 Power factor at the distribution substation

It is preferred to have a power factor as close to unity as possible as a lower power

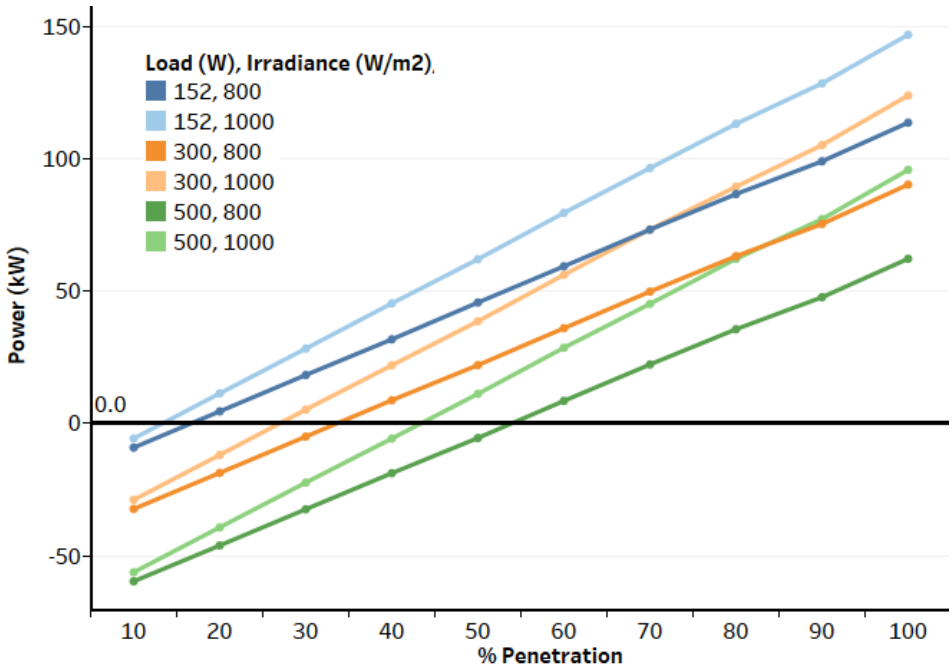

Figure 5-15: Net power at the secondary of the substation for different penetration levels of PV and different loading conditions

factor means the grid capacity has to be higher to transfer the same amount of real power to the loads. As most commercial PV inverters are operating at or close to unity power factor, the reactive power requirement of the loads remains unchanged with the installation of PV systems. As seen from the substation, this implies that the power factor deteriorates with increasing penetration of PV as shown in Figure 5-16. This is irrespective of the load power factor. The increase in power factor after it reaches its minimum is due to the reversal of the direction of real power flow. It can also be observed from Figure 5-16 that when the load on the feeder increases or the solar irradiance level reduces the percentage contribution of PV can reach higher values without decrease of power factor at the substation. It should, however, be noted that the deterioration of power factor does not indicate an increase in the reactive power requirement of the loads which commonly occurs in a system with low power factor. The distribution network operator should look at the absolute value of reactive power before deciding on taking actions to improve the low power factor at the substation level. The power factor at 30% penetration for 300 W load at 1000 W/m^2 and 800 W/m^2 has the same magnitude, but the direction of active power

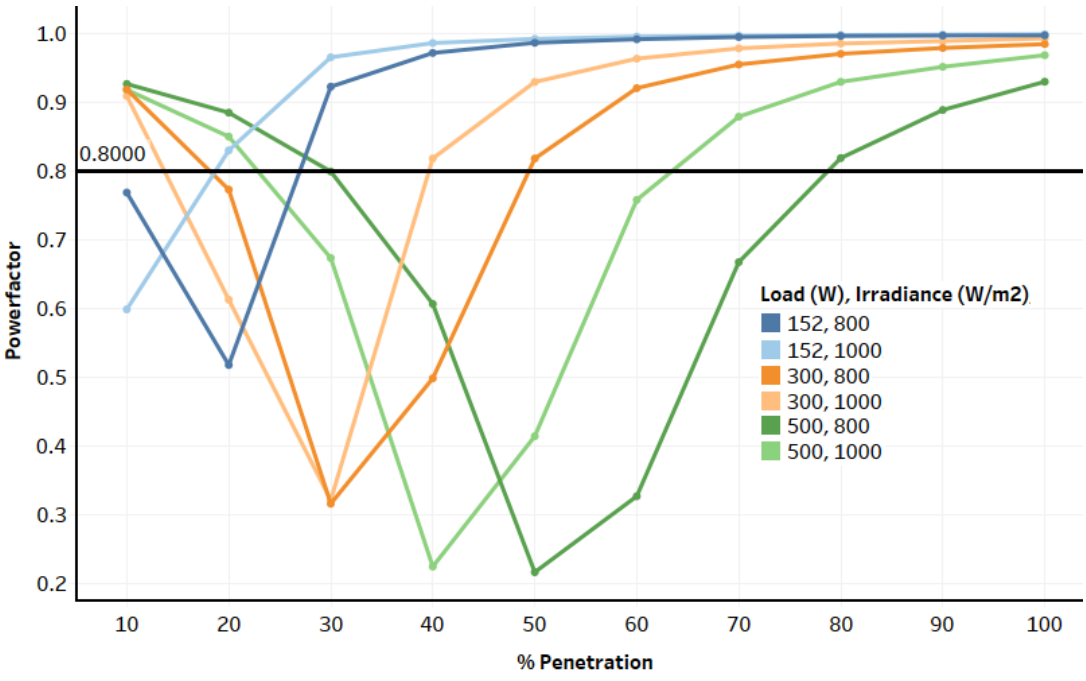

Figure 5-16: Power factor at the secondary of the substation for different penetration levels of PV and different loads

is different. At 800 W/m^2, the direction of active power is from the substation to the feeder whereas at 1000 W/m^2 the direction of active power is from the feeder to the substation as generation is higher than load.

5.5.5 Impact of change in operating power factor of PV on the performance parameters

To observe the impact of the reactive power supply by PV systems, the PV systems were made to operate at 0.98 pf and 0.95 pf lagging (using a generator convention, i.e. exporting/supplying reactive power). The UK guidelines allow the operation of PV systems between 0.95 pf lagging and 0.95 p. f. leading [86], though commercial inverters are typically set to operate at unity pf. The simulations were performed for penetration levels from 0 to 100% in steps of 10%. From Figure 5-17, it can be observed that the power factor at the substation is best under all penetration levels when PV systems are operating at 0.95 p. f. lagging. However, the 0.95 p. f. and 0.98 p. f. lagging operation of PV system results in the voltage profile violating the upper limit at 20% penetration of PV system as shown in Figure 5-18(a) and (b). Figure 5-19 shows the net reactive power at the substation for different penetration

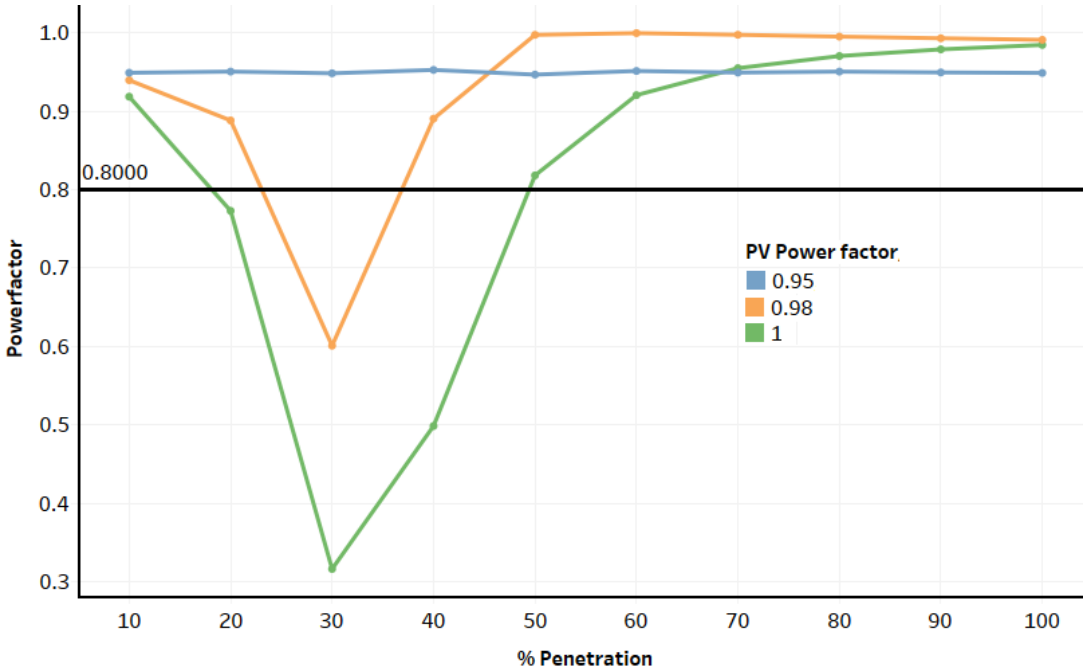

Figure 5-17: Power factor at the secondary of the substation for different penetration levels of PV at 300 W load and 800 W/m^2 irradiance with PV operating at different power factors

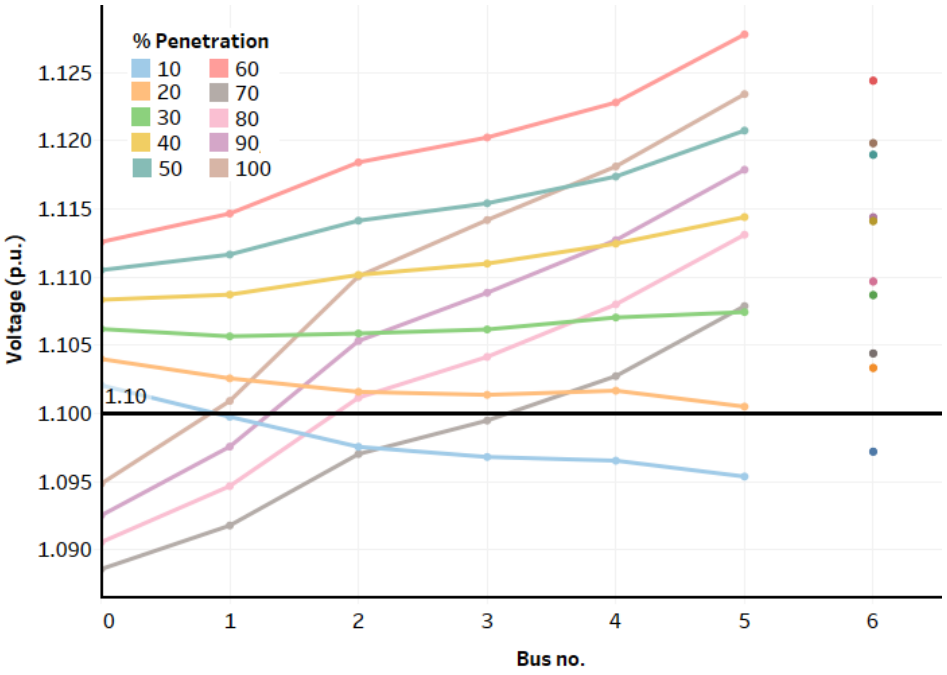

(a) 0.95 lagging

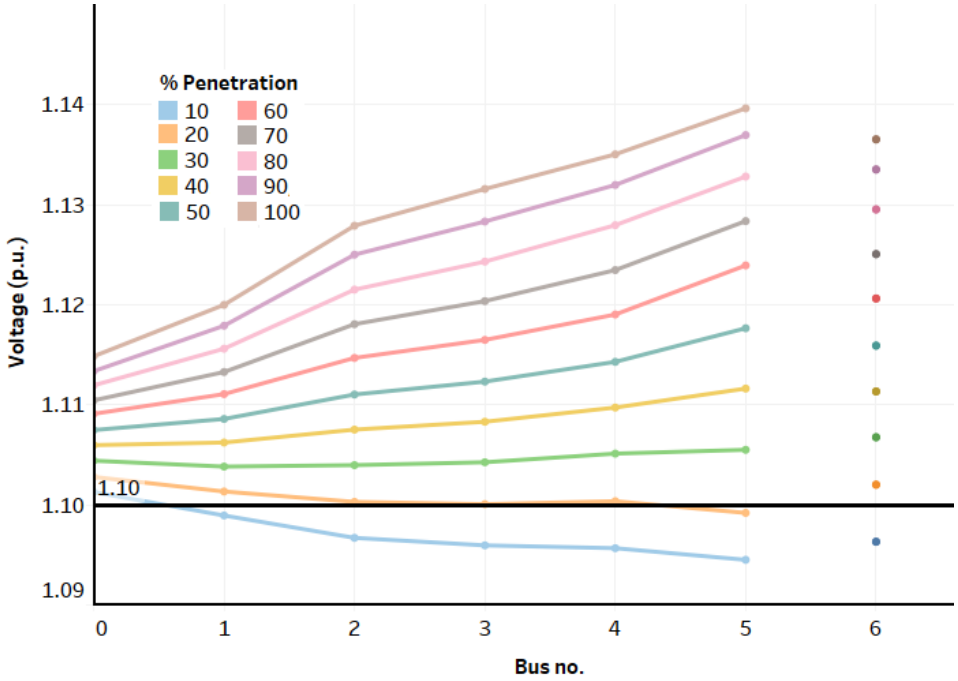

(b) 0.98 lagging

Figure 5-18: Voltage profile of the three-phase distribution network for different penetration levels at 300 W load, 800 W/m^2 irradiance and PV power factor of 0.95 lagging and 0.98 lagging

levels and differs for PV systems operating at different lagging power factors. The reactive power reversal under 0.95 pf lagging occurs after PV penetration increases from 30% which is almost at the same percentage under which reversal of real power occurs. If the PV systems are required to operate at lagging power factor, i.e.

to supply reactive power, then, at the more probable scenario of 300 W and 800 W/m^2, action would be required at just above 20% PV penetration to prevent voltage rise.

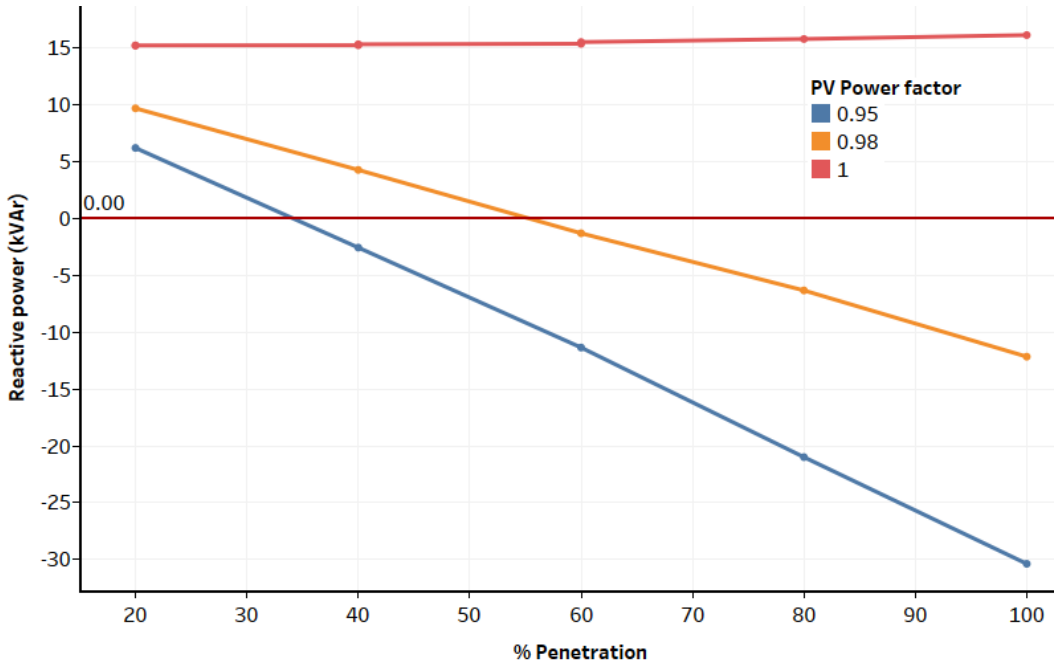

Figure 5-19: Net reactive power at the secondary of the substation for different penetration levels of PV and different operating power factors at 300 W load, 800 W/m^2 irradiance

5.5.6 Impact of distribution of PV on the performance parameters

For balanced distribution of PV, the percentage unbalance is around 0.1% at the far end of the feeder at 10% PV penetration and goes up to 0.5% at 60% penetration. This could be attributed to the fact that even though the number of houses and the number of PV systems in each phase is the same, it is not uniformly distributed across the different buses, which can occur in a practical distribution network. The difference is more clearly visible in bus 5, where the unbalance increases with the increase in penetration of PV systems. Though the absolute values of unbalance are not high, the percentage increase in unbalance for an increase in PV penetration is around 400%. This implies that if the initial unbalance at a bus is high, the introduction of PV may accentuate the unbalance and this can affect the performance of any three-phase load connected to that bus. Figure 5-20 shows the percentage unbalance across the feeder for different penetration levels from 10-

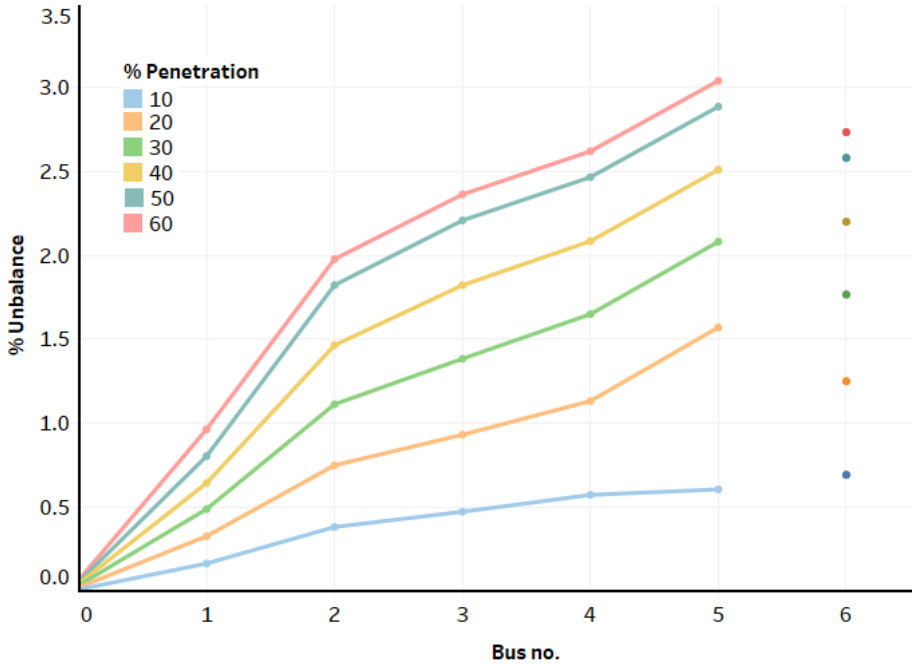

Figure 5-20: Percentage unbalance across the three-phase distribution feeder for unbalanced distribution of PV and different penetration levels of PV at 300 W load and 800 W/m^2 irradiance

60% for PV distribution only on the A-phase of the network, 300 W load and 800 W/m^2 irradiance. At 10% PV penetration the percentage unbalance is around 0.7% at bus 6 with the percentage unbalance increasing with increasing penetration of PV systems and reaches about 3% at 60% penetration which is the worst possible unbalance as any PV penetration percentage above 60% would introduce PV on the next phase and reduce the overall unbalance. At 30% PV, the percentage unbalances reaches the maximum permissible unbalance level mentioned by Engineering Recommendation P29 [83]. However, the probability of connection of all PV systems in a feeder to the same phase is quite low. Also, the background unbalance levels considered are very low which may not be true in practical scenarios.

5.6 Summary

The performance of a single-phase and three-phase distribution network, representative of the UK residential power network, have been evaluated under different PV penetration levels in terms of the voltage profile across the feeder, total

harmonic distortion of the current, net power flow and power factor at the secondary of the substation transformer.

For the single-phase feeder, power factor is a major parameter which decreases with an increase in penetration levels and reaches close to zero at 40% penetration. However, the low power factor in this scenario does not indicate an increase in reactive power requirement as often indicated by low power factor. Zero power factor means that the substation transformer is only supplying reactive power and no real power. Changing the tap setting to reduce the substation transformer voltage to 240 V (phase to neutral) maintains the voltage across the feeder within statutory limits for higher penetration levels, but this results in the power factor falling below 0.8 earlier than when the voltage was maintained at 250 V. The analysis of other performance parameters highlight that as the penetration level increases the presence of PV adversely affect the performance of the distribution network at irradiance levels greater than or equal to 800 W/m^2.

The three-phase distribution network is evaluated mainly for two scenarios viz., the typical worst-case scenario (load of 152 W and irradiance of 1000 W/m^2) and the realistic worst-case scenario (load of 300 W and irradiance of 800 W/m^2). At 300 W, the tap changer at the 33/11 kV substation moves from 0 to -1 resulting in a higher voltage across the feeder than at 152 W load. This results in voltage profile violating the upper limit at PV penetration level greater than 20% as against 30% at the typical worst-case scenario. The parameter that is affected next is the net power flow at the substation. The net power at the substation becomes negative at 20% penetration for the worst-case scenario and at 30% penetration at realistic worst-case scenario. Another parameter that is affected by PV is the net power factor at the substation, which is directly related to the amount of power a PV system can supply. At the futuristic scenario with load of 500 W and 800 W/m^2, the performance parameters were not affected up to 60% PV penetration.

The results highlight that the more probable scenarios pertaining to the network, in terms of both the load and irradiance, should be used for deciding the limit on the contribution of PV systems. Under the realistic worst-case scenario, steps would be necessary to regulate the voltage profile as the penetration of PV increases above 20% and to improve the capacity of the distribution network to handle the reverse power flow as PV penetration increases above 30%.

Though voltage rise can be mitigated by reducing substation voltage, caution has to be used to prevent under voltage at heavy loading conditions. The ability of PV inverters to supply reactive power, if used, could result in improvement of the power factor at the substation but result in the voltage profile violating the upper limit at lower penetration levels of 20%. The amount of reactive power that each inverter should supply is dependent on the load power factor and penetration level of PV. Evaluation of potential solutions to increase the contribution of PV in a distribution network in the UK is presented in chapter 7.

CHAPTER 6

DYNAMIC PERFORMANCE OF A DISTRIBUTION NETWORK WITH MULTIPLE SINGLE-PHASE PV SYSTEMS

A system is said to be in a dynamic-state if the variables defining the system operating conditions are time varying in nature [128]. As an electric power system is comprised of many individual elements and interconnections, different types of dynamic interactions are possible. Some of these interactions may affect only a section of the system or may affect the whole of the system and can be categorised based on the cause, reaction, time frame, physical character or place of occurrence of the event. Two main causes of power system dynamics are disturbances and changing power demand/generation. The disturbances in a power system are categorised as voltage dips, voltage surges, overvoltage, harmonics, power frequency variations, voltage fluctuations, voltage imbalance, short and long voltage interruptions, under voltage and transients, as per EN50160 [81]. The causes of the above-mentioned disturbances, except harmonic disturbances, are system faults, inductive/capacitive loading/switching, switching on/off of large loads and lightning. The harmonic disturbances arise from non-linear loads, industrial furnaces and transformers/generators.

Faults in overhead lines of a distribution network are typically caused by strong winds or accumulation of ice resulting in breakage of the line. In underground cables, it is resultant of natural decay or careless street digging [18]. Large currents and associated voltage sag in the distribution network during a fault can affect the system stability and cause further damage if action is not taken immediately to detect and disconnect a fault. Protective equipment is used to detect and disconnect a fault, the operation of which must be fast, reliable and selective [128]. PV systems

act as additional current sources that contribute to the net fault current and may affect the distribution network performance as the existing protection mechanism may not be designed for this contribution. This chapter, therefore, aims to analyse the performance of a distribution network with multiple single-phase inverters during a fault. The chapter then discusses the impact of multiple inverters on the protective equipment in a 400 V distribution network in the UK, typically fuses at all feeders and a relay at the substation transformer. The chapter also provides a discussion on the observations made based on the G-83 guidelines against the trip times stipulated by different standards.

6.1 Review on Impact of Fault on a Distribution Network with PV

Electricity networks are rapidly changing from passive distribution networks with unidirectional power flow to active distribution networks with bi-directional power flow [129]. The term distributed generation (DG), which includes generation based on rotating devices (synchronous generators and induction generators) and based on power electronic devices (inverter-based generators), has been used in studies on dynamic performance/fault performance [130-135]. Fault headroom of the protective equipment, a relay, was used to determine the impact of DG on the distribution network in [130] and the report concluded that for DG penetration up to 100%, i.e. all households with a 1 kWp Combined Heat and Power (CHP) generation unit, the fault contribution does not form a limiting constraint. However, Freris and Infield have raised concerns that even small contributions to the fault current from DG may be enough to violate the limits of the switchgear component, resulting in the need to upgrade the equipment [131]. The impact of DG in a medium voltage distribution network in Italy has been analysed in [132] and issues in the fault location/isolation procedures in the distribution network with increasing contribution from DG has been highlighted.

Kaddah, El-Saadawi and El-Hassanin used an IEEE 13-node test feeder at 4.16 kV to analyse the impact of DG for percentage contributions from 0 – 30% of total connected load and concluded that above 10% penetration, protection co-ordination may be affected [133]. Difficulty in the detection of the fault using simple over and under voltage relaying schemes in an exporting feeder has been discussed by Sun and concluded that the changes to protective equipment setting are dependent on the operation of the DG, due to the intermittent nature of their operation [134]. The recent review paper by Manditereza and Bansal on protection challenges in the presence of DG concluded that the traditional protection mechanism is not sufficient to perform its function when the contribution from DG increases [135]. However, they do not provide a clear differentiation between the types of generators and their different characteristics during fault/voltage sag.

Experimental tests performed in Japan using a 200 kWp PV system and high resistance faults, to replicate faults at different distances from the PV, indicated that the substation overcurrent relay failed to detect the fault in many instances [136]. The ability of an inverter-based generation to disconnect within a few cycles after detection of a fault (fast disconnection) has been discussed in [131], with the requirement for extra care during the design of protection devices that rely on high fault currents. Further concern has been raised in [137] on the ability of the inverter to detect a fault and thus continuing to feed the fault, resulting in nuisance fuse operation. The report also observed that if the PV increases the fault current, the minimal melt time of the fuse may be reduced significantly, resulting in lack of coordination with the upstream instantaneous trip mechanism. An experimental test was performed on a 1.7 kW commercial inverter in Thailand to estimate the time delay for detection and switching-off of the inverter by Phuttapatimok et al. and they observed that, although standards in Thailand allowed 2s to disconnect, the inverter took only 84.8 ms (<5 cycles) to disconnect the system [138].

Malmedal, Kroposki and Sen discussed the impact of fault current contribution from the PV inverter on a 12.47 kV distribution feeder in the US with lumped load at 480 V and concluded that, at the residential level, the presence of PV has no impact on interrupting ratings of equipment [22]. They, however, assumed that the inverters contribute to the fault current for less than 1 cycle under short-circuit and feed around 1-2 times their rated current. Though they provided a detailed analytical approach to discuss the fault current contribution from rotating generators, the conclusion on PV inverters was drawn mostly from the assumptions on the characteristics of the inverter. They, additionally, have discussed the possibility of over-voltages in healthy phases during a single-phase to ground fault in the presence of three distributed generation systems, resulting in tripping of transformer protection. Morren and Haan analysed a medium voltage distribution network in the Netherlands and concluded that the impact of PV on protection was minimal as the response of inverter can be defined depending on the voltage at the terminal and thus controlled [139]. Trucotte and Katiraei simulated the fault current contribution from megawatt-scale PV power plant located at the end of a 25 km long feeder for faults at the substation and at the end of the feeder and observed that the fault current was limited to 1.1 to 1.5 times the rated current [140].

Results of testing two inverters at the laboratory facility of NREL and at the manufacturer have been presented in [113]. The inverters rated 1 kW and 500 kVA, 60 Hz, were tested based on guidance given by Underwriters Laboratories (a global safety consulting and certification company and publisher of different safety standards) and fault contributions from the inverter lasted between 1.1 – 4.25 ms (< 1 cycle). However, the fault current contribution from the 1 kW inverter was 42.7 A which is approximately 5 times the rated current. The test was performed only on one single-phase inverter and used a DC source of 16 kW rating which could have resulted in a higher current being supplied during a fault. Hence, this result cannot

be directly extended to other single-phase PV systems. Le-Thi-Minh et al. analysed two types of medium voltage distribution networks, rural and urban, prevalent in France with two PV systems rated 500 kW or 2 MW each and concluded that a fault in an adjacent feeder resulted in unnecessary tripping of PV in the healthy feeder [141]. They, however, do not discuss the reason for the drop of PV terminal voltages in the healthy feeder to near '0' for a fault in the adjacent feeder.

Katiraei et al. used simulation based and analytical methods to calculate the contribution for PV inverters, rated 500 kW each, during fault and concluded that the contribution from PV is not a limiting factor [142]. They categorised the inverters as fast disconnection type, which disconnected in less than 1 cycle under fault, and generic model type, which took around 10 cycles to disconnect even when the voltage drops to less than 50% of the rated voltage. The fault current contribution from each inverter was assumed to be in the range of 1 to 1.2 times the rated current. The unwanted tripping of inverters for faults located outside their scope of operation gave rise to discussion of low voltage ride through (LVRT) or fault ride through (FRT) for PV inverters, the need for which, along with requirement of reactive power supply during fault at distribution level, has been discussed by Yang et al. [143]. They, however, do not discuss at what voltage levels and at what contribution levels from PV it would become necessary to have LVRT. Margossian, Sachau and Deconinck discussed the impact of FRT requirements in Germany for a 65 kV and 20 kV distribution network and concluded that the FRT requirement cannot be generalised and that the requirement is dependent on the strength of the network, type of protection and location of PV [144].

Traditionally, the fault current contribution from PV is ignored as the systems are comparatively smaller than the contribution from synchronous generators and also due to their fast disconnection on detection of fault [145]. The research on the impact of PV on distribution network during fault so far considers mainly medium voltage

with the exception of [22], where loads are lumped on the 480 V low voltage distribution network. However, even this work does not discuss the protection present at 480 V, which is typically fuses, and the details of the low voltage distribution feeder. Also, this work is for a network in the US, which operates under different standards of grid connection than those of the UK. With discussions of LVRT becoming prevalent, the inverters will remain connected to the grid for a longer duration than has been assumed in the literature (<1 – 10 cycles). The UK guidelines G-83 (discussed in chapter 3) for tripping of inverters already gives longer time for tripping (around 25 cycles) than the IEEE guidelines of 0.16 s and longer than the tripping time considered in the literature. This chapter, therefore, aims to analyse the impact of multiple single-phase PV systems on an LV distribution network in the UK, using part of an actual network in the UK and considers PV to stay connected for time durations as mentioned in G-83. The impact of fault at different locations of the distribution network on the PV system is also analysed in terms of the fault current and settling time after fault clearance. The impact of PV on the dynamic performance of the distribution network is evaluated in terms of the net fault current, net current at the distribution substation, voltage profile during a fault and impact on the protection system.

6.2 Methodology of Dynamic Analysis

Fault analysis may be performed by direct solution of network equations, network reduction and back substitution or simulation [146]. The simulation-based approach is used in the present study, as it allows easy incorporation of the non-linear nature of PV systems as well as the details of the three-phase unbalances as also highlighted in [147]. MATLAB Simulink model of the PV system and the distribution network as discussed in chapter 4 are used for the dynamic analysis. A self-clearing single-phase to ground (SLG) fault is introduced in the feeder at one of two different locations, near the 11/0.433 kV substation of the detailed feeder and at the far end

of the detailed feeder, as shown in Figure 6-1 (marked as F1 and F2). The fault duration is assumed as 1 s, as an intermediate value between the two trip times of 0.5 s and 2.5 s for different voltage drops stipulated by G-83/2 [86]. The inverter model uses the time delay for disconnection as 0.5 s when the voltage at its terminals drops below 184 V and 2.5 s when the voltage drops below 200.1 V in-line with the G-83/2 guidelines.

The performance of the distribution network in terms of settling time after fault clearance, total fault current, fault current contribution from the inverter and voltage fluctuation during and after fault clearance for three penetration levels is analysed in the next section. The simulations were performed for the following parameter variations:

a. 0%, 40% and 100% PV penetration levels
b. Load of 500 W (the performance of the distribution network is independent of the connected load at the instant of fault)
c. Irradiance of 400, 800 and 1000 W/m^2.

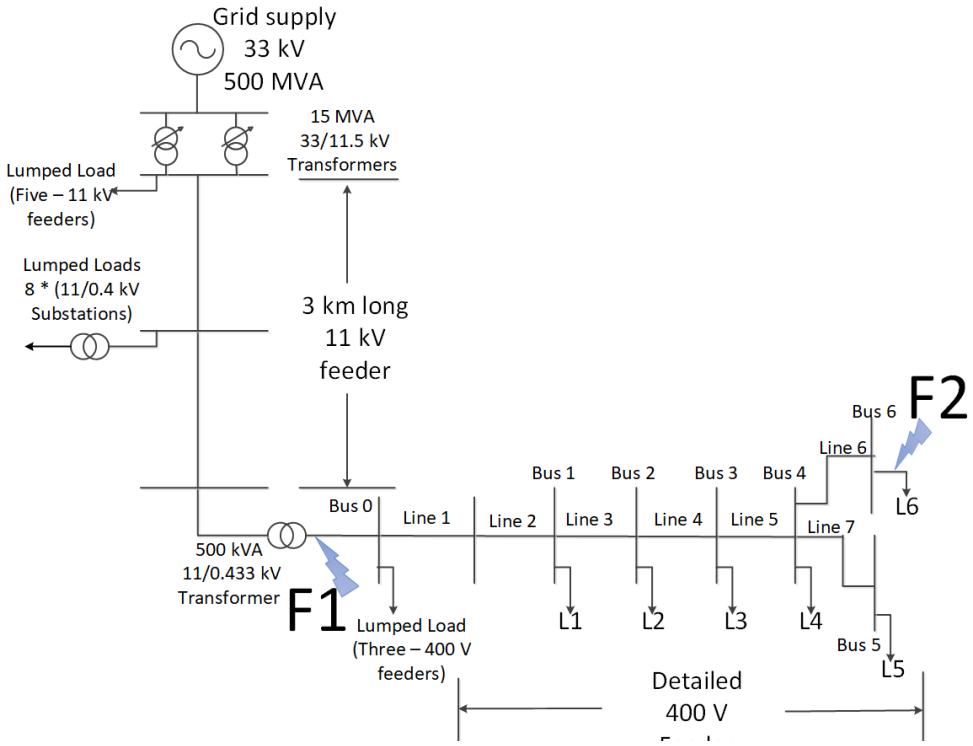

Figure 6-1: Distribution network with fault locations F1 and F2 marked

d. Fault located near the substation (F1) and at the far end of the feeder (F2)
e. PV distributed uniformly near the substation (F1) or at the far end of the feeder (F2)

These combinations were chosen because at 500 W load, 40% penetration indicates a scenario just before the occurrence of reverse power flow. PV penetration of 100%, results in a scenario with reverse power flow or power being fed into the substation from the PV systems in the distribution feeder. The fault is simulated as a single-phase to ground fault in phase A and occurs at time instant t = 1 s and is cleared at t = 2 s. For representative purpose, the time delay for reconnection is considered as 0.5 s after the network returns to the normal conditions (see section 3.1 and section 4.2).

For a fault near the substation, i.e at F1, the voltage at the secondary of the substation and all points from the substation to the end of the feeder drop to near '0', resulting in the disconnection of all the inverters connected to the feeder. As this fault is before the four distribution feeders split, the other three feeders represented by lumped loads and lumped PV system also experience the same voltage drop to near '0' value and this results in disconnection of the PV system within 0.5 s. Also, for a fault at this point, it is the fuse at the secondary of the 11/0.4 kV substation that has to operate first followed by the relay at the primary of the 11/0.4 kV substation as a backup protection.

6.3 Results and Discussion

A fault affects the performance of the PV system and the PV system may affect the performance of the distribution network during and after the fault. This section therefore first discusses the impact of fault on the PV output and then discusses the impact of PV on the dynamic performance parameters of the distribution network.

Once the fault is cleared, the time taken by the system to reach a steady-state, which may be the same state as before fault or different depending on the action of the protective device, is called the settling time. The impact of fault on the output current of the PV system is discussed in detail. The parameters of the distribution network that may be affected during fault by the presence of PV systems are the net fault current at the fault location, net current at the secondary of the substation during the fault and voltage profile during the fault. The impact of the use of a lumped PV model as a representation of the PV systems in the adjacent feeder is also discussed. The impact of PV on the existing protection mechanism and the impact of different technical regulations are then discussed.

6.3.1 Impact of fault on PV output current

The output current of the PV system is dependent on the voltage across its terminals and the irradiance level during the fault. Figure 6-2 shows the voltage and current of the PV inverter before, during and after a fault at location F1 and with the PV connected to bus 1. The inverter takes less than 10 cycles after reconnection to reach a steady-state. The inverter output current has a first peak almost three times the rated current similar to the published experimental results in [116]. In the experiment conducted in [116], the inverter trips after the first peak itself, however in order to evaluate the impact of continued supply from the inverter for the maximum allowable duration mentioned in G-83, the inverter model was allowed to stay connected for a duration of 0.5 s after fault detection. If the inverters are to have LVRT, modifications have to be made to the inverter control strategy to prevent saturation of the controller and build-up of DC link voltage during a voltage sag. Different control strategies for LVRT in inverters to enable them to stay connected to the grid during fault/voltage sag have been discussed in [111, 148-151]. Figure 6-3 shows the inverter output current of an inverter at bus 1, before and during a fault at F1 for different irradiance levels of 1000 W/m^2, 800 W/m^2 and 400 W/m^2. It

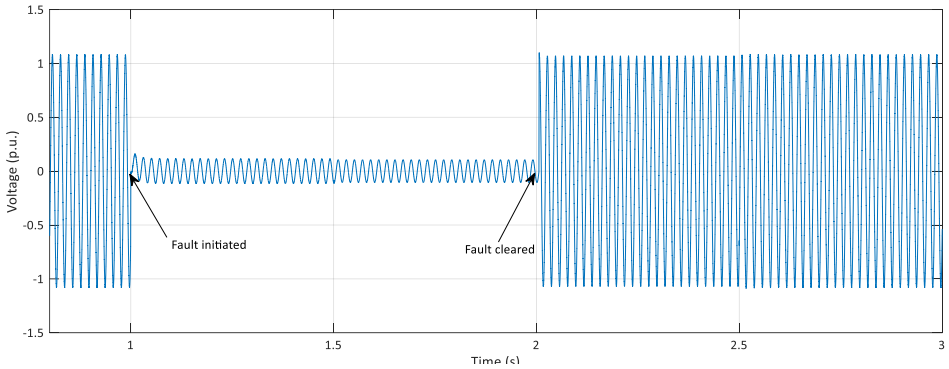

(a) Voltage at the inverter terminals

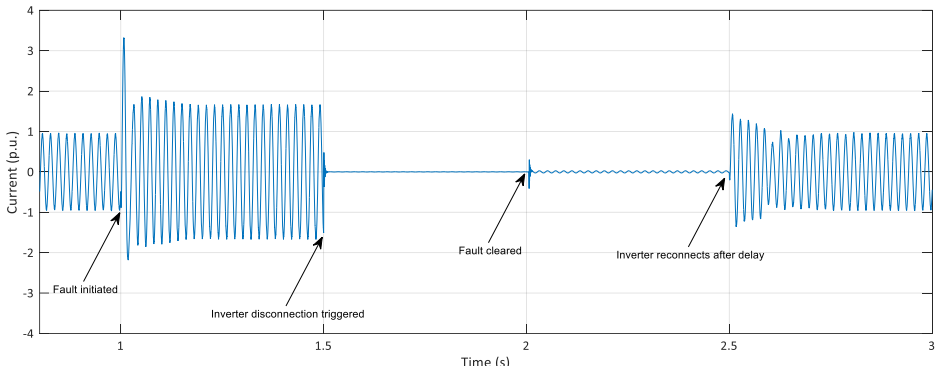

(b) Inverter output current

Figure 6-2: Voltage and current output of PV system connected to bus 1 before, during and after fault at F1

can be observed that, though the magnitude of the first peak at 800 and 400 W/m^2 irradiance levels are lower than the peak at 1000 W/m^2, the continued contribution from the inverters are close to 2 p. u. (twice the rated current) irrespective of the irradiance levels. The current is limited to 2 p. u. due to the controller action whereas the DC link current results in an increased current at the first cycle. Most commercial inverters currently do not wait for the duration of 0.5 s before disconnecting from the

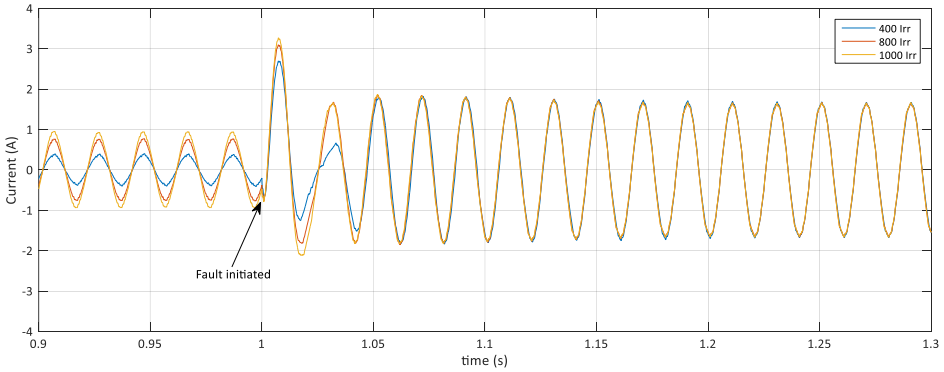

Figure 6-3: Output current of an inverter at bus 1 before and during fault at F1 for different irradiance levels

grid in case of a fault. However, while introducing LVRT at low voltage distribution network, it is important to consider this continued contribution from the inverters for longer time durations than considered in the G83. Figure 6-4(a) shows the output current of PV inverter in bus 1 for a fault at F2 at 40% PV penetration. At 40% penetration, the voltage at bus 1 is close to the boundary voltage of 184 V (185 V) and hence the inverter trips after 0.5 s of fault occurrence. However, for the similar conditions at 100% penetration, the voltage at bus 1 is 188 V, higher than the limit of 184 V, and therefore the inverter stays connected for the 1 s duration as shown in Figure 6-4(b).

Figure 6-5 shows the output current of the PV inverter in bus 1 before, during and after a fault at F2. It can be observed that the peak, as well as the continued contribution of fault current from the PV, decreases with a decrease in irradiance. The decrease in contribution is more pronounced for a fault at F2 than for a fault at

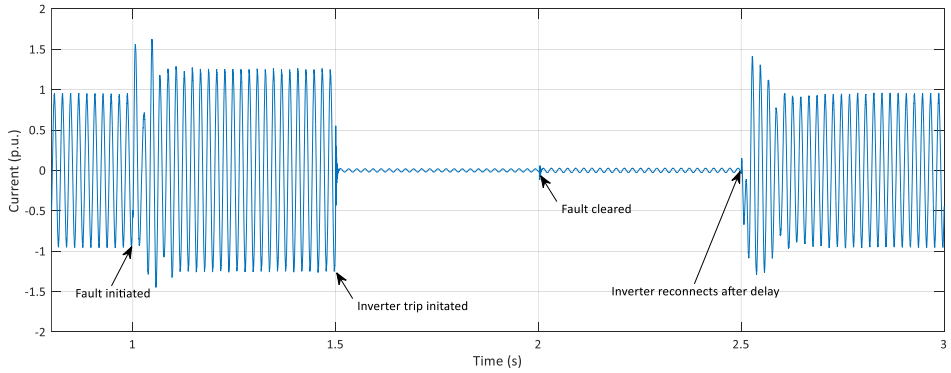

(a) 40% PV penetration

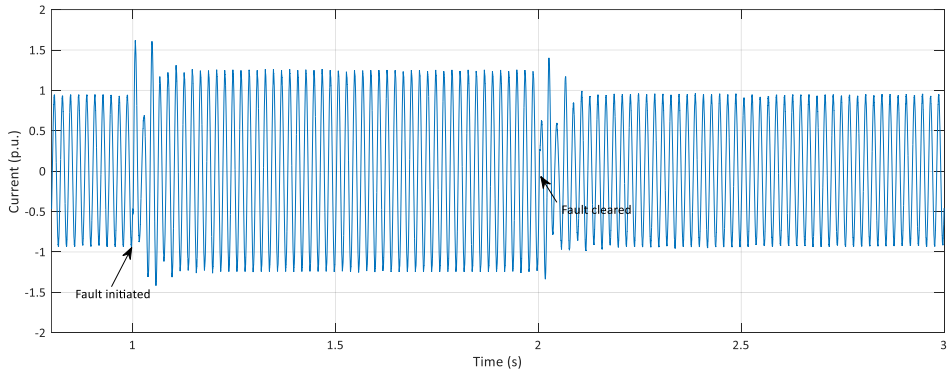

(b) 100% PV penetration

Figure 6-4: Instantaneous output currents of PV inverter at bus 1 before, during and after fault at F2 for different penetration levels

F1. For a fault at F1, the lumped PV also trips within 0.5 s as the voltage across one of the phases is lower than the limits mentioned by G-83. This is not similar to a practical scenario, where the PV would be single-phase in nature and distributed across the three-phases, resulting in disconnection of inverters connected to phase A and not the disconnection of all inverters in the feeder. For a fault at F2, the lumped PV experiences only a voltage sag and remains connected to the grid. This is similar to a practical scenario, where fault at F2 is representative of a fault in the adjacent feeder, for which the inverters should not trip or trip only on sustained voltage sag.

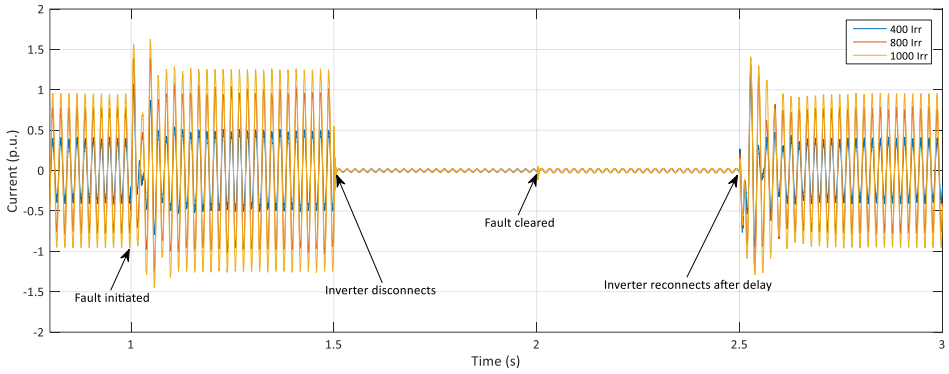

(a) Output current

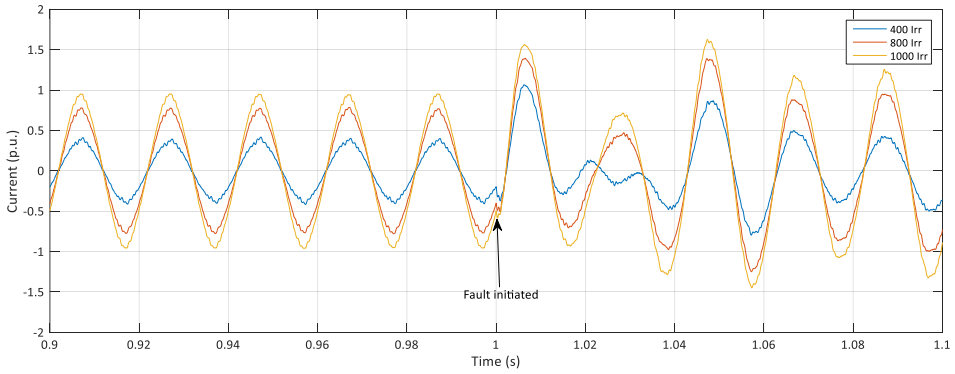

(b) Zoom view of the current for time interval 0.9 to 1.1

Figure 6-5: Output current of PV inverter in bus 1 for fault at F2 for different irradiance levels

6.3.2 Impact of PV on performance of distribution network during fault

The presence of PV may affect the settling time, net fault current, the net current at the substation, voltage profile during fault and the protection mechanism. Though the reconnection of the inverter after a fault introduces fluctuations in the current, this is similar to the fluctuation introduced every time the inverter is synchronised and starts supplying the grid. Even though all the inverters are modelled to reconnect after a time delay of 0.5 s, the net current at the substation does not show a significant disturbance at the time of reconnection. Therefore the impact of PV on the settling after a fault due to reconnection of the PV systems is considered insignificant and not discussed further.

Net fault current at the point of fault

For a fault at F1, the presence of PV systems increases the net fault current at the point of fault as shown in Figure 6-6. However, the increase is only nominal and

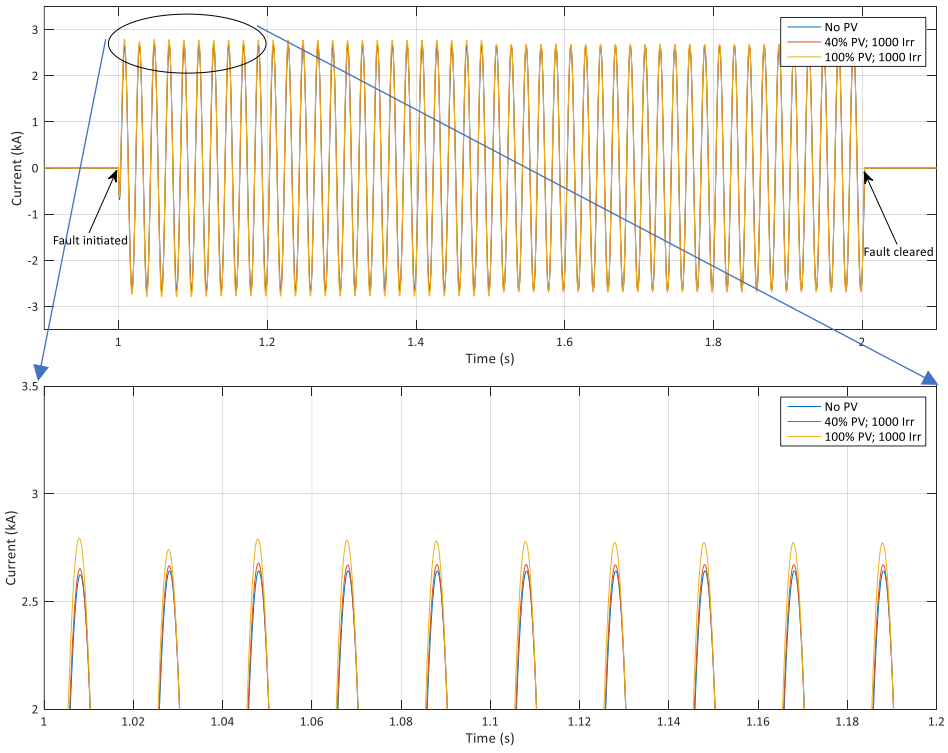

Figure 6-6: Net fault current at 0, 40 and 100% PV penetration with PV distributed near the substation for a fault at F1

can be considered as negligible for both 40 and 100% penetration of PV systems irrespective of the location of PV systems. Also, the level of irradiance has no significant impact on the net fault current for a fault at F1. Table 6-1 shows the net fault current for faults at F1 and F2 at 0, 40 and 100% penetration of PV at an irradiance level of 1000 W/m^2.

Table 6-1: Net fault current for different fault locations and different PV penetration levels

Fault location	PV location	Irradiance (W/m^2)	% penetration of PV	Net fault current (kA)
F1	NA	1000	0	24.9325
F1	Near S/S	1000	40	25.2612
F1	Near S/S	1000	100	25.7458
F1	Far from S/S	1000	40	25.2602
F1	Far from S/S	1000	100	25.7051
F2	NA	1000	0	2.642
F2	Near S/S	1000	40	2.6791
F2	Near S/S	1000	100	2.7937
F2	Far from S/S	1000	40	2.8073
F2	Far from S/S	1000	100	3.0033

For a fault at the far end of the feeder, i.e. at F2, the increase in net fault current is dependent on the location of the PV systems as shown in Figure 6-7 and Figure 6-8. When the PV systems are considered to be distributed at the far end of the feeder, the net fault current increases by 6% and 13% for 40% and 100% PV penetration respectively. However, if the PV systems are considered to be distributed closer to the substation, then the increase in net fault current is around 1% and 6% for 40% and 100% PV penetration. The net fault current for fault at F2 is also dependent on the irradiance level during the fault duration. The net fault current decreases with a decrease in irradiance at the given penetration level for a fault at F2 as shown in Figure 6-9.

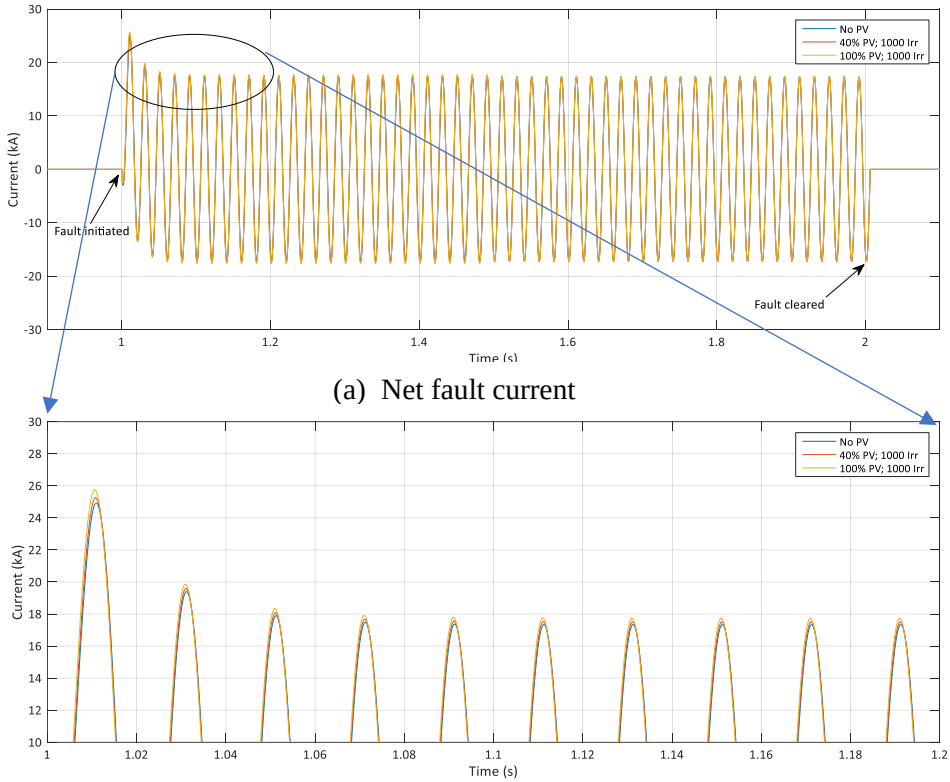

(a) Net fault current

(b) Zoom view of the circled signal of part (a)

Figure 6-7: Net fault current at 0, 40 and 100% PV penetration with PV distributed near the substation for a fault at F2

Net current at the secondary of the distribution substation

The presence of PV does not significantly affect the net current at the substation during the fault for a fault at F1. The presence of PV decreases the net current at the substation from 25 kA to 24.6 kA i.e. about 2% decrease. For a fault at the far end of the feeder i.e. at F2, the net current at the substation for 0 and 40% penetration of PV systems with PV systems distributed near the substation is as shown in Figure 6-10. At 40% penetration, the current at steady-state is close to zero as most of the load is met by the PV. The fault is initiated at 1 s and after 0.5 s delay, the inverters connected to bus 1 disconnect from the network as the voltage at bus 1 is around 184 V (the boundary voltage as per G-83). This results in a slight increase in current drawn from the substation, as the fault current that was being supplied by the inverter is now supplied by the substation. However, the lumped PV remains connected to the grid as it experiences only a voltage sag. Therefore, the

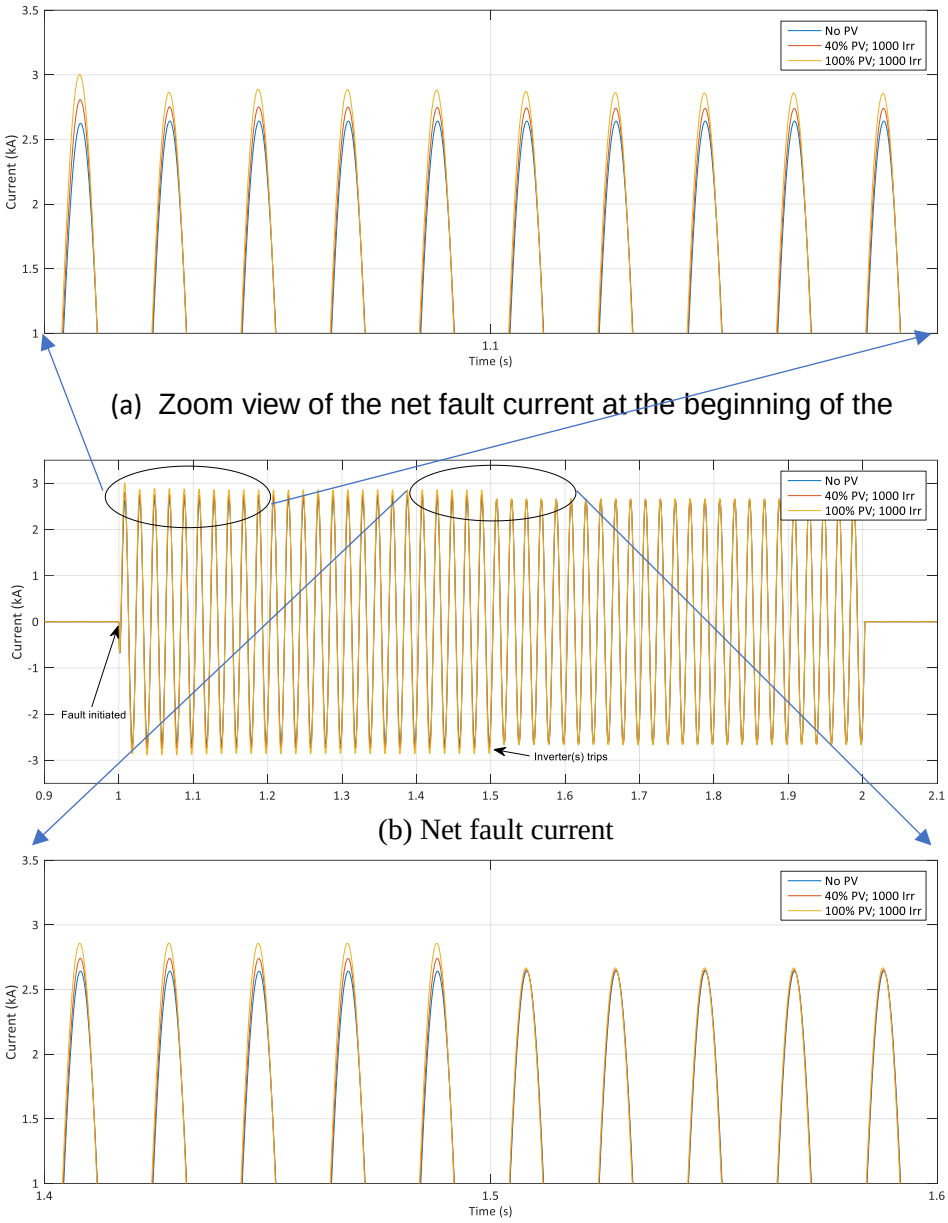

(a) Zoom view of the net fault current at the beginning of the

(b) Net fault current

(c) Zoom view of the currents during the time interval the inverters trip

Figure 6-8: Net fault current before, after and during fault at F2 for 0, 40 and 100% PV penetration with PV distributed far from the substation

net current at the substation during fault at 40% penetration of PV is not the same as no PV scenario for the duration from 1.5 s to 2 s. The fault is cleared at 2 s and the inverters at bus 1 reconnect to the network after a delay of 0.5 s, i.e. at 2.5 s, and the network returns to the steady-state conditions. The net current at the substation before, during and after the fault at F2 for 0% and 100% penetration of PV systems is as shown in Figure 6-11. The current during steady-state at 100% PV penetration is higher than the current at no PV, as at this penetration level current is being fed to the substation (generation higher than load). Similar to the 40%

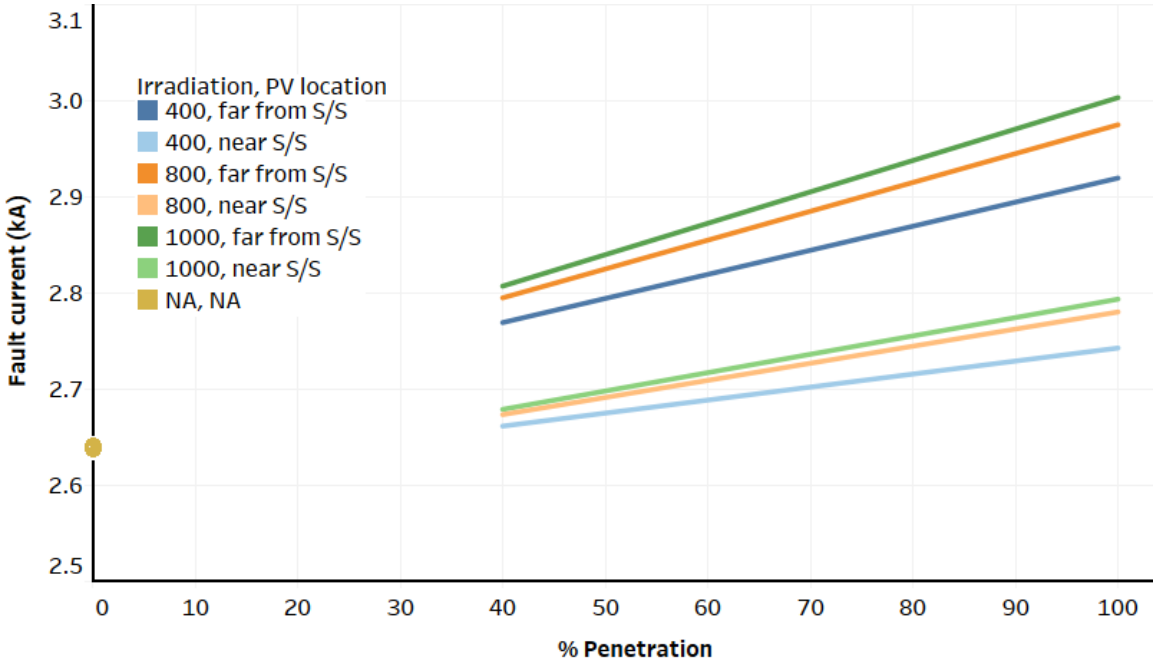

Figure 6-9: Net fault current for different penetration levels and different irradiance levels for fault at F2

penetration level, the inverters connected to buses 2 and 3 disconnect after a delay of 0.5 s resulting in an increase in current supplied by the substation after 1.5 s. However, the PV systems connected to bus 1 remain connected to the grid as the voltage is higher than 184 V and the lumped PV system also remains connected to the distribution network. During the fault, the net current at the substation decreases from 3000 A (peak) at no PV to 2600 A (peak) and 2100 A (peak) at 40% and 100% PV penetration respectively i.e. a reduction of 13% and 30%. The reduction in current at the substation remains at similar percentages for PV distribution at the far end of the feeder for a fault at F2. The net current at the substation during fault at a given PV penetration is also dependent on the irradiance level during a fault. At low irradiance level of 400 W/m^2, the decrease in substation current is only around 5% as against 13% at a high irradiance level of 1000 W/m^2 for 40% PV penetration.

Voltage profile during fault

When a fault occurs at the far end of the feeder with no PV systems, the voltage in phase A at the substation drops to 232 V (1.01 p. u.) from a steady-state voltage of

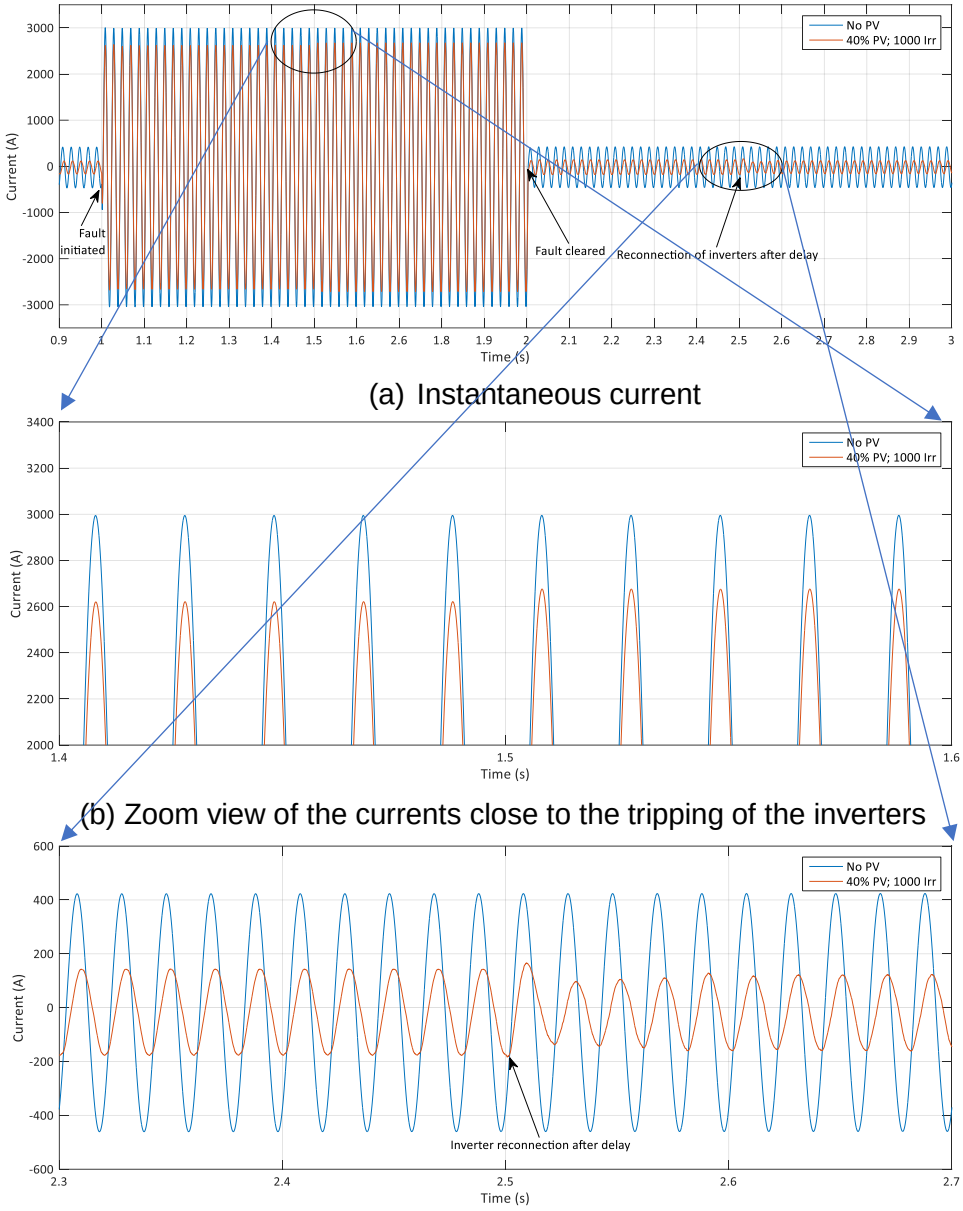

(a) Instantaneous current

(b) Zoom view of the currents close to the tripping of the inverters

(c) Zoom view of the currents during the reconnection of the inverters

Figure 6-10: Instantaneous current at the secondary of the substation for 0 and 40% penetration of PV systems near the substation for a fault at F2

247 V (1.07 p. u.). The voltages in phase A at the substation during the fault are 232.7 V (1.01 p. u.) and 235.5 V (1.02 p. u.) for 40% and 100% PV penetration respectively as shown in Figure 6-13. For a similar fault but with PV distributed at the far end of the feeder, the voltage in phase A at the substation for 40% PV penetration is 1.016 p. u. (233.8 V), 0.5% higher than when the PV was distributed close to the substation. For a single-phase to ground fault in phase A at F2, the variation in voltage profiles during fault, in phase A, introduced by the PV systems is not significant compared to the voltage drop due to the fault. However at 100%

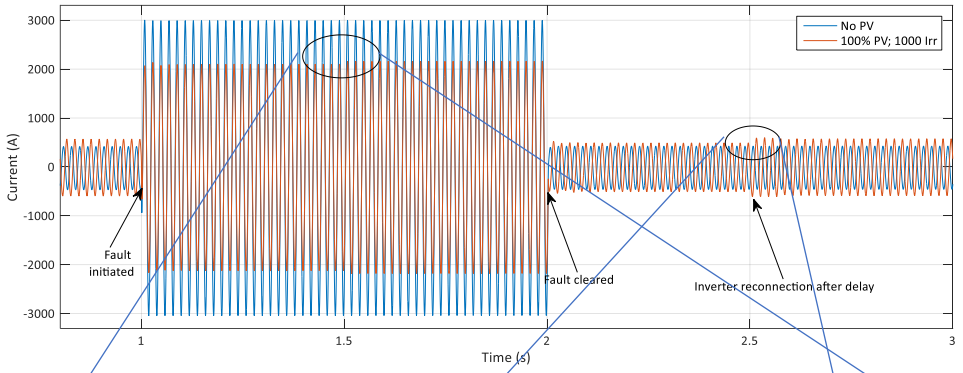

(a) Instantaneous current

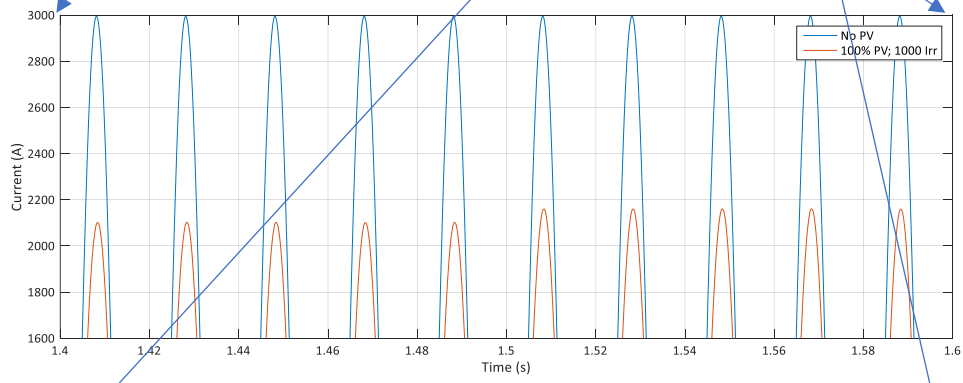

(b) Zoom view of the current near the tripping time of the inverters

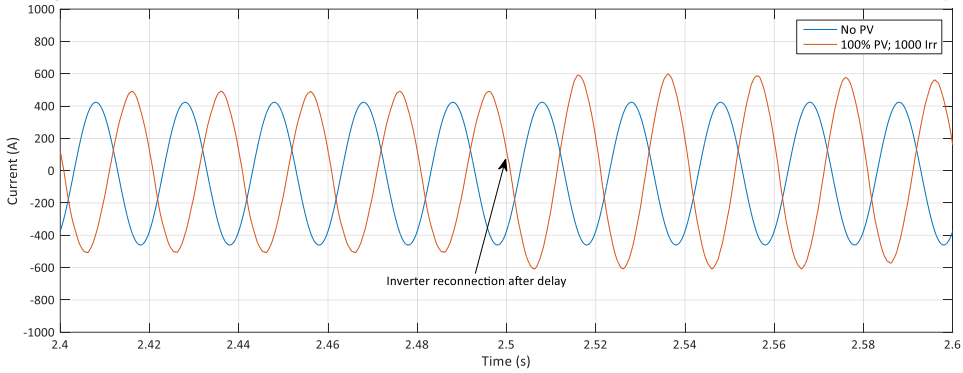

(c) Zoom view of the currents as the inverters reconnect to the grid

Figure 6-11: Instantaneous current at substation for 0 and 100% PV penetration before, during and after a fault at F2

penetration, there is a slight over-voltage in phases B and C at buses 4, 5 and 6 for a fault at F2 as shown in Figure 6-12. This may be due to the presence of the three-phase lumped PV system where voltage sag in one phase affects the voltages across the other two phases and the resultant currents. Overvoltage in healthy phases during a single line to ground fault has been raised as a concern in [22].

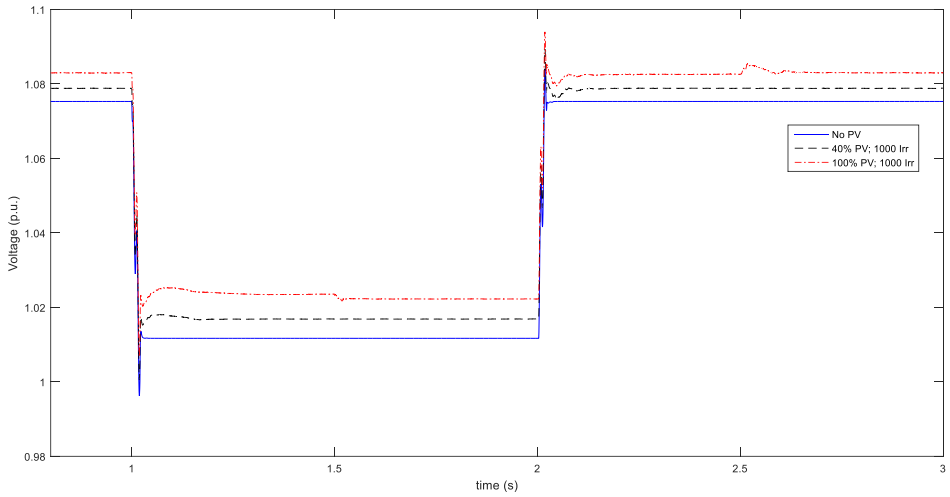

Figure 6-13: RMS Voltage in phase A at substation before, during and after fault at the far end of the feeder for different penetration levels of PV (PV distributed near the substation, solar irradiation of 1000 W/m^2)

At 100% penetration of PV, the voltage at bus 1 during a fault is higher than 184 V allowing the PV systems to remain connected to the network for 2.5 s. However, if the PV systems were following the German regulation VDE 0126-1-1 (see section 3.3), the PV systems connected to bus 1 would be disconnected for 40% and 100% penetration levels for a fault at F2. If the PV systems were following the European regulation IEC 61727 or the US regulation (refer chapter 3 for details), the

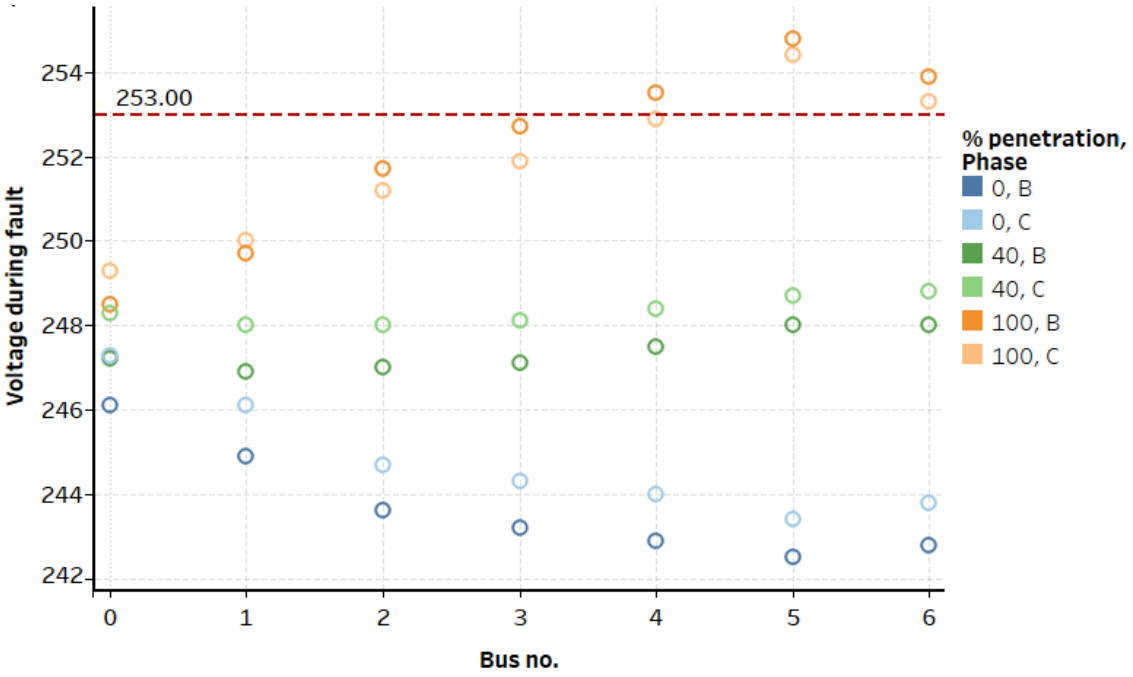

Figure 6-12: Voltage in the other two phases during fault for 100% PV penetration

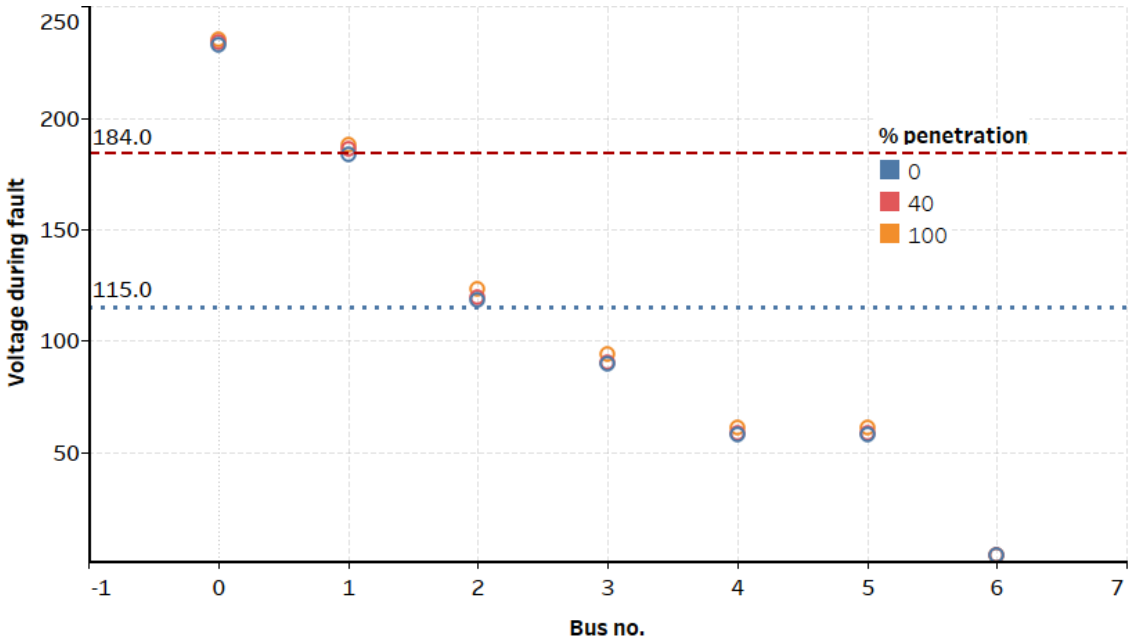

Figure 6-14: Voltage profile of A phase, during fault for different penetration levels of PV systems for a fault at F2

voltage level at which the PV systems should disconnect is 50% of the rated voltage, i.e. at 115 V for 230 V rated condition. This indicates that the PV systems at bus 1 and bus 2 would remain connected to the grid for both the penetration levels for a fault at F2, irrespective of the location of the PV system with respect to the substation. The voltage profile of A phase, during a fault at F2 for different penetration levels of PV systems distributed near the substation, is as shown in Figure 6-14. The dotted lines at 184 V and 115 V indicate the boundary conditions for disconnection of the PV system in the event of under voltage as given by G-83 and IEC/US regulation respectively. While evaluating the impact of PV on the distribution network performance, it is important to consider the regulations adopted.

6.3.3 Impact of PV on the protection system of low voltage distribution network

A fault is considered as cleared if it results in the disconnection of the faulted item of the system without tripping of any unwanted circuit breakers [146]. Fault clearance time typically ranges from <0.1 s to 1 s or more depending on the fault level and the protective device used. Overcurrent protection is typically used to

provide fault clearance and uses fuses, direct-acting trip mechanisms on circuit breakers or relays. In order to understand the impact of PV on the protection system, it is necessary to have an understanding of the protection device on the distribution network, its ratings and its coordination. Relays at different voltage levels and in different sections of a distribution network use time grading to distinguish the faults in different sections of the network. For time grading, the operating time for the protective equipment at the lowest voltage level is chosen first and a margin of 0.4 s or 0.5 s is added to each stage back to the main station/grid [146]. For the network under consideration in this research, the lowest voltage level is 400 V with protective equipment of fuses and at 11 kV there are four relays in sequence resulting in a delay of 1.8 to 2.2 s at the grid supply relay. Theoretical calculations for fault currents arising from a fault at F2, under no PV scenario, yields a minimum fault current of 1.9 kA with one supply transformer disconnected (typical process to calculate minimum fault current for the design of relays). Details of the theoretical calculation are given in Appendix G.

The distribution feeder at 230/400 V is protected mainly by fuses located in each branch of the network and in each service feeder to the residence. The fault clearance time of a fuse is the sum of pre-arcing time and arcing time. To achieve discrimination between fuses in series, the network operators typically use the same type of fuses with a ratio of ratings of the two fuses not less than 2. For the distribution network under consideration, the service feeders use 35 mm^2 combined neutral earth conductor (CNE). The service feeder for each house is provided with a fuse of 60 A rating for a single-phase residence, by the respective distribution network operator (DNO). 200 A heavy duty fuses are typically used in each branch of the 400 V distribution network [152]. Energy Networks Association Technical Specifications (ENATS) 37 -2 published in 2005 recommends that the fuse used in single transformers up to 500 kVA rating should be capable of withstanding 18 kA

fault current for up to 0.5s [153]. The code of practice of Northern Power Grid [154] (one of the network operators in the UK) provides a guidance on the selection of fuses at a substation and mentions that, for a 500 kVA substation, a 500 A fuse is used at the low voltage side and 40 A expulsion fuse is used at the high voltage side. However, Electricity Northwest Limited (another network operator in the UK) uses a 400 A and 25 A fuse respectively at low and high voltage sides of the transformers [155], which could be attributed to the ratings of the cables used or the load served by the respective network operators. The time-current zones of low voltage fuses of different ratings are as shown in Figure 6-15 [156].

For a fault at the far end of the feeder i.e. at F2, which represents physically a fault at any individual house/load, the 60 A fuse at the service head trips within 0.1s irrespective of the contribution of PV. If the fault at the far end represents a physical location on the last branch, i.e. on the branch between bus 4 and bus 6, the first protection mechanism to work would be the 200 A fuse near bus 4. Fault current of 1.8 kA at no PV would trip the fuse at 0.2 s. With PV, even a 1-2% increase in net fault current would result in faster tripping of this fuse. The fuse at the low voltage of the transformer can also be considered as a backup protection for a fault at the far end of the feeder. For a 400 A fuse, the operating time changes from 3 s under no PV scenario to 6 s and 11 s under 40% and 100% PV respectively. If a 500 A fuse was used with the transformer this change in current at the substation reflects a change in operating time from 6 s under no PV scenario to 12 s and 40 s under 40% and 100% PV respectively. Though the probability of failure of all the fuses in each branch is very low, the change in operating time for a 500 A fuse is significant as a typical time-delay of operation of the fuse in a low voltage network varies from 30 s to 60 s [157]. For a fault at the secondary of the substation, the secondary substation will trip within 0.1 s irrespective of the PV penetration.

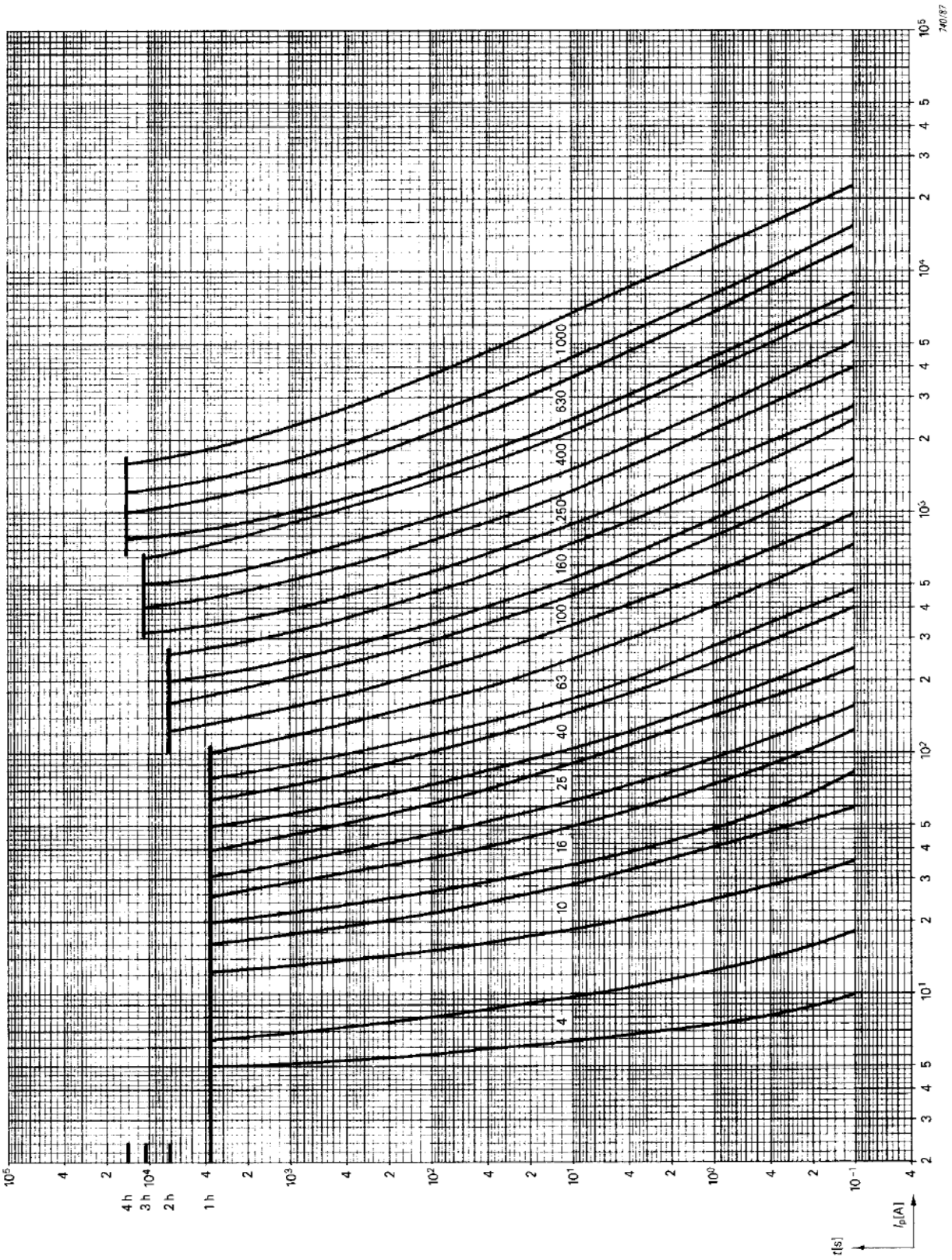

Figure 6-15: Time current zones for "g-G" fuses [136]

For a fault at F1, the fuses (fuse in individual service feeder or that at the branch) will clear a fault near it within a maximum of 0.1 s and for a fault at F2, the fault will be cleared within a maximum of 0.2 s. A fault at F1 would result in a significant voltage drop, as discussed in the previous section. However, a fault at F2 may result

in a voltage sag close to the boundary condition mentioned in G-83. The boundary condition of 50% voltage drop stipulated by IEC would enable the PV systems to be connected for longer duration (2 s) for a fault further from the PV system, which could be representative of a fault at the far end of the feeder when PV is located close to the substation or a fault at the adjacent feeder that would be reflected as a voltage sag. Disconnection of the inverter for a voltage sag due to a fault in an adjacent feeder is undesirable as it leads to generation loss and may result in a further drop in voltage as the load that was being supplied by the PV system would now be supplied by the grid. Figure 6-14 indicates that the lower boundary condition of 50% voltage sag would enable more PV systems to stay connected in the event of a fault at F2.

The results indicate that IEC regulations would enable more PV systems to stay connected in the event of a fault and prevent unnecessary disconnection. Typical relay disconnection time is around 0.2 s maximum and the following reclosing occurs after a typical delay of 15 s to check whether the fault is permanent or not. For a fault at F1, the relay would disconnect the feeder within 0.2 s resulting in a voltage drop to zero and before the next reclosing the inverters would have disconnected. Therefore a time delay of 0.5 s for a fault at F1 is sufficient. For a fault at F2, the relay is the worst-case backup protection, which would act with a delay of 3 s or 6 s depending on the transformer protection under no PV scenario. As the delay is increased under the presence of PV, disconnection after a delay of 2.5 s indicates that the local protection mechanism close to the fault failed to operate, requiring the backup protection to act, which should be within 0.7 s (adding the time grading between fuses). So the inverter disconnecting within 2.5 s allows ample time for the backup protection to act. However, if that fuse also fails to act and the fuse at the secondary of the substation has to act, disconnecting within 2.5 s would still allow the relay to pick up the fault. This implies that the time delays considered

in G-83 are sufficient for the protection mechanism in a distribution network in the UK. However, a lower cut-off of under-voltage disconnection would enable more PV to stay connected to the network without adversely affecting the performance of the distribution network under fault.

6.4 Summary

The fault current contribution of inverters was most often ignored in previous research on impact of PV on distribution network owing to their fast disconnection times and relatively lower currents than for the synchronous generators. However, with increasing contribution from PV at residential levels, it is important to understand the impact on protection systems at low voltage levels. Also, as the UK guidelines for inverters provide a higher disconnection delay than the IEEE standards, it is important to understand the performance of inverters that take longer to disconnect. This is also particularly relevant in the recent times with discussions of low voltage ride through/fault ride through. This chapter discussed the impact of fault at different locations of the distribution network on the PV systems and the impact of PV systems on the performance of the distribution network during and after a fault.

The fault current as seen by the substation decreases with increasing penetration of solar PV. The reduction was a maximum of 30% for 100% PV penetration for PV distributed near the substation or at the far end of the feeder. Also, this reduction was not significantly affected by variation in irradiation from 1000 W/m^2 to 400 W/m^2. The impact of PV on the protection device at this voltage level, fuse and its coordination with relays at the substation was also discussed. The longer duration of fault enables the observation of the impact of a sustained fault on the inverter output. Also, the inverters staying connected to the grid for 0.5 s, in-line with G-83, enables observation of the impact of continued current contribution from the

inverters on the fault current and protection mechanism. It can be observed that, in a radial distribution network, faults that are far from the PV terminals would be cleared within 0.2 s, indicating that delayed tripping of the inverters (0.5 s) as suggested by G-83 is more appropriate than the shorter time of fewer than 10 cycles as assumed in the literature. However, a lower cut-off voltage for under-voltage disconnection than stipulated in G-83 would enable more PV systems to stay connected during fault and avoid unnecessary loss of generation.

CHAPTER 7

TECHNICAL BARRIERS AND SOLUTIONS TO INCREASE PV PENETRATION IN THE UK

As discussed in chapters 5 and 6, the increased penetration levels of PV may adversely affect the steady-state and dynamic performance of the distribution network. This chapter starts with a summary of the penetration levels at which the presence of PV may adversely affect the performance of the distribution network and then presents the technical solutions to address these effects. The solutions applicable to a low voltage distribution network are further evaluated based on a set of chosen criteria to identify three top-ranked solutions. The chapter then evaluates the effectiveness of chosen technical solutions for one case study in the city of Newcastle upon Tyne, UK, using solar irradiance data for the city and load profile data for the UK. The discussion on the data of irradiance and load profile was given in section 5.2. The solutions are ranked based on their effectiveness for increasing PV penetration in residential distribution networks in the UK.

7.1 Technical Barriers

The maximum percentage of PV which can be accommodated without adversely affecting the performance of the distribution network is called the hosting capacity of the network for PV systems [158]. The performance parameters used to evaluate the steady-state (see section 5.4) and dynamic-state (see section 6.3) performance of the distribution network are used to evaluate the hosting capacity. They are:

1. Voltage profile (P1)
2. Total harmonic distortion (P2)
3. Net active power at substation (P3)
4. Power factor at secondary of substation (P4)

5. Voltage unbalance (P5)
6. Protection mechanism (P6)

The voltage profile is considered within limits when the values are within +10/-6% of the nominal value. Similarly THD is considered within limits if the value is less than 5%. Net active power is considered as adversely affected when the direction of power reverses, i.e. when the direction of power changes from “grid to distribution network” to “distribution network to grid”. As it is preferable to have power factor as close to unity as possible, a power factor below 0.8 is considered as the limit. Voltage unbalance greater than 3% resulting in the abnormal operation of three phase loads connected to the distribution network and is chosen as the upper limit for unbalance. The protection mechanism at distribution level in the UK is mainly fuses at branch level and a relay at the substation. The increase in operating time of the fuses and relay is considered as the limiting factor for the parameter P6.

From the results of steady and dynamic-state performance, it can be concluded that the performance of the distribution network was adversely affected at the worst-case scenarios as the percentage of PV increases. The worst-case scenarios from the chapters 5 and 6 are therefore extended here to evaluate the hosting capacity. The scenarios to evaluate the hosting capacity are the typical worst-case scenario used in the literature, the realistic worst-case scenario for the UK (see section 5.2) and a slightly higher load, representative of a futuristic scenario where demand-side management is used to increase the daytime load at noon. The slightly higher load is also representative of a distribution network with more percentage of high consuming customers than the UK average percentage. For the performance evaluation, the percentage penetration of PV was increased in steps of 10%. The following list summarises the scenarios in terms of the load, irradiance level and PV location:

- S1 – Worst-case scenario used in the literature i.e. load of 152 W, irradiance of 1000 W/m^2, PV located at the far end of the feeder
- S2 – Realistic worst-case scenario i.e. load of 300 W, irradiance of 800 W/m^2, PV located at the far end of the feeder
- S3 – Futuristic scenario with load of 500 W, irradiance of 800 W/m^2, PV located at the far end of the feeder

Table 7-1 summarises the permissible penetration levels for each of the scenarios for different parameters. The percentages in each cell indicate the percentage penetration of PV up to which the presence of PV does not adversely affect the performance of the distribution network, based on the results discussed in sections 5.4 and 6.3.

Table 7-1: Percentage PV penetration at which different performance parameters may be adversely affected for different scenarios

		Hosting capacity		
No.	Performance parameter	S1	S2	S3
1	Voltage profile (P1)	30%	20%	100%
2	Total harmonic distortion (P2)	100%	100%	100%
3	Net active power at substation (P3)	10%	30%	40%
4	Power factor at secondary of substation (P4)	10%	20%	30%
5	Voltage unbalance (P5)	30%	30%	30%
6	Protection mechanism (P6)	40%	40%	40%

The performance parameters that may be adversely affected at S1 by increasing penetration of PV systems in the order of their occurrence are

1. Net active power at secondary of substation (P3)
2. Power factor at secondary of substation (P4)
3. Voltage profile (P1)
4. Voltage unbalance (P5)

5. Protection mechanism (P6)

For scenario S2, the barriers in the order they may be observed, as the percentage of PV increases, are

1. Voltage profile (P1)
2. Power factor at secondary of substation (P4)
3. Net active power at secondary of substation (P3)
4. Voltage unbalance (P5)
5. Protection mechanism (P6)

For scenario S3, the barriers in the order they may be observed, as the percentage of PV increases, are

1. Voltage unbalance (P5)
2. Power factor at secondary of substation (P4)
3. Net active power at secondary of substation (P3)
4. Protection mechanism (P6)
5. Voltage profile (P1)

The results highlight that, at the probable boundary conditions, the first parameter to be adversely affected is the voltage profile, which is in-line with the discussions in the existing literature. The distribution network used in this research has been in used in [118] to evaluate the impact of an increase in contribution from combined heat pumps (CHP), which is also an inverter based generator, on the network performance. A simplified load flow based approach with CHP as a constant current source was used in [118] and only the voltage profile was evaluated. Though the maximum penetration has been mentioned as 48%, the authors have not clearly mentioned the definition of percentage penetration they have used. The network was further used in [119] to extend the analysis in [118] to include reverse power

flow and unbalance with the definition of percentage penetration as the ratio of the number of houses with PV to the total number of houses. The percentage penetration at which over voltage occurs is around 40%, which is around 30% as per the definition used in this thesis. However, the penetration at which reverse power flow occurs is different (40% in this research as against 80% in [119]) which could be attributed to the difference in generation profiles of PV and CHP.

Unbalance in voltage becomes significant only at about 60% penetration with all PV connected in the same phase. However, the probability of occurrence of such an event is very low as also highlighted in [119]. Impact of the presence of PV on the voltage profile of a larger network with 1262 houses has been analysed in [29]. The authors, however, use mean of voltages throughout the network at 1-minute intervals for one typical day each in summer and winter to evaluate the impact. They observe that the voltage mean violates the upper limit only at 50% penetration, which translates to 76% as per the definition in this thesis. However, the use of a mean profile tends to cancel the increase in voltage due to PV generation against the voltage sag due to heavy load at any other part of the distribution network. The higher permissible penetration level of PV could be attributed to the use of mean voltage. The time interval used in this thesis is 1 minute for irradiance data and 30 minutes for load profile. Though the time interval is higher than that used in [29], the data is based on larger number of houses and measured over a longer period. The use of a more probable boundary scenario, based on practical conditions, results in more practical permissible penetration levels of PV. Also, the use of the net capacity of PV in the definition of penetration enables the extension of the results to a network with different individual ratings of PV systems. However, care has to be taken to extend the results to networks in other parts of the UK. Correlation of the local irradiance values with the load profile of customers in that network and the comparison of tap changer settings would be required before the extension of the

results of this thesis. The percentage of PV at which its presence may adversely affect the steady state performance considering the most probable boundary conditions is about 20%, lower than the penetration levels (converted to percentage as per the definition in this thesis) discussed in [17, 29, 31, 118, 119] as shown in Table 7-2.

Table 7-2: Comparison of hosting capacity as discussed in the literature

Author(s), (Year)	Performance parameter(s)	Hosting capacity (%)	
		as per author's definition	as per definition in this thesis
Ingram, S., S. Probert, and K. Jackson (2003)	Voltage profile	48	Not sufficient information
Econnect ventures Ltd. (2007)	Voltage profile	40	30
	Reverse Power Flow	100	80
Thomson M. and Infield D. G. (2007)	Voltage profile	50	76
Suwanapingkarl P. (2012)	Voltage profile	15	46
Ali, S., N. Pearsall, and G. Putrus (2012)	Voltage profile	50	115

While mitigating the barriers, caution has to be taken to ensure that other performance parameters are not adversely affected by the solution. For example, the option of modifying the operating power factor of the PV systems may have an adverse impact on the voltage profile (as described in section 5.4.5). The next section discusses the different solutions discussed in the literature to mitigate the adverse effects of PV system on the performance parameters of the electricity network (transmission and distribution) and also rank them in the order of its effectiveness for electricity distribution network in the UK.

7.2 Technical Solutions

The contribution of PV could be increased without adversely affecting the distribution network performance using the capability of the PV inverter itself or by

making changes to or replacing different components of the distribution network. Though the capability of PV inverters to modify the network parameters favourably has been a topic of research for more than a decade, for eg. [159], it was only recently that the capability was considered as an option to help increase the contribution of PV systems in the network.

Technical solutions to help increase DG contribution, at 33 kV and below, in the UK have been discussed by Collinson et al. in [160]. Active network management (ANM) has been suggested as an option to increase DG contribution. The report categorises different technical solutions for ANM as follows:

1. Fault level management
2. Network voltage control
3. Network power flow management

The solutions have been evaluated using their implications on customers, distributed generator owners and distribution network operators (DNO). The report identifies network enhancement or uprating as a solution that falls into all three categories of technical solutions and serves as a benchmark to evaluate other solutions. The high cost of replacing different components of the network, which is also dependent on the voltage level and increases with increasing voltage level, has been identified as a key issue to implement this solution. Fault management of the network with DG has been highlighted as the main issue for which a detailed discussion of solutions has been carried out. These solutions may not be applicable for PV systems as they are inverter based generators with limited contribution to the fault current.

The literature on solutions to increase the contribution of PV systems can be broadly categorised as those addressing:

1. Overvoltage
2. Active power flow/congestion
3. Rapid fluctuations in power flow
4. Voltage total harmonic distortion (VTHD)
5. Performance of PV inverter during fault

The following sections discuss in detail the literature on each of these categories.

7.2.1 Mitigate overvoltage

Voltage rise may be mitigated by:

1. Using PV inverter capability to control the reactive power output
2. Using shunt elements to control reactive power flow in the network
3. Adjusting the tap changer settings
4. Modifying/adding series voltage regulators
5. Controlling the active power flow (curtailment and storage)
6. Relaxing of the upper voltage limit of the standards

Relaxing the upper limit by 1% or 2% has been suggested in [161] without the evaluation of its potential to increase the PV contribution. Also, the impact that the relaxation of upper voltage limit may have on other loads connected to the distribution network has not been discussed.

The impact of the use of inverter capability to control the voltage of the network is dependent on the type of electricity network to which it is connected. The impact of the use of inverter capability to supply or absorb reactive power in a transmission network has been discussed in [161, 162]. Tan analysed a 500 kV, 10 bus test network representative of the transmission network in the US for increasing penetration of PV from 0 to 10% and concluded that at lagging power factor (supplying reactive power) the voltage profile fluctuation for a given fluctuation in irradiance was lower than at unity power factor or leading power factor (absorbing

reactive power) [162]. The PV system was modelled to operate at a constant power factor between 0.85 lagging and 0.85 leading. Tan also analysed the capability of the inverter to control the real-time reactive power output dependent on the voltage at its terminals and concluded that this did not result in significant improvement in voltage profile fluctuation arising from a fluctuation in irradiance. However, a similar control strategy implemented by Prakash for a transmission network in the US showed a higher reduction in the number of buses facing overvoltage than a reconfiguration of existing shunt devices under light and heavy loading conditions [161]. However, the details of voltage set points used to arrive at the final configuration of the PV inverter was not provided.

The impact of the use of inverter capability to vary its reactive power output to control the voltage profile in a distribution network has been discussed in [163-167]. Zhou discussed the impact of control of reactive power output of the PV inverter, based on the reactive power – voltage droop characteristic for a single-phase transformer-less PV inverter, on modified IEEE 34 bus network and concluded that the method was effective in mitigating the voltage rise [163]. Ackermann et al. evaluated the possibility of varying the reactive power output of the inverter as a function of real power or voltage and concluded reactive power control to be less effective than the active power control in LV networks due to their relatively higher R/X ratios [164]. A study by Vandenbergh et al., on LV and MV distribution networks in the Czech Republic, Germany, Italy and Spain highlighted that use of inverter reactive power supply capability would result in improvements in voltage fluctuations resulting from PV generation variation [165]. The reactive power output was controlled as a function of real power or as a function of the voltage at the inverter terminals and they also discussed the use of SCADA interaction with individual PV inverters to control the reactive power output. Schauder discussed the impact of control of reactive power output of a 5 MVA PV inverter connected to a 13.8 kV MV

distribution line in the US and concluded that the reactive power from PV can be used to mitigate voltage fluctuations introduced by PV and also to mitigate pre-existing voltage issues in the MV network [166]. However, the literature discussing the impact of reactive power control on a distribution network still consider large three-phase PV systems and lumped three-phase loads. The LV distribution system, as discussed in chapter 4, has single-phase PV systems and loads and the distribution lines have higher R/X ratio than transmission networks. The impact of reactive power control on such a network has not been quantified in the literature. With the discussions of inclusion of reactive power control as a standard feature in future PV inverters, it is important to evaluate and quantify its impact on an LV distribution network in the UK.

A theoretical three-phase symmetrical rural distribution network has been analysed in [167] with three different control strategies for reactive power control. In the first strategy, the inverters operate at constant power factor irrespective of the voltage at the terminals. In the second strategy, the inverters that experience overvoltage absorb reactive power until the voltage has been brought within the limits. In both strategies, the additional reactive power has to be supplied by the grid whereas, in the third strategy considered, reactive power absorbed by the PV inverter farthest from the substation was compensated by reactive power generation by the PV inverter near the substation. Though the third strategy does not contribute to an increase in instantaneous current at the secondary of the substation, communication between the PV inverters becomes a mandatory requirement to implement this solution.

Voltage regulation by modifying the existing control mechanisms in on-load tap changers (OLTC) at HV/MV transformers and additional OLTC at the MV/LV transformer has been suggested in [165] and the authors have observed that OLTC at MV/LV is effective in controlling the voltage fluctuations. The effectiveness of

modifications to the control strategy of OLTC at the HV/MV transformer has been observed as dependent on the uniform loading on all the feeders supplied by the transformer and also on how representative of the entire feeder is the location of measurement of voltage used to regulate the output voltage of the transformer. The use of OLTC at the MV/LV substation has also been discussed in [168] and the authors observed that the effectiveness of this solution is dependent on the length of the distribution feeder. The higher the length of the feeder, the higher is the effectiveness of the solution.

In the context of the LV distribution network in the UK, changes could be made to the OLTC in the 33/11 kV distribution transformer and/or to the off-load tap changer in 11/0.433 kV substation transformer. The modifications to the OLTC would be more effective for a uniform increase in penetration of PV in all the feeders supplied by the 33/11 kV transformer than for a clustered increase in penetration in one of the feeders supplied by the transformer. There is a possibility of using additional voltage sensors at different parts of the LV distribution network to control the tap-changers (active voltage control), but that would require more infrastructure than currently available to decide which voltage would result in optimum performance of the distribution network. The possibility of changing the setting of the off-load tap changer in the 11/0.433 kV transformer is a simple solution to prevent overvoltage at the increased penetration of PV. However, care has to be taken to ensure that this does not result in under voltage at heavy loading conditions with no PV and also under normal loading conditions with no PV.

Zhou evaluated the effectiveness of the use of a static voltage compensator (SVC) to regulate voltage with reactive power control of PV inverter and concluded that the SVC was more effective in limiting the voltage fluctuations than the reactive power control using PV at 5% and 10% PV penetration in a 10-bus network representative of the US transmission network [162]. However, the rating of SVC is dependent on

the network capacity and the total PV capacity connected to the network and may require replacement when the PV penetration increases beyond a particular level, incurring a further cost to the network operation. The inverters were operated at a constant lagging power factor of 0.95 for the above comparison. The use of existing reconfigurable shunt devices that could be controlled in a coordinated manner and the addition of new shunt devices to regulate voltage in a transmission network have been discussed in [161]. The effectiveness of the use of shunt devices was evaluated for two extreme demand conditions, one arising from the past that has light loading condition and one futuristic high loading condition with PV penetration from 7.5% to 45%. The use of additional shunt devices was more effective than co-ordinated control of existing shunt devices for the network under consideration, though this would result in higher implementation costs.

Etherden evaluated the increase in generation of wind or PV systems, in MW, that could be obtained in an MV/LV distribution network in Sweden with lumped generation/load at 400 V at 2% and 5% curtailment in a year [169]. The curtailment in [169] is defined as the percentage of time in a year that the generators will have to reduce its output with a reduction in generation dependent on the overloading of the distribution network. The research highlights the possibility of the use of hosting capacity as an index to compare integration of different types of renewable generation in different networks but does not discuss the percentage increase in hosting capacity achieved or increase in hosting capacity in terms of the performance parameters of the distribution network. Different DG curtailment strategies, viz. last in first out (LIFO), proportional reduction and most technically appropriate scheme, have been discussed, by Sun, as a solution to prevent overvoltage in [134]. An optimal load flow based approach was used to evaluate the impact of different curtailment strategies in the UK generic distribution system (UKGDS) with multiple wind farms. However, the increase in the contribution of wind

generation achieved by using the curtailment was not quantified. Though works discussing curtailment strategies are available, they do not focus on the LV distribution network and in most cases assume a balanced network with lumped three-phase loads at 400 V.

Petinrin and Shaaban reviewed different strategies to mitigate overvoltage in a distribution network with wind and PV generation [170] with the main highlights on demand-side management and energy storage. They concluded that smart grid technologies like demand-side management and energy storage are more effective in mitigating voltage rise with minimum network enhancement than changes to tap changers or reactive power control. Vandenberg et al. evaluated that storage by either the network operator or by the prosumer (a consumer who performs generation as well) was effective in regulating the voltage, albeit with high initial cost [165]. Ackermann et al. discussed the use of storage to reduce the amount of energy curtailed and concluded that about 30-40% of the annual demand of Europe could be met by PV without violating the voltage limits by providing storage at optimal locations of the network [164]. Implementation of smart meters at individual customers may provide information to implement demand-side management and energy storage management. There have also been discussions on the use of electric vehicles for energy storage. However, the implementation of the smart grid solutions, viz. demand-side management and energy storage, would involve arriving at a consensus with multiple stakeholders, which could be considered as a future work of this research. The evaluation of the effectiveness of these solutions would also require higher time and geographical resolution for the load profile and irradiance.

7.2.2 Control the net active power

Vandenberg et al. discussed the use of storage, active power curtailment and demand-side management in the low voltage distribution network to control the net power [165]. The possibility of storage both at the distribution level and at the individual consumer level was discussed and they concluded that storage at individual customer level has a higher impact than at network level on reducing the voltage fluctuations and reverse power flow issues arising from increasing contribution of PV systems. They also observed that regulatory changes are urgently required to allow for customer storage in Spain and the Czech Republic. The solution of active power control using PV inverters has also been identified as a high impact solution requiring regulatory changes in the four countries considered. Alexander, Richardson and James discussed different types of storage, viz. pumped storage, liquid air storage, hydrogen storage as a solution to reduce overloading of equipment in the network and concluded that though there are technical issues for each of the above storage solutions, a mix of the storage technologies would form a potential solution to create a 100% renewable electricity network for the UK [171]. As reverse power flow is one of the barriers limiting the contribution of PV, the options of active power curtailment and storage are included in this research in the initial assessment of solutions.

7.2.3 Limit rapid fluctuations in power flow

Shaobo et al. discussed battery storage as a solution to prevent rapid changes of power flow [172]. The optimal capacity, in kW and kWh, of battery storage in-order to minimize the power fluctuations at MW scale PV plants was evaluated. However, they do not indicate the voltage level at which the methodology can be adopted and the expected reduction in power flow fluctuation at the point of common coupling (PCC) with the transmission line. Storage has been further discussed in [169] for the MV/LV network, with lumped loads and generations at LV, using real-time

assessment and communication strategy to increase the hosting capacity of the network. Shivashankar et al. presented a review of battery storage as a solution to limit power fluctuations in a network with an observation that detailed analysis along with better load and irradiance forecasting is required to evaluate the potential of battery storage to increase the contribution of PV systems [173]. They also highlight that there is limited research focusing on the voltage at grid side and reverse power flow while also considering the fluctuations in solar power output. As the time step for analysis of power fluctuations is between the time steps for steady-state analysis and dynamic analysis, this aspect has not been evaluated in detail in this research.

7.2.4 Limit the voltage total harmonic distortion

Dartawan et al. discussed the use of harmonic filters to help increase the contribution of PV systems in distribution networks with background harmonics have been discussed in [40]. They presented a case study based on a 12.47 kV distribution network, with 0% and 2% background harmonics, and multiple 500 kW PV systems, with 3% or 6% current total harmonics, to elaborate the impact of PV on the voltage harmonics at 69/12.47 kV substation. Though an option of the use of a high pass filter and a notch filter in parallel to reduce the harmonics has been discussed, the increase in the contribution of PV that could be attained through this solution has not been evaluated. The results of steady-state performance evaluation at different penetration levels of PV highlights that the total harmonic distortion at the secondary of the substation was not significantly adversely affected by the presence of PV. Hence, the effectiveness of solutions to limit the total harmonic distortion has not been evaluated.

7.2.5 Control the performance of PV system during fault

Yang et al. proposed a modification of the grid code to allow the PV to stay connected during a fault (LVRT) and supply reactive power to increase the

contribution of PV systems in distribution networks [143]. They highlighted that tripping of the PV system under fault results in voltage flickers, power outages and system instability. Though control strategies to implement LVRT in single-phase PV systems were presented, the impact of LVRT on the performance parameters was not analysed. A novel controller that can perform islanding detection for an inverter with LVRT capability was presented by Zhou in [163] and its impact on the IEEE 34 bus test distribution network at 29.4 kV was simulated for 30% PV penetration and 90% voltage sag with a sag duration of 3 s. Zhou observed that though the inverters stayed connected to the grid, the voltage at many parts of the network dropped below the under-voltage protection threshold defined in IEEE 1547 which could be attributed to the limit on the amount of reactive power (in this case is 0.45 p. u.) a PV system can supply. Active network management has been discussed as a solution to increase the fault headroom available in a UK urban network, with the conclusion that increase in PV/inverter based generation may release fault headroom enabling more connection of DG [174]. The evaluation of the impact of single-phase PV systems on the performance of a distribution network during a fault (as discussed in chapter 6) indicates that at LV, the presence of PV does not significantly affect the performance of the distribution network. Therefore, the solutions to control the performance of PV systems during fault have not been considered for detailed analysis.

7.3 Methodology to Identify and Evaluate Technical Solutions

From the results of dynamic-state performance analysis (detailed in chapter 6), it can be concluded that the presence of PV does not significantly affect the protection mechanism in low voltage distribution networks. Also, the UK guidelines provide a significant time delay to prevent unnecessary tripping of the inverters. The results of steady-state performance analysis indicate that the voltage profile is the first performance parameter affected, followed by reverse power flow and power factor

at the secondary of the substation. Though rapid fluctuation of the PV output is of concern at higher PV capacities, at low voltages, the fluctuations smooths out due to the physical distribution of the residential PV systems and the fluctuations in the demand in residential loads. Therefore, it is not a barriers at the distribution network level.

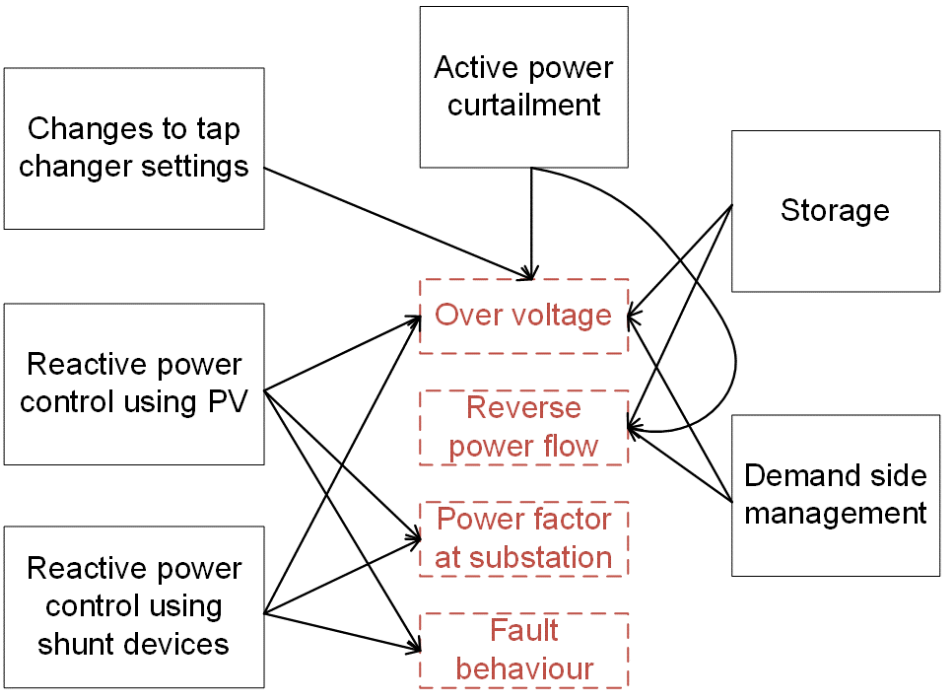

Figure 7-1: Summary of solutions discussed in literature

Figure 7-1 shows the summary of the different solutions discussed in the literature, excluding network reinforcement, and the links to the performance parameter(s) that may be affected by them. From the figure, it can be observed that most of the solutions have an impact on more than one performance parameter. For example, reactive power control using PV would have an impact on the voltage profile, power factor at substation and fault performance. The authors of [165] proposed two indices, a cost-benefit index and a regulatory priority index, to prioritize the solutions applicable to LV and MV distribution networks in Italy, Spain, Germany and the Czech Republic. The cost-benefit indicator was a weighted average based on cost, impact on voltage and impact on congestion/power flow with weights of 0.4, 0.4 and 0.2 respectively. The authors attribute the higher weight for impact on voltage to the

discussions in the literature on voltage problems limiting the hosting capacity. The regulatory priority index was based on binary options for technology availability and applicability within existing regulation.

A similar approach, as in [165], is proposed here to prioritise the solutions applicable to LV distribution networks in the UK but with equal weight to all the criteria. Equal weight was used because, although voltage was the first parameter to be affected at the realistic worst-case scenario (S2), reverse power flow was the first parameter to be affected in the other scenarios (S1 and S3). The criteria used to perform the initial assessment, to shortlist the solutions that are analysed in detail to quantify the percentage increase in the contribution of PV resulting from the solutions, are as given in Table 7-3. The higher the score, the better the solution and the solutions with the 3 highest scores were considered for detailed assessment. These solutions were analysed in detail, based on the criteria given in Table 7-4, to arrive at the final ranking of solutions to increase the contribution of PV in the distribution network in the UK.

7.4 Initial Assessment of Solutions

The details of the scores obtained by different solutions for the initial assessment criteria are as shown in Table 7-5. Grid reinforcement involves adding to or replacing the existing components of the distribution network to enable additional PV to be connected to the network without adversely affecting the performance. Grid reinforcement is easier to implement technically compared to other solutions, however, it is less economically feasible due to high initial costs [164]. Therefore, grid reinforcement has not been included in the table. Though reactive power control using PV and using shunt devices have the same score, the ranking for reactive power control using PV is assigned a higher position as the solution can be

Table 7-3: Initial assessment criteria

Initial assessment criteria/Score	1	2	3	4	5
Is the solution applicable to LV distribution network? (C1)	No		May be		Yes
Technology readiness of the solution (C2)	Only concepts are available	Early research	Successful in the laboratory	Successful in pilot projects	Commercial product
Applicability within existing regulatory framework in the UK (C3)	Changes required				No changes required
Cost of implementation (C4)	Very high cost	High cost	Average cost	Low cost	Very low cost
Additional infrastructure required for implementation (C5)	Extra infrastructure required		May be required		No additional infrastructure required

Table 7-4: Detailed assessment criteria

Detailed assessment criteria	Values	Additional comments
Percentage increase in contribution of PV	0-100%	
Any changes to existing hardware?	Yes/No	If yes, how costly are the changes?
Will the solution affect any other performance parameter?	Yes/No	If yes, what is the new limit of PV contribution?
Changes to existing design of inverter	Yes/No	If yes, what change is required?
Will the solution disrupt power during implementation?	Yes/No	If yes, then for how long?
Will the solution result in loss of generation?	Yes/No	If yes, then by how much (%)?
Cost of implementation	1-5	Very high / High / Average / Low / Very low

Table 7-5: Initial assessment of solutions

Solution/Criteria	C1	C2	C3	C4	C5	Total Score	Rank
Changes to Tap changer settings	5	5	5	5	5	25	1
Reactive power control using PV	5	5	1	4	5	20	3
Reactive power control using shunt devices	5	5	5	2	3	20	4
Active power curtailment	5	5	5	4	5	24	2
Storage	5	5	1	2	3	16	5
Demand side management	5	4	1	3	1	14	6

implemented with minor changes to the regulatory framework, which are already being considered in other countries.

Based on the initial assessment, changes to the tap changer, active power curtailment and reactive power control have been chosen to be analysed in detail. These solutions are further evaluated using the models developed in chapter 4 to

determine the effectiveness of the solution to increase the penetration of PV systems.

7.5 Detailed Assessment of the Selected Technical Solutions

This section describes the detailed assessment of the selected solutions viz. changes to the tap changer settings, active power curtailment and reactive power control.

7.5.1 Evaluation of impact of changes to off-load tap changer settings

A distribution network in the UK typically has transformers stepping down the voltage from 33 kV to 11 kV and from 11 kV to 0.433 kV. The 33/11 kV transformer has an on-load tap changer (OLTC) regulating the voltage at the 11 kV side of the transformer. The literature available discusses the possibility of changing the voltage regulation characteristic of the OLTC and modifying the bus voltage that is used to calculate the tap setting. An example would be to monitor the voltage at the bus furthest from the 33/11 kV transformer instead of the secondary voltage of the transformer to perform the voltage regulation. However, such a modification would only be beneficial if all the feeders that the 33/11 kV transformer is supplying have a uniform distribution of load and PV systems, which is generally not the case. If the feeder at the far end of the distribution network has a high penetration of PV systems resulting in an overvoltage at that feeder, and the OLTC was modified keeping in view this feeder, the feeders in the middle may experience under voltage. Another option is to use voltage measured at different parts of the feeder to control the secondary side, 11kV, voltage. However, this would require multiple sensors, communication between them and a complex calculation. Therefore, the changes to OLTC are not considered to mitigate the overvoltage issue at the LV distribution network arising from the presence of PV systems.

The 11/0.433 kV transformer typically has an off-load tap changer. The off-load tap changer is set to maintain a higher voltage than 1 p. u. at no load condition, so as to ensure the voltage at the point farthest from the transformer does not face under-voltage during high loads e. g. evening peak. Changes to the off-load tap changer may not be a popular option as it would require disruption of the service and manual modification of the tap setting. Also, the network operator has to ensure that this change does not result in over/under-voltage at low load/high load with no PV generation. However, this is a suitable option if a one-time change to the setting would allow for increased contribution of PV without adversely affecting any other performance parameter of the distribution network with and without PV generation.

Before analysing the impact of the solution of changing the off-load tap changer settings, a set of simulations were performed to identify the boundary loading conditions. The boundary loading conditions are the loads close to the tap-changer movement from one value to another, for example from -1 to -2. The distribution network was simulated at initial tap changer settings and no PV for loads varying from 150 W to 900 W (values of loads were chosen based on Figure 5-3) in steps of 50 W. A load per house of 300 W resulted in movement of tap changer from 0 to -1 resulting in the voltage profile being very close to the upper limit. Any load which results in a similar profile has to be considered in combination with the highest possible irradiance at the load to ensure that the solution is effective in that scenario as well and would not result in a worsening of the performance of the distribution network. The loading conditions that occur before each change of tap changer are also identified, as there is a probability of under-voltage at these loading conditions when PV generation is low/zero. The boundary loading conditions as identified in this step are 250 W, 300 W, 550 W, 600 W, 850 W and 900 W. Figure 7-2 shows the voltage profile at the boundary conditions. It can be observed that the voltage profile at 300 W is closer to the upper limit than the voltage profile at 250 W (contrary

to the expectation that the voltage would drop due to increase in load) due to the tap changer movement from 0 to -1. A similar trend can be observed with loads 550 W and 600 W as well as 850 W and 900 W.

To evaluate the impact of reducing the secondary voltage of the 11/0.433 kV transformer on the distribution network performance, the following scenarios were simulated:

1. Boundary loading conditions at no PV
2. 30% PV penetration, 300 W per house load, 800 W/m^2 irradiance and substation voltage of 415 V (the scenario at which over-voltage was experienced as per steady-state performance analysis)

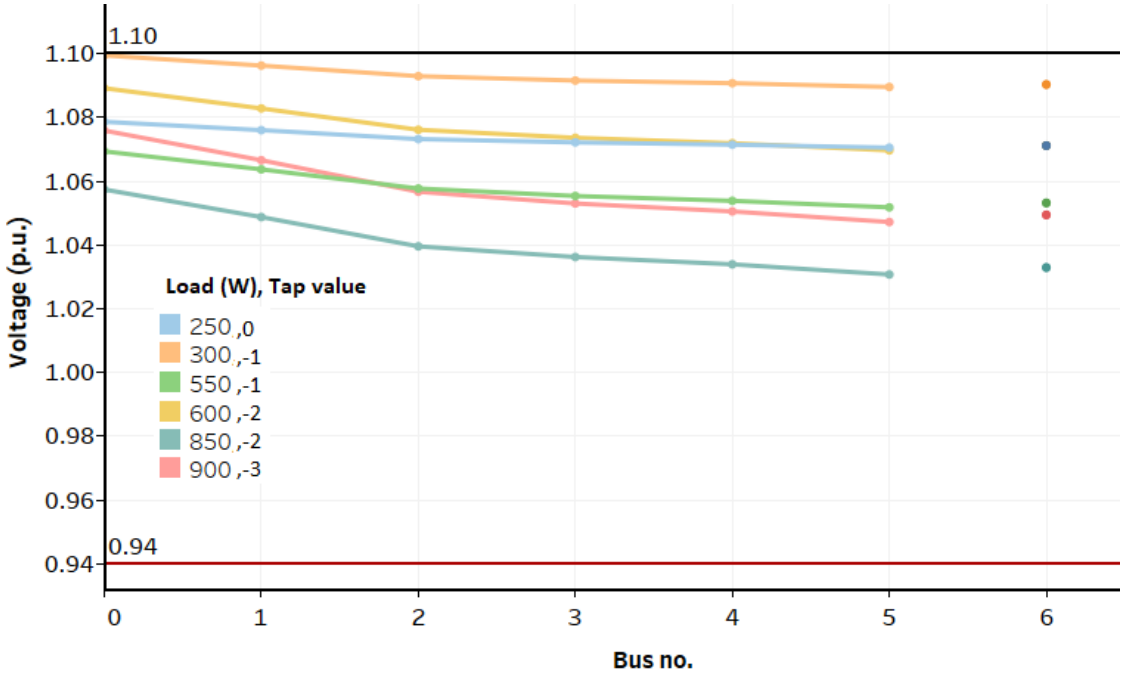

Figure 7-2: Voltage profiles at different loading conditions resulting in an action by the tap changer

3. 30% PV penetration, 550 W per house load, 800 W/m^2 irradiance and substation voltage of 415 V.
4. 30% PV penetration, 600 W per house load, 800 W/m^2 irradiance and substation voltage of 415 V.

5. 40% PV penetration, 300 W per house load, 800 W/m^2 irradiance and substation voltage of 415 V
6. 40% PV penetration, 550 W per house load, 800 W/m^2 irradiance and substation voltage of 415 V.
7. 40% PV penetration, 600 W per house, 800 W/m^2 irradiance and substation voltage of 415 V.

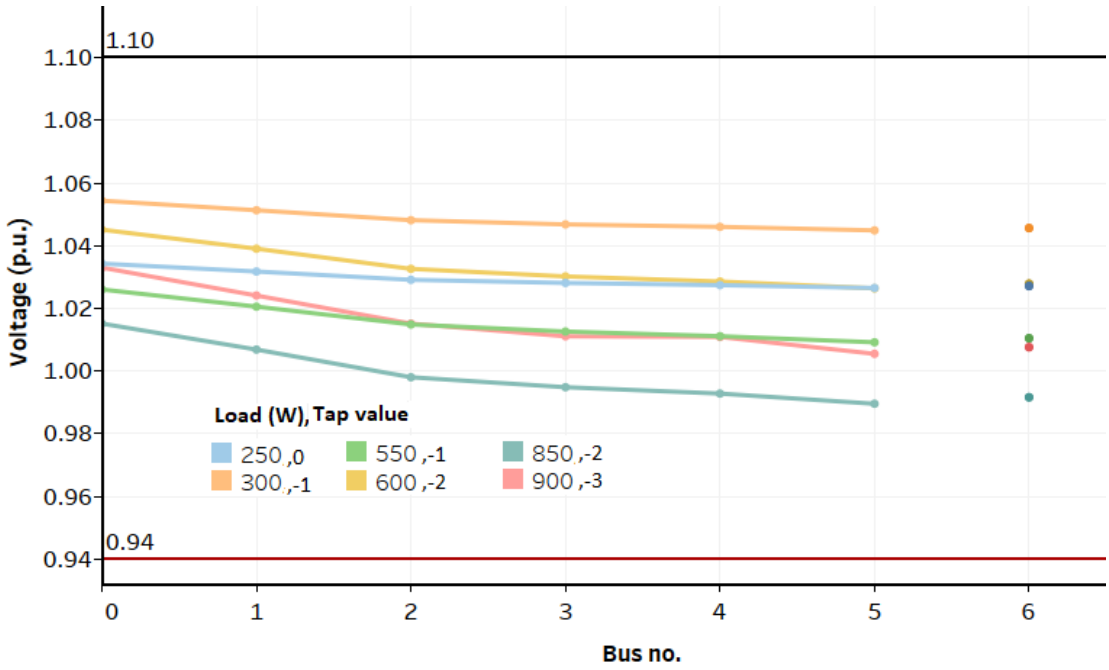

Figure 7-3: Voltage profile at the boundary scenarios for reduced secondary voltage at 11/0.433 kV substation

Figure 7-3 shows the voltage profile at the boundary conditions for the secondary of the 11/0.433 kV substation set at 415 V at no PV scenario. It can be observed that this change in tap changer setting does not result in under-voltage even at 900 W load (highest average demand as obtained from actual demand monitoring in the UK) at no PV. As PV contribution at high loads does not result in over-voltage, these conditions were not considered for observing the impact of an increase in PV penetration level. Figure 7-4 shows the voltage profile at 30% and 40% PV penetration at 300 W load and secondary substation voltage of 415 V. The results

show that the upper voltage limit is not violated at 40% and the penetration could go above 40%. However, at PV penetration levels above 40%, reverse power flow becomes the new barrier. Therefore, the scenarios above 40% have not been considered to evaluate the impact of changes to off-load tap changer settings. If reverse power flow is ignored, it may be possible to increase the penetration to about 100% before reaching the upper voltage limit.

7.5.2 Evaluation of curtailment

Curtailment of active power has an impact on the voltage profile as well as on the net power at the 11/0.433 kV substation. With no curtailment, the network faces overvoltage at 30% PV penetration and reversal of power flow at less than 40% PV penetration. The strategies for curtailment as discussed in the literature include last in first out approach (LIFO), first in first out approach (FIFO) and technical efficient approaches. The approaches LIFO and FIFO introduce uncertainty in terms of the location of the PV system curtailed and may not result in desired performance enhancement. The technically efficient approaches typically provide better control

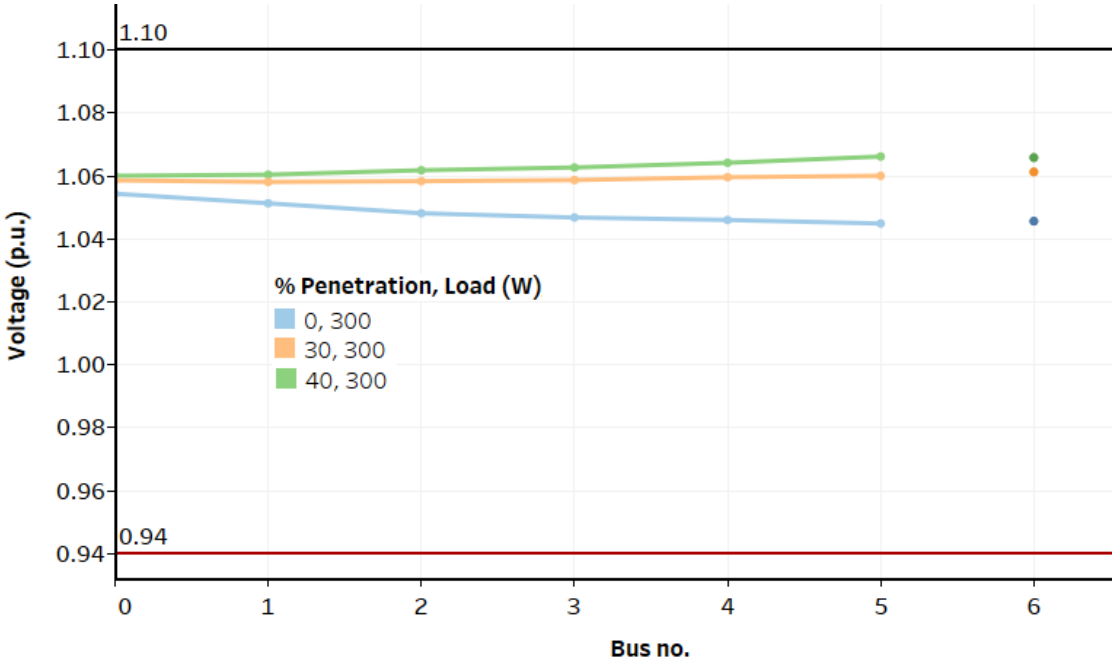

Figure 7-4: Voltage profile at different penetration levels of PV at the far end of the feeder for 300 W load and secondary voltage of 415 V

on the impact of curtailment on the performance of the distribution network and also may result in a lower number of PV systems being curtailed. The possible strategies for curtailment of energy from PV systems in an LV feeder other than LIFO/FIFO are:

1. Whenever overvoltage is detected in any part of the feeder, all the PV inverters in that feeder are required to shutdown
2. Whenever overvoltage is detected in any part of the feeder, the PV systems that face overvoltage are shut down
3. Whenever overvoltage is detected in any part of the feeder, the output of all the PV systems are curtailed to 50% of their respective rated capacities
4. Whenever overvoltage is detected in any part of the feeder, the PV systems that face overvoltage are curtailed to 50% of their respective rated capacities

In the case of a radial network with PV clustered at the far end of the network, the overvoltage due to the presence of PV would be felt almost throughout the feeder as shown in Figure 5-11. Therefore the impact of strategies 1 and 2 and strategies 3 and 4 would be the same, that is, the number of PV systems shut down for strategies 1 and 2 would remain the same. Also, the number of PV system curtailed in strategies 3 and 4 would be the same. The implementation of strategy 1 or 2 would result in disconnection of all PV systems in the feeder and the network performance would replicate that of a no PV scenario. Similarly, when strategy 3 is adopted, a condition of overvoltage would result in all PV systems operating at half their rated capacity which would be similar to PV systems operating at 500 W/m^2. Figure 7-5 shows the voltage profile for strategy 3 at 20%, 30% and 40% PV penetration levels. From the figure, it can be observed that 50% curtailment does not mitigate overvoltage at all buses. Figure 7-6 shows the net active power at the secondary of the 11/0.433 kV transformer for different penetration levels of PV. From the figure,

it can be observed that the net active power is positive until the percentage penetration reaches above 50%. That is, 50% PV curtailment is effective in mitigating the reversal of power flow until about 50% PV penetration.

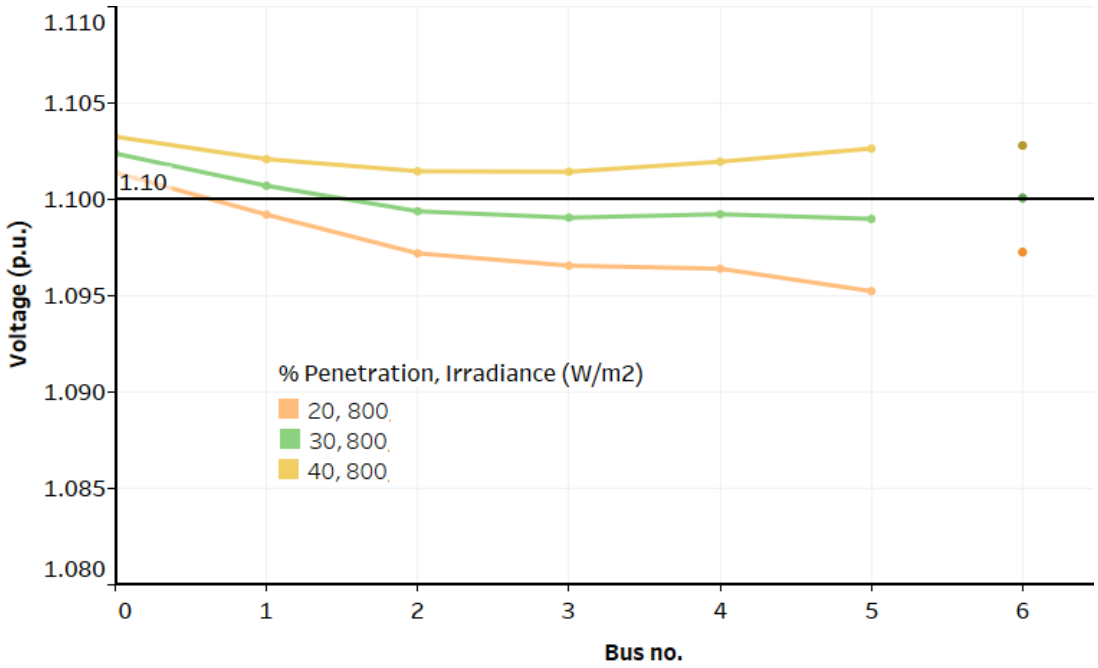

Figure 7-5: Voltage profile at different penetration levels with 50% curtailment, 300 W load and 800 W/m^2 irradiance, PV at the far end of the feeder

Strategy 1 would result in control of over-voltage for higher percentages albeit with increased potential for energy generation that is wasted. For example, at 30% penetration, curtailment would be required for irradiance greater than 600 W/m^2. Traditionally total curtailed energy is calculated as the product of the curtailed

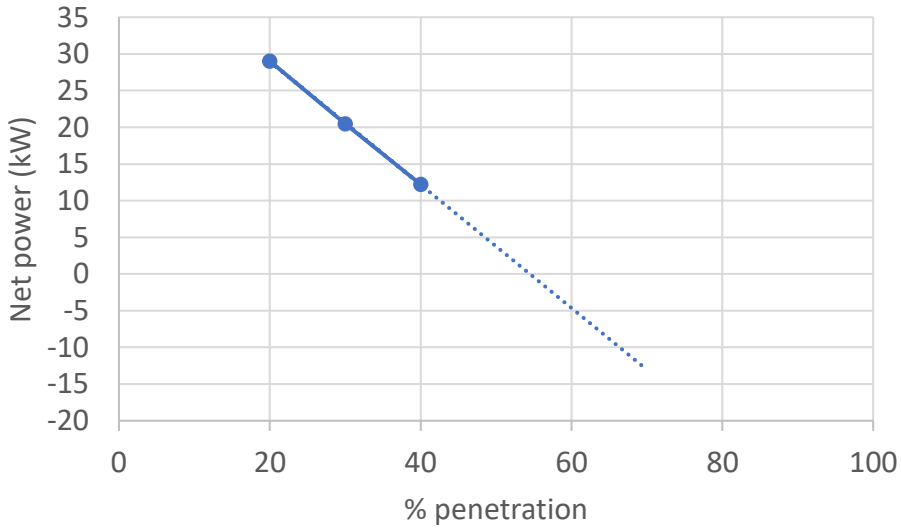

Figure 7-6: Net active power at the secondary of the 11/0.433 kV substation for different penetration levels of PV systems

capacity, capacity factor, power factor and operating hours of the generator [175]. If a shutdown of the PV system is performed to prevent overvoltage, it would result in a loss of around 133 MWh of energy generation (almost 100% of the energy generated by PV) in a year as penetration increases from 20 to 30% PV penetration, for the network considered. If a reduction of power to 50% of rated capacity is considered, then a loss of around 66 MWh may occur. For the UK, based on the data of irradiance, irradiance greater than 600 W/m^2 could occur for about 250 to 500 hours/year or about 5-10% of the daylight hours, depending on the orientation of the PV system (see section 5.3). Considering this irradiance data, as the percentage penetration increases from 20 to 30%, curtailment would be required for a maximum of 500 hours/year. This would result in a loss of generation about 30 – 60 MWh for strategy 1 or about 10 – 20 MWh for strategy 3 depending on the orientation of PV systems. Though in strategy 3, PV systems are required to operate at half its rated capacity, the energy curtailed is lower than half of the energy curtailed due to strategy 1 as irradiance is not always around 1000 W/m^2 when curtailment is performed. That is if the irradiance is around 600 W/m^2 for one hour, strategy 3 would result only in curtailment of 2.5(600-500)/1000 kWh, i.e. 0.25 kWh, for a 2.5 kWp PV system, not 1.25 kWh. The curtailed energy calculation for strategy 1 also includes the variation in irradiance from 600 – 1300 W/m^2.

The above calculations, however, do not consider that at higher loading conditions than 300 W per house and 600 W/m^2 irradiance voltage is within limits. From the correlation of load with the irradiance data, it can be observed that load remains in the range of 300 – 350 W only for a part of the time that the irradiance is greater than 600 W/m^2 as shown in Figure 7-7. Considering this correlation, it can be observed that as penetration increases from 20 to 30%, curtailment would be required for about 90-100 hours instead of the 250 to 500 hours in order to prevent overvoltage. This implies that curtailment would be required for less than 2% of a

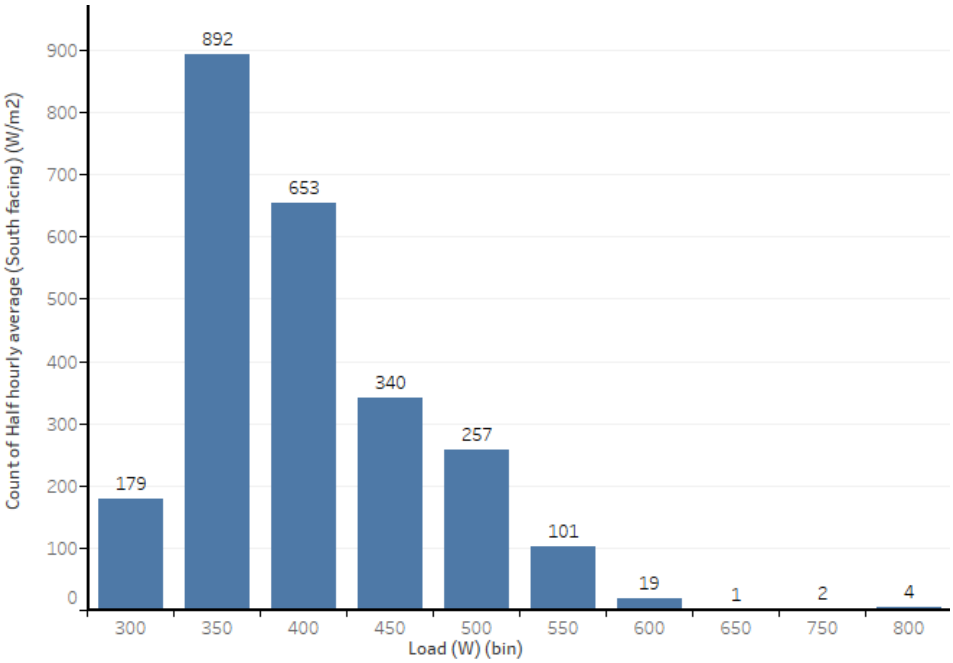

(a) South facing wall

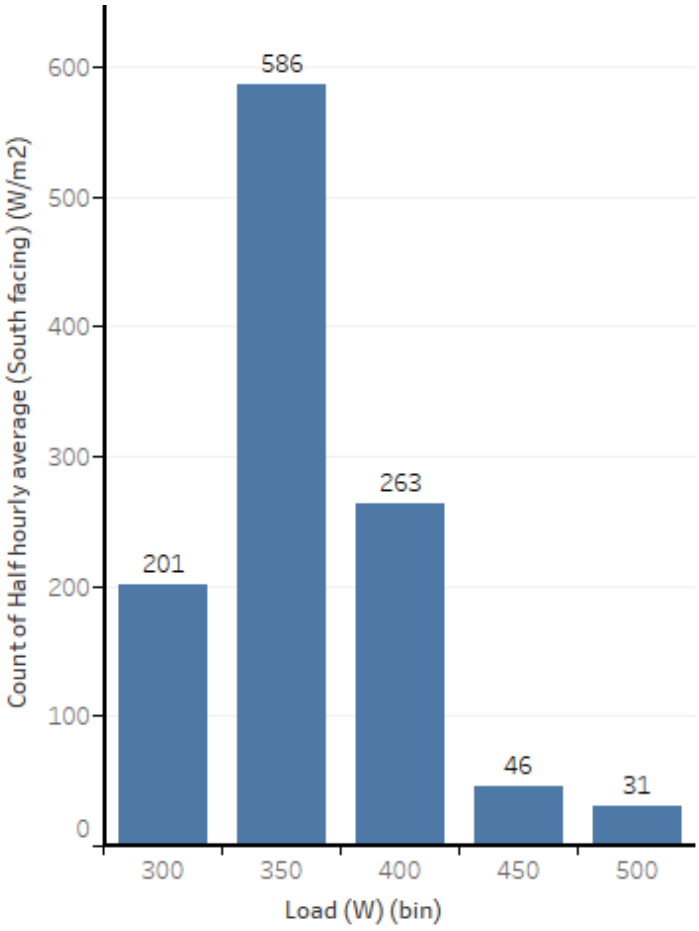

(b) Horizontal surface

Figure 7-7: Count of half hourly average irradiance greater than 600 W/m² on a south facing wall and horizontal surface for different loads

year to prevent overvoltage as penetration increases from 20 to 30%. The use of strategy 1, along with the consideration of load and irradiance correlation, may result

Table 7-6: Summary of results of curtailment using different strategies

	Penetration increases from 20 to 30%					Penetration increases from 30 to 40%					Penetration increases from 40 to 50%				
Parameter / Scenario	PV_{gen} (MWh)	E_{curt} (MWh)	h_{curt} (h)	h_{curt} (%)	E_{curt} (%)	PV_{gen} (MWh)	E_{curt} (MWh)	h_{curt} (h)	h_{curt} (%)	E_{curt} (%)	PV_{gen} (MWh)	E_{curt} (MWh)	h_{curt} (h)	h_{curt} (%)	E_{curt} (%)
No curtailment	110 - 130	NA	NA	NA	NA	155 - 170	NA	NA	NA	NA	200 - 225	NA	NA	NA	NA
Strategy 1 (irr data only)	110 - 130	30 - 60	250 - 500	4 -5%	25 - 50%	155 - 170	40 - 80	250 - 500	4 -5%	25 - 50%	200 - 225	51 - 100	370 - 600	4 - 7%	25 - 50%
Strategy 3 (irr data only)	110 - 130	10 - 21	250 - 500	4 -5%	8 - 17%	155 - 170	13 - 30	250 - 500	4 -5%	8 - 17%	200 - 225	17 - 40	370 - 600	4 - 7%	8 - 17%
Strategy 1 (load & irr correlation)	110 - 130	10 - 11	89 - 100	1 - 1.2%	7 - 10%	155 - 170	13 - 15	89 - 100	1 - 1.2%	7 - 10%	200 - 225	22 - 25	125 - 150	1.4 - 1.6%	7 - 10%
Strategy 3 (load & irr correlation)	110 - 130	3 - 3.5	89 - 100	1 - 1.2%	2.5 - 3%	155 - 170	4 - 4.5	89 - 100	1 - 1.2%	2.5 - 3%	200 - 225	5.8 - 6.3	125 - 150	1.4 - 1.6%	2.5 - 3%

in a loss of a generation of 10-12 MWh per year whereas the use of strategy 3 may result in a loss of a generation of 3-4 MWh per year. If curtailment is used as a strategy to increase PV penetration only considering the reverse power flow and assuming that overvoltage was mitigated by other solutions, curtailment would be required as PV penetration increases above 30%. From Figure 7-6, it can be observed that with 50% curtailment, penetration can be increased up to 50%, beyond which reverse power flow again becomes the barrier. At 50% PV penetration, reverse power flow would occur when the irradiance is higher than 500 W/m^2. Considering this and the correlation between the load and irradiance, the amount of generation that may be curtailed is around 22-25 MWh for strategy 1 and around 5-6 MWh for strategy 3, as against the traditional curtailment of about 178 MWh. Table 7-6 summarises the increase in a generation that could be achieved by an increase in PV penetration, the amount of PV generation that is curtailed and the number of hours of curtailment as penetration increases from 20 to 30%, 30 to 40% and 40 to 50%. Strategy 3 is better than strategy 1 as it reduces the generation lost in curtailment, however, strategy 3 would require modifications to the control strategy of the inverter capability to move its operating point away from the MPP. Also, consideration of the correlation between load and irradiance highlights that, in a practical network, energy lost due to curtailment may be much less than that calculated using traditional approaches. A cost-benefit analysis could be further done to provide more clarity on the benefits of the use of the more probable scenario with a correlation of load and irradiance. However, the percentage of total generation that would be curtailed does provide a clear indication of the relative benefit of the use of correlation of load with irradiance over the traditional methods to evaluate the economic feasibility of curtailment

7.5.3 Evaluation of reactive power control

The UK guidelines currently allow operation of PV between 0.95 p. f. lagging and 0.95 p. f. leading (Chapter 3). In order to eliminate the need for any regulatory or policy changes, the power factor of PV systems while operating on reactive power control is maintained between these levels. The impact of operating PV systems at 0.95 and 0.98 lagging power factors have been discussed in section 5.5.5. It was observed from the results that the lagging power factor operation improved the power factor at the secondary of the 11/0.433 kV transformer. However, it also resulted in the voltage upper limit being violated at lower penetration levels than when the PV was operating at unity power factor. As the overvoltage was the first barrier to be mitigated, the PV system was operated at leading power factors (absorbing reactive power) to observe the effectiveness of reactive power control (RPC) in mitigating the overvoltage.

The possible strategies for RPC are:

1. All PV systems are operated at a constant power factor, the value of this being determined by the network operator depending on the percentage penetration of PV on that feeder.
2. PV systems that face overvoltage are operated at leading power factor of 0.95 or 0.98
3. PV systems facing overvoltage are operated at leading power factor while PV systems not facing overvoltage are operated at lagging power factor. This could ensure that no additional reactive power is drawn from the transmission network due to the reactive power control.

Based on the voltage profile at the realistic worst-case scenario, it can be observed that when an overvoltage occurs, almost all the buses face overvoltage. Also, with PV being clustered at the far end, overvoltage would be felt simultaneously by all

the PV systems. This would be mean that no PV systems would be available to operate at lagging power factor for implementation of strategy 3. Therefore, strategy 3 is not a practical option for the LV radial distribution network with PV clustered at the far end of the feeder. Also, as strategies 1 and 2 would have a similar impact on the number of PV systems to be controlled, only strategy 1 is discussed further.

To evaluate the impact of reactive power control on the performance of the distribution network, the PV systems were operated at 0.95 or 0.98 p. f. leading and PV penetration level was increased from 30 to 50% in steps of 10%. Figure 7-8 shows the voltage profiles at 0.95 and 0.98 leading power factors at 30, 40 and 50% PV penetration level. From the figure, it can be observed that when PV systems are operated at 0.98 p. f. leading, the voltage upper limit is reached at greater than 30% PV penetration whereas when PV systems are operated at 0.95 p. f. leading, the voltage upper limit is reached after 40% PV penetration. Figure 7-9 shows the net reactive power at the secondary of the 11/0.433 kV transformer for different penetration levels of PV operating at 0.95 and 0.98 leading power factors. From the figure, it can be observed that the requirement of reactive power almost doubles at

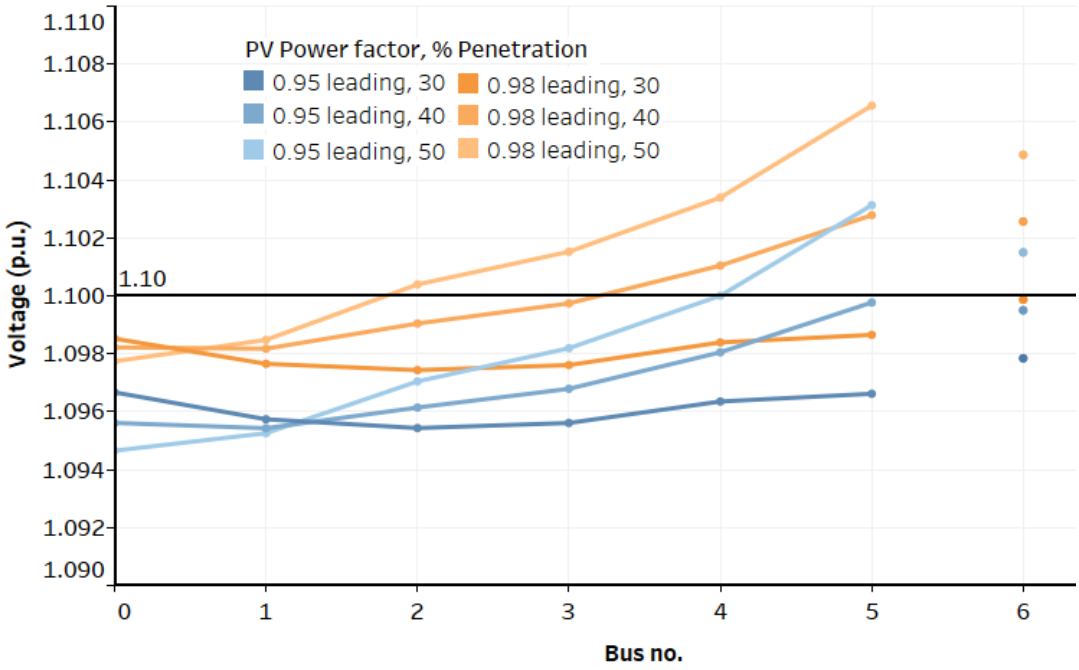

Figure 7-8: Voltage profile at different PV penetration levels with PV operating at leading p.f.

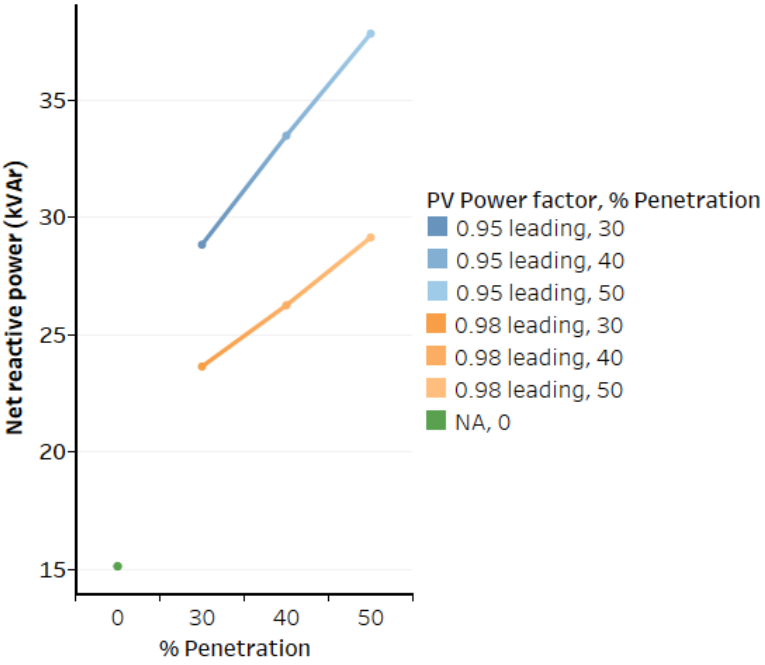

Figure 7-9: Net reactive power at the secondary of the substation at different penetration levels when PV is operated at leading p.f

50% penetration level at 0.98 p. f. leading operation and almost triples at 0.95 p. f. leading operation. It can be concluded from the results that the use of reactive power control would mitigate the overvoltage barrier up to 40% penetration, where reverse power flow is the barrier. However, the additional requirement on the transmission network to supply reactive power during periods of higher generation may result in inefficient operation of the transmission network. Therefore, an implementation of this solution would require more evaluation from the transmission network operator perspective.

7.6 Ranking of Solutions

The following table, Table 7-7 summarises the impact and effectiveness of the solutions based on the criteria described in Table 7-4. The higher the score, the higher is the effectiveness of the solution. Based on the score, the discussed solutions can be arranged in their decreasing order of effectiveness as:

1. Changes to off-load tap changer settings – Rank 1
2. Reactive power control - Rank 2

3. Active power curtailment – Rank 3

Table 7-7: Summary of detailed assessment for the solutions considered (scores in bracket)

Detailed assessment criteria	Solution 1 (Changes to tap changer settings)	Solution 2 (Active power curtailment)	Solution 3 (Reactive power control)
Percentage increase in contribution of PV	100 (1)	50 (0.5)	100 (1)
Any changes to existing hardware?	No (1)	Yes (0)	Yes (0)
Cost of changes to existing hardware	No cost (5)	Low cost (4)	Low cost (4)
Will the solution affect any other performance parameter?	No(1)	No (1)	Yes (net reactive power requirement from transmission network) (0)
Changes to existing design of inverter	No (1)	Yes (0)	Yes (0)
Will the solution disrupt power during implementation?	Yes (0)	No (1)	No (1)
Will the solution result in loss of generation?	No (1)	Yes (0)	No (1)
Cost of implementation of solution	Very low cost (5)	Low cost (4)	Low cost (4)

However, solutions ranked 1 and 2 address only the overvoltage problem and not the reverse power flow. To increase the contribution of PV in a low voltage distribution network, a more beneficial strategy would be to mitigate the overvoltage to increase the penetration from 20 to 40% PV penetration followed by a solution to mitigate the reverse power to increase the penetration from 40 – 60%. Beyond 60% penetration of PV other solutions like storage, demand-side management would be required to ensure that the overall performance of the distribution network is not

adversely affected by the presence of PV and also to ensure that higher proportion of PV generation is not lost due to curtailment.

7.7 Summary

This chapter summarises the technical barriers limiting the contribution of PV systems on a low voltage distribution network based on the results of the steady-state and dynamic performance evaluation. The chapter then discusses the different solutions considered in the literature and maps them to the barriers that it addresses. An initial assessment based on a set of criteria resulted in a choice of three solutions, viz. change to tap changer settings, active power curtailment and reactive power control, for the detailed analysis. In order to rank the solutions based on their effectiveness, a set of further criteria were defined based on the discussions in literature.

In order to evaluate the effectiveness of the solution, the performance of the distribution network with different penetration levels of PV and different solutions were simulated. The results of the evaluation of the impact of changes to tap changer settings indicated that a change of off-load tap changer settings from 433 V to 415 V results in mitigating the over-voltage to beyond 40% penetration. The evaluation of the impact of curtailment of the performance highlights that the solution is more effective on the barrier of reverse power flow rather than on the over-voltage. The solution of reactive power control is effective in mitigating the barrier of overvoltage. However, the operation of PV at leading power factor would mean that the distribution feeder requires more reactive power than with no PV. This additional reactive power will have to be met by the transmission network which makes the transmission network less efficient.

Based on the scores for each of the criteria, the solutions in the decreasing order of effectiveness are changes to off-load tap changer settings, reactive power control

and active power curtailment. However, a technically beneficially strategy to increase the contribution of PV would be to implement the changes to tap-changer setting to increase the PV contribution from 20 to 40%, followed by active power curtailment which would enable the increase of PV contribution from 40 to 60%. A phased approach like this would enable the regulators to plan for the transitionary period. This would also allow time to have the regulations that enable curtailment and communication strategies between the PV and the network operator to be defined. This would also enable the network operator to arrive at an agreement with a customer with PV systems and be prepared for the changes in load/generation. It is also relevant to note here that the future electricity demand would also include electric vehicles which could be used effectively as a storage using smart control systems.

CHAPTER 8

CONCLUSIONS AND FUTURE WORK

The fundamental objectives of the UK energy policy are to reduce CO_2 emissions, to maintain and increase energy security and to keep the price of energy competitive and affordable. These are commonly referred to as the 'energy trilemma of the UK'. Decarbonisation of the electricity sector is a major step that helps achieve the emission reduction objective at relatively low cost and low uncertainty. Small-scale renewables are one of the four options to aid decarbonisation of the electricity sector. The recent decrease in cost of PV systems has resulted in a significant increase in the number of PV systems being installed in the UK over the last decade. About 90% of installed PV systems in the UK have rated capacity less than 4 kW and this research has focused on this sector of PV systems which are typically connected to the LV distribution networks.

The percentage penetration of PV has been defined as the ratio of total PV capacity to after diversity maximum demand of all the houses in the network. The literature also uses a definition based on the number of houses with PV as the ratio of number of houses with PV to the total number of houses in the network. Such a definition may result in a higher or lower penetration percentage than the definition used in this thesis depending on the rating of individual PV systems considered in the respective literature.

8.1 Conclusions

The aim of this research was to investigate the key technical barriers and develop associated solutions for high penetration of photovoltaic systems in the UK. The research undertook a mixed method approach using software simulations, actual data from field trials and experimental results.

Dynamic model of PV system

The first objective was to develop a generic dynamic model of a single-phase PV system and an LV distribution network representative of the UK. A survey that ended in 2017 by CIGRE/CIRED highlighted the lack of a generic model of inverter-based generators for use in power system studies. The inverter models available in the literature typically focus on improving the topology of the inverter or the control strategy to increase the efficiency. However, in many cases, this results in additional components and complex calculations which affect the overall reliability and cost of the inverter. Also, these models typically do not include the protection mechanisms suggested by G-83 guidelines. To address these gaps, a dynamic model of a PV system with a common topology and control strategy along with the protection mechanism was developed. The model can represent PV systems of capacity varying from 1kW to 4 kW. The key parameters can be modified using the user interface of the model. The performance of the inverter was validated against the standards and experimental results. As this model is not pertaining to a single manufacturer, it can be used in dynamic studies of distribution networks with PV systems. As the SIMULINK model can be interfaced with IPSA software, common software among the distribution network operators (DNOs) in the UK for infrastructure planning, the model developed in this research can be further used by the DNO to evaluate the performance of their respective distribution network with inverter-based generation. Use of such a model would also enable the researchers to analyse the performance of an LV distribution network with multiple inverter-based generators more accurately than with the use of a negative load model for PV systems. With increasing suggestions on the use of PV to meet ancillary requirements of the distribution network, a detailed model as presented in this research would enable the planners to observe the impact of these ancillary services

on both the network and the customer and plan for any contingencies that may develop in future.

Evaluation of realistic worst-case scenarios

The second objective was to analyse the local irradiance and load profile data of the UK to identify the realistic worst-case scenarios to evaluate the impact of PV systems on the LV distribution network. The literature analysing the impact of PV on the distribution network typically uses a high irradiance value of 1000 W/m^2 and after diversity minimum demand of the network as the worst-case scenario. The 1-minute data measured on horizontal and south facing surfaces over a three year period showed that the irradiance was greater than 800 W/m^2 for 2% of sunshine hours for the horizontal surface and 5% of the sunshine hours for the south facing surface. Based on this analysis, a realistic worst-case scenario with an irradiance of 800 W/m^2 was used in this research. The analysis of the CLNR data showed that the minimum demand always occurred in the time interval 1 a.m. to 4 a.m. when there is little/no sunshine. A scatter plot based approach was used to analyse the correlated load and irradiance at different half hour intervals of the year which highlighted that the typical worst-case used in literature never occurred and that the load during hours of daylight was almost twice the after diversity minimum demand of the network.

The implication of this result was that the maximum permissible PV penetration levels arrived using the worst-case scenario have to be re-evaluated. As the value of irradiance is from a single location in the UK, care has to be advised before generalising the results to other parts of the UK. This research provides an approach for analysing the local irradiance data alongside the load profile of the network under consideration to arrive at realistic worst-case scenarios for the evaluation of the impact of PV on the distribution network under consideration. The minimum load

during hours of daylight considered in this research is based on the average percentage composition of different categories of households in the UK. However, this might be different if the area under consideration has a different composition than the national average. The approach suggested in this research becomes more feasible with the completion of installation of smart meters at every house in the UK, a project currently under implementation, which enables the DNO to have more details of half-hourly load profile of each house connected on their network. This would enable the DNO to forecast the net demand from the distribution network and plan for the energy purchase accordingly.

Evaluation of steady-state performance at realistic worst-case scenario

The third objective of this research was to evaluate the steady-state performance of the distribution network at different penetration levels of PV using the models developed in objective 1. The use of a realistic worst-case scenario, based on practical conditions, results in more practical permissible penetration levels of PV. Also, the use of the net capacity of PV in the definition of penetration enables the extension of the results to similar networks with different individual ratings of PV systems. However, care has to be taken to extend the results to networks in other parts of the UK. Correlation of the local irradiance values with the load profile of customers in that network and the comparison of tap changer settings would be required before the extension of the results of this thesis.

The results highlight that, at the realistic worst-case scenario, the first parameter to be adversely affected is the voltage profile, which is in-line with the discussions in the existing literature. However, the literature does not discuss the issues of reverse power flow and power factor in the context of the impact of PV on the low voltage distribution network and the influence of one parameter on another performance parameter of the network. The percentage of PV at which its presence may

adversely affect the steady-state performance considering the realistic scenario is 20% which is lower than the penetration levels discussed in the existing literature, after corrections to the variations in definitions of percentage penetration of PV.

Evaluation of dynamic performance

The fourth objective of this research was to evaluate the impact of PV penetration on the dynamic performance of the distribution network. The contribution of PV to the net fault current has generally been ignored in previous studies due to the fast disconnection and self-limiting capabilities of the inverter. However, the disconnection time as stipulated by G-83 is higher than those considered in the literature. With discussion on the introduction of low voltage ride through (LVRT) to prevent disconnection of too many PV systems for a fault, it is important to understand the impact of PV on both the net fault current and the protection mechanism when PV stays connected for a longer duration than considered in the literature. For a fault at the far end of the feeder, the net fault current at the distribution substation decreases slightly with the increase in penetration of PV, with a 30% drop in current at 100% PV penetration. The results add to the body of knowledge on the impact of PV on the dynamic performance of the low voltage distribution network.

The LV distribution network is typically protected using fuses at different branches, fuses at connections to individual customers and a relay at the primary of the 11/0.4 kV substation. The reduction of current at the substation during fault at the far end of the feeder may significantly increase the tripping time of the fuse at the 11/0.4 kV substation and also result in lack of coordination with the relay at the primary. However, for a fault at the far end of the feeder, only the failure of fuses at all the branches from the location of the feeder to the substation will result in the tripping

of the fuse at the substation. The probability that all these fuses fail to act is quite low.

The results of this analysis may be extended to any radial low voltage distribution network in the UK as the use of fuses and relays is the standard practice in low voltage distribution networks. The results were discussed in the light of regulations adopted by the UK, Europe, Australia and the USA. Another result to be highlighted is that the time delay of 0.5 s stipulated by G-83 ensures that sufficient time is available for faults occurring away from the PV to be cleared by the action of the respective fuse, in contrast to 0.16 s stipulated by IEEE 1547. However, a lower cut-off voltage for under-voltage disconnection than stipulated in G-83 would ensure more PV stays connected to the network during a fault that has occurred far from the PV installations.

Evaluation of hosting capacity at realistic worst-case scenario

The fifth objective of this research was to evaluate the PV hosting capacity of the network based on the results of performance analysis at steady and dynamic-states. The technical parameters used to evaluate the hosting capacity are voltage profile, total harmonic distortion, net active power at the substation, power factor at the secondary of the substation, voltage unbalance and protection mechanism. The scenarios considered are the typical worst-case scenario, the realistic worst-case scenario and a futuristic scenario.

When the typical worst-case scenario is used as a boundary condition, the reverse power flow is the first barrier and this is followed by overvoltage. However, for the realistic worst-case scenario, over-voltage is the first barrier, followed by the reverse power flow. These results aid in analysing the solutions to increase the hosting capacity of the distribution network. The third scenario considered is futuristic, i.e. if the daytime load can be increased slightly by the use of demand-side management,

the contribution of PV could be increased by 400% considering the typical worst-case scenario and by 200% considering the realistic worst-case scenario.

The results of the three scenarios may also be used by the DNO while deciding the hosting capacity of their network by comparing their scenario with the scenarios discussed in this thesis. Reverse power flow at 11/0.4 kV does not significantly affect the distribution network. However, the DNOs prefer to be aware of its occurrence and take action before the reverse power flow occurs at the 33/11 kV transformer and the 33 kV lines, where directional protection is used for detection and isolation of fault.

Evaluation of technical solutions

The sixth and last objective of this research was to identify, evaluate and rank the technical solutions that are applicable to the low voltage distribution network. A review of technical solutions was performed and evaluated against an initial set of criteria to generate a list of solutions applicable to the low voltage distribution network. The top three solutions based on the score for initial assessment criteria were implemented in the simulations to evaluate the impact of solutions on the increase of PV penetration. The solutions were then ranked, based on the score achieved in the detailed assessment criteria. The solution with the highest score was given the highest position. The solutions along with the ranks, using realistic worst-case scenario, are:

- Changes to off-load tap changer settings – Rank 1
- Active power curtailment – Rank 2
- Reactive power control – Rank 3

The results add to the body of knowledge of solutions to increase the contribution of PV. Though some of the solutions have also been assessed in existing literature, they do not quantify the increase in hosting capacity that could be achieved using

the solutions and the correlation between the generation and load profiles. Different strategies for curtailment based on technical or non-technical criteria have been suggested in the literature to increase the hosting capacity. However, most of them use a capacity factor based approach to quantify the amount of generation lost due to curtailment.

The results of this research, show that the use correlation of irradiance values with the load profiles to evaluate the hours of curtailment required provides a more realistic estimate of the energy curtailed than the traditional capacity factor based calculations. The performance of the network with different solutions suggests that the use of changes to settings of the off-load tap changer followed by curtailment would enable an increase in PV penetration from 20% to 60% at relatively low cost and low implications to both the network operator and the customer. Such a phased implementation of solutions would enable the planners to establish the required regulatory changes to implement the second solution i.e. curtailment. This would also provide sufficient time to the DNO to arrive at a consensus with the PV customer on the cost of the generation that would be lost by curtailment.

8.2 Future work

The results of the methodology to identify technical barriers can be extended further by including the irradiance data from different parts of the UK alongside socio-economic factors that are used to categorise the households in the UK. A characterisation of different types of distribution networks across the UK would enable the generalisation of this work to different parts of the UK. Also, as the contribution from small-scale renewables increase in the UK, there is a probability that a feeder has different types of renewable generators connected to the same bus or to different buses. The work in this thesis can be extended further to analyse the impact of the presence of different types of small-scale generators and evaluate

the hosting capacity based on the generation and load profiles of the distribution network under consideration.

Also, in the future, there would be an increase in the use of electric vehicles (EV) which acts as both a load and a storage device. With the implementation of smart meters and extension of time of day tariffs to domestic customers, it is important to evaluate the performance of the network with renewables, EVs and demand-side management (DSM). The models developed in this research are applicable to any inverter-based generation and would require a careful choice of boundary conditions to evaluate the performance of the network with multiple generators, EVs and DSM. The presence of EVs and DSM provides an opportunity to further increase the contribution of renewables.

REFERENCES

1. *BP Statistical Review of World Energy June 2017*. 2017, BP P. L. C. : London. p. 1-52.
2. Birol, F., L. Cozzi, D. Dorner, and T. Gül, *World Energy Outlook Special Report: Energy and Climate Change*. 2015, International Energy Agency,: Paris, France.
3. Philibert, C., C. Tam, Y. Abdelilah, H. Bahar, Q. Marchais, S. Mueller, U. Remme, M. Waldron, and H. Wiesner, *Technology Roadmap Solar Photovoltaic Energy*. 2014, International Energy Agency.
4. European Commission, *A Roadmap for moving to a competitive low carbon economy in 2050*. 2011, European Union: Brussels.
5. International Energy Agency. *IEA finds CO2 emissions flat for third straight year even as global economy grew in 2016*. 2017 [cited 2017 30/08/2017]; Available from: https://www.iea.org/newsroom/news/2017/march/iea-finds-co2-emissions-flat-for-third-straight-year-even-as-global-economy-grew.html.
6. DTI, *Energy White Paper*. 2003: London, UK.
7. Ekins, P., N. Strachan, I. Keppo, W. Usher, J. Skea, and G. Anandarajah, *The UK energy system in 2050: Comparing Low-Carbon, Resilient Scenarios*. 2013, UKERC: London, UK.
8. *Climate Change Act*. 2008, Government, H. M.: United Kingdom.
9. Department of Energy and Climate Change, *2013 UK Greenhouse Gas Emissions, Final Figures*. 2015: London, UK.
10. National Atmospheric Emissions Inventory. *Overview of greenhouse gases* 2013 [cited 2017 2nd Dec]; Available from: http://naei.defra.gov.uk/overview/ghg-overview.
11. Gardner, P., *UK Generation and Demand scenarios for 2030*. 2011, Garrad Hassan and Partners Limited: Glasgow, Scotland.
12. Gosden, E., *EDF admits Hinkley Point funding not finalised as it extends life of old reactors*, in *The Telegraph*. 2016, Telegraph Media Group Limited: London, UK.
13. Department of Energy and Climate Change, *UK Renewable Energy Roadmap*. 2011: London, UK.
14. Department of Energy and Climate Change, *Renewable Energy Roadmap UK: Update 2013*. 2013: London, UK.
15. *Solar Photovoltaics deployment*. 2016 26th October 2016 [cited 2016 16th Nov]; Available from: https://www.gov.uk/government/statistics/solar-photovoltaics-deployment.
16. Mott MacDonald, *System Integration of Additional Micro-generation*. 2004, Department of Trade and Industry: London, UK.
17. Suwanapingkarl, P., *Power Quality Analysis of Future Power Networks*, in *Faculty of Engineering and Environment*. 2012, Northumbria University: Newcastle Upon Tyne.
18. Jenkins, N., R. Allan, P. Crossley, D. Kirschen, and G. Strbac, *Embedded Generation* 2000, Stevenage, UK: Institution of Engineering and Technology.
19. Department of Energy and Climate Change, *UK Solar PV Strategy Part 1: Roadmap to a Brighter Future*. 2013: London, UK.
20. Boot, P., J.d. Jong, and N. Hoogervorst, *For accomodating increasing amounts of wind and solar in the power market*, in *Reflections on coordination mechanisms*, D. Sherwood, Editor. 2014: Hague, Netherlands.
21. Department of Energy and Climate Change, *UK Solar PV Strategy Part 2*. 2014: London, UK.
22. Malmedal, K., B. Kroposki, and P.K. Sen, *Distributed Energy Resources and Renewable Energy in Distribution Systems: Protection Considerations and Penetration Levels*, in *IEEE Industry Applications Society Annual Meeting*. 2008, IEEE: Edmonton, AB, Canada.
23. Beck, F. and E. Martinot, *Renewable Energy Policies and Barriers.* Encyclopedia of Energy, 2004. **5**: p. 365 - 383.
24. Margolis, R. and J. Zuboy, *Nontechnical Barriers to Solar Energy Use: Review of Recent Literature*. 2006, NREL: Colorado, USA.
25. Burges, K. and J. Twele, *Power systems operation with high penetration of renewable energy - the German case*, in *International Conference on Future Power Systems*. 2005: Amsterdam, Netherlands.

26. Fitzer, J. and W.E. Dillon, *Impact of Residential Photovoltaic Power Systems on the Distribution Feeder.* IEEE Transactions on Energy Conversion, 1986. **EC-1**(4): p. 39-42.
27. Favuzza, S., G. Graditi, F. Spertino, and G. Vitale. *Comparison of power quality impact of different photovoltaic inverters: the viewpoint of the grid*. in *IEEE International Conference on Industrial Technology*. 2004. Hammamet, Tunisia.
28. Katiraei, F., K. Mauch, and L. Dignard-Bailey, *Integration of photovoltaic power systems in high-penetration clusters for distribution networks and mini-grids* International Journal of Distributed Energy Resources, 2007. **3**(3): p. 207-223.
29. Thomson, M. and D.G. Infield, *Network Power-Flow Analysis for a High Penetration of Distributed Generation.* Power Systems, IEEE Transactions on, 2007. **22**(3): p. 1157-1162.
30. McDermott, T.E. *Voltage control and voltage fluctuations in distributed resource interconnection projects*. in *IEEE PES T&D 2010*. 2010.
31. Ali, S., N. Pearsall, and G. Putrus, *Impact of High Penetration Level of Grid-Connected Photovoltaic Systems on the UK Low Voltage Distribution Network.* International Conference on Renewable Energies and Power Quality, Santiago de Compostela (Spain), 28th to 30th March, 2012.
32. Demirok, E., *Control of Grid Interactive PV Inverters for High Penetration in Low Voltage Distribution Networks*, in *Department of Energy Technology*. 2012, Aalborg University: Aalborg, Denmark.
33. Yan, R., B. Marais, and T.K. Saha, *Impacts of residential photovoltaic power fluctuation on on-load tap changer operation and a solution using DSTATCOM.* Electric Power Systems Research, 2014. **111**: p. 185-193.
34. Denholm, P. and R. Margolis, *Very Large-Scale Deployment of Grid-Connected Solar Photovoltaics in the United States: Challenges and Opportunities*, in *Solar 2006*. 2006: Denver, Colorado.
35. Katiraei, F. and J.R. Aguero, *Solar PV Integration Challenges.* IEEE Power and Energy Magazine, 2011. **9**(3): p. 62-71.
36. Saad, N.M., M.S. Sujod, L.H. Ming, M.F. Abas, N.R.H. Abdullah, R. Ishak, and M.S. Jadin, *The impacts of photovoltaic distributed generation (PVDG) on distribution power system network*, in *International Conference on Electrical, Electronic, Communication and Control Engineering (ICEECC2017)*. 2017: Kuala Lumpur.
37. Kotsopoulos, A., P.J.M. Heskes, and M.J. Jansen. *Zero-crossing distortion in grid-connected PV inverters*. in *IECON 02, IEEE 2002 28th Annual Conference of the Industrial Electronics Society*. 2002.
38. Patsalides, M., A. Stavrou, V. Efthymiou, and G.E. Georghiou, *Towards the establishment of maximum PV generation limits due to power quality constraints.* International Journal of Electrical Power & Energy Systems, 2012. **42**(1): p. 285-298.
39. Fekete, K., Z. Klaic, and L. Majdandzic, *Expansion of the residential photovoltaic systems and its harmonic impact on the distribution grid.* Renewable Energy, 2012. **43**: p. 140-148.
40. Dartawan, K., L. Hui, R. Austria, and M. Suehiro, *Harmonics issues that limit solar photovoltaic generation on distribution circuits* in *World Renewable Energy Forum (WREF 2012)*. 2012: Colorado Convention Centre, Denver, USA.
41. Pandi, V.R., H.H. Zeineldin, W. Xiao, and A.F. Zobaa, *Optimal penetration levels for inverter-based distributed generation considering harmonic limits.* Electric Power Systems Research, 2013. **97**: p. 68-75.
42. Oliveira, L.G.M., W.d.C. Boaventura, G. Amaral, J.V.G.C. Mello, V.F. Mendes, W.N. Macedo, P.F. Torres, A.S. Piterman, T.J.R. Corrade, and B.M. Lopes. *Assessment of Harmonic Distortion in small grid-connected photovoltaic systems*. in *2016 17th International Conference on Harmonics and Quality of Power (ICHQP)*. 2016.
43. Heskes, P.J.M. and J.H.R. Enslin, *Power Quality behaviour of different photovoltaic inverter topologies*, in *24th International Conference PCIM* 2003, 20 - 23 May: Nurnberg, Germany.
44. Rangarajan, S.S., E.R. Collins, and J.C. Fox. *Interactive impacts of elements of distribution systems and PV on network harmonic resonance*. in *2017 IEEE 6th International Conference on Renewable Energy Research and Applications (ICRERA)*. 2017.

45. Rangarajan, S.S., E.R. Collins, and J.C. Fox. *Harmonic resonance repercussions of PV and associated distributed generators on distribution systems*. in *2017 North American Power Symposium (NAPS)*. 2017.
46. Baran, M.E., H. Hooshyar, Z. Shen, and A. Huang, *Accommodating High PV Penetration on Distribution Feeders.* IEEE Transactions on Smart Grid, 2012. **3**(2): p. 1039-1046.
47. Azmi, A.N., I.N. Dahlberg, M.L. Kolhe, and A.G. Imenes. *Impact of increasing penetration of photovoltaic (PV) systems on distribution feeders*. in *2015 International Conference on Smart Grid and Clean Energy Technologies (ICSGCE)*. 2015.
48. Mourad, N. and B. Mohamed. *Short circuit current contribution of distributed photovoltaic integration on radial distribution networks*. in *2015 4th International Conference on Electrical Engineering (ICEE)*. 2015.
49. Zhang, Z., T. Zheng, R. Xie, and P. Zhang. *Protection for distribution network with photovoltaic integration*. in *2016 IEEE PES Asia-Pacific Power and Energy Engineering Conference (APPEEC)*. 2016.
50. Xie, R.R., T. Zheng, Z.K. Zhang, and P.Z. Zhang. *Voltage based protection for10kV distribution network with photovoltaic integration*. in *2016 IEEE PES Asia-Pacific Power and Energy Engineering Conference (APPEEC)*. 2016.
51. Tekpeti, B.S., X. Kang, and X. Huang, *Fault analysis of solar photovoltaic penetrated distribution systems including overcurrent relays in presence of fluctuations.* International Journal of Electrical Power & Energy Systems, 2018. **100**: p. 517-530.
52. Yue, M. and X. Wang, *Assessing Cloud Transient Impacts of Solar and Battery Energy Systems on Grid Inertial Responses.* Electric Power Components and Systems, 2014. **43**(2): p. 200-211.
53. Wang, Z.Y., G. Chen, Z.Y. Dong, L.Y. Zhang, and D.J. Hill, *Vulnerability Analysis for Power Grid Given Renewable Energy Sources Integration*, in *AORC Technical meeting*. 2014: Tokyo, Japan.
54. Achilles, S., S. Schramm, and J. Bebic, *Transmission System Performance Analysis for High-Penetration Photovoltaics*, in *Subcontract Report*, NREL, Editor. 2008.
55. Sovacool, B.K., *Rejecting renewables: The socio-technical impediments to renewable electricity in the United States.* Energy Policy, 2009. **37**(11): p. 4500-4513.
56. Fu, Q., *Modeling, Analyses and Assessment of Microgrids Considering High Renewable Energy Penetration.* Theses and Dissertations, Paper 248, 2013.
57. Chen, W. and H. Yin, *Optimal subsidy in promoting distributed renewable energy generation based on policy benefit.* Clean Technologies and Environmental Policy, 2017. **19**.
58. del Río, P. and P. Mir-Artigues, *Support for solar PV deployment in Spain: Some policy lessons.* Renewable and Sustainable Energy Reviews, 2012. **16**(8): p. 5557-5566.
59. Burer, M.J. and R. Wustenhagen, *Which renewable energy policy is a venture capitalist's best friend? Empirical evidence from a survey of international cleantech investors.* Energy Policy, 2009. **37**(12): p. 4997-5006.
60. Grubb, M., *Technology Innovation and Climate Change Policy: an overview of issues and options.* Keio Journal of Economics, 2004. **41**(2): p. 103 - 132.
61. del Rio, P. and E. Cerda, *The policy implications of the different interpretations of the cost-effectiveness of renewable electricity support.* Energy Policy, 2014. **64**: p. 364-372.
62. Mitchell, C. and P. Connor, *Renewable energy policy in the UK 1990–2003.* Energy Policy, 2004. **32**(17): p. 1935-1947.
63. DTI. *Analysis of the responses to the consultation paper*. 2001 [cited 2017 2nd Dec]; Available from: http://webarchive.nationalarchives.gov.uk/20070603164510/http://www.dti.gov.uk/renewables/publications/pdfs/response.pdf.
64. DTI. *The Renewables Obligation Preliminary Consultation*. 2001 [cited 2017 2nd Dec]; Available from: http://webarchive.nationalarchives.gov.uk/+/http:/www.berr.gov.uk/files/file21097.pdf.
65. Ofgem, *The renewables obligation - Ofgem's second annual report*. 2005: London, UK.

66. Foxon, T.J., R. Gross, A. Chase, J. Howes, A. Arnall, and D. Anderson, *UK innovation systems for new and renewable energy technologies: drivers, barriers and systems failures.* Energy Policy, 2005. **33**(16): p. 2123-2137.
67. Foxon, T.J. and P.J.G. Pearson, *Towards improved policy processes for promoting innovation in renewable electricity technologies in the UK.* Energy Policy, 2007. **35**(3): p. 1539-1550.
68. Dinica, V., *Support systems for the diffusion of renewable energy technologies—an investor perspective.* Energy Policy, 2006. **34**(4): p. 461-480.
69. Fouquet, D. and T.B. Johansson, *European renewable energy policy at crossroads—Focus on electricity support mechanisms.* Energy Policy, 2008. **36**(11): p. 4079-4092.
70. Falconett, I. and K. Nagasaka, *Comparative analysis of support mechanisms for renewable energy technologies using probability distributions.* Renewable Energy, 2010. **35**(6): p. 1135-1144.
71. Lipp, J., *Lessons for effective renewable electricity policy from Denmark, Germany and the United Kingdom.* Energy Policy, 2007. **35**(11): p. 5481-5495.
72. Harmelink, M., M. Voogt, and C. Cremer, *Analysing the effectiveness of renewable energy supporting policies in the European Union.* Energy Policy, 2006. **34**(3): p. 343-351.
73. *Aggregated energy balances showing proportion of renewables in supply and demand*. 2017, Department for Business, Energy and Industrial Strategy,: London, UK.
74. Constable, J. and L. Moroney. *Renewables Output in 2010*. 2011 [cited 2017 28 November]; Available from: http://www.ref.org.uk/publications/229-renewables-output-in-2010.
75. DTI, *The Energy Challenge - Energy Review Report*. 2006: London, UK.
76. Pollitt, M.G., *UK Renewable Energy Policy since Privatisation*. 2010: University of Cambridge.
77. Pearson, P. and J. Watson, *UK Energy Policy 1980 - 2010; A history and lessons to be learnt*. 2012, The Parliamentary Group for Energy Studies: London, UK.
78. Ofgem. *Feed-In Tariff (FIT) rates*. 2017 [cited 2017 20th October]; Available from: https://www.ofgem.gov.uk/environmental-programmes/fit/fit-tariff-rates.
79. National Solar Centre, *Planning guidance for the development of large scale ground mounted solar PV systems*. 2013, Building Research Establishment: Cornwall, UK.
80. UK Power. *Regulations for Installing Solar PV*. [cited 2017 24/07/2017]; Available from: https://www.ukpower.co.uk/solar-panels/regulations-for-installing-solar-pv.
81. British Standards Institution, *Voltage characteristics of electricity supplied by public electricity networks*. 2010.
82. The Electricity Council, *Engineering Recommendation P28: Planning limits for Voltage Fluctuations caused by Industrial, Commercial and Domestic Equipment in the United Kingdom*. 1989: London, UK.
83. The Electricity Council, *Engineering Recommendation P29: Planning Limits for Voltage Unbalance in the United Kingdom*. 1990: London, UK.
84. Energy Networks Association, *Engineering Recommendation G5/4 - 1: Planning Levels For Harmonic Voltage Distortion And The Connection Of Non-Linear Equipment To Transmission Systems And Distribution Networks In The United Kingdom*. 2005: London, UK.
85. British Standards Institution, *Photovoltaic (PV) systems - Characteristics of the utility interface*. 1996: London, UK.
86. Energy Networks Association, *Engineering Recommendation G83, Issue 2: Recommendations for the Connection of Type Tested Small-scale Embedded Generators (Up to 16A per Phase) in Parallel with Low-Voltage Distribution Systems*. 2012: London, UK.
87. British Standards Institution, *BS EN 61000-3-2: Electromagnetic compatibility (EMC), Part 3-2: Limits - Limits for harmonic current emissions (equipment input current <= 16 A per phase)* 2014: London, UK.
88. Stetz, T., M. Kraiczy, K. Diwold, B. Noone, A. Bruce, I. MacGill, B. Bletterie, R. Bründlinger, C. Mayr, K.d. Brabandere, C. Dierckxsens, W. Yibo, S. Tselepis, A. Iaria, A. Gatti, D. Cirio, Y. Ueda, K. Ogimoto, K. Washimara, M. Rekinger, D. Marcel, C. Bucher, and B. Mather, *High Penetrations of PV in Local Distribution Grids*, in *IEA-PVPS Task 14: High-Penetration of PV Systems in Electricity Grids. Subtask 2: Case-Study Collection*. 2014: Kassel, Germany.

89. Teodorescu, R., M. Liserre, and P. Rodriguez, *Grid converters for photovoltaic and wind power systems*. 2011, Sussex, UK: John Wiley and Sons Ltd.
90. Lammert, G., K. Yamashita, L.D.P. Ospina, H. Renner, S.M. Villanueva, P. Pourbeik, F.-E. Ciausiu, and M. Braun, *International industry pactice on modelling and dynamic performance of inverter based generation in power system studies.* CIGRE Science and Engineering, 2017. **8**.
91. Messenger, R.A. and J. Ventre, *Photovoltaic Systems Engineering*. 3rd ed. 2010, London, UK: CRC Press.
92. BRE, E. Technology, H. Group, and S. Energy, *Photovoltaics in Buildings: Guide to the installation of PV systems*, DTI, Editor. 2006: London, UK.
93. Fedkin, M. *Efficiency of Inverters*. Utility Solar Power and Concentration [cited 2017 29 November]; Available from: https://www.e-education.psu.edu/eme812/node/738.
94. Sangwongwanich, A., Y. Yang, D. Sera, F. Blaabjerg, and D. Zhou, *On the Impacts of PV Array Sizing on the Inverter Reliability and Lifetime.* IEEE Transactions on Industry Applications, 2018: p. 1-1.
95. Rashid, M.H., *Power Electronics Handbook*. 2001, San Diego, USA: Academic Press.
96. Kouro, S., J.I. Leon, D. Vinnikov, and L.G. Franquelo, *Grid-Connected Photovoltaic Systems: An Overview of Recent Research and Emerging PV Converter Technology.* IEEE Industrial Electronics Magazine, 2015. **9**(1): p. 47-61.
97. Majhi, B., *Analysis of Single-Phase SPWM Inverter*, in *Department of Electrical Engineering*. 2012, National Institute of Technology, Rourkela.
98. Bowtell, L. and T. Ahfock, *Comparison between unipolar and bipolar single phase gridconnected inverters for PV applications*, in *Australasian Universities Power Engineering Conference*. 2007: Perth, WA, Australia. p. 1-5.
99. Pazynych, A., *A study of the harmonic content of distribution power grids with distributed PV systems* in *Electrical Engineering*. 2014, Tampere University of Technology: Tampere, Finland.
100. Xiao, W., N. Ozog, and W.G. Dunford, *Topology Study of Photovoltaic Interface for Maximum Power Point Tracking.* IEEE Transactions on Industrial Electronics, 2007. **54**(3): p. 1696-1704.
101. FARANDA, R. and S. LEVA. *Energy comparison of MPPT techniques for PV Systems*. in *WSEAS TRANSACTIONS on POWER SYSTEMS*. 2008. Roberto Faranda, Sonia Leva.
102. Dolara, A., *Energy Comparison of Seven MPPT Techniques for PV Systems.* Journal of Electromagnetic Analysis and Applications, 2009. **01**(03): p. 152-162.
103. Hornik, T. and Q.-C. Zhong, *A Current-Control Strategy for Voltage-Source Inverters in Microgrids Based on H∞ and Repetitive Control.* IEEE Transactions on Power Electronics 2011. **26** (3): p. 943 - 952.
104. Crowhurst, B., E.F. El-Saadany, L.E. Chaar, and L.A. Lamont, *Single-Phase Grid-Tie Inverter Control Using DQ Transform for Active and Reactive Load Power Compensation*, in *IEEE International Conference on Power and Energy*. 2010: Kuala Lumpur, Malaysia.
105. Samerchur, S., S. Premrudeepreechacharn, Y. Kumsuwun, and K. Higuchi. *Power control of single-phase voltage source inverter for grid-connected photovoltaic systems*. in *Power Systems Conference and Exposition (PSCE), 2011 IEEE/PES*. 2011.
106. Sultani, J.F., *Modelling, design and implementation of d-q control in single-phase grid-connected inverters for photovoltaic systems used in domestic dwellings* in *Faculty of Technology*. 2013, De Montfort University: Leicester.
107. Zhong, Q.-C. and T. Hornik, *Control of Power Inverters in Renewable Energy and Smart Grid Integration*. 2013, New Jersey, USA: Wiley-IEEE press.
108. IEEE, *IEEE Application Guide for IEEE Std 1547(TM), IEEE Standard for Interconnecting Distributed Resources with Electric Power Systems*, in *IEEE Std 1547.2-2008*. 2009: New Jersey, USA. p. 1-217.
109. Rahman, S.A. and R.K. Varma. *PSCAD/EMTDC model of a 3-phase grid connected photovoltaic solar system*. in *North American Power Symposium (NAPS)*. 2011. Boston, USA: IEEE.

110. Liserre, M., F. Blaabjerg, and S. Hansen, *Design and control of an LCL-filter-based three-phase active rectifier.* IEEE Transactions on Industry Applications, 2005. **41**(5): p. 1281-1291.
111. Neves, F.A.S., M. Carrasco, F. Mancilla-David, G.M.S. Azevedo, and V.S. Santos, *Unbalanced Grid Fault Ride-Through Control for Single-Stage Photovoltaic Inverters.* IEEE Transactions on power electronics 2016. **31**(4).
112. Mirhosseini, M., J. Pou, and V.G. Agelidis, *Single- and Two-Stage Inverter-Based Grid-Connected Photovoltaic Power Plants With Ride-Through Capability Under Grid Faults.* IEEE Transactions on sustainable energy 2015. **6**(3).
113. Keller, J. and B. Kroposki, *Understanding Fault Characteristics of Inverter-Based Distributed Energy Resources*. 2010, NREL: Colorado, USA.
114. Bravo, R.J., R. Yinger, S. Robles, and W. Tamae, *Solar PV Inverter Testing for Model Validation*, in *IEEE Power and Energy Society General Meeting*. 2011, IEEE: San Diego, CA. p. 1-6.
115. Abdulhadi, I., F. Coffele, A. Dysko, C. Foote, C. Kungu, and M. Lee, *Hardware based characterisation of LV inverter fault response*, in *24th International Conference on Electricity Dsitribution (CIRED)*. 2017, IET: Glasgow, UK.
116. Kroposki, B. and J. Keller, *Understanding Photovoltaic Inverter Fault Current and Low Voltage Ride-Through*, in *25th European Photovoltaic Solar Energy Conference and Exhibition*. 2010: Valencia, Spain.
117. Goh, H.S., *The Effect of Grid Operating Conditions on the Harmonic Performance of Grid-Connected PV Inverters*, in *School of Electrical, Electronic and Computer Engineering*. 2011, Newcastle University: Newcastle upon Tyne.
118. Ingram, S., S. Probert, and K. Jackson, *The impact of small scale embedded generation on the operating parameters of distribution networks*. 2003, P B Power, Department of Trade and Industry: London, UK.
119. Econnect Ventures Ltd., *Embedded controller for LV networks with distributed generation*. 2007, DTI: London, UK.
120. Bucher, C., *Analysis and simulation of distribution grids with photovoltaics*, in *EEH - Power systems laboratory*. 2014, ETH Zurich: Zurich.
121. Stokes, M., M. Rylatt, and K. Lomas, *A simple model of domestic lighting demand.* Energy and Buildings, 2004. **36**(2): p. 103-116.
122. Vasanasong, E. and E.D. Spooner, *The Prediction of Net Harmonic Currents Produced by Large Numbers of Residential PV Inverters: Sydney Olympic Village Case Study*, in *Ninth International Conference on Harmonics and Quality of Power*. 2000: Orlando, Florida, USA.
123. SCHWANZ, D., S. RÖNNBERG, and M. BOLLEN, *Voltage unbalance due to single-phase photovoltaic inverters* in *24th International Conference on Electricity Distribution (CIRED)*. 2017, The IET: Glasgow.
124. Newborough, M. and P. Augood, *Demand-side management opportunities for the UK domestic sector.* IEEE Transactions on Generation, Transmission and Distribution, 1999. **146**(3).
125. *Customer Led Network Revolution Project Data*. 2015 [cited 2017 31/10/2017]; Available from: http://www.networkrevolution.co.uk/resources/project-data/.
126. *The Electricity Safety, Quality and Continuity Regulations*, in *VII*. 2002: London, UK.
127. Schwarzer, D.V. and D.R. Ghorbani, *Transient Over-Voltage Mitigation and its Prevention in Secondary Distribution Networks with High PV-to-Load Ratio*. 2015, Hawaii Natural Energy Institute: Honolulu, Hawaii.
128. Machowski, J., J.W. Bialek, and J.R. Bumby, *Power system dynamics: Stability and Control*. 2nd ed. 2008, West Sussex, UK: John Wiley and Sons.
129. Chowdhury, S., S.P. Chowdhury, and P. Crossley, *Microgrids and Active Distribution Networks*. 2009, Stevenage, UK: IET publications.
130. limited, K., *The contribution to distribution network fault levels from the connection of distributed generation*. 2005, DTI: London, UK.
131. Freris, L. and D. Infield, *Renewable energy in power systems*. 2006, New Jersey, USA: Wiley-Blackwell.

132. Conti, S., *Analysis of distribution network protection issues in presence of dispersed generation.* Electric Power Systems Research, 2009. **79**(1): p. 49-56.
133. Kaddah, S.S., M.M. El-Saadawi, and D.M. El-Hassanin, *Influence of Distributed Generation on Distribution Networks During Faults.* Electric Power Components and Systems, 2015. **43**(16): p. 1781-1792.
134. Sun, W., *Maximising Renewable Hosting Capacity in Electricity Networks*. 2015, University of Edinburgh: Edinburgh.
135. Manditereza, P.T. and R. Bansal, *Renewable distributed generation: The hidden challenges – A review from the protection perspective.* Renewable and Sustainable Energy Reviews, 2016. **58**: p. 1457-1465.
136. Kobayashi, H., K. Takigawa, E. Hashimito, A. Kitamura, and H. Matsuda. *Problems and countermeasures on safety of utility grid with a number of small-scale PV systems*. in *IEEE Conference on Photovoltaic Specialists*. 1990. Florida, USA.
137. Intelligent Energy Europe, *State of the art on dispersed PV power generation: Publications review on the impacts of PV Distributed Generation and Electricity networks Annexes*. 2007, European Commission: Brussels, Germany.
138. Phuttapatimok, S., A. Sangswang, M. Seapan, D. Chenvidhya, and K. Kirtikara, *Evaluation of fault contribution in the presence of PV grid connected systems*, in *33rd IEEE Photovoltaic Specialists Conference*. 2008: San Diego, CA, USA.
139. Morren, J. and S.W.H.d. Haan, *Impact of distributed generation units with power electronic converters on distribution network protection*, in *9th IET International conference on developments in power system protection (DPSP)*. 2008, IET: Glasgow, UK. p. 664-669.
140. Turcotte, D. and F. Katiraei, *Fault Contribution of Grid-Connected Inverters*, in *IEEE Electrical Power Conference*. 2009: Quebec, Canada.
141. C.Le-Thi-Minh, T. Tran-Quoc, S. Bacha, C. Kieny, P. Cabanac, D. Goulielmakis, and C. Duvauchelle, *Behaviors of photovoltaic systems connected to MV network during faults*, in *26th European Photovoltaic Solar Energy Conference and Exhibition*. 2011: Hamburg, Germany.
142. Katiraei, F., J. Holbach, T. Chang, W. Johnson, D. Wills, B. Young, L. Marti, A. Yan, P. Baroutis, G. Thompson, and J. Rajda, *Investigation of Solar PV Inverters Current Contributions during Faults on Distribution and Transmission Systems Interruption Capacity*, in *Western Protective Relay Conference*. 2012, Quanta Technology: North Carolina, USA.
143. Yang, Y., P. Enjeti, F. Blaabjerg, and H. Wang. *Suggested Grid Code Modifications to Ensure Wide-Scale Adoption of Photovoltaic Energy in Distributed Power Generation Systems*. in *IEEE Industry Applications Society Annual Meeting*. 2013. Lake Buena Vista, FL.
144. Margossian, H., J. Sachau, and G. Deconinck, *Distribution network protection considering grid code requirements for distributed generation.* IET Generation, Transmission & Distribution, 2015. **9**(12): p. 1377-1381.
145. Reiman, A.P., *An analysis of distributed photovoltaics on single-phase laterals of distribution systems*, in *Graduate Faculty of The Swanson School of Engineering*. 2015, University of Pittsburgh: Pittsburgh.
146. Aggarwal, R.K., N. Ashton, K.A. Coates, P.C. Colbrook, L. Csuros, D. Day, E. Dolby, L.C.W. Frerk, E. Hamilton, J. Harris, J.W. Hodgkiss, L.Jackson, G.S.H. Jarrett, M. Kaufmann, E. Mellor, K.G. Mewes, P.J. Moore, J.H. Naylor, C. Ohl6n, H.S. Petch, J. Rushton, E.C. Smith, C. Turner, H.W. Turner, and J.C. Whittaker, *Power System Protection*. 2 ed, ed. The Electricity Training Association. 1995, London, UK: The Institution of Electrical Engineers.
147. Nimpitiwan, N., G.T. Heydt, R. Ayyanar, and S. Suryanarayanan, *Fault Current Contribution From Synchronous Machine and Inverter Based Distributed Generators.* IEEE Transactions on Power Delivery, 2007. **22**(1): p. 634 - 641.
148. Hagh, M.T., A. Jalilian, S.B. Naderi, M. Negnevitsky, and K.M. Muttaqi, *Improving Fault Ride-Through of Three Phase Voltage Source Inverter During Symmetrical Fault Using DC Link Fault Current Limiter*, in *Australian Universities Power Engineering Conference (AUPEC)*. 2015: New South Wales, Australia.

149. Bottrell, N. and T.C. Green, *Comparison of Current-Limiting Strategies During Fault Ride-Through of Inverters to Prevent Latch-Up and Wind-Up.* IEEE Transactions on Power Electronics, 2014. **29**(7): p. 3786-3797.
150. Bianchi, F.D., A. Egea-Alvarez, A. Junyent-Ferré, and O. Gomis-Bellmunt, *Optimal control of voltage source converters under power system faults.* Control Engineering Practice, 2012. **20**(5): p. 539-546.
151. Plet, C.A., M. Graovac, T.C. Green, and R. Iravani. *Fault response of grid-connected inverter dominated networks*. in *IEEE PES General Meeting*. 2010. Rhode Island, USA.
152. Haggis, T. and A. Land, *Cables, Cable laying and accessories manual*. 2004, Central Networks: Bristol, UK.
153. Association, E.N., *ENA TS 37-2: Substation Cable Distribution Boards*. 2005: London, UK.
154. Northern Power Grid, *Code of Practice for the economic development of the HV system*. 2017: Newcastle upon Tyne, UK.
155. *Code of practice 331, Protection of LV Underground and Overhead Distributors and HV Protection of Distribution Transformers*. 2014, Electricity Northwest Limited.
156. British Standards Institution, *BS EN 60269-2: Low voltage fuses: Supplementary requirment for fuses for use by authorized persons (fuses mainly for industrial applications) - Examples of standardised systems of fuses A to K*. 2013: London, UK.
157. Northern Power Grid, *Code of Practice for the economic development of the LV system*. 2017: Newcastle upon Tyne, UK.
158. Yang, Y. and M. Bollen, *Power quality and reliability in distribution networks with increased levels of distributed generation*. 2008: Stockholm, Sweden.
159. Porter, D., G. Strbac, and J. Mutale, *Ancillary service provision from distributed generation*, in *18th International Conference on Electricity Distribution*. 2005: Turin.
160. Collinson, A., F. Dai, A. Beddoes, and J. Crabtree, *Solutions for the connection and operation of Distributed Generation*. 2003, Distributed Generation Co-ordinating Group (Technical Steering Group): London, UK.
161. Prakash, N., *Mitigating the Detrimental Impacts of Solar PV Penetration on Electric Power Transmission Systems*, in *Theses and Dissertations*. 2013, Arizona State University: Arizona, USA.
162. Tan, Y.T., *Impact on the power sytem with a large peneration of photovoltaic generation* in *Department of Electrical Engineering and Electronics*. 2004, The University of Manchester Institute of Science and Technology (UMIST): Manchester, UK.
163. Zhou, Y., *The Next Generation Grid-Connected PV Inverters for High Penetration Applications*, in *Department of Electrical and computer Engineering*. 2013, The Florida State University, College of Engineering: Florida, USA.
164. Ackermann, T., S. Cherevatskiy, T. Brown, R. Eriksson, A. Samadi, M. Ghandhari, L. Soder, D. Lindenberger, C. Jagemann, S. Hagspiel, V. Cuk, P.F. Ribeiro, S. Cobben, H. Bindner, F.R. Isleifsson, and L. Mihet-Popa, *Smart modeling of optimal integration of high penetration of PV - Smooth PV*. 2013: Darmstadt, Germany.
165. Vandenbergh, M., D. Craciun, V. Helmbrecht, R. Hermes, R. Lama, P.M. Sonvilla, M. Rekinger, and G. Concas, *Prioritization of technical solutions available for the integration of PV into the distribution grid* 2013, DERLab: Berlin, Germany.
166. Schauder, C., *Advanced Inverter Technology for High Penetration Levels of PV Generation in Distribution Systems*, in *NREL Subcontract Report*. 2014: Massachusetts, USA.
167. Pompodakis, E.E., I.S. Lelis, I.A. Drougakis, and M.C. Alexiadis, *Photovoltaic systems in low-voltage networks and overvoltage correction with reactive power control.* IET Renewable Power Generation, 2016. **10**(3): p. 410-417.
168. Bletterie, B., J.L. Baut, S. Kadam, R. Bolgaryn, and A. Abart, *Hosting capacity of LV networks with extended voltage band*, in *International Symposium on Smart Electric Distribution Systems and Technologies (EDST)*. 2015: Vienna.
169. Etherden, N., *Increasing the Hosting Capacity of Distributed Energy Resources Using Storage and Communication*. 2014, Lulea University of Technology: Lulea, Sweden.
170. Petinrin, J.O. and M. Shaaban, *Impact of renewable generation on voltage control in distribution systems.* Renewable and Sustainable Energy Reviews, 2016. **65**: p. 770-783.

171. Alexander, M.J., N. Richardson, and P. James, *Energy storage against interconnection as a balancing mechanism for a 100% renewable UK electricity grid.* IET Renewable Power Generation, 2014. **9**(2): p. 131-141.
172. Shaobo, L., H. Minxiao, F. Ruixiang, and H. Xiaodong. *Configuration of energy storage system for distribution network with high penetration of PV*. in *IET Conference on Renewable Power Generation (RPG)*. 2011. Edinburgh, UK: IET.
173. Shivashankar, S., S. Mekhilef, H. Mokhlis, and M. Karimi, *Mitigating methods of power fluctuation of photovoltaic (PV) sources – A review.* Renewable and Sustainable Energy Reviews, 2016. **59**: p. 1170-1184.
174. *Facilitating Distributed Generation connections*. 2014, UK Power Networks Holdings Limited: London, UK.
175. Hidayat, M.N. and F. Li, *Impact of Distributed Generation Technologies on Generation Curtailment*, in *IEEE Power & Energy Society General Meeting*. 2013, IEEE: Vancouver, Canada.

APPENDIX A:

DETAILS OF THREE-PHASE INVERTER MODEL

As discussed in section 4.4 the steady-state performance of an inverter is validated in two parts, viz. validation of the MPPT model and validation of the DC/AC converter. Figure A-1 shows the efficiency of the MPPT model at different ratings of PV systems for signals a – n. It can be observed that the efficiency is above 90% for all signals except for signals k and l, in-line with the results in [101]. Figure A-2 and Figure A-3 shows the odd and even harmonic currents as a percentage of the rated current for different ratings of PV systems. From the figures, it can be observed that the harmonic currents are within the maximum permissible levels for all harmonic orders.

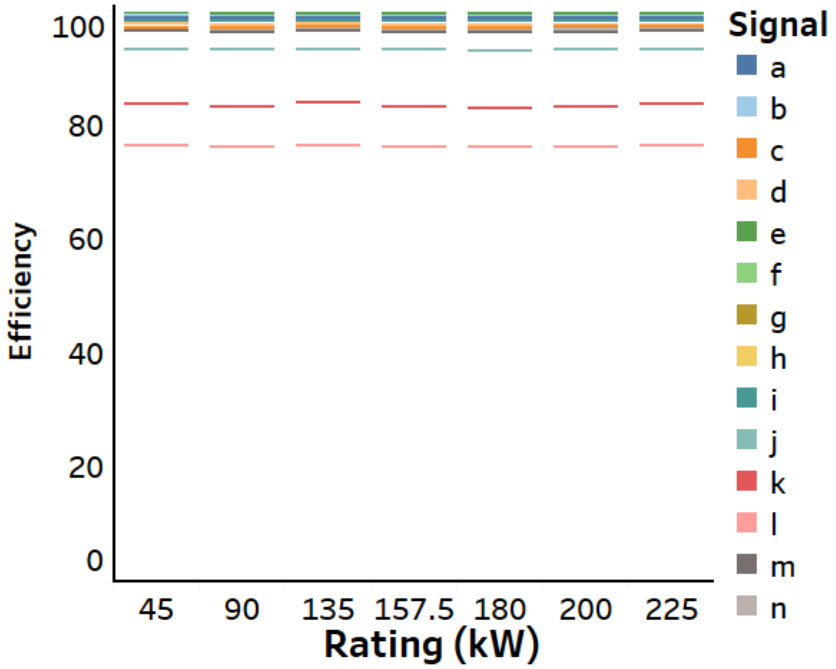

Figure A-1: Efficiency of the three-phase MPPT model at different ratings of PV systems for signals a-n

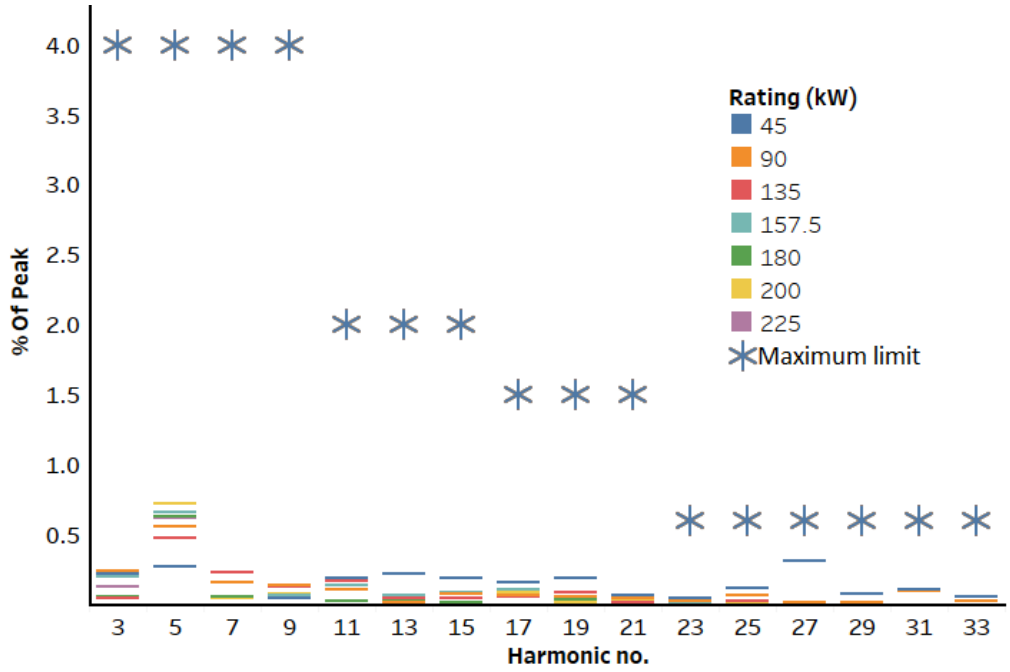

Figure A-2: Odd harmonic currents as percent of rate current for different ratings of inverter and the maximum permissible limits

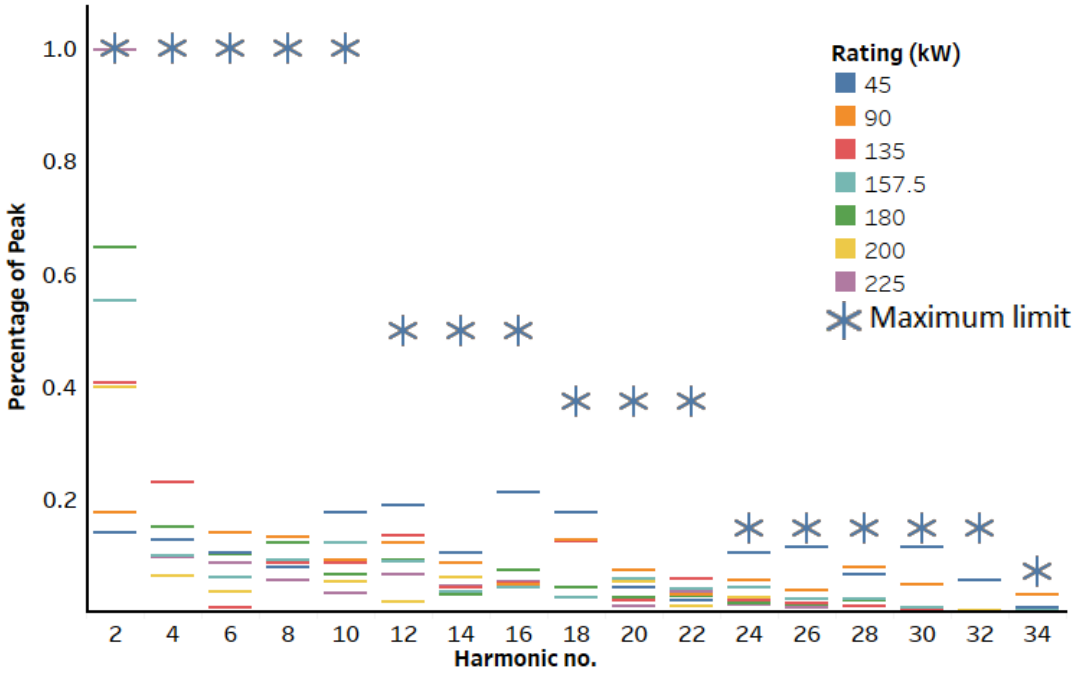

Figure A-3: Even harmonic currents as percent of rate current for different ratings of inverter and the maximum permissible limits

APPENDIX B:

DETAILS OF SIMULINK MODEL OF DIFFERENT COMPONENTS

B.1. PV array

MATLAB provides a built-in block “PV Array” which implements an array of PV modules as shown in Figure B-1(a). This block has a five parameter model using current source *IL* (same as I_{ph}), diode, series resistance R_s and shunt resistance R_{sh} to represent the irradiance and temperature dependent I-V characteristics of the modules. The diode is characterised by its reverse saturation current I_D and the quality factor (diode emission coefficient) *N*. The default value for *N* is 1.5. The block also has a set of pre-defined modules, the values of which are available. Figure B-1(b) shows the array parameters block in MATLAB. The module “Trina Solar TSM-250PA05.08” is used for all the simulations in this thesis. The specifications of the solar PV module used are as given in Table B-1.

Table B-1: Specifications of the solar PV module used for modeling

Parameter	Value
Rated capacity	250 Wp
Open circuit voltage (V_{oc})	37.8 V
Short circuit current (I_{sc})	8.55 A
Maximum power point voltage (V_{mpp}) @ STC	31 V
Maximum power point current (I_{mpp}) @ STC	8.06 A
Temperature coefficient of V_{oc} ($\beta_{V_{oc}}$)	-0.35%/˚C
Temperature coefficient of I_{sc}	0.06%/˚C

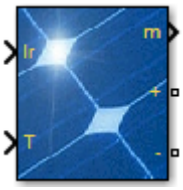

(a) Built-in block

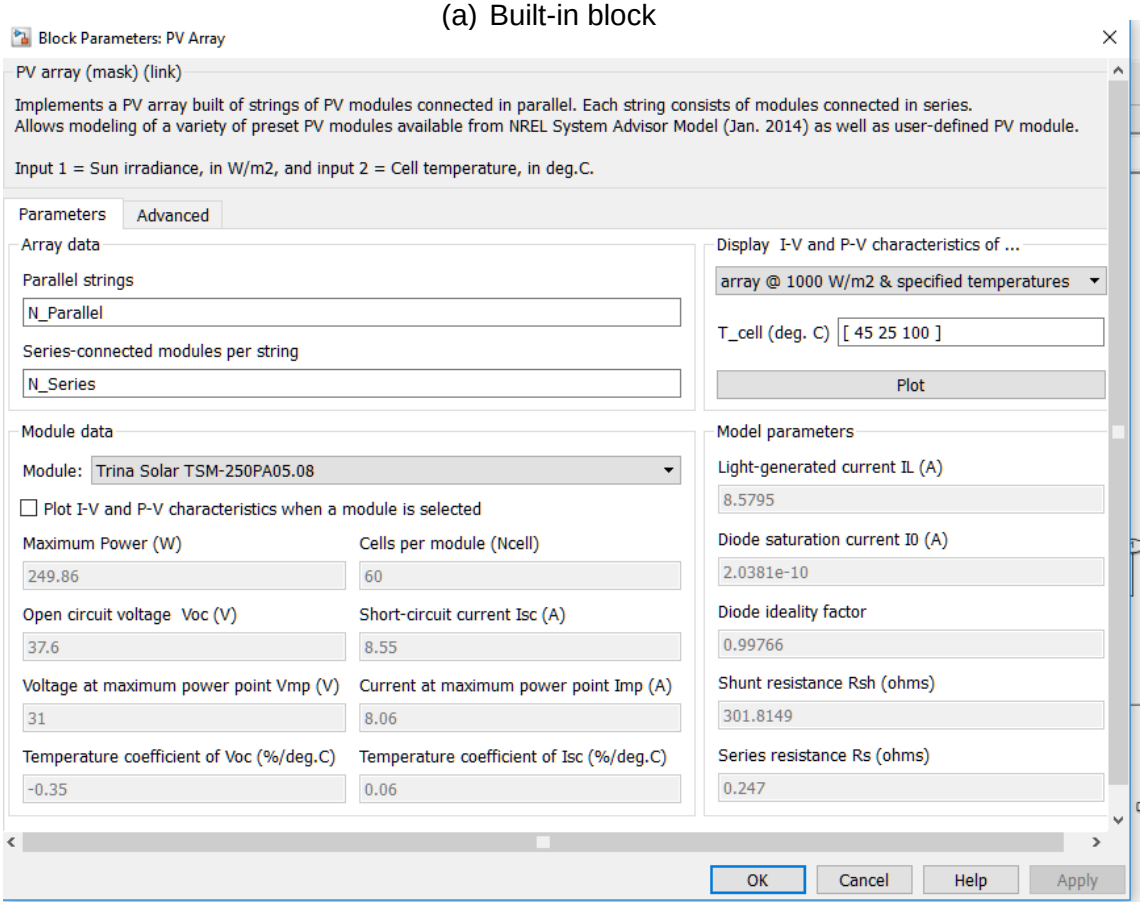

(b) Built-in block parameters

Figure B-1: PV array built-in block in MATLAB and its parameters

B.2 Code of P&O MPPT

Following was the code used to implement modified P&O MPPT in the developed model of PV system.

```
function D  = PandO(Param, Enabled, V, I)

% MPPT controller based on the Perturb & Observe algorithm.

% D output = Reference for DC link voltage (Vdc_ref)

% Enabled input = 1 to enable the MPPT controller

% V input = PV array terminal voltage (V)
```

```
% I input = PV array current (A)

% Param input:

Dinit = Param(1);  %Initial value for Vdc_ref

Dmax = Param(2);   %Maximum value for Vdc_ref

Dmin = Param(3);   %Minimum value for Vdc_ref

deltaD = Param(4); %Increment value used to increase/decrease Vdc_ref

persistent Vold Pold Dold;

% To ensure the values are stored between calls to the function

dataType = 'double';

if isempty(Vold)

    Vold=0;

    Pold=0;

    Dold=Dinit;

end

P= V*I;

dV= V - Vold;

dP= P - Pold;

if dP ~= 0 & Enabled ==1

    if dP < 0

        if dV < 0

            D = Dold + deltaD;
```

```
        else
            D = Dold - deltaD;
        end
    else
        if dV < 0
            D = Dold - deltaD;
        else
            D = Dold + deltaD;
        end
    end
else D=Dold;
end
if D >= Dmax | D<= Dmin
    D=Dold;
end
Dold=D;
Vold=V;
Pold=P;
```

B.3 Phase locked loop for grid synchronisation

The built-in block in MATLAB Simulink shown in Figure B-2(a) gives the measured frequency in Hertz and ωt varying between 0 and 2π, synchronised on the rising zero crossing of the fundamental component of the input signal. Figure B-2(b) shows

the parameters of the PLL block and the values used. $Fnom$ is the nominal frequency of the PV system being modelled (set as 50 Hz for the model) and the rest of the parameters are set to the default values mentioned in the built-in block.

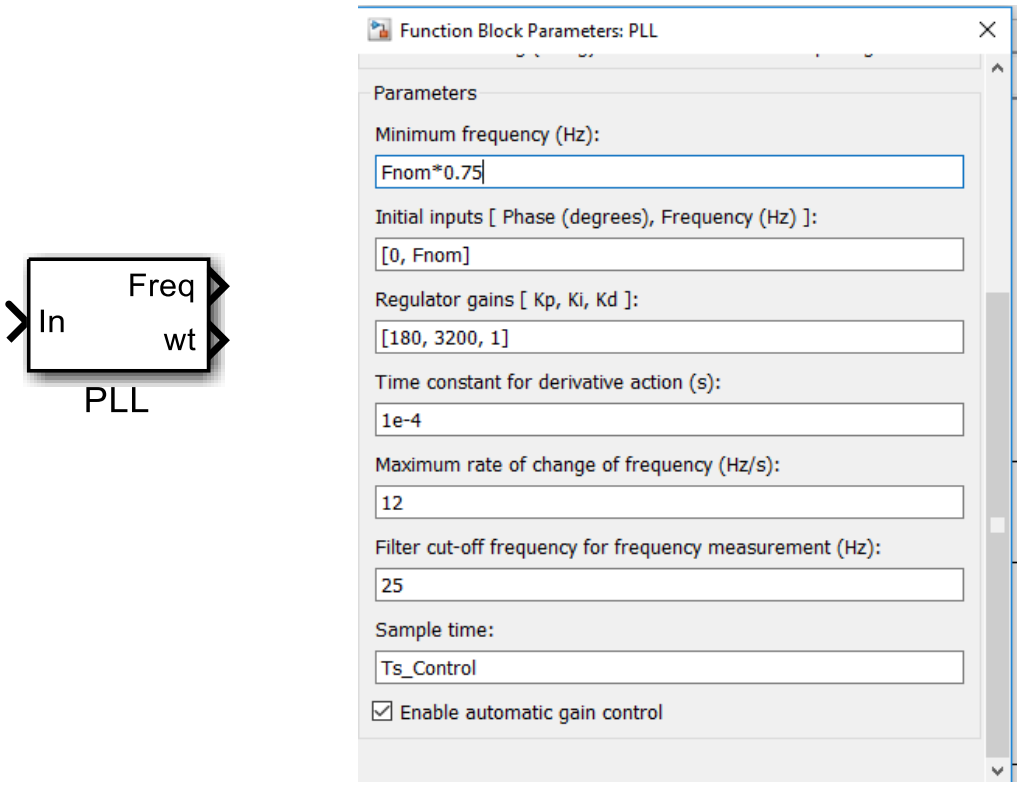

(a) Built-in block (b) Block parameters

Figure B-2: Built-in PLL block in MATLAB Simulink and its parameters

Figure B-3 shows the single phase transformation of the grid current or the inverter output current. Inverter current signal is converted to per unit value using the nominal rating of the inverter and the nominal rating of the PV system as base values. The per unit inverter current signal is then delayed by π/2 radians and fed

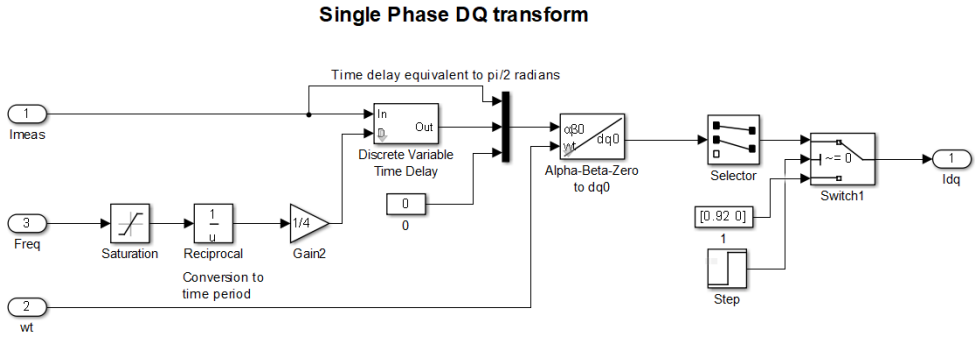

Figure B-3: Single phase d-q transformation of grid current

into the alpha-beta-zero to dq0 built-in block in MATLAB Simulink along with the original per unit current signal and constant zero signal. Switch1 block is used to transmit an initial value of 0.92 and 0 for d and q components respectively during the first time-step during which the controller is calculating the respective values. The d-q components of inverter current are passed through a low pass filter to eliminate the higher order harmonics introduced by the PWM controller in the signal. As grid voltage is the reference signal for the d-q transformation, the grid voltage can be directly converted to d-q by splitting the waveform into real and imaginary components as shown in Figure B-4.

Direct axis current reference value is obtained from the DC-link voltage and DC reference value is as shown in Figure B-5. The difference in value between the reference DC link voltage and the measured DC link voltage is converted into per unit by dividing the error/difference by the reference DC value, which is then integrated to obtain the reference signal. The constants k_p and k_i of proportional controller are chosen as 9.25 and 200 respectively based on trial and error to ensure

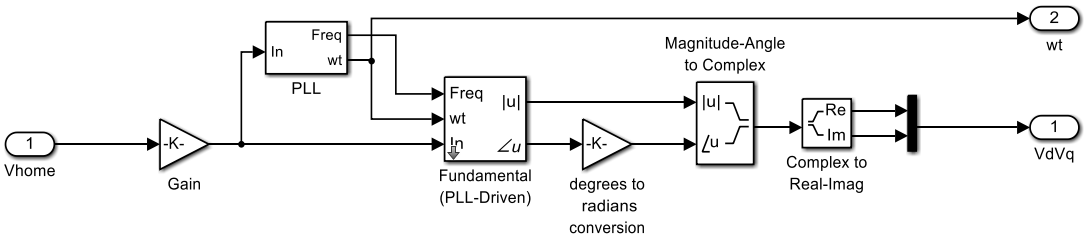

Figure B-4: d-q transformation of grid voltage

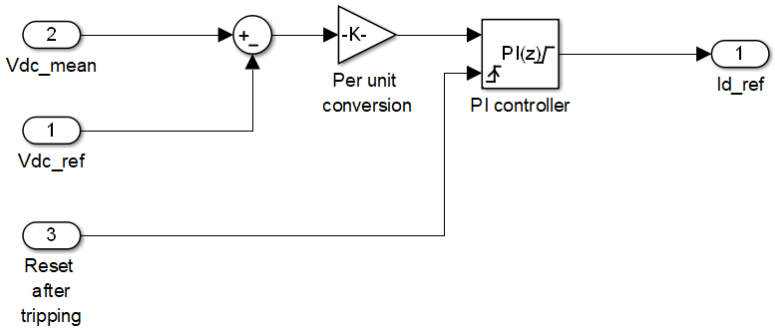

Figure B-5: Direct axis current reference signal generation

a reasonable settling time and overshoot. The PI controller is reset on the rising edge of the external reset signal. The voltage reference signals are compensated for this voltage drop as shown in Figure B-6. The voltage drop compensated direct and quadrature axis voltages are the magnitudes of output waveform of the H-bridge configuration. This is divided by the DC voltage in per unit (nominal AC voltage of the system as base) to calculate the modulation index of the PWM signal.

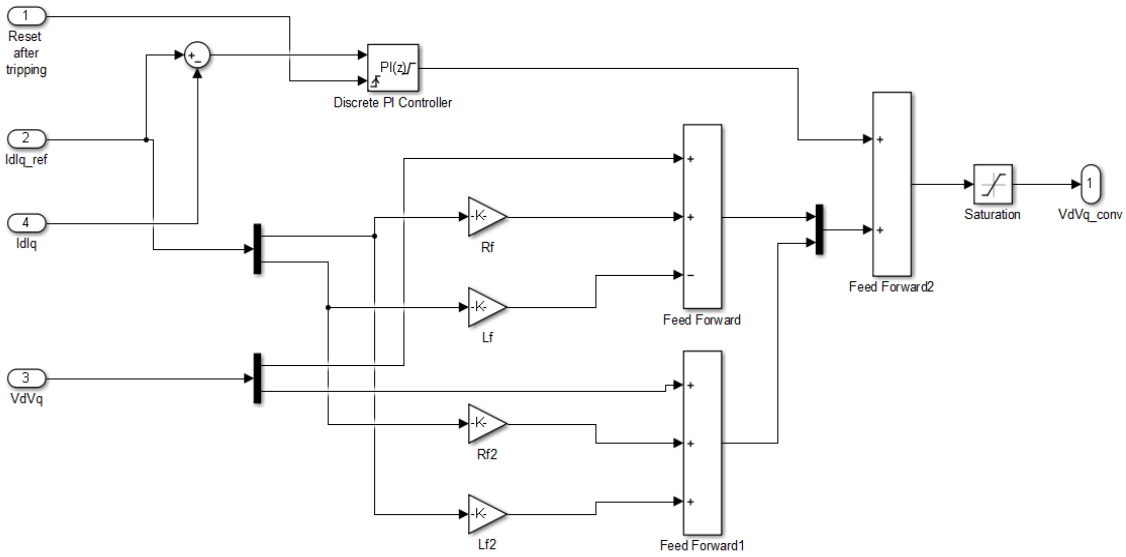

Figure B-6: Compensation for voltage drop in filter

The amplitude of this signal is controlled by the d-q controller, which is compared with the triangular signal at the high frequency to generate the switching pulses for the inverter switches. As the phase of the waveform has to be corrected for the time-delay introduced by calculations, the magnitude and the phase angle of the signal are separated. After addition of the phase delay, the sinusoidal reference signal for PWM is generated marked, as *Uref* in Figure B-7. MATLAB Simulink built-in block of the PWM generator is used to generate pulses for controlling the output of the single-phase universal bridge (built-in block)

B.4 Overall inverter model

The overall model of the PV system is as shown in Figure B-8 and Table B-2 gives the parameters of 2.5 kWp PV system used for performance evaluation of distribution network with PV. The next sections describe the equations used to arrive

at the values of different components of the inverter and a sample calculation for a 2.5 kWp system.

Table B-2: Parameters of 2.5 kWp solar PV system

Parameter	Value
PV rating	2500 Wp
Module rating	250 Wp
Number of modules in series	10
Number of strings in parallel	1
DC voltage, V_{dc}	425
PV capacitor, C_{pv}	3.65 µF
Inductance of DC/DC converter,L_{dc}	12 mH
DC/DC converter switching frequency	10 kHz
DC Link Capacitor, C_{dc}	900 µF
Inverter switching frequency, F_C	10 kHz
Inductance of LCL filter, L	3.4 mH
Resistance of Inductance of LCL filter, R_L	2.1 mOhms
Capacitance of LCL Filter, C	3.76 µF
Active power loss in the capacitance	7.5 Watts
K_p and K_i of Current regulator	0.38, 10.36
K_p and K_i of voltage regulator	9.25, 200

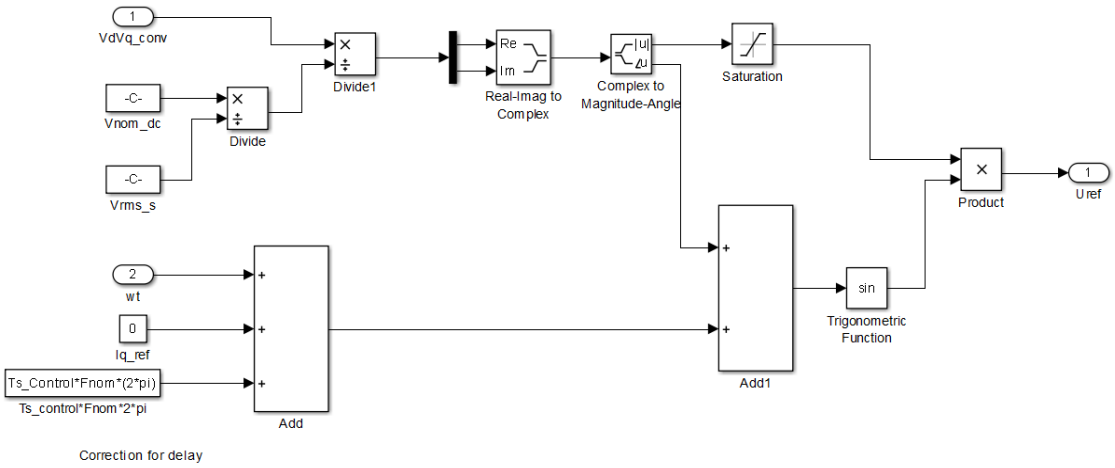

Figure B-8: Generic model of PV system

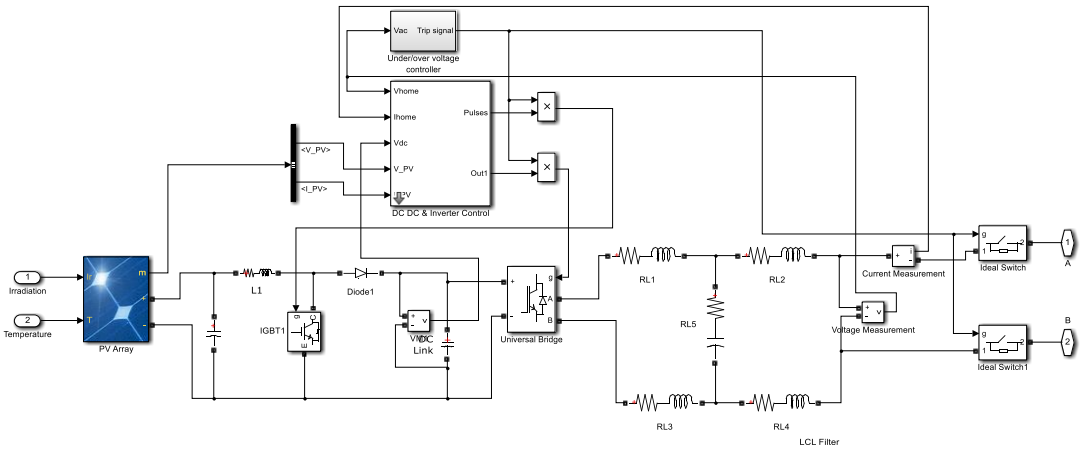

Figure B-7: Modulation index and reference signal for PWM generation

B.5 Design of boost converter for 2.5 kWp PV system

Base voltage for per unit calculations, $V_{base} = 230\ V$

Base VA for per unit calculations, $P_{base} = 2500\ VA$

Base current for per unit calculations, $I_{base} = {}^{P_{base}}/_{V_{base}} = 10.87\ A$

Base impedance for per unit calculations, $Z_{base} = {}^{V_{base}}/_{I_{base}} = 10.869\ Ohms$

Base capacitance for per unit calculations, $C_{base} = 150\ \mu F$

Rated DC current, $I_{dc} = {}^{Rated\ Power}/_{DC\ input\ voltage} = 8.0645\ A$

Permissible fluctuation in DC current, $\Delta I_{dc} = 10\%\ of\ I_{dc} = 0.80465\ A$

Minimum inductance of the DC/DC boost converter, $L_{dc,min} = \frac{V_{mp} \times (V_{dc} - V_{mp})}{\Delta I \times f_{dc} \times V_{dc}}$

$= 10\ mH$

Value of inductance of DC/DC boost converter used in this design,

$L_{dc} = 1.2 \times 10\ mH = 12\ mH$

DC-link capacitance, $C_{dc} = \frac{P_{base}}{\Delta V_{dc} \times V_{dc} \times \omega_{grid}} \quad = 900\ \mu F$

PV side capacitance, $C_{pv} = \frac{DT^2 V_{pv}}{4 \Delta V_{pv} L_{dc}} \ = 3.65\ \mu F$

Maximum capacitance of the LCL filter, $C_{max} = 0.05 C_{base} \quad = 7.5\ \mu F$

Value of capacitance of the LCL filter used in this design, $C = {C_{max}}/{2} = 3.75\ \mu F$

Frequency of resonance of the LCL filter, $f_{res} = \frac{F_c}{5} = 2000\ Hz$

Value of resistance in series with the capacitor, damping resistance,

$$R_d = \frac{1}{3 \times 2\pi f_{res} C} = 7.07\ \Omega$$

Value of inductance of the LCL filter used in this design, $L = \frac{2}{(2piF_{nom})^2 * C}$

$= 3.4\ mH$

Value of resistance in series with inductance of the LCL filter, $R_L = \frac{0.01 P_{nom}}{100 I_{rated}^2}$

$= 2.1\ m\Omega$

APPENDIX C:

SPECIFICATIONS OF THE INVERTER

Table C-1 provides the technical parameters of the 1 kW inverter used in the experiments for validation of dynamic performance of the dynamic model of PV system.

Table C-1: Technical parameters of 1 kW inverter

Parameter	Value
Rated Power	1000 Watt
DC input range	20-45 Vdc
MPPT voltage range	24 – 38 Vdc
AC output	230 Vac (190 – 260 Vac)
Frequency	50/60 Hz (Auto control)
Power factor	>98%
THD	<5%
Peak efficiency	88%
Stable efficiency	86%
Protection	Islanding; short-circuit; low voltage; overvoltage; over temperature
Grid Detection	DIN VDE 1026; UL 1741

APPENDIX D:

SPECIFICATIONS OF THE TYPICAL NETWORK

Table D-1 provides the details of the typical distribution network representative of the distribution networks in the UK.

Table D-1: Specifications of the typical distribution network

Component	Specifications
33 kV Source	33 kV source with 500 MVA fault level
33/11.5 kV Transformers	15 MVA 18% impedance on 15 MVA base YY0 windings X/R ratio of 15 Two transformers in parallel -20/20% tap changer with 2.5% tap steps Automatic voltage control scheme with 2.5% bandwidth Voltage set point between 11 and 11.1 kV Off load ratio of 33/11.5 kV
11 kV Feeder circuits	Five feeders modelled with lumped 11 kV – three-phase load of 2 MVA. Power factor same as the sixth detailed feeder.
11 kV detailed feeder circuit	1.5 km of 185 sq. mm. 3 core PICAS plus 1.5 km of 95 sq. mm. 3 core PICAS cable Impedance of 185 sq. mm. is 0.164 + j0.080 Ω/km Impedance of 95 sq. mm. is 0.32 + j0.087 Ω/km
11/0.433 kV transformer	500 kVA 5% impedance Dy11 windings X/R ratio of 15 Off load ratio of 11/0.433 kV
400 V detailed feeder	Impedance of 240 CNE is 0.1258 + j0.0685 Ω/km Impedance of 120 CNE is 0.2533 + j0.0685 Ω/km Impedance of 70 CON is 0.4430 + j0.0705 Ω/km

APPENDIX E:

DETAILS OF THE CLNR PROJECT

Table E-1 provides the details of the different classes of houses and its average percentage of the total houses in the UK. Table E-2 provides the details of the percentage of different classes of houses in the CLNR data.

Table E-1: Classes of houses and its percentage of total houses in the UK

No.	Class		% of houses
1	A	Alpha territory	3.53
2	B	Professional Rewards	8.16
3	C	Rural Solitude	4.37
4	D	Small Town Diversity	8.99
5	E	Active Retirement	4.42
6	F	Suburban mindsets	11.3
7	G	Careers and kids	5.76
8	H	New homemakers	5.88
9	I	Ex-council community	8.62
10	J	Claimant cultures	5.41
11	K	Upper floor living	5.04
12	L	Elderly needs	5.35
13	M	Industrial heritage	7.56
14	N	Terraced melting pot	7.13
15	O	Liberal opinions	8.48

Table E-2: Details of number of houses and its percentage in each class in the measured data

No.	Mosaic Class	Class name	Houses in each class	Percentage of houses in each class for the data
	Z	no data	217	2.46
1	A	Alpha territory	182	2.07
2	B	Professional Rewards	796	9.03
3	C	Rural Solitude	211	2.39
4	D	Small Town Diversity	1063	12.06
5	E	Active Retirement	390	4.43
6	F	Suburban mind-sets	1042	11.83
7	G	Careers and kids	378	4.29
8	H	New homemakers	193	2.19
9	I	Ex-council community	1251	14.20
10	J	Claimant cultures	556	6.31
11	K	Upper floor living	100	1.13
12	L	Elderly needs	714	8.10
13	M	Industrial heritage	886	10.06
14	N	Terraced melting pot	581	6.59
15	O	Liberal opinions	251	2.85
		Total	8811	100

APPENDIX F:

ADDITIONAL RESULTS OF STEADY-STATE PERFORMANCE EVALUATION OF THE SINGLE-PHASE FEEDER

Section 5.3 discussed the steady state performance of the single phase feeder at 152 W and 300 W loads, 1000 and 800 W/m^2 irradiance and PV distributed near and far from the substation for penetration levels from 0 to 100%. This appendix discusses the rest of the evaluation.

F.1 Impact of PV on the voltage profile of the single phase feeder

Figure F-1 shows the voltage profile of the feeder at 152 W load, 800 W/m^2 irradiance and PV distributed at the far end of the feeder. It can be observed that the voltage upper limit is not violated till 30% penetration, higher than the penetration at which upper limit is violated at 1000 W/m^2 irradiance, with other parameters remaining the same. Figure F-2 shows the voltage profile at 600, 400 and 200 W/m^2

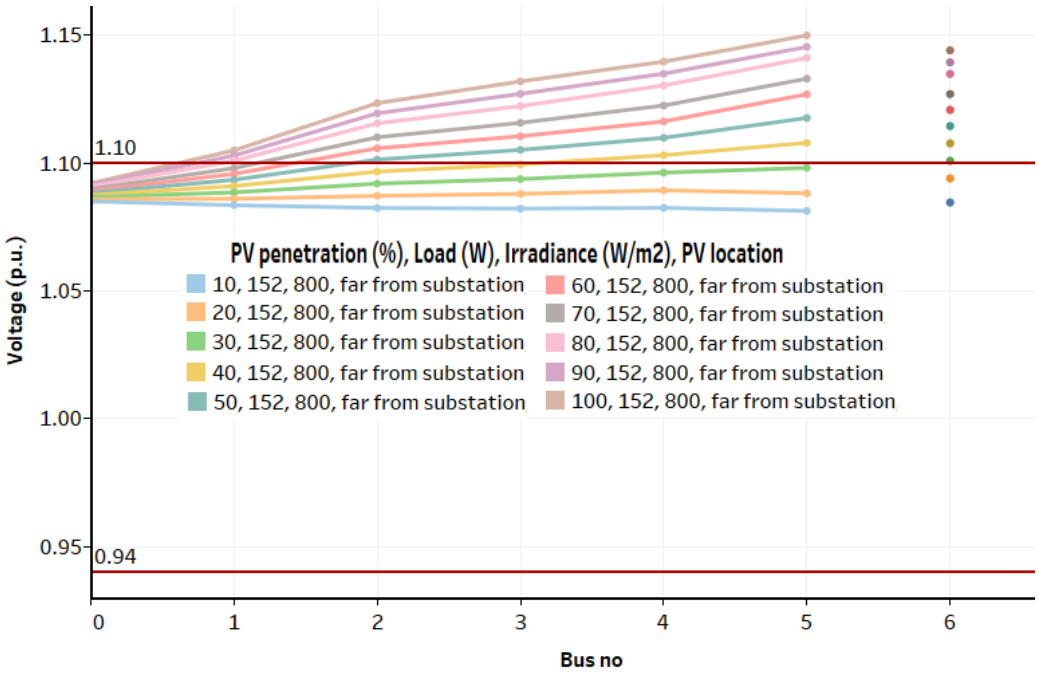

Figure F-1:Voltage profile of the single phase feeder at 152 W load, 800 W/m^2 irradiance and PV distributed at the far end of the feeder

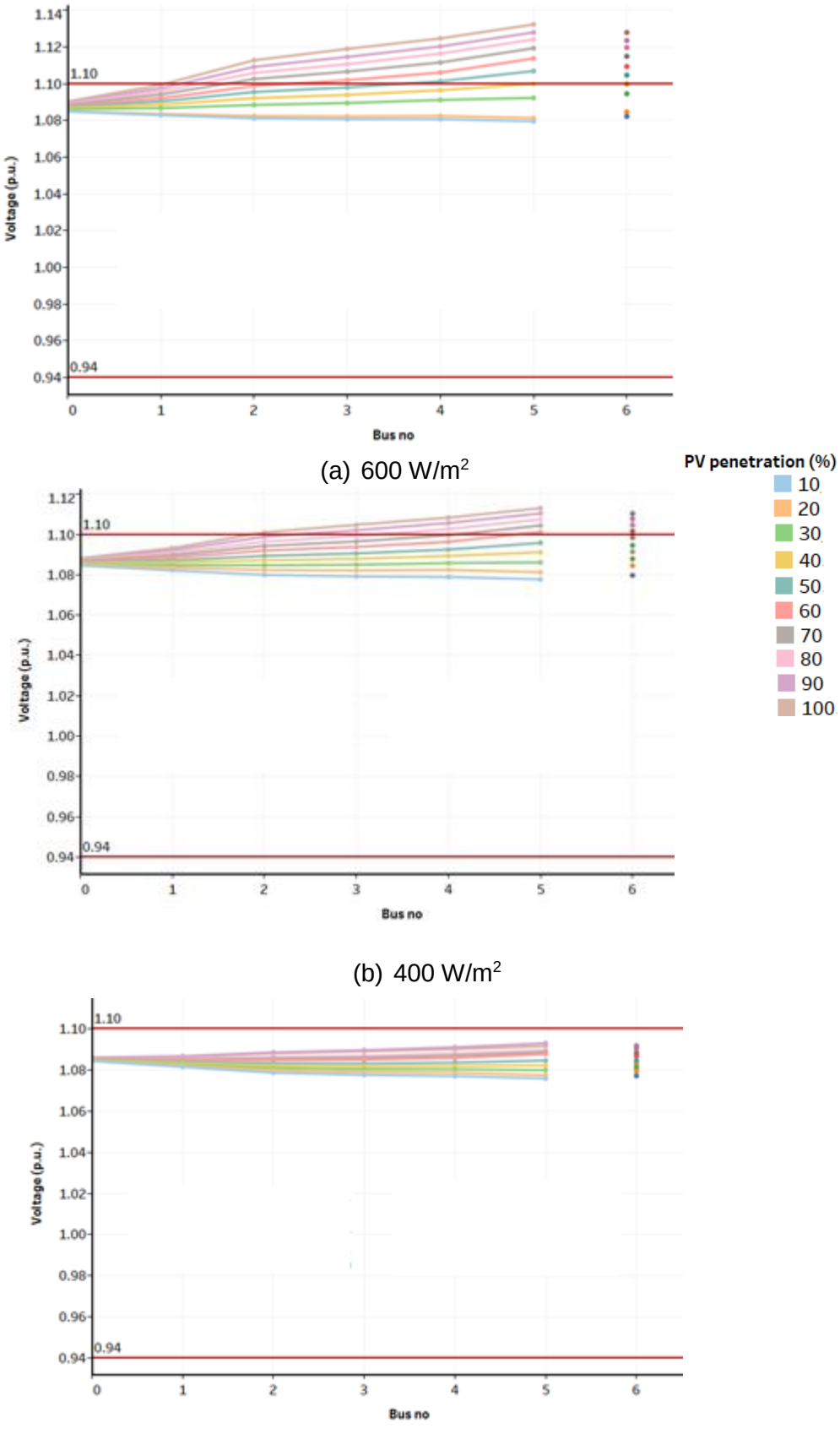

(a) 600 W/m^2

(b) 400 W/m^2

(c) 200 W/m^2

Figure F-2: Voltage profile of the single phase feeder at 152 W load with PV distributed at the far end of the feeder at different irradiance levels

irradiance and it can be observed that the penetration level at which the upper limit of the voltage is violated increases as the irradiance level decreases. Figure F-3

shows the voltage profile of the single phase feeder at 152 W load at different irradiance levels and penetration levels. It can be observed that the penetration level at which voltage upper limit is violated for PV distributed near the substation is higher than the penetration level for respective conditions with PV distributed at the far end of the feeder. The voltage profile of the single phase feeder at 300 W load at different irradiance levels and penetration levels with PV distributed at the far end of the feeder and near the substation shows a similar trend.

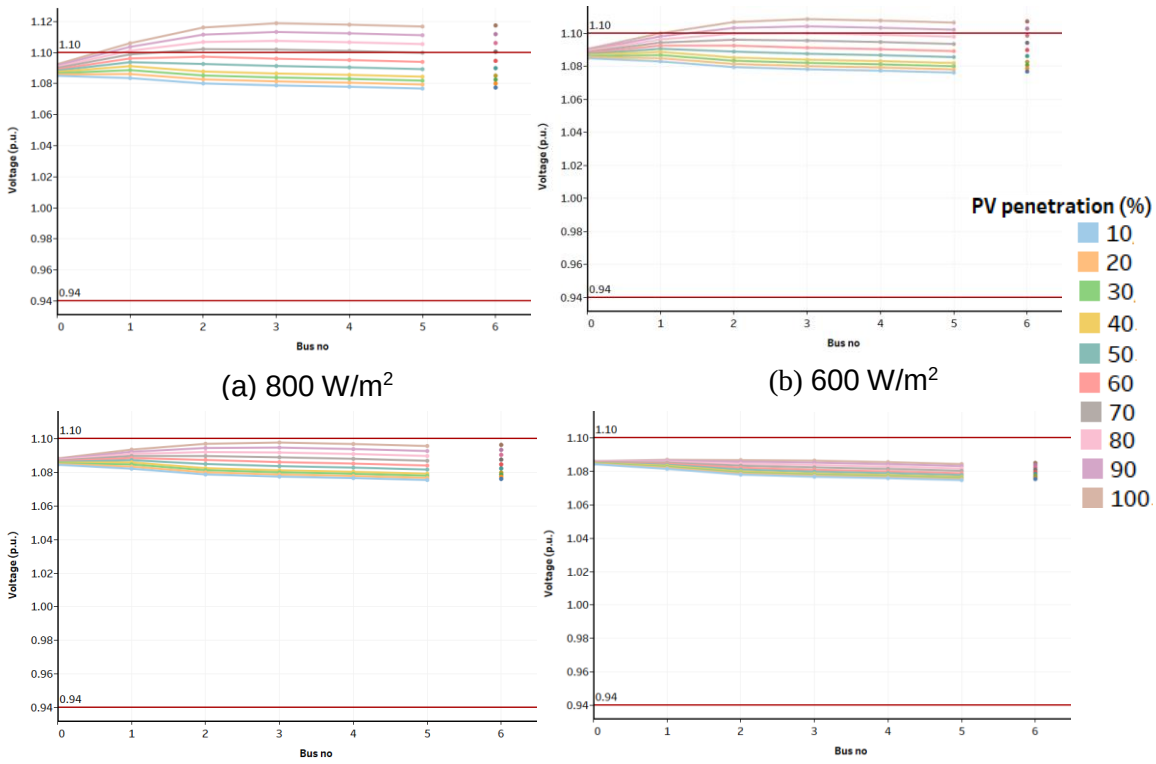

(a) 800 W/m^2 (b) 600 W/m^2

(c) 400 W/m^2 (d) 200 W/m^2

Figure F-3: Voltage profile of the single phase feeder at 152 W with PV distributed at the far end of the feeder and at different irradiance levels

F.2 Impact of PV on the THD of the single phase feeder

Figure F-4 shows the variation of THD of the current at the secondary of the substation transformer at different penetration levels of PV systems for irradiance levels of 1000 W/m2 and 800 W/m2 and a load of 152 W and 300 W. for PV distributed at the far end of the feeder. From this figure and Figure 5-7 it can be observed that the location of PV does not have a significant impact on the current THD at the secondary of the substation. However, at lower irradiance levels, the

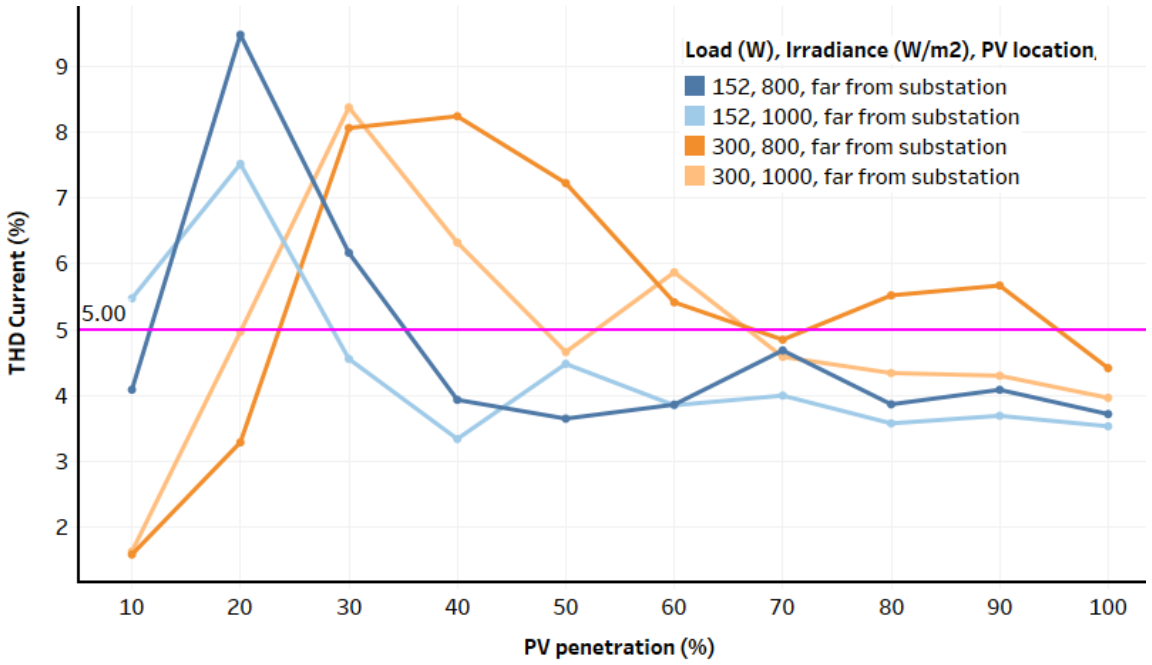

Figure F-4: THD of current at the secondary of the substation transformer for different penetration levels for loads of 152 W and 300 W with PV distributed at the far end of the feeder for irradiance levels of 1000 and 800 W/m^2

current THD increases above 20% as penetration increases above 70% at 200 W/m^2 irradiance, 152 W load, as shown in Figure F-5(a). For a similar set of parameters at 300 W load, the current THD is less than 20% up to 100% PV penetration as shown in Figure F-5(b). The trends are similar for PV distributed at the far end of the feeder. The combination of loads between 152 W to 300 W with irradiance between 50 to 200 W/m^2 occurs for 1% of the time in a year in the time period 4 a.m. to 6 a.m. mostly in the months June to August (based on correlation of load and irradiance).

F.3 Impact of PV on the net power at the substation of the single phase feeder

Figure F-6 shows the variation of net active power at the secondary of the substation transformer for different penetration levels and for irradiance levels of 200 to 600 W/m2. From the figure, it can be observed that as irradiance decreases, the percentage penetration of PV at which reverse power flow occurs increases as the generation from PV decreases with a decrease in irradiance.

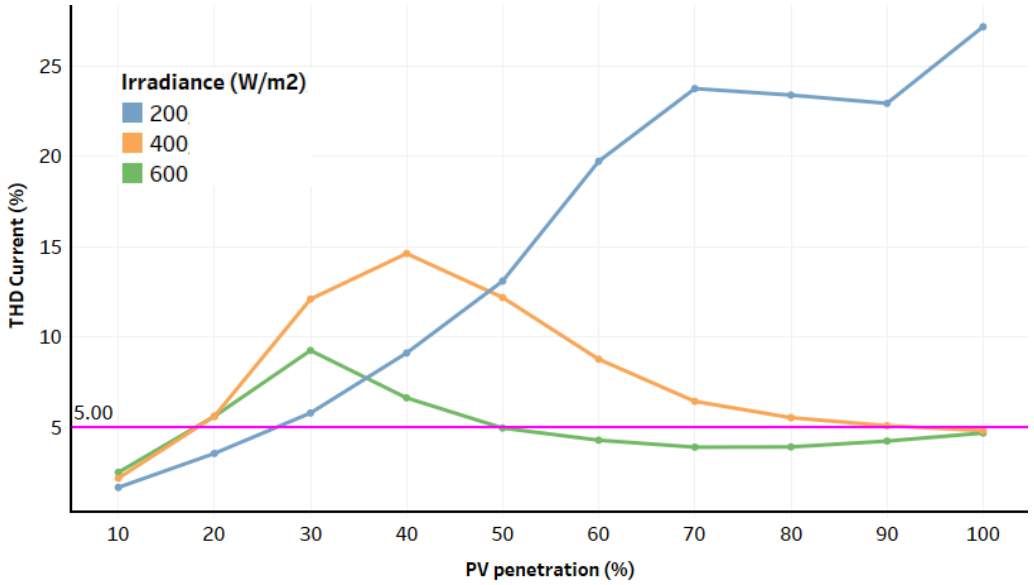

(a) 152 W load

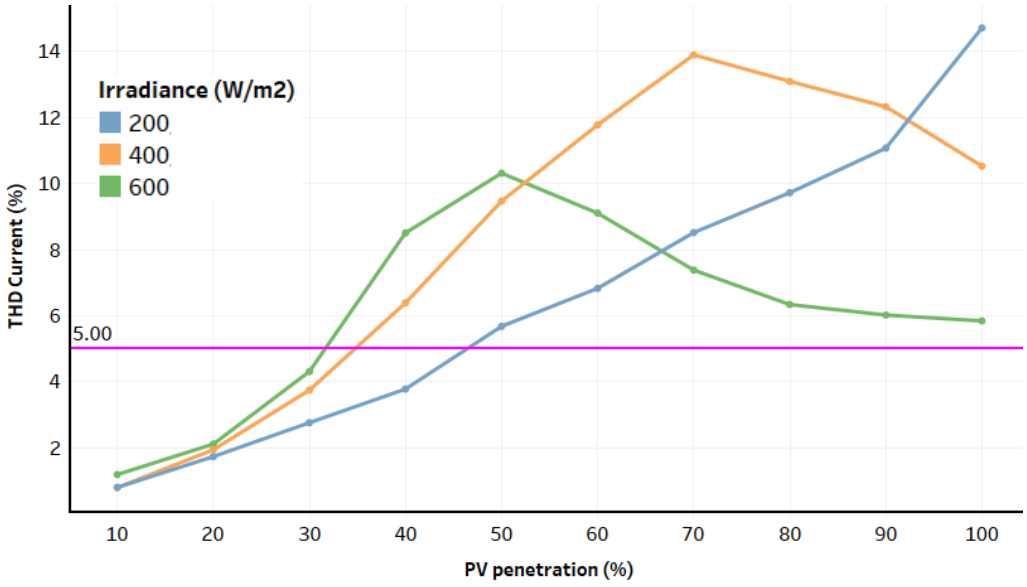

(b) 300 W load

Figure F-5: THD of current at the secondary of the substation transformer for different penetration levels and different irradiance levels for different loads

F.4 Impact of PV on the power factor at the substation of the single phase feeder

Figure F-7 shows the variation of power factor at the substation transformer for different penetration levels, loads of 152 W and 300 W, and irradiance of 200, 400 and 800 W/m2. From the figure, it can be observed that the penetration of PV at which the power factor at the substation decreases below 0.8 p. f. is higher for lower irradiance level as against the similar conditions at higher irradiance levels.

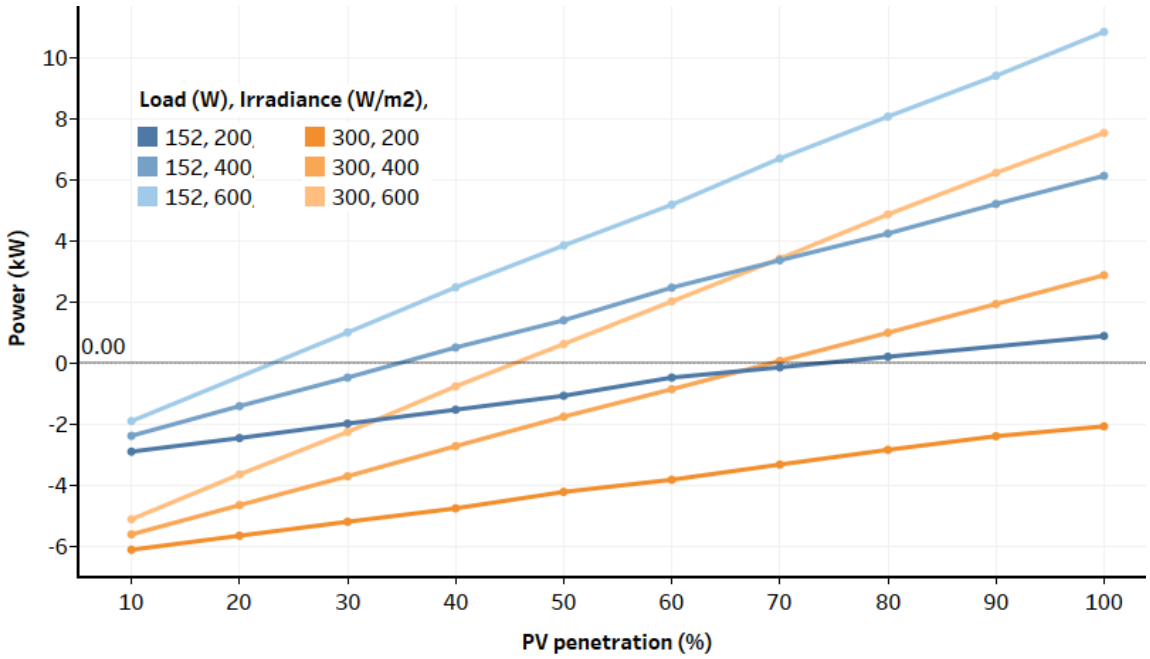

Figure F-6: Net active power flow at the substation transformer for different penetration levels of PV for different scenarios

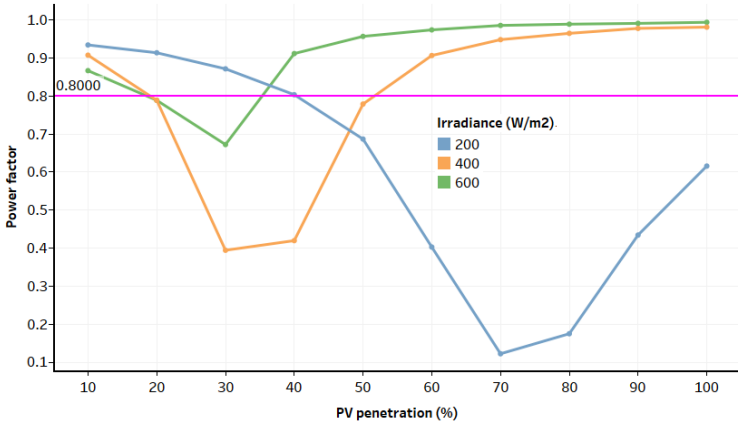

(a) 152 W load

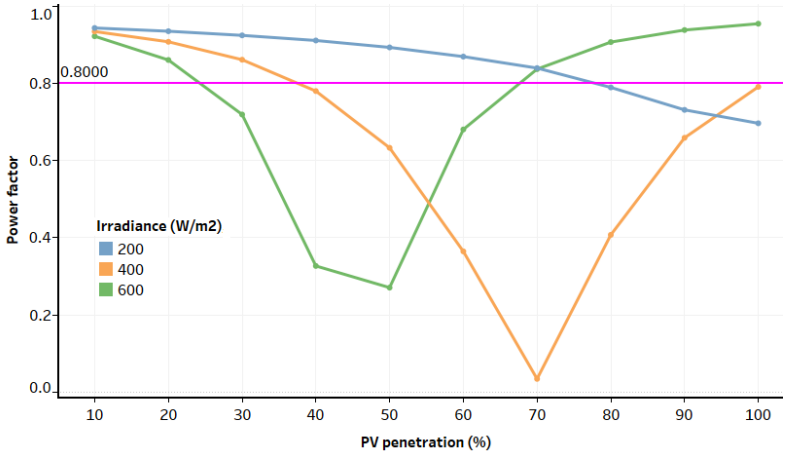

(b) 300 W load

Figure F-7: Power factor at the substation for different penetration levels of PV at different loads

APPENDIX G:

THEORETICAL CALCULATION OF FAULT CURRENT IN A DISTRIBUTION NETWORK WITH NO PV

The source in the distribution network is a generator with 500 MVA fault level at 33 kV. The impedance of the source has been given as j2.178 Ω in [118]. Fault current calculations are typically performed on a per unit basis. For this network, the base values chosen are

Base MVA, $MVA_{base} = 100\ MVA$

Base voltage, $V_{base} = \frac{11}{\sqrt{3}} kV$

Base current, $I_{base} = \frac{MVA_{base}}{\sqrt{3} * V_{base}}$

Base impedance, $Z_{base} = \frac{V_{base}}{I_{base}}$

To calculate the fault current, the first step is to calculate the per unit Thevenin equivalent impedance of the distribution network up to the fault location. The per unit impedance of different components of the distribution network are calculated first and then added to arrive at the Thevenin equivalent impedance. The different parts of the network that are in series with the source including the fault impedance is as shown Figure G-1. The next component in series with the source is the 15 MVA transformer.

Rating of the 33/11 kV transformer = 15 MVA

Percentage impedance of the 33/11 kV transformer on rating, $\%\ impedance\ on\ rating = 18$

Per unit impedance of the transformer $Z_{p.u.\_tfr} = MVA_{base} * \frac{\%\ impedance\ on\ rating}{Rating\ of\ transformer} = 1.2\ p.u$

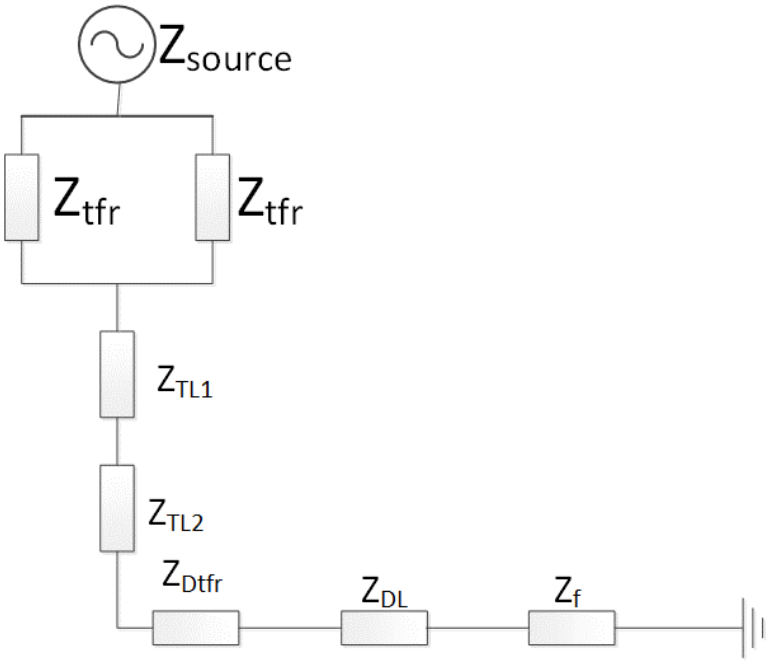

Figure G-1: Thevenin equivalent circuit of the distribution network under consideration

The X/R ratio of the transformer has been given as 15 resulting in $Z_{tfr} = 0.0798 + j1.1973\ p.u.$

The impedance of the transmission lines are also converted into per unit and added.

$$Z_{TL1} = \frac{(0.164 + j0.08) * 1.5\ km}{Z_{base}}$$

$$Z_{TL2} = \frac{(0.32 + j0.087) * 1.5\ km}{Z_{base}}$$

Rating of the 11/0.433 kV transformer = 0.5 MVA

Percentage impedance of the 11/0.433 kV transformer on rating, $\%\ impedance\ on\ rating = 5$

Per unit impedance of the transformer $Z_{p.u.\_Dtfr} = MVA_{base} * \frac{\%\ impedance\ on\ rating}{Rating\ of\ transformer} = 0.333\ p.u$

The X/R ratio of the transformer has been given as 15 resulting in $Z_{Dtfr} = 0.022 + j0.3323\ p.u.$

The total impedance of the distribution line is calculated as

$Z_{DL} = \frac{\sum(impedance * length\ of\ branch)}{Z_{base}}$,

where impedance values are as given in (Table C-1)

$$R_f = 1\ m\Omega$$

The Thevenin equivalent impedance $Z_{th} = 0.6981 + j2.9617$

Fault current is given as $I_f = \frac{V_{base}}{Z_{th}} p.u.$

The fault current in per unit multiplied by base current value gives the magnitude of the fault current in kA which has both active and reactive component. The magnitude of I_f is 1.8 kA.